A MULTIFUNCTIONAL NANOPARTICLE FORMULATION FOR SIRNA DELIVERY TARGETING NEURODEGENERATIVE DISEASES AND CANCER

Meenakshi Malhotra

Biomedical Technology and Cell Therapy Research Laboratory
Department of Biomedical Engineering
Faculty of Medicine
McGill University
Montreal, Quebec, Canada

April 2013

A thesis submitted to McGill University in partial fulfillment of the requirements of the degree of Doctor of Philosophy

To my parents

ACKNOWLEDGMENTS

I would like to express my gratitude to my research supervisor Dr. Satya Prakash. I am very grateful for his positive outlook, intellectual support, encouragement and advice, which were very helpful for the accomplishment of my research. His ever welcoming nature and patience with my questions, doubts and random visits to his office helped me gain lot of confidence with my ability to take decisions and following my research objectives. I am very grateful for the support and advice provided by my committee members Dr. Henrietta Galiana from the department of Biomedical Engineering and Dr. David Burns from the department of Chemistry for their questions and guidance, which helped my project at various stages, from planning to execution.

It is an honor for me to acknowledge the support of my colleagues, who helped me shape my analytical and critical thinking. Catherine Tomaro-Duchesneau and Shyamali Saha deserves much credit as she provided with an extensive help at various stages from designing to execution of the experiments, along with trouble shooting and proof reading of the manuscripts. Her help with RTPCR and statistical analysis is greatly appreciated.

I would also like to thank my fellow colleagues, Jasmine Bhathena, whose encouragement constructive discussions and questions during the lab meetings helped me immensely with my project. Arun Kulamarva for his encouragement, support and helping me improve my scientific writing skills. Christopher Martoni, for showing me to work with Hitachi 911 and helping me throughout to work with the machine, trouble shooting and for having immense patience with my never ending questions.

I would earnestly thank Ciaran Lane, who helped at a very crucial stage of my thesis. His help with setting up chemical reactions in the laboratory, working with solvents and providing me with basics of FTIR and NMR, helped me clear many doubts. Ambika Srinivasan from the Department of Neurosciences is warmly thanked for her expertise in western blot and RTPCR analysis and for developing the blots at the facility in her department. Her help with PCR gene expression analysis, antibody selection for protein analysis and quantifying total RNA using nanodrop in her lab is highly

appreciated. Mrs. Anjali Sharma from the department of Chemistry is warmly thanked for her intellectual inputs, with my chemical reactions and with NMR analysis.

I would also like to sincerely acknowledge Prof. Maryam Tabrizian and Biomat'x laboratory for letting me use the equipment facility in her lab that aided me to generate data for my thesis and special thanks go to Jamal Daoud, Sania Mansouri, Steve Shapka, Nicola Duceppe and many others. I also appreciate the excellent research environment provided to me by the BTCTRL group at the Department of Biomedical Engineering. My special thanks go out to all my other colleagues at BTCTRL (Arghya Paul, Safaa Sebak, Maryam Mirzaei, Imen Kahouli, Wei Shao, Sana Abbasi and Afshna Khan) for their insightful comments that helped me at assorted stages of my project, for making various issues clear to me.

I would also like to thank Mr. David Liu for help with electron microscopy, Ms. Tara for help with running NMR samples at FEMR facility at McGill, Mr. Petr Fiursak for help and training with FTIR, Otto Mass building, McGill. Dr. Jo-Ann Bader and Ms. Caroline Therien at Goodman cancer research center for processing the tissue samples and providing with histology slides. Dr. Marilene Paquet for her helpful input on assessing the histology slides. Furthermore, I'd like to thank the technicians at the McGill University Animal Resources Centre, especially Anna Jimenez, Rosalie Michaud, Genevieve Berube for their assistance with animal handling and training provided to follow the animal use protocol.

Ms. Pina Sorrini, Ms. Lina Vuch, Ms. Patricia Cap and Ms. Nancy Abate are kindly thanked for their endless supply of help and good cheer over the years. Dr. Ross Wagner must also be acknowledged for his time and assistance.

I would like to sincerely acknowledge the McGill Internal Studentship, Eileen's peter McGill Major Scholarship and the Fonds de Recherche en Santé du Québec for graduate scholarships. Support from these generous sources was instrumental.

I would like to thank my best friend Mr. Sanjeev Panigrahy, who provided me with endless moral support and encouragement in the pursuit of my dreams, showing me hope in the darkest days and especially bringing me food while working late night on long chemical reactions in the lab and giving me ride back home even in stormy weather. They say angels come in human form. I couldn't have focused so well if the basic needs

were not taken care of. I would also thank my friends in “Art of Living Foundation” (NGO) who cared about my well being at various stages of my work and their countless blessings has truly helped me in innumerable ways.

I would also like to thank Sr. Celsa, who has been a role model for me ever since I was a child and I am very fortunate for having her presence in my life. I am very grateful to my undergraduate teacher Dr. V.R. Swamy, who showed me the path towards research and introduced me to Nanomedicine. I can never forget his inspiring words and his belief in me. He has been a true inspiration and has always reminded me to follow my dreams.

Last but the not the least I am very grateful to my family for their enormous and unwavering support in the pursuit of this degree. My father, Mr. S.K. Malhotra, who has been struggling with a neurodegenerative disease, has been my biggest strength. From him, I learnt that with “will” one can change a state of “helplessness” into “power”. Seeing the repercussions such a disease holds for not only him but for the entire family, I have been moved to deliver the best of my skills to people around me, be it work or social circle. It has left a deep impression in me to never let anyone be helpless. My Mother, Mrs. Anand Malhotra, has been my backbone, supporting and motivating me with her inspirational talks. She has been the best of friend one can ever ask for.

PREFACE

In accordance with McGill University Thesis Preparation guidelines, as an alternative to the traditional thesis format, I have opted to present my thesis as original papers. The thesis includes articles, already published/accepted or to be submitted for publication. This collection of papers, of which I am the first author along with other co-authors, are presented in Chapters 3, 4, 5, 6 and 7 and are each divided into sections consisting of an abstract, introduction, materials and methods, results and discussion. A common abstract, introduction, literature review, a general discussion, conclusions and a bibliography are included in this thesis in accordance to the guidelines.

TABLE OF CONTENTS

siRNA	Small interfering ribonucleic acid
RNAi	RNA interference
miRNA	Micro RNA
ds RNA	Double stranded RNA
shRNA	Short hairpin RNA
RISC	RNA induced silencing complex
mRNA	Messenger RNA
DA	Degree of N-acetylation
DDA	Degree of deacetylation
HMWC	High molecular weight chitosan
LMWC	Low molecular weight chitosan
CHOS	Chitosan oligosaccharides
TPP	Sodium tripolyphosphate
PEG	Polyethylene glycol
MGF	Mechano growth factor
TAT	Trans-activating transcriptional activator
CPP	Cell penetrating peptide
CTP	Cell targeting peptide
WHO	World health organization
NMR	Nuclear Magnetic Resonance
FTIR	Fourier Transform Infrared
AD	Alzheimer's disease
NDDs	Neurodegenerative diseases
CNS	Central nervous system
PD	Parkinson's disease
HD	Huntington's disease
MS	Multiple Sclerosis
ALS	Amyotrophic lateral sclerosis
SCA	Spino cerebellar ataxia

BBB	Blood brain barrier
BCB	Blood-cerebrospinal fluid barrier
BCEC	Brain capillary endothelial cells
CSF	Cerebrospinal fluid
CED	Convection enhanced delivery
EEG	Electroencephalogram
CT	Computerized tomography
MRI	Magnetic resonance imaging
SPECT	Single proton emission computed tomography
PET	Positive electron tomography
MDR	Multidrug resistance
DNA	Deoxyribonucleic acid
IFN	Interferon
PKR	Protein kinase R
DRBD	Double-stranded RNA-binding domain
UTR	Untranslated region
TNF	Tumor necrosis factors
TLR	Toll-like receptors
ssRNA	Single stranded RNA
VEGF	Vascular endothelial growth factor
PLA	Polylactic acid
PGA	Poly glycolic acid
EPR	Enhanced permeation and retention
RES	Reticuloendothelial system
MPS	Mononuclear phagocyte system
PTD	Protein transduction domain
PSN1	Presenilin 1
PLK1	Polo-like kinase 1
LMW	Low molecular weight
MMW	Medium molecular weight
HMW	High molecular weight

TEM	Transmission electron microscopy
EDTA	Ethylenediaminetetraacetic acid
TBE	Tris borate EDTA
µg	microgram
ng	nanogram
µl	micro litre
µM	microMolar
mL	millilitre
N:P	Nitrogen:Phosphate
w/v	weight/volume
CO_2	Carbon dioxide
g	Grams
h	Hours
°C	degree celcius
n	Size of statistical sample
rpm	rotations per minute
bp	base pair
NaCl	Sodium chloride
PEI	Polyethyleneimine
NaH	Sodium hydride
$SOCl_2$	Thionyl chloride
$AlCl_3$	Aluminium chloride
THF	Tetrahydrofuran
DMF	N,N-dimethylformamide
EMEM	Eagle's minimum essential medium
FBS	Fetal bovine serum
TOSS	Total suppression of side bands
TOSDL	TOSS – dipolar dephasing
PBS	Phosphate buffered saline
NLS	Nuclear localization signal
EDC	1-ethyl-3-[3-dimethylaminopropyl]carbodiimide hydrochloride

DMAP	4-(Dimethylamino) pyridine
HRP	Horse radish peroxidase
MTS	3-(4, 5-Dimethyl-2-thiazolyl)-2, 5-diphenyl-2H-tetrazolium bromide
CS	Chitosan
PH	Phthalic anhydride
CSPH	Phthaloyl chitosan
NP-40	Nonyl phenoxypolyethoxylethanol-40
DTT	Dithiotreitol
SDS	Sodium dodecyl sulfate
TBST	Tris buffered saline – tween
Ig	Immunoglobulin
GLM	General linear model
SPSS	Statistical product and service solution
DMSO	Dimethylsulfoxide
NHS	N-hydroxy succinimide
FAD	Familial Alzheimer's disease
NT	Non-targeting
PFA	Paraformaldehyde
DAB	Diaminobenzidine
TUNEL	Terminal deoxynucleotidyl transferase-mediated dUTP nick-end labeling
PCR	Polymerase chain reaction
CRP	C-reactive protein
ALT	Alanine aminotransferase
AST	Aspartate transaminase
ALP	Alkaline phosphatase
CRE	Creatinine
UA	Uric acid
P53	Protein 53
PLL	Poly-l-lysine
GAPDH	Glyceraldehyde 3-phosphate dehydrogenase
PMSF	Phenylmethylsulfonyl fluoride

BCA	Bicinchoninic acid
KD	Kilo Dalton
LNA	Locked Nucleic acid
TTR	Transthyretin
PKN3	Protein Kinase N3
SNALP	Stable nucleic acid lipid nanoparticle
EPH A2	Ephrin Type A2
HIF 1α	Hypoxia inducible factors 1α
RRM2	Ribonucleoside-diphosphate reductase subunit M2
KSP	Kinesin spindle protein
KRAS	V-Ki-ras2 Kirsten rat sarcoma viral oncogene homolog
HPMA	N-(2-hydroxypropyl) methacrylamide

ABSTRACT

The thesis project focuses on the development of a novel, non-viral nanoparticle formulation for delivery of nucleic acids, drugs and other molecules. These nanoparticles were developed with an aim to administer the therapeutic molecules, non-invasively, to the targeted diseased tissue. The current thesis illustrates the design, characterization and optimization of the nanoparticles. The design of this novel nanoparticle formulation involves a series of chemical reactions on a parent polymer, chitosan, which is a cationic, biocompatible and biodegradable in nature. Chitosan was then surface graphed with another hydrophilic polymer called polyethylene glycol (PEG). PEG was used as a linker to further attach a peptide, which was meant to target a specific receptor on the cell's surface of the diseased tissue. In this work, we have utilized three peptide sequences, a cell penetrating peptide TAT, a neuronal targeting peptide MGF, and a colon targeting peptide CP15. These novel nanoparticles prepared using a novel synthetic scheme have shown successful delivery of the therapeutic molecules (siRNA) to the targeted tissue both in-vitro and in-vivo. The nanoparticle system as proposed can be used for intranasal delivery of siRNA's targeting brain or be used for systemic delivery to cancerous tissues. This project claims for the development of a nanoparticle based therapeutic delivery device, which can be tailor-made in terms of size, shape, surface charge of the nanoparticle, targeting peptide and therapeutic payload such as; siRNA/DNA/RNA and drugs. The formulation possesses the ability to bypass the blood-brain-barrier and other physiological barriers for the application treating neurodegenerative diseases and cancer respectively.

RESUME

Le projet de thèse porte sur l'élaboration d'une formule innovatrice et non virale de nanoparticules pour livrer des acides nucléiques, drogues et autres molécules. Ces nanoparticules ont été élaborées dans le but d'administrer, de façon non-invasive, des molécules thérapeutiques, pour cibler les tissus malades. La thèse présentée illustre la conception, la caractérisation et l'optimisation des nanoparticules. La conception de cette nouvelle formulation de nanoparticules consiste en une série de réactions chimiques sur un polymère parent, la chitosane, qui est cationique, biocompatible et biodégradable. Chitosane était alors modifiée en surface avec un autre polymère hydrophile, le polyéthylène glycol (PEG). PEG a été utilisée pour lier un peptide, qui avait pour but de cibler un récepteur spécifique localisé sur la surface de la cellule du tissu malade. Dans ce travail, nous avons utilisé trois séquences peptidiques, un peptide de pénétration cellulaire TAT, un peptide de ciblage neuronal MGF et un peptide qui cible le colon, CP15. Ces nouvelles nanoparticules, préparées à l'aide d'un nouveau schéma de synthèse, ont montrées une livraison réussie des molécules thérapeutiques (siRNA) au tissu ciblé, in vitro et in vivo. Le système de nanoparticules proposé est utile pour cibler le cerveau par une administration intranasale ainsi que pour cibler des tissus cancéreux par administration systémique. Ce projet propose le développement d'un dispositif de livraison thérapeutique basée de nanoparticules, qui peut être personnalisées en fonction de la taille, la forme, la charge superficielle de la nanoparticule, le peptide de ciblage et la charge utile thérapeutique tels que: siRNA/ADN/ARN et d'autres molécules thérapeutiques. La formule possède la capacité de contourner la barrière hémato-encéphalique et autres barrières physiologiques pour traiter les maladies neurodégénératives et les tissus cancéreux.

CHAPTER 1: GENERAL INTRODUCTION, RATIONALE, RESEARCH HYPOTHESIS, THESIS OBJECTIVES AND OUTLINE

Nanotechnology is the understanding and control of matter at dimensions of roughly 1 to 100 nm, where unique phenomenon enables the delivery of novel drugs, genes, proteins, peptides, vaccines for therapeutic applications [1]. It is an interdisciplinary field which involves an integration of surface science, organic chemistry, molecular biology, semiconductor physics, microfabrication etc, for a detailed study of the diseases at a molecular level.

The nanoparticles based delivery methods, for RNAi therapeutics, holds a great promise in the realm of drug discovery/development research. In comparison to the traditional drug technologies, RNAi promises to be at a therapeutic advantage for neurological and proliferative disorders. Most of the existing treatments and drugs available for neurodegenerative diseases provide symptomatic relief, but cannot stop, prevent or reverse the progression of the disease, the destruction of neurons and cognitive impairment. Thus, a significant opportunity exists for a novel product which has the potential to address the current unmet need. A recent report by the Alzheimer's Association predicts that number of cases in America with Alzheimer's disease (AD) above the age of 65 will increase dramatically by mid-century [2]. This will lead to a total care giving cost for individuals from $172 B to more than $1 trillion by 2050 [2]. This astonishing number calls for a dramatic improvement in the health care and medicare system. Even therapies that lead to delay in the onset of the disease 5 years can majorly impact the socio-economic status of the disease.

Proliferative-associated disorder such as cancer is characterized by uncontrolled growth of group of cells that infest adjacent tissues and often metastasize to other organs via lymphatic system or blood stream. The Global Cancer Report issued by the World Health Organization (WHO) estimates that there are over 10 million new cases of cancer every year with over 6 million annual deaths caused by the disease [3]. The current

treatment options available for cancer are surgery, chemotherapy, hormone blocking therapy, immunotherapy and radiation therapy. The toxicity of these methods has severely limited the safety and effectiveness of the treatment.

RNA interference has emerged as a new model for gene therapy in cancer, with the advantage of specifically blocking the genes that are involved in the biochemical pathways of cancerous cells and/or neurodegenerative diseases. Moreover, the poor-target specificity and side-effects of other existing drugs, makes siRNA based RNAi therapeutics to fall under a new class of advanced drugs, which are target-specific and addresses the translation gap between genetic and non-genetic disorders. However, owing to the transient nature of the siRNA it has become essential to optimize the chemistry and delivery aspects of the siRNA candidates. Many efforts in RNAi research deals with safe chemistry procedures to protect the siRNA from degradative enzymes when administered into the body [4]. However, it may sometimes compromise the efficiency of the siRNA candidate [4]. To address this issue, nanoparticle based delivery is quite an appealing approach. This novel system does not alter the chemistry of the siRNA, rather encapsulates the molecule to protect it from biological enzymes and fluids for safe delivery at the targeted site. Nanoparticles based delivery has an advantage to offer targeted delivery, which can identify ligands specific for disease biomarkers, thus distinguishing between abnormal and normal cells. This can reduce side-effects and facilitate uptake of therapeutics by the cells.

1.1 Research Hypothesis

A multifunctional nanoparticle formulation can be designed and administered non-invasively for siRNA delivery, targeting neurodegenerative diseases and/or cancer, in-vivo.

1.2 Research Objectives:

1) Characterize and optimize chitosan nanoparticles to achieve a size in the range of 5-20 nm to target neuronal cells and of size 100-120 nm to target cancer cells. This objective includes determining the correct pH, concentration, N:P ratio of

polymer:siRNA, maximum gene loading efficiency, particle size, surface charge, percentage uptake by cells in comparison to the commercially available transfection reagents and cellular toxicity of the nanoparticles.

2) Design and synthesize a derivative of chitosan polymer that proves to be less cytotoxic. The synthesis would involve a novel scheme to functionalize the polymer with a hydrophilic polymer and attaching a cell penetrating or a cell targeting peptide (CPP/CTP) on it.
3) Characterize the modified chitosan polymer and analyze the substitution of specific functional groups via Nuclear Magnetic Resonance (NMR) and Fourier Transform Infrared (FTIR) analysis, develop nanoparticles complexing siRNA and determine size and in-vitro cellular uptake, toxicity analysis and gene silencing analysis.
4) Validate the developed siRNA-nanoparticle formulation in an animal model Alzheimer's disease (AD), by delivering the formulation via intranasal route and determine the percentage gene silencing and safety/toxicity analysis.
5) Validate the developed siRNA-nanoparticle formulation in a xenograft animal model of colorectal cancer, by delivering the formulation via systemic route and determine the percentage gene silencing and safety/toxicity analysis in cancer tissue.

1.3 Thesis Outline

This thesis contains 10 chapters. The background and objectives of the thesis research are stated in Chapter 1, and an exhaustive literature survey of relevant subject matter in Chapter 2. Chapters 3-7 are five original papers that are already published, accepted/ to be submitted to peer-reviewed journals. These research articles include the main studies performed to test above stated research hypothesis and to achieve the above stated research objectives. Chapter 8 sums up the findings obtained in these studies and Chapter 9 summarizes claimed contributions to knowledge and conclusions. Recommendations for future research (Chapter 10) are given at the end of this thesis.

2.1 Introduction to Nanomedicine

Nanomedicine is gaining importance in the pharmaceutical and other industries with developing target specific carriers to achieve higher therapeutic efficacy. Its main focus can be classified as: 1) drug delivery, 2) in-vitro and in-vivo diagnostics, 3) imaging and 4) regenerative medicine. Specifically, the emergence of nanoparticle based drug/gene delivery carriers is posed to edge over chemotherapy and radiation therapy as cancer therapeutics. This is primarily because nanomedicine engages controlled production parameters in the making of engineered particles with specific size, shape, and other essential properties. It is widely expressed that these materials will significantly contribute to the next generation of medical care technology and pharmaceuticals in the areas of disease diagnosis, disease prevention and many other treatment procedures. This thesis focuses on the design and development of a multifunctional polymeric nanoparticle **(figure 2.1)**, which shows great potential as an effective therapeutic delivery vehicle. The advantage of such a delivery system would be to show no or tolerable levels of toxicity/side effects and with efficient delivery of a high potency therapeutic in much less quantity than required otherwise. Specifically, the multifunctional, non-viral nanoparticles were developed from a cationic polymer, chitosan to deliver siRNA. The surface of the nanoparticle is camouflaged under a layer of hydrophilic linear polymer, polyethylene glycol (PEG), which is further tagged with CPP/CTPs). The nanoparticle system developed was used for in-vitro and in-vivo application, to test the composition's physical state, solubility, stability, therapeutic effect, efficacy, rate of in-vivo release, and rate of in-vivo clearance. Following is the general description of nanoparticle's components (**figure 2.1**) involved in the synthesis.

2.1.1 Chitosan – cationic polymer

In the current study the cationic polymer used is chitosan. Chitosan is a polysaccharide and is known to be biocompatible in nature. It is obtained by N-deacetylation of chitin. In industrial scale procedures, chitosan is obtained from chitin by alkali treatment of crustacean shells. It is also present in nature in the cell walls of some

fungi and algae and in insects. It is mainly composed of β-1,4-linked D-glucosamine units with a variable content of N-acetyl-D-glucosamine units **(figure 2.2)**. The percentage of N-acetyl-D-glucosamine units is defined as the degree of N-acetylation of chitosan ("DA"), while the percentage of D-glucosamine units is also called the degree of deacetylation ("DDA") of chitosan **(figure 2.2)**. Most commercial preparations of chitosan are characterized by DDA values between 70 and 99% [5, 6]. Native chitosan molecules, as isolated from natural organisms or obtained after alkaline N-deacetylation of chitin, are of high molecular weight (HMWC), in the range of millions of Daltons, with degrees of polymerization reaching several thousand units. While various applications were described for such HMWC, for most applications a narrower, optimal range of molecular weight is preferred. Chitosan polymers with shorter than native chains are often divided into low molecular weight chitosan (LMWC), with a range of molecular weight roughly between 5 KDa and 100 KDa and chito-oligosaccharides (or chitosan oligosaccharides; CHOS) with a lower limit of 0.4 KDa (glucosamine dimer) while the higher limit is less defined (5 to 10 kDa). The CHOS are fully soluble in water and are essentially prepared as undefined mixtures of oligomeric molecules of various molecular weights and degrees of N-acetylation [5, 6].

Chitosan is a cationic polymer due to the presence of amine groups at the C6 position of its pyranose ring and, in its native unmodified state, is only soluble in mild acidic conditions (pH $\leq$5.5). The free amine groups present on chitosan polymer can be modified, by conjugating other compounds. However this can lead to the loss of its cationic nature. The presence of free amine groups (*e.g.* a net positive charge) on chitosan can help in complexing with negatively charged agents (due to ionic interactions), can help in cellular uptake and, once inside the endosomal cavity, can create a "proton sponge effect" (*e.g.* a swelling behavior of chitosan observed when encountering an acidic pH inside the cell's endosome) [5, 6].

2.1.2 Small interfering RNAs (siRNAs) – anionic therapeutic agent

siRNA is a nucleic acid molecule capable of mediating RNA interference "RNAi" or gene silencing. Specifically, they are 18-22 nucleotides in length and are double

stranded; wherein, one strand comprises the sense region and the second strand comprise the antisense region. It bears a net negative charge and can be formulated inside the internal core formed by the cross-linked cationic polymer.

2.2 RNA interference

Following the initial discovery of (RNAi)-mediated gene silencing [7], the therapeutic use of siRNA is gaining in popularity. The pioneering work of Fire et al. (1998) led to the identification of dsRNAs with the potential to selectively and efficiently turn off genes in *Caenorhabditis elegans* [8]. In vertebrates, however, the dsRNAs were shown to cause cell death by the induction of the Interferon (IFN) response and the activation of dsRNA-dependent protein kinase R (PKR). Later, Elbashir et al. (2001) pioneered gene silencing in mammals by proving that diced dsRNAs can side-step the IFN pathway and effectively switch off a targeted gene [9]. This mechanism opened a plethora of opportunities; one among them was the use of gene silencing against a variety of human diseases through an approach termed 'RNAi therapeutics'.

2.2.1 Mechanism of RNAi

RNAi is a post-transcriptional gene silencing process that is induced by a miRNA or a dsRNA (a small interfering RNA (siRNA) or small hairpin RNA (shRNA)) and has been used to modulate gene expression. The mechanism of RNAi involves degradation/repression of the messenger RNA by an RNA induced silencing complex (RISC) that carries the antisense strand of siRNA to the targeted mRNA region and thereby preventing the translation of the transcribed targeted mRNA [4]. The two major players in RNAi mechanism are 1) Dicer and 2) A multiprotein RNA-induced silencing complex (RISC), containing Argonaute. **Figure 2.3** illustrates the mechanism of RNAi on introduction of dsRNA into the cytoplasm of a cell, wherein Dicer along with its associated cofactors, consisting of an N-terminal RNA helicase domain, an RNA-binding Piwi/Argonaute/Zwille domain, two RNase III domains and a double-stranded RNA-binding domain (DRBD), trigger the generation of a pool of siRNAs. The formed siRNAs are ~ 21 base pairs (bp) in length with 2 nucleotide overhangs at both 3' ends. The processed siRNAs are then delivered to an Argonaute-containing RISC. With a

perfect sequence complementarity of the RNA duplex loaded onto the RISC, the Argonaute cleaves the passenger strand through RNA helicase activity. This produces activated RISC, retaining the guide strand with lower stability at the 5' end, to act as a RISC-targeting cofactor. RISC is a stable protein-RNA complex guided by the bound strand of siRNA to the target mRNA [10]. The siRNA bound strand confers sequence-based specificity to its associated Argonaute containing-RISC complex, allowing recognition and base pairing with the target mRNA. This reaction is carried out by the Piwi domain in RISC that folds into an RNaseH-like structure. The Argonaute in the RISC complex contains an endonuclease activity which causes a single-site cleavage of the target mRNA roughly in the middle of the siRNA binding region [11, 12]. The resulting cleaved fragments of the target mRNA have unprotected ends and are, hence, subsequently degraded by the cellular nucleases.

2.2.2 The essentials of siRNA – overcoming off-target effects

The most important barrier in developing a successful siRNA design is to avoid siRNA silencing of unintended mRNA transcripts containing partial homology. This undesirable effect is known as the 'off-target effect' [13, 14]. As in the case with miRNAs, which cause translational repression, they are 22 nucleotides in length and bear imperfect complementarity with the target mRNA to be silenced. Due to which, they may cause more off-target effects as compared to siRNAs. Thus, sequence specificity of the siRNA is very stringent, as a single base pair mismatch between the siRNA and its target mRNA can dramatically reduce the efficacy of silencing.

The incidence of nonspecific targeting is dependent on the concentration of the siRNA, with a higher concentration leading to a greater off-target effect. Thus, subnanomolar concentrations of highly active siRNAs are used in order to minimize off-target effects [13, 14]. Off-target effects, from high concentrations of siRNAs in the cells, are likely to result from the sense strand or from the dsRNA-binding proteins that stimulate the antiviral-response pathways, inducing the expression of antiviral-response genes. The use of sub-nanomolar concentrations of siRNA allows the transfection of multiple siRNAs simultaneously, an important advantage. Seed-region analysis

determines the number of exact matches of the siRNA seed-region with the mRNA's 3' untranslated regions (UTR)s. Complementarity between the 3'UTR of the mRNAs and the seed-region of the antisense (guide) strand, especially with the nucleotides at positions 2 - 7 or 2 - 8, has been associated with off-targeting (**Figure 2.4**) [15]. It has been observed that siRNAs with low seed-region frequency are less likely to cause off-targeting when compared to siRNAs with higher seed-region frequencies [15, 16]. Interestingly, it was reported that long dsRNA does not evoke off-targeting because a pool of siRNAs with different sequences arise following Dicer digestion [17], which subsequently reduces the concentration of a particular siRNA in relation to the total siRNA. This, in turn, reduces off-targeting. Therefore, the use of a pool of chemically synthesized siRNAs, with different sequences, plays a key role in reducing off-target effects [18].

The loading of the sense (passenger) strand to the RISC may be another source of off-target effects. Even if a siRNA sequence satisfies the conditions aforementioned, the possibility of a small percentage of sense (passenger) strand being incorporated into RISC and serving as a guide strand can change the expression of many genes. In such a case, chemical modifications of the sense strand would serve to solve this problem [13]. Longer and unmodified siRNAs are more likely to trigger off-target effects. In the cytoplasm, such effects are associated with the activation of PKR that is not sequence dependent (**Figure 2.3**). The sequence-dependent immunostimulatory effects, that is, IFN and tumor necrosis factor (TNF)-mediated innate immunity, are induced by specific siRNA motifs that activate toll-like receptors 7 and 8 (TLR7/8) [19, 20] and the retinoic acid-inducible gene I pathway [21]. The systemic therapeutic delivery of siRNA in vivo is intrinsically related to a potential recruitment by the immune cells, as both TLR7 and TLR8 are located in the endosomal compartment and can sense endocytosed single-stranded RNA (ssRNA)/dsRNA (**Figure 2.3**) [18]. Such immunostimulatory activation caused by siRNAs can be mitigated by different chemical modifications [22, 23].

Recent advancements in siRNA mediated gene therapy is focusing on the incorporation of specific nucleotide chemistries in the siRNA sequence, such as 2'-O-

methyl-modified nucleotides, in order to improve its pharmacologic and nuclease resistant properties and low immuno-stimulatory effect. **Table 2.1** shows the examples of chemically modified siRNAs and its effect on siRNA's biological activity [24]. Bifunctional siRNA approaches combining gene silencing and immunostimulation for the enhancement of antiviral and antitumoral synergy between innate immune recruitment and gene-specific targeting have recently been published [4, 24]. A recent review describes the details on recognizing and avoiding different siRNA off-target effects [25].

2.2.3 Effective siRNA delivery strategies

Once an siRNA has been successfully designed and synthesized, the next challenge is to effectively deliver siRNAs into the target cell/tissue. Synthetic siRNA are transient in nature and need to be delivered by either viral or non-viral vectors. For siRNAs to migrate and cross the physiological barriers to initiate a successful gene silencing is very crucial. The following sections describe various methods used for siRNA delivery and their advantages and disadvantages.

2.2.3.1 Viral mediated siRNA delivery

Recombinant viruses have been successfully used to transfect cells because their envelope is replaced by another virus to achieve the tropism of the desired cell target. This is done using a technique called pseudotyping, which involves deletion of disease promoting genes and incorporation of glycoproteins from another virus. This helps them to effectively transduce cells such as neurons [26]. In the case of short hairpin RNAs (shRNAs) that bear a tight hairpin turn, require the use of an expression vector for its delivery into the nucleus of the cell in order to integrate with the host genome [27]. The shRNAs are then transcribed in the nucleus by polymerase II and III, forming a pre-microRNA, which is processed by Drosha and is exported to the cytoplasm with the help of exportin 5 and follows the RNAi mechanism [27]. However, the use of an expression vector has raised safety/toxicity concerns. Studies do support the cause of cellular toxicity [28] and activation of immune response [29] against viral expression vectors, nullifying their effect as carriers.

2.2.3.2 Commercially available transfection reagents

Various commercially available delivery/transfection reagents do fulfill the need of siRNA delivery in substantially lower doses than siRNA delivered alone, but they lack to emphasize on issues such as target specificity, cytotoxicity, immunological responses, stable systemic delivery and off-target effects of these reagents. Moreover, the efficacy of most of these commercially available transfection reagents is limited to in-vitro use [30-33]. For in-vivo applications, delivery via systemic route targets multiple sites, which may not be an idea for many biomedical applications. Systemic delivery is currently a major obstacle in the development of siRNA and other nucleic acid-based therapeutics. Before siRNAs can be used therapeutically, researchers must overcome the problems of in-vivo instability [29, 34], off-targeting [35, 36] and unwanted immune system activation [20, 21].

2.2.3.3 Local delivery of siRNA

Recent studies have demonstrated rapid advancements in overcoming the efficient delivery challenges in RNAi-based therapeutics. Animal studies involve either naked or formulation-based siRNA delivery to the target tissue. The advantages of administering siRNA locally are the utilization of lower siRNA dose and reduced systemic side effects. However, this form of delivery is invasive in nature, whereas formulation based siRNA delivery involves a higher dosage but remains less invasive. The success of local and formulation-based siRNA delivery has been demonstrated to be well tolerated and efficacious in animal models of ocular neovascularization and scarring, targeting vascular endothelial growth factor (VEGF) and is now being further tested in a clinical setting as a treatment for age-related macular degeneration [37-39]. Further success with RNAi therapeutics has been shown for pulmonary diseases targeting viral genes, respiratory syncytial virus and parainfluenza virus [40, 41] and in CNS by local administration of naked siRNA via intracerebroventricular or intrathecal infusion [42, 43]. However, the formulation-based siRNA requires 10 times lesser dose with efficient silencing [44, 45]. An extensive review on siRNA based therapies, delivery strategies and clinical studies, has been published elsewhere [46-49].

2.2.3.4 Non-viral mediated siRNA delivery

Non-viral nanoparticles mediated drug delivery is an upcoming revolution in the field of nanomedicine. Some of the key properties of nanoparticles mediated drug/gene delivery are its ability to enhance drug bioavailability at the targeted site, improve controlled release of the drug, enable targeted drug delivery [50, 51], reduced toxicity [52] and stabilize of the therapeutic molecule from degradative enzymes [53]. Polymeric nanoparticles exist in the range of 1 to 1000 nm in diameter [54] and can be developed from a combination of different polymers and surfactants. Most of the commonly used nanoparticles are developed from cyclodextrin [55-57], poly-L-Lysine, polyamidoamines, dendrimers [58, 59], polyethyleneimine [60, 61], liposomes [62, 63], cationic lipids [64, 65], lipid conjugant, and stable nucleic acid lipid conjugates [66, 67]. Polymers like polylactic acid (PLA), polyglycolic acid (PGA), or a copolymer of PLA and PGA, have also been used for the delivery of proteins and genes [68, 69], vaccines [70, 71], anticancer drugs [72-74], ocular drugs [75, 76], and cytokines [77]. Other natural cationic polymers that have been used for siRNA delivery are chitosan [78, 79] and atelocollagen [80,81]. **Table 2.2** describes the current ongoing clinical trials with various RNAi-nanoparticle formulations [www.clinicaltrials.gov].

2.3 Multifunctional nanoparticles

Biomedical applications of nanotechnology have shown a clear edge over conventional methods. It promises effective treatment in a cost-effective way, wherein the diseases will be combated with maximum therapeutic effect and minimum intervention. It will lead to a decrease in both time and money, invested in developing new medicines where modeling, targeting and safety assessment of the drug require a large amount of resources. The use of particles of the scale of biomolecules enables better interaction and monitoring of the cells, intercellular interactions and intracellular pathways, thus providing with an important tool for the targeted drug delivery applications, in vivo imaging, in vitro diagnostics and regenerative medicine. **Table 2.3** lists the commercially available nanoparticles being used for various biomedical applications [82].

The benefits of a multifunctional drug/gene delivery system are numerous, and can involve, but are not limited to: 1) targeted delivery, allowing for an increased drug concentration at the desired site, reducing systemic exposure to a potentially toxic compound, 2) a constant rate of drug delivery to allow for the maintenance of a constant therapeutic dose at the site of delivery, and 3) an increase in drug stability due to protection from degradation and loss of drug [83, 84]. It also opens an opportunity for "personalized medicine" through which a therapy/medicine could be suggested according to the molecular characteristics of the patient. The current clinical trials with various kinds of nanoparticles and drug conjugants are listed in **Table 2.4** [84].

The multifunctional nanoparticle-based delivery systems have wide application and can empower a single nanoscale device to perform in-vivo imaging and therapeutic delivery simulatenoeusly. The work performed by Yang and coworkers, combined magnetic nanocrystals with therapeutic antibodies and doxorubicin for specific delivery of the therapeutic at the diagnosed cancer site [85]. Another approach followed by Farokhzad and coworkers, used aptamer tagged nanoparticles to deliver docetaxel, specifically targeting the antigen on the prostate cancer cells [86]. Apart from drugs, researchers have also delivered siRNAs using multifunctional nanoparticles. A work by Medarova and coworkers, conjugated siRNA to magnetic nanoparticles tagged with fluorescent probe Cy5.5 molecule for optical imaging. [86].

Just as cancer therapeutics the use of multifunctional nanoparticles for translocating drugs across the BBB, also appears to be a promising approach. Few nanoparticle conjugated anticancer drugs such as loperamide and doxorubicin, have been shown to cross the BBB, with efficient drug release at the targeted site [87, 88]. A recent commercialized nanoparticle formulation, Visudyne from Novartis prepared a liposomal-drug (verteporfin) conjugant for systemic delivery application, treating age-related macular degeneration [89]. Another study by Zhang and coworkers showed liposomal gene formulations, delivered systemically into rhesus monkeys. The formulation was tagged with a monoclonal antibody against human insulin receptor that facilitated the formulation to cross the blood–retinal barrier [90]. Though, antibody tagged nanoparticle

formulations provide target-specificity, their high molecular weight makes the overall size of the nanoparticles big, which can in turn, be a hindrance to achieve optimal biodistribution at the targeted site.

The main features of nanoparticles that influence their uptake, biodistribution, clearance, toxicity in-vivo is dependent on two factors, i.e. Enhanced Permeation and Retention (EPR) effect and Reticuloendothelial system (RES).

2.3.1 Enhanced Permeation and Retention (EPR) effect

The tumor microenvironment comprises of a fast-growing, hyperproliferative cancer cells having a high metabolic rate and demand for the recruitment of new vessels (neovascularization) in order to supply them with oxygen and nutrients [91]. The pathophysiologic condition of a tumor is its utilization of the glycolysis pathway to obtain additional energy, resulting in the generation of an acidic environment [92]. Tumor cells also release growth factors and enzymes such as matrix metalloproteinases, which lead to an imbalance of angiogenic regulators dilating the tumor vessels, resulting in large gap junctions, ranging from 200 to 2000 nm in size, between endothelial cells, as compared to the normal junction which are 5-10 nm in range [91]. Moreover, the higher interstitial pressure generated by a compromised lymphatic drainage and a lower intravascular pressure limit the movement of macromolecules/particulate materials out of the tumor blood vessels into the extra-vascular compartment [93]. This enhanced vascular permeability and the lack of adequate lymphatic drainage at tumor sites facilitates passive targeting using polymeric nanovectors. The phenomenon is termed the EPR [94-96] (**Figure 2.5**).

2.3.2 Reticuloendothelial system (RES)

The EPR effect is attributed to the molecular weight, surface charge and nature of the composed material (polymer). For nanoparticles to accumulate in or at the tumor site, it is essential that they circulate longer in the system. Large macromolecules are usually taken up by the mononuclear phagocyte system (MPS), also called the RES and thus nanoparticles can also be cleared by MPS from circulation [97]. The MPS includes bone

marrow progenitors, blood monocytes and tissue macrophages and also Kupffer cells of the liver and macrophages of the spleen. Thus, to avoid opsonisation by MPS cells, nanoparticles are surface grafted with hydrophilic polymers like PEG to form "stealth" nanoparticles [98]. The incorporation of PEG has shown to impart, better steric stability to nanoparticles, preventing protein adsorption and interaction with immune cells. The type of PEG used in the thesis has at least two distinct and different end, each of which can be covalently associated with either the cationic polymer or the targeting/penetrating peptide. The PEG used in this study has a molecular weight of 2000 Daltons, with a formula $H(OCH_2CH_2)nOH$, where "n" defines the number of units [99].

2.3.3 Size and surface characteristics of nanoparticles

The conjugation of drugs/genes to polymers avoids the random bioavailability of the low molecular weight drugs and enables size dependent specificity. However, the molecular weight of the nanoparticles plays an equally important role in the delivery, as a molecular weight of less than 50 kDa or of a size less than 6 nm are rapidly cleared by the kidney following systemic administration [100-103]. On the other hand, this size is crucial for non-biodegradable polymers, in order to be eliminated by the renal system, following drug delivery. Other studies have also shown that a size of around 20 nm though have rapid permeation in tumors but have poor retention at the tumor site [104] and a size above 100-120 nm was observed to have low permeation at tumor site [105].

In addition, surface charge of the nanoparticles have also shown to affect tumor accumulation, wherein, cationic nanoparticles, though have shown enhanced uptake by the tumor cells but are also susceptible to glomerular filtration and activation of immune response, as the negative charge on the glomerular capillary results in a charge selective barrier. The neutral or anionic nanoparticles have not shown to pose any such complications. The nanoparticles of around 500 nm resulting from high molecular weight polymers have shown to accumulate more in the liver and lungs [106-108].

Nanoparticles that abide the above mentioned size and surface characteristics escape the RES and are able to circulate longer in the bloodstream with a greater chance

of reaching the targeted site. Another advantage of using nanoparticles is their ability to be functionalised by cell targeting ligands that increases their affinity towards targeting the intended cell type, expressing the receptor specific for the ligand and in turn, limiting the non-specific uptake of the nanoparticles by other cells.

2.4 Specific targeting with nanoparticles

The use of targeting molecules provides multifunctionality to polymeric nanoparticles. This ensures nanoparticles entry via carrier/adsorptive/receptor mediated endocytosis **(Figure 2.6)**. The coupling between the polymer surface and the ligands for vector-mediated delivery is facilitated either via covalent coupling of active functional groups naturally present on either of the molecules or by the introduction of a chemically modified, reactive functional moiety. Thus, the introduction of ligands provides cell type selectivity to nanoparticles by facilitating receptor-mediated endocytosis. Various ligands that have been employed for targeting are small molecules [109], aptamer [110], peptides [111], proteins [112], or antibodies [55]. The incorporation of ligands facilitates the avidity of the nanoparticle with the receptors. This can specifically be used for drug conjugates that failed because of low binding affinity to the target. It has been shown in previous studies that incorporation of ligands may not specifically enhance the biodistribution of nanoparticles in the tumor; for example, polymer-based [113], lipid-based [55, 57, 114-116], and gold nanoparticle [117] systems, but can significantly enhance the ligand-density dependent, cellular internalization of nanoparticles via receptor-mediate endocytosis [117]. Thus, the nanoparticle accumulation mainly depends on the size of the nanoparticles, followed by affinity dependent uptake [116]. A study modelling study based on ligand mediated uptake revealed that ligands of either smaller or higher molecular weight than 25 KD, achieved greater uptake in the tumor tissues. As, smaller ligands achieve high receptor binding affinity due to the high surface-volume ratio and larger ligands achieve higher retention due to their size, even if the binding is low [116].

2.4.1 Cell penetrating/targeting peptides

The incorporation of ligands, such as CPPs/CTP's can greatly enhance the cellular uptake of nanoparticles. The two main features that underlie any efficient delivery parameter are the target specific internalization and/or the release from the endosome. Thus, it becomes interesting to combine the best features of the two and form a multifunctional nanoparticle. The CPPs are protein transduction domains (PTDs) that consist of positively charged amino-acid sequences, usually less than 20 amino acid sequences and mainly consisting of arginine and lysine. These arginines and lysines interact with the negatively charged head groups present on the cell membrane, such as heparin sulfate, sialic or phospholipidic acid [113, 117-119] allowing for the diffusion across the cell membrane and the delivery of the siRNA directly into the cytoplasm. The CPPs triggered delivery of therapeutic molecules is an added advantage over traditional intracellular methods of delivery such as, microinjection, electroporation, or pH-sensitive liposomes, which are invasive and damage the integrity of the cell membrane. CPPs such as penetratin and transportan have been used to conjugate siRNA and enhance cellular uptake [120]. Other cationic peptides that have been used for gene delivery are MPG (27-mer peptide) [121] and cholesteryl oligo-D-arginine (Chol-R9) [122].

For CPPs different routes of endocytosis have been proposed, such as, caveolae [123], macropinocytosis [124, 125], through a clathrin-dependent pathway [126], via a cholesterol-dependent clathrin-mediated pathway [126] or in the trans-Golgi network [126]. Also, direct translocations via lipid membrane [127] and energy independent pathways [128,129] have also been published. The CPP-mediated nanoparticle delivery was first reported using TAT peptide conjugated to iron oxide nanoparticles (40 nm) in-vivo [130]. The modification with TAT peptide resulted in approximately 100-fold higher uptake efficiency than the unmodified iron oxide particles. TAT peptide-modified nanoparticles have also been investigated for delivering diagnostic and therapeutic agents across the BBB [131].

Cell targeting peptides are specific ligands that show high specificity and affinity towards a specific receptor that is exclusively over expressed by a particular cell. RGD

peptide has been the most extensively studied cell targeting peptide towards integrin (αvβ3) receptor [132]. These cell targeting peptides hold an advantage over the use of antibodies, as the high molecular weight of antibodies limit their use as a targeting moiety on nanoparticles. Most of the CTPs are identified by phage display technology. This technique involves the combinatorial generation of short peptide sequences, which are inserted in the extracellular protein of a filamentous phage [133]. The phage amplifies once it interacts with the extracellular receptor of a specific cell type and causes infection. The transfected cell suspension then goes through a several rounds of selection with limited dilutions and a single phage type is isolated. Subsequently, the "active" combinatorial sequence is identified by sequencing, which is usually 8 to 12 amino acids in length.

This way, certain ligands are selected with a specific affinity towards a particular cell type. The ligand modified nanoparticles present an enhanced nanoparticle/therapeutic formulation, which show the promise of nanomedicine to offer a sensitive, specific and a reliable therapeutic option in the coming future. It can have a substantial impact on different medical applications ranging from pharmaceutical, medical devices, diagnostics and imaging sectors. With the advancement in knowledge and techniques a better understanding to determine the biodistribution, pharmacokinetics and toxicity of the nanoparticles would be needed. This will enable the configuration of a safe and an efficient on-target delivery system to treat cancers, immunological and neurological disorders.

The targeting/penetrating peptide (CPP/CTP) used in this thesis is 8-15 amino acids in length. This thesis includes a CTP, MGF, mechano growth factor (splice variant of insulin growth factor-1) for targeting neuronal and Purkinje cells in the brain and a CP-15 for targeting colorectal cancer cells. Alternatively or complementarily, the peptide can also possess a biological characteristic that enables it to penetrate through the cell membrane and aid in the delivery of the payload. In this thesis TAT (transcriptional activator protein encoded by human immunodeficiency virus type - 1) was used as a CPP [1].

The multifunctional nanoparticles developed were used for two applications: Neurodegenerative diseases and Cancer focussing on their current treatment modalities and their advantages and limitations. The need to address these disease applications is represented by the target population and the therapeutic market, especially focussing on Alzheimer's disease and colorectal cancer.

2.5 Neurodegenerative diseases

Central nervous system (CNS) is a highly intricate and a sensitive organization, which is vulnerable to any changes that can affect its molecular mechanism and regular functions [1]. Among the neurological disorders, neurodegenerative diseases (NDDs) encompass a separate domain, which are characterized by progressive loss of neurons. The etiology of NDDs is most often multifactorial, likely a result of gene–environmental interaction, which may lead to diseases like Parkinson's diseases (PD), Alzheimer's disease (AD), Huntington's disease (HD), Multiple Sclerosis (MS), Amyotrophic lateral sclerosis (ALS) and Spino Cerebellar Ataxia (SCA). These diseases tend to progress slowly over the time and generally target older population. According to WHO with the result of a growing and ageing population, NDDs will become world's second leading cause of death, after cardiovascular disease, overtaking cancer by 2040 [134]. The treatments available to date only mitigate the symptoms of the disease. Thus, designing an inhibitor for any neurodegenerative disease that effectively halts its pathogenicity is yet to be achieved.

The major challenge in brain drug delivery lies in crossing the blood brain barrier (BBB)/blood–cerebrospinal fluid barrier (BCB) to reach the catalytic pockets of the enzyme/protein involved in the molecular mechanism of the disease process [135]. The low/selective permeability across the BBB is due to a membranous network of brain capillary endothelial cells (BCEC) connected through tight junctions, which forms the physiological barrier of the cerebrovasculature (**figure 2.7**). Though a close-knit microenvironment of the CNS protects it from the intrusion of harmful chemical/ substances, it also poses a major obstacle to the delivery of neuroprotective drugs for the treatment of neurological disorders. It has been reported that most of the neuropeptides and hydrophilic therapeutic agents, such as antibiotics, anticancer agents cannot cross the

BBB after systemic administration [136]. Only small, lipophilic compounds with a molecular mass < 400–500 Da, are known to cross the BBB, but target only a small number of CNS diseases [137]. The large surface area of approximately $20m^2$ of the brain's cerebrovasculature promises successful drug administration *via* trans-endothelial route, only if the physiological barrier formed by the endothelia cells could be overcome.

The current clinical strategy to deliver drug/gene to the central nervous system involves surgical interventions, which can later pose post surgical complications like fluid retention in the ventricles etc., having fatal side-effects [138]. The invasive approach of delivering the drugs involves mechanically breaching the BBB and can be broadly categorized as, (a) interstitial delivery, which involves techniques like injections, catheters and pumps for delivering drugs directly into the brain interstitium [138]. (b) intracerebro-ventricular delivery, wherein the drug is delivered directly into the cerebral ventricles in order to bypass BBB. However, its limitation is that it creates an intracranial pressure, when the drug is infused into small ventricular volumes. This results in a high clinical incidence of hemorrhage, cerebrospinal fluid (CSF) leaks, neurotoxicity and CNS infections [139]. The other technique is (c) intracerebral delivery, wherein the drug is introduced directly into the brain parenchyma using intrathecal catheter, controlled release matrices [140], microencapsulated chemicals [141] or recombinant cells [142]. However the only limitation is the slow movement of drug, which decreases exponentially with distance [143]. d) The last invasive method is the convection enhanced delivery (CED), which involves insertion of a small calibre catheter, to actively pump the infusate into the brain parenchyma that penetrates into interstitial space [143].

In contrast to the invasive techniques, intravascular and intranasal delivery through olfactory pathway has shown success to be used as non-invasive therapeutic delivery techniques to the brain. Since BBB restricts the entry of hydrophilic substances due the tight endothelial junctions and allows only lipophilic drugs to pass through, substances like mannitol and arabinose that are hyperosmolar in nature have been injected in the cerebral circulation in order to shrink the endothelial cells, leading to transient opening of

tight junctions [144]. Similar results have also been obtained by using pharmacological substances that are analogs of bradykinin and nitric oxide [145, 146]. Such strategies have proved beneficial for the treatment of brain tumours [147]. Another approach to facilitate the drug uptake mechanism is to manipulate the endogenous transport system present at the surface of BBB like carrier mediated and receptor mediated transport [148, 149]. However, one limitation with this method is, even after traversing the BBB the drugs encounter basal lamina, which traps opsonised proteins and particles, thus making the BBB opening strategy less efficient [150]. The intranasal route, on the other hand is an alternative pathway to transport drugs along the olfactory sensory neurons to yield significant concentrations in the olfactory bulb and CSF. The nasal drug delivery to the CNS is thought to involve either an intraneuronal or extraneuronal pathway [151, 152]. In spite of the inherent difficulties in delivery, the direct nose-to-brain transport [153] and access to CSF of three neuropeptides bypassing the bloodstream has been shown in human trials [152]. This mode of delivery could be an effective therapeutic option of delivering proteins such as brain-delivered neurotropic factor (BDNF) to the olfactory bulb as a treatment for Alzheimer's disease [154]. Some of the limitations that have to be overcome with intranasal route of administration would be to bypass enzymatically active and low pH of nasal epithelium, the possibility of mucosal irritation or the possibility of large variability caused by nasal pathology, such as common cold. Though it is a non-invasive strategy but to achieve effective therapeutic drug concentrations is yet to be determined.

In the current thesis, the nanoparticles developed in the range of 5-10 nm were administered intranasally to target brain. Depending on the targetability of the nanoparticles to deliver the siRNA maximally in the cerebral cortex, lead to the extension of the study to target an animal model of AD. As in AD, the neurons in the cerebral cortex undergo degeneration.

2.5.1 Alzheimer's disease

Alzheimer's is the most common form of dementia, which is incurable and degenerative. It is characterized by the presence of misfolded protein in the form of senile

plaques and neurofibrillary tangles in the brain [155]. It is predicted to affect 1 in 85 people globally by 2050 [156]. The mean life expectancy of an individual is drastically reduced to 7 years after the onset of the disease. Currently, there is no cure available that can halt the progression of the disease. However, therapies and drugs are available in the markets that merely mitigate the symptoms of the disease. The currently approved treatments for AD include cholinesterase inhibitors, such as Donepezil (Aricept), Rivastigmine (Exelon), Galantamine (Razadyne). These inhibitors block the activity of cholinesterase enzyme which breaks apart acetylcholine, which is a vital neurotransmitter. The other approved treatment is Memantine (Namenda), which is a neuroprotective agent that blocks excitotoxicity [157].

The underlying pathological mechanism of AD is still unknown but the accumulation of amyloid-beta peptides is thought to be the central triggering event of the disease, which is believed to disrupt the cell's calcium ion homeostatis, leading to apoptosis [158]. The amyloid plaques in Alzheimer's disease are composed of dense, insoluble deposits of amyloid-beta peptide in and around the neuron. These peptides are the fragment of a larger transmembrane protein called amyloid precursor protein (APP) [159-161]. APP is essential for neurons growth survival and post injury repair [162, 163]. The formation of amyloid-beta peptides is initiated by a sequential cleavage of APP by an enzyme, protease beta-secretase, also known as BACE1 (beta site APP cleaving enzyme) and then by a gamma–secretase, an aspartyl protease complex, which generates toxic C-terminal fragments inside the cell and releases a fragment called amyloid-beta peptide extra cellularly [159, 164].

The identification of the biological and pathological abnormalities triggered the studies on recognizing the genes responsible for causing inherited forms of AD [158]. On such form is autosomal dominant familial AD, which is caused due to the mutations in the APP and components of gamma-secretase (Presenilins 1 and 2) [165-167] that lead to increased production of amyloid-beta 2 protein, the main component of senile plaques [168, 169]. Several transgenic animal models have been developed based on various

genetic mutations to understand the etiology and possible pathological mechanism of the disease and to investigate various therapeutic options [170-171].

Advancement in RNAi therapy has facilitated the understanding of pathobiological mechanisms of the disease with most of the researches focusing on phenotype rescue due to dominantly acting mutant genes and loss-of function analysis [172, 173]. Based on the etiology of the AD, the key targets for RNAi therapy are assumed to be APP, BACE [174] and gamma-secretase [175, 176] and tau, which can eliminate the production of toxic C-terminal fragments and amyloid-beta peptides. siRNAs has been delivered to the central nervous system both naked or with the help of some transfection reagents in-vivo, targeting different molecular targets in different parts of the nervous system, showing effective gene silencing. In the current thesis, we have targeted PSN1 gene in an animal model of AD, with a siRNA targeted delivered through multifunctional nanoparticles, administered intranasally, as described in chapter 6 of the thesis.

2.6 Cancer

Another application where specific drug-delivery and/or upregulated cellular uptake of therapeutics is important is in cancer. Cancer is characterized as a disorder which arises following a number of mutagenesis steps, allowing cancerous cells to grow and divide uncontrollably. These processes allow cancer cells to acquire properties of unlimited proliferation potential, self-sufficiency in growth signals and resistance to both anti-proliferative and apoptotic cues which would, otherwise, contain their growth [177]. Tumors have also evolved methods to gain further support through interactions with surrounding stromal cells, promoting their angiogenesis, their evasion of immune detection and their metastasis to distal organs [178]. As recently published in Nature communications (Oct 2012 issue), wherein scientists have reported a clue on cancer metastasis. According to their discovery, the cancer spreads to other parts of the body due to the change in its adhesion properties, which are guided by the molecular interactions between cell and the extracellular matrix [179], specifically the interaction of integrin on the cell's surface with fibronectin and galectin-3 proteins in the extra cellular matrix. The

researchers are now focussing on mechanisms to block this interaction that causes metastasis [179].

The primary factor for the cause of 90-95% of cancer cases is reported from environmental factors such as, tobacco, obesity, diet, radiation, stress, infections, lack of physical activity and environmental pollutants and only 5-10% are of genetic origin [180]. The five most prevalent types of cancer are Lung, stomach, colorectal, liver and breast. It can be said that, as of yet, for a number of reasons, an adequate therapy for cancer has not been developed. Some of these reasons include: late stage diagnosis, inadequate methods for controlling aggressive metastasis, and a lack of methods to overcome multi-drug resistant (MDR) cancer [181].

Current cancer therapies can be broadly categorized into two groups: cytotoxic therapies and molecular targeted drugs [182]. Examples of traditional cytotoxic therapies include radiation and chemotherapeutic compounds such as platinum-based drugs [182, 183]. Radiation, utilizing photons, damages the deoxyribonucleic acid (DNA) of cancer cells by creating free radicals, leading to the inhibition of cell division and, eventually, causing cell death. Cancer cells are most abundantly found in the mitotic phase, in a state of continuous DNA replication, allowing radiation to be more toxic to tumor cells than normal cells, providing a therapeutic window [184]. The current medical anticancer treatments involve applications where therapies are provided by removing the diseased cells (surgery), burning them out (radiation therapy), or poisoning the diseased cells faster than the healthy cells (chemotherapy) with drugs such as 5-Fluorouracil, oxaliplatin and Leucovorin [185], all of which do cause damage to healthy cells [186, 187]. Thus, most of these treatment modalities also show a level of toxicity to noncancerous cells since these are still proliferating, albeit at a slower rate than cancerous cells. Moreover many these treatments also give rise to serious side effects such as nausea, hair loss, neuropathies, neutropenia and kidney failure [83].

The effectiveness of any therapeutic drug is dependent on the early screening and diagnosis of cancer. The treatment of cancer at a benign stage is mostly successful than

treating at a metastatic stage. Chemotherapies employed on treating a metastatic cancer leads to un-intended toxicity and side-effects to tissues that are non-cancerous. Thus, at a later stage the therapy itself becomes the cause of mortality. For these reasons, an effective mode of therapeutic intervention is needed that can enhance the efficacy of drugs targeted at the tumor site, barring the normal tissues. Moreover, an enhanced therapeutic molecule, which may limit the toxicity of drugs even if delivered at an un-intended site, would be of advantage.

In this thesis, we have focussed on the colorectal cancer, which is the fourth most common type of cancer in US and is more common in people of over 50 years of age. It affects the large intestine and the rectum. It begins as benign polyps that grow from the mucosal layer of the lumen [188]. These polyps are termed hyperplastic polyps and usually have very low chances of becoming a cancer. The other type of polyps is adenomatous and hamartomatous polyps, these types of polyps usually develop in cancer and are associated with heredity. The adenomatous polyps grow into a small-mushroom like shape over the period of time and invade the successive layers of the lumen [188]. The malignant adenomas are called adenocarcinomas, which when metastasize, spread the cancer to other organs. The genetic pathway to the development of colorectal cancer depicts point mutations in the tumor-suppressor genes such as, APC, P53 and in a proto-oncogene K-ras [189].

In this thesis, we utilized siRNA mediated delivery and gene silencing by the multifunctional nanoparticles, wherein the siRNA was targeted against another type of proto-oncogene, serine/threonine-protein kinase (PLK1). PLK 1 plays a significant role in the cell cycle regulation, especially in the functional maturation of the centrosome and in the establishment of the bipolar spindle. PLK1 is over-expressed in a variety of human cancers [190, 191] and is directly associated with p53, a tumor suppressor gene. PLK1 on interaction with p53, inhibits its transactivation and pro-apoptotic activity [192], leading to uncontrolled cell proliferation. Studies have shown that PLK1 inhibition can induce pro-apoptotic pathway and inhibit growth of cancerous tissues. In this thesis, as described in chapter 7, we have focused on delivering siRNA against PLK1 gene,

delivered by multifunctional nanoparticles, administered intra-peritoneally. The nanoparticles developed were from HMW chitosan, instead of the LMW chitosan used for NDD study. The choice of HMW chitosan was to obtain nanoparticles in the range of 100-120 nm as compared to 10-20 nm in the case of NDD study. This was essential, to avoid glomerular filtration of small nanoparticles in circulation.

2.7 Conclusions

Nanotechnology is a vast, fast-developing field whose potential is attracting a great deal of interest from scientists, technologists, many industries, investors and governments. Having seen major applications of nanomedicine it is evident that nanomedicine clearly scores over the conventional healthcare practices. Nanomedicine offers effective treatment in a cost-effective way, as dose will be reduced and medical treatments will be less wasteful. Diseases will be combated more efficiently, as maximum effect can be extracted with minimum intervention. Use of particles of the scale of biomolecules will lead to better interaction with and monitoring of cells, intercellular interactions, intracellular pathways and the molecules that control these cells, thus, providing us with an important tool for targeted drug delivery, in-vivo imaging, in-vitro diagnostics and regenerative medicine. Apart from this, nanomedicine will lead to decrease in the time and money put into developing new medicines where modeling, targeting and safety assessment of the drug require large amount of resources. Also, due to combination of targeted imaging, RNAi technology and therapy, 'personalized medicine' would be possible. This would lead to early diagnosis of treatment’s efficacy on an individual and the medicine would be given according to the molecular characteristics of the patient. Further, careful implementation of this technology would be needed to avoid having unprecedented environmental, socio-economic and toxic effects.

Building on the current literature, the present thesis research attempts to fuse the most desired characteristics of nanomedicine into one nanoparticle for therapeutic delivery applications, enabling the therapeutics, such as siRNA to reach the targeted site. This thesis presents the design, synthesis and development of a multifunctional nanoparticle with its delivery efficacy tested in both in-vitro and in-vivo models.

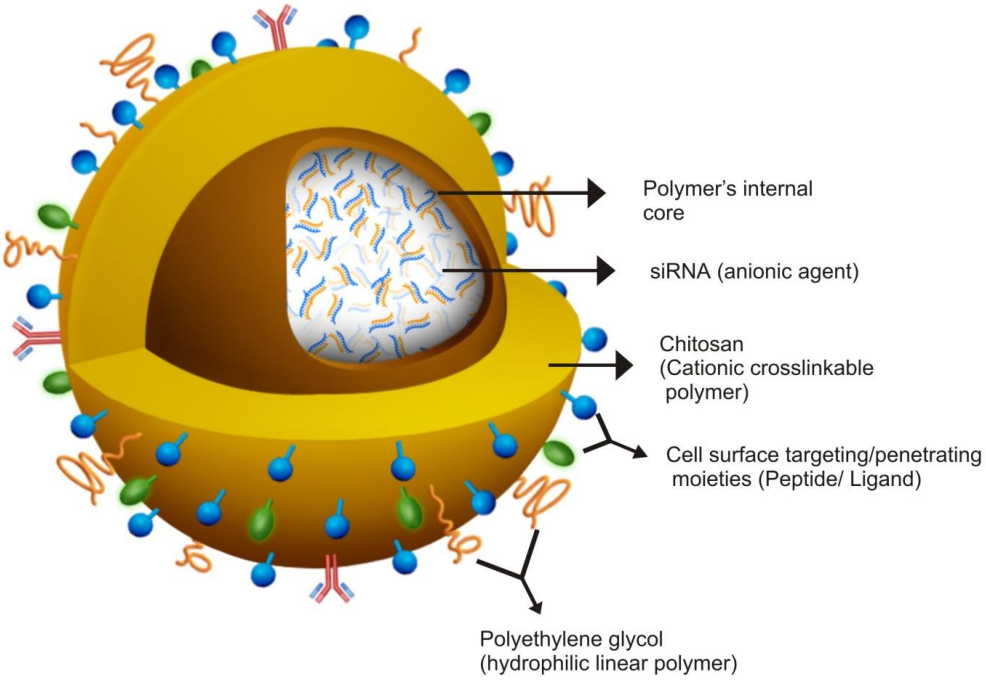

Figure 2.1: A multifunctional nanoparticle formulation, comprising of an anionic agent as a therapeutic payload, a cationic crosslinkable polymer, an internal core, a hydrophilic linear polymer and cell targeting/penetrating moieties.

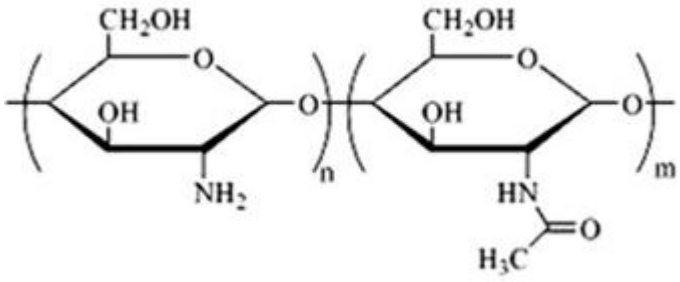

Figure 2.2: Chemical structure of Chitosan polymer, which is mainly composed of β-1,4-linked D-glucosamine units with a variable content of N-acetyl-D-glucosamine units.

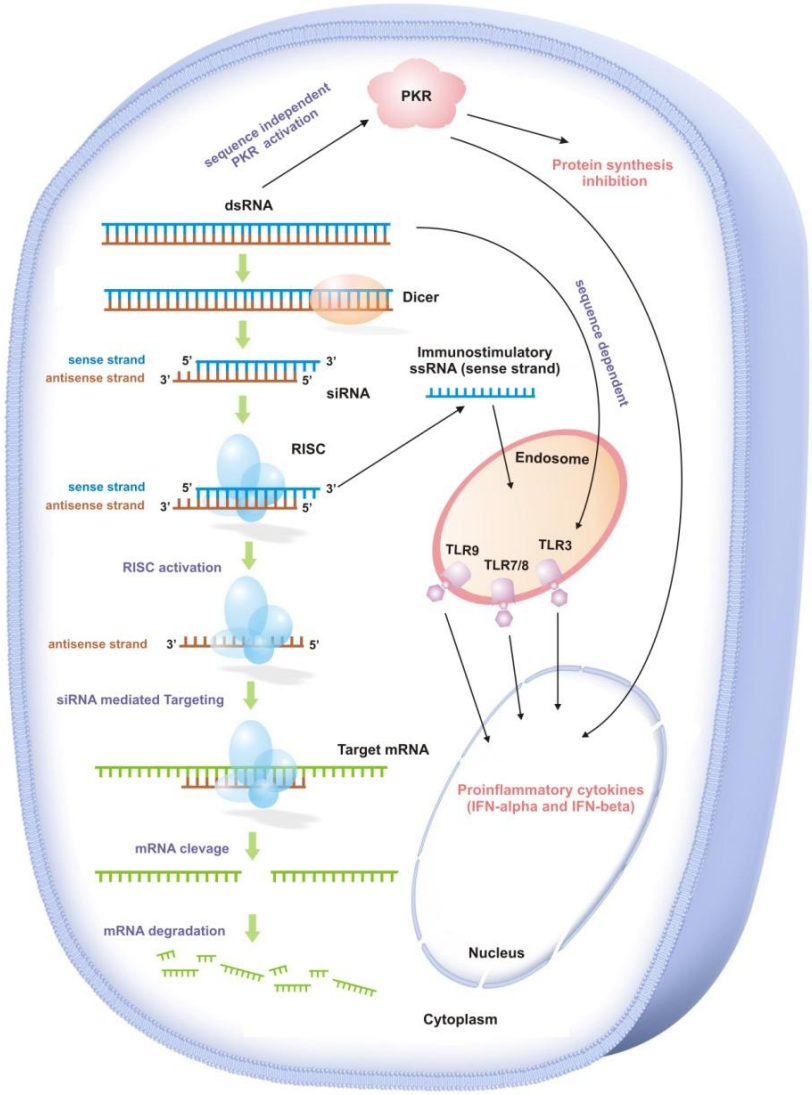

Figure 2.3: siRNA-mediated gene silencing and off-target effects. Long dsRNA entering into the cell is processed into siRNAs by Dicer. These siRNAs assemble into RISCs that unwind the sense strand. The antisense strand along with the RISC is guided to the complimentary mRNA strand. After the complimentary binding, RISC cleaves the target mRNA that is further degraded by cellular nucleases. dsRNA activates the dsRNA-dependent Protein Kinase RNA-activated (PKR) leading to a global inhibition of protein synthesis. Toll-like receptors present in the endosome recognize double-stranded and single-stranded siRNAs in a sequence-dependent manner and induce pro-inflammatory cytokines [4]

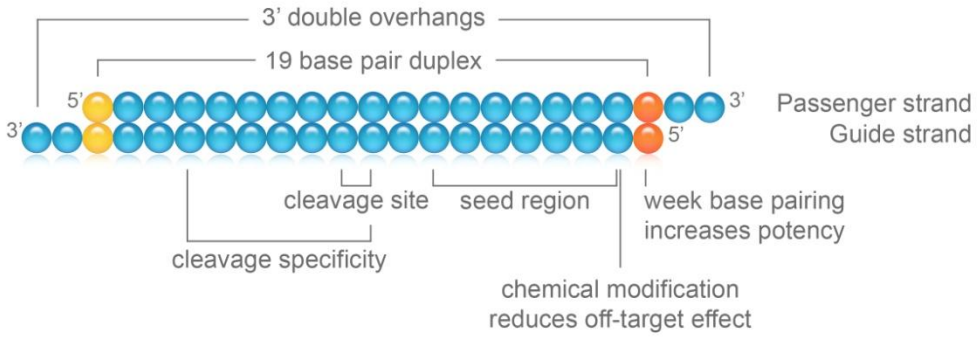

Figure 2.4: Schematic representation of an siRNA duplex. siRNAs have a well-defined structure, usually 21-nucleotide-long followed by two nucleotide 3' overhangs. Each strand has a 5' phosphate group and a 3' hydroxyl group. This structure is the result of processing by Dicer, an enzyme that converts either long dsRNAs or hairpin RNAs into siRNAs. Important sequence specific features like seed region, cleavage specificity region, mRNA cleavage site and key sites for chemical modifications and potency enhancement are shown [4]

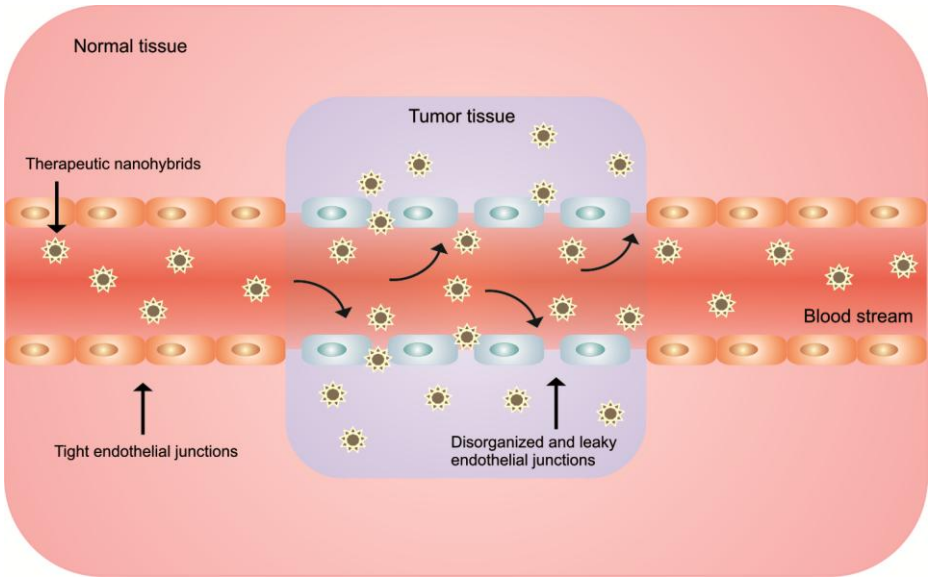

Figure 2.5: Schematic of tumor targeting by nanohybrids via Enhanced Permeation and Retention (EPR) effect [1]

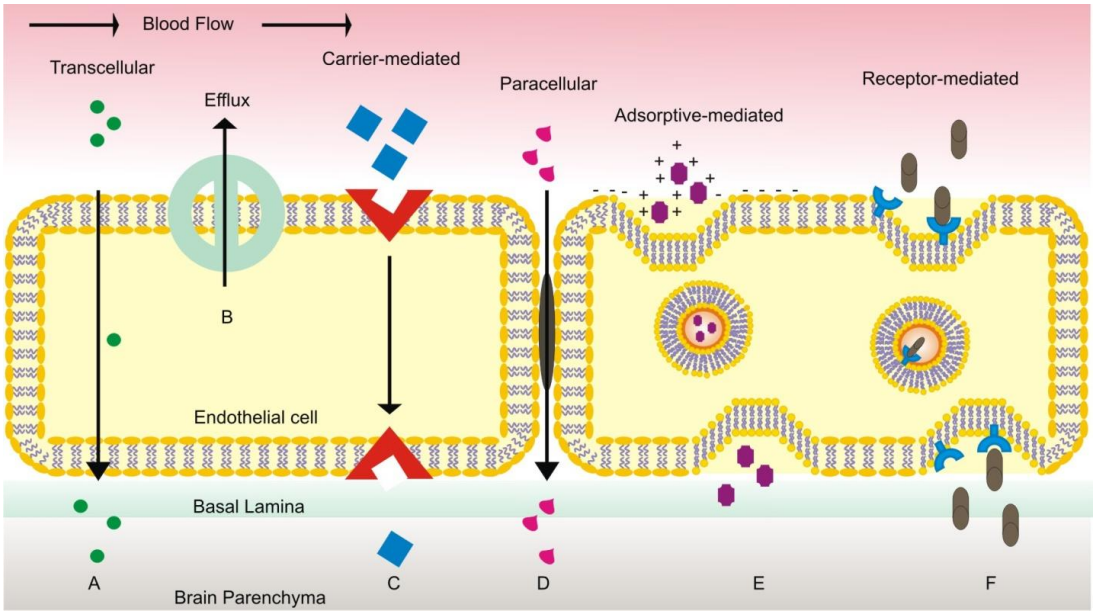

Figure 2.6: Schematic of potential transportation routes of therapeutic molecules and nanoparticles across the Blood-brain barrier. (A) Transcellular route for transport of lipid soluble substances like glucose, O_2, CO_2, etc. (B) Efflux transporters, that flush out some of the passively diffused lipophilic molecules; (C) Carrier mediated transport of molecules like glucose, amino acids, small peptides, nucleosides, monocarboxylates etc.; (D) Paracelluar transport for small amount of water soluble substances; (E) Adsorptive mediated transport for positively charged molecules; (F) Receptor-mediated transport for essential proteins like insulin, transferrin and cytokines [1]

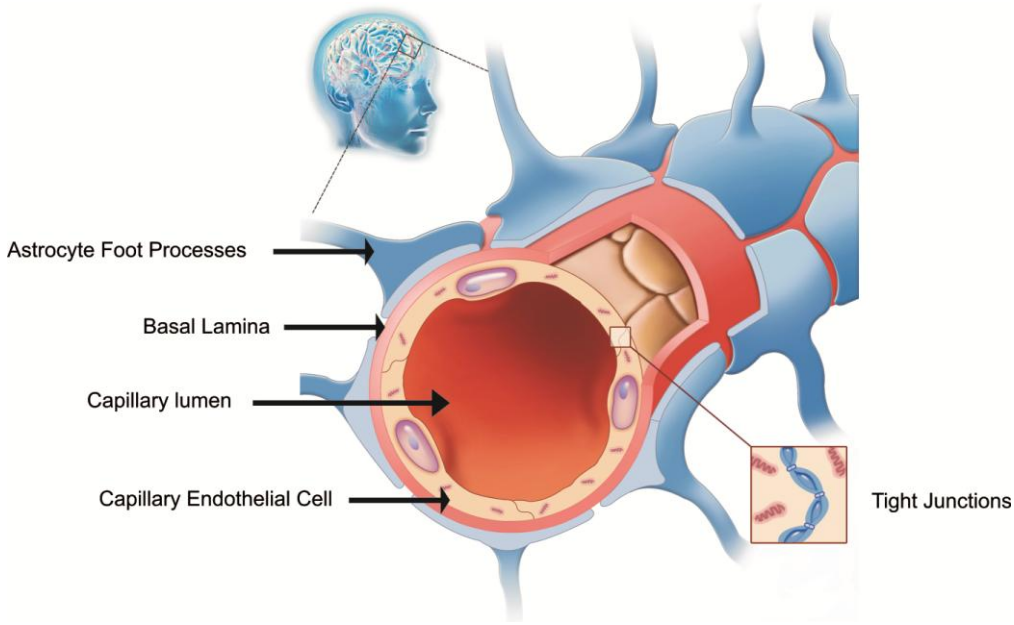

Figure 2.7: Schematic of physiological barrier (blood-brain barrier) involved in delivery of therapeutic molecules [1]

Table 2.1: Effect of few chemical modification and bioconjugation on siRNA. RNAi function (when compare with the gene silencing effect of unmodified siRNA): not affected - >50% gene silencing; moderately affected - 20-50% gene silencing; severely affected - <20% gene silencing. The increase in RNAi activity is not because of the direct influence of chemical modification on silencing activity of the guide strand. The enhanced potency of siRNA due to chemical modifications like nuclease stability, off-target reduction and specificity, results optimal guide strand entry into RISC and facilitate multiple turnover [4].

Passenger Strand	**Guide Strand**	**RNAi Function**	**siRNA character**
2'-OMe, 2'-F and related substitutions	Unmodified	Increased	Endonuclease resistance, Reduced off-target
Unmodified	2'-OMe at position 2	Not affected	Off target reduction
2'-O-MOE	Unmodified	Not affected	Endonuclease resistance
Unmodified	2'-O-MOE	Moderate to severe based on position	Endonuclease resistance
2'-OMe and 2'-O-MOE	Unmodified	Not affected	Endonuclease resistance, Reduced off-target
Phosphorothioate backbone	Unmodified	Not affected	Exonuclease resistance
Unmodified	Phosphorothioate backbone	Moderately affected	Exonuclease resistance
Phosphorothioate backbone	Phosphorothioate backbone	Moderately affected	Exonuclease resistance
3' end modification by 2'-OMe and phosphorothioate substitutions	Unmodified	Increased	Higher nuclease stability
Unmodified	Blocking of the 5-hydroxyl terminus	Severely affected	No significance
Blocking of the 3' terminus	Unmodified	Not affected	No significance
Bioconjugation with cholesterol or carrier molecule	Unmodified	Not affected	Increased cellular uptake, biodistribution and site specificity

Table 2.2: Current clinical trials for RNAi-based therapeutics involving a delivery vehicle [www.clinicaltrials.gov]

Company	**Drug**	**Delivery agent**	**Target**	**Disease**	**Route**	**Phase**
Alnylam	ALN-VSP02	SNALP lipid nanoparticles	KSP/ VEGF	Liver cancer	Systemic	I
Calando	CALAA-01	Cyclodextrin Nanoparticle	RRM2	Solid tumors	Systemic	I
Santaris/ Enzon	EZN-2968	LNA oligonucleotide	HIF-1α survivin	Solid tumors/ lymphoma	Systemic	I
Silence	Atu027	Liposome	PKN3	Solid tumors	Systemic	I
M.D. Anderson	siRNA-EphA2-DOPC	Liposome	EphA2	Advanced cancers	Systemic	I
Silenseed Ltd	siG12D LODER	LODER (polymer matrix)	KRASG 12D	Pancreatic cancer	local	I
Silenseed Ltd	siG12DLODER + Gemcitabine or FOLFIRINOX	LODER (polymer matrix)	KRAS G12D	Advanced Pancreatic cancer	local	II
Tekmira	TKM-PLK1	SNALP lipid nanoparticles	PLK1	Solid tumors	Systemic	I
Alnylam	ALN-TTR02	SNALP lipid nanoparticles	TTR	transthyretin-mediated amyloidosis	Systemic	I

Table 2.3: Commercial use of nanoparticle formulations for various biomedical applications [82]

Company	Application	Nanoparticle	Therapeutic use
Liplasome Pharma, Schering – Plough Corp	Drug delivery	Liposomes	Cancer
Berna Biotech AG	Drug delivery	Liposomes	Vaccines: Influenza and Hepatitis A
Enzon, Gilead Science	Drug delivery	Liposomes	Fungal infection
Starpharma	Therapeutics	Dendrimers	HIV, Cancer, Ophthalmology, Inflammation
Nanomix	In-vitro diagnostics	Carbon nanotubes	Respiratory function monitoring
Carbon nanoprobes Inc	Imaging	Carbon nanotubes	Atomic force microscopy probe tip
Evident technologies, Quantom dot Corp, Nanoco technologies Ltd.	In-vitro diagnostics, Imaging	Quantom dots	Labeling reagents: Western blotting, flow cytometry, biodetection
Immunicon	In-vitro diagnostics	Magnetic nanoparticles	Cancer
Advanced Magnetics	Imaging, therapeutics	Magnetic nanoparticles	Liver tumors, cardiovascular disease, anemia
Nanospectra Biosciences Inc	Therapeutics	Magnetic nanoparticles	Cancer
Amersham/GE	In-vitro diagnostics	Gold nanoparticles	HIV
Nanoprobes	In-vitro diagnostics, Imaging	Gold nanoparticles	Labeling reagents (PCR, RNA, Western blotting), angiography and kidney

Table 2.4: Selected list of polymer-drug conjugate/encapsulated compounds and their clinical status [84]

Polymer	**Drug**	**Clinical Name**	**Clinical Status**
Albumin	Paclitaxel	Abraxane®	Market
Carbon nanotube	Methotrexate	N/A	Preclinical
N-(2-hydroxypropyl) methacrylamide (HPMA) copolymer	Doxorubicin	PK1, FCE28068	Phase II
N-(2-hydroxypropyl) methacrylamide (HPMA) copolymer	Gly-Gly-en-Pt	AP5280	Phase II
N-(2-hydroxypropyl) methacrylamide (HPMA) copolymer	Gly-Phe-Leu-Gly-en-Pt (terminating with 1,2-diaminocyclohexyl palatinate)	AP5346, ProLindac™	Phase II
N-(2-hydroxypropyl) methacrylamide (HPMA) and Galactosamine copolymer	Doxorubicin	PK2, FCE28069	Phase II
PEO-P(Asp)-and Poly(ethylene glycol)	Doxorubicin	NK911	Phase II
Poly(ethylene glycol) and poly(D,L lactide) copolymer	Paclitaxel	Genoxol-PM	Phase II
Poly-L-glutamic acid (PGA)	Camptothecin	CT-2106	Phase I
Poly-L-glutamic acid (PGA)	Paclitaxel	CT-2103, Xyotax™, OPAXIO™	Phase II

Presented in the following five chapters are the studies performed in order to investigate the stated research hypothesis and to achieve the stated research objectives. Each chapter discusses various important aspects of the thesis research project.

Chapter 3: Chitosan, a biodegradable and a biocompatible polymer was chosen to form nanoparticles encapsulating siRNA. The goal of the study was to achieve smallest possible particle size in order to be used for targeting neurodegenerative diseases, by crossing the blood-brain barrier. Specifically this chapter investigates the preparation and characterization of chitosan nanoparticles, complexing siRNA. The study involves optimization of pH, concentration and N:P ratio of chitosan:siRNA to have maximum siRNA loading into the nanoparticles with nanoparticles of <50 nm in size.

Chapter 4: The nanoparticles as prepared in the previous chapter were tested for their transfection and cytotoxicity on Neuro2a cells. Though efficient transfection was achieved, however, the nanoparticles were cytotoxic. Towards this goal, this chapter demonstrates a novel synthesis scheme that was incorporated to reduce the toxicity of the nanoparticles. For which, the chitosan polymer was surface graft with a hydrophilic polymer, polyethylene glycol (PEG). The synthesized polymer was characterized by FTIR and nanoparticles were formed as previously described in chapter 3. The nanoparticles were tested for siRNA loading efficiency, transfection efficiency and cytotoxicity.

Chapter 5: The PEGylated nanoparticles formed though were efficient for transfection and had reduced toxicity but were not suitable for specific targeting to be used in-vivo. Towards this goal, this chapter describes another novel synthesis scheme, wherein the chitosan polymer was surface grafted with PEG and was further tagged with a cell penetrating peptide, TAT, which was used as a model peptide, to form multifunctional nanoparticles. The synthesis was successfully performed and characterized by FTIR and NMR and nanoparticles were formed as described in chapter 3. These nanoparticles were then tested for transfection, cytotoxicity and their ability to deliver a functional siRNA in Neuro2a cells.

Chapter 6: As surface functionalized, peptide tagged PEGylated chitosan nanoparticles were prepared in the previous chapter. The similar synthesis scheme was utilized to form nanoparticles tagged with a cell penetrating peptide, TAT and a cell targeting peptide, MGF. The nanoparticles were prepared to deliver siRNA to the brain, when administered intranasally. The purpose of the study was to enable the therapeutic delivery non-invasively with high efficiency. Towards this goal, this chapter demonstrates a pilot study, wherein the siRNA delivery, to the brain, through the nanoparticles was investigated in an experimental animal model C57BL/6J. The analysis was performed based on safety, biodistribution and toxicity of the nanoparticles in the organ tissues. This study was further extended to an animal model of Alzheimer's disease as most of the nanoparticles were observed to target the cerebral cortex of the brain, which is the most affected area of degeneration in Alzheimer's disease. This extended study illustrates delivery of a functional siRNA targeting Presenilin 1 (PSN1) gene by nanoparticles, via intranasal route to an animal model of Alzheimer's disease.

Chapter 7: This study was performed to explore the multifunctionality of the nanoparticles prepared through a synthetic scheme, as described in chapter 5. The synthetic scheme developed enables to tag any peptide on the nanoparticles, which is specific to target a particular cell surface receptor. Towards this goal, we utilized CP15 peptide on PEGylated chitosan nanoparticles to target colorectal cancer tissue in-vivo. The siRNA used in this study was targeted against a pro-oncogene polo-like kinase 1 (PLK1), which is highly expressed in most of the tumor tissue types. The study analyzed the relative gene expression (mRNA) and protein suppression by the siRNA delivered by nanoparticles in comparison to other treatment groups and the control group. The biodistribution, tumor accumulation, serum safety analysis was also performed.

Chapter 8 summarizes the findings of the thesis work.

Chapter 9 details claims of original contributions to knowledge and conclusions.

Chapter 10 includes the recommendations for future research.

During this thesis research period, I contributed to 29 original research articles/reviews/book chapter, of which 24 are currently published or in press, 25 first author and 24 collaborative research abstracts or proceedings and a US provisional patent. In this thesis, I have elected to use 5 articles, of which I am the first author.

CONTRIBUTION OF AUTHORS

As first author of the original research articles included in this thesis, I was responsible for the planning and execution of each study, including a review of the literature, specific research objectives and methodology to be implemented. Furthermore, I deigned and conducted the experiments, analyzed and discussed the data accumulated from in-vitro and in-vivo studies and prepared manuscripts. For all research articles, Dr. Satya Prakash, as research advisor, was the corresponding author. Specific co-author contributions per chapter are listed below.

Chapter 3: Arun Kulamarva helped with cell culture experiments and in writing of the manuscript. Safaa Sebak helped with collection of particle sizing and zeta potential measurements. Arghya Paul, Jasmine Bhathena and Maryam Mirzaei helped with in-vitro lab techniques and trouble shooting at various stages of the experiment. All other authors discussed the results and commented on the manuscript.

Chapter 4: Ciaran lane jointly helped to design the setup of the chemical reactions and also helped with the data analysis. Catherine-Tomaro Duchesneau helped with statistics and along with Shyamali Saha, who helped with in-vitro studies on cell culture and manuscript proof-reading.

Chapter 5: Catherine Tomaro-Duchesneau helped with statistics, in-vitro cell study and proof-read the manuscript.

Chapter 6: Catherine-Tomaro Duchesneau and Shyamali Saha helped with performing intranasal injections in the preliminary animal study. Catherine helped with statistics and data analysis. All the authors contributed in discussion of the results and proof reading of the manuscript.

Chapter 7: Catherine–Tomaro Duchesneau contributed with design of the study, PCR, statistics and data analysis. Shyamali Saha contributed in the data analysis. All the authors contributed with discussion of results and proof read the article.

Original article 1

CHAPTER 3: ULTRA-SMALL NANOPARTICLES OF LOW MOLECULAR WEIGHT CHITOSAN AS AN EFFICIENT DELIVERY SYSTEM TARGETING NEURONAL CELLS

Meenakshi Malhotra, Arun Kulamarva, Safaa Sebak, Arghya Paul, Jasmine Bhathena, Maryam Mirzaei and Satya Prakash*

Biomedical Technology and Cell Therapy Research Laboratory
Department of Biomedical Engineering, Artificial Cells and Organs Research Center
Faculty of Medicine, McGill University
3775 University Street, Montreal, Quebec, H3A2B4, Canada

*Corresponding author: Tel: 514-398-2736; Fax: 514-398-7461,
Email: satya.prakash@mcgill.ca

Preface: Chitosan, a biodegradable and a biocompatible polymer was chosen to form nanoparticles encapsulating siRNA. The goal of the study was to achieve smallest possible particle size in order to be used for targeting neurodegenerative diseases, by crossing the blood-brain barrier. Specifically this chapter investigates the preparation and characterization of chitosan nanoparticles, complexing siRNA. The study involves optimization of pH, concentration and N:P ratio of chitosan:siRNA to have maximum siRNA loading into the nanoparticles with nanoparticles of <50 nm in size.

Article published in ***Drug development and Industrial Pharmacy.*** **2009; 35(6):719-726**
http://informahealthcare.com/doi/abs/10.1080/03639040802526789

3.1 Abstract: Cell transfection with nanoscale cationic polymeric particles using chitosan has been extensively explored. Because of its properties such as cationic charges, biocompatibility, biodegradability, and low toxicity, it has been used as a potential gene, siRNA, protein (including antibodies), and drug carrier system. This work describes the development of chitosan nanoparticles of <50 nm in diameter for a potential siRNA delivery application. The particles were prepared using an ionic gelation method, using sodium tripolyphosphate as a cross-linker. The effect of variation in pH was investigated on particle size and surface charge. Gene loading efficiency by chitosan nanoparticles was performed by varying weight ratios of chitosan:siRNA. Transfection efficiency was evaluated on Neuro2a cells. Conclusion: These particles have potential in the delivery of siRNA to neural tissues.

Key words: Delivery, neuronal cells, siRNA, transfection, ultra-small nanoparticles

3.2 Introduction:

The efficacy of many therapeutic molecules is often limited due to the potential physiological and anatomical barriers in reaching the target site of therapeutic action. Crossing the BBB is a major challenge in delivering drugs for the treatment of NDDs [193]. Hence, developing a delivery system that optimizes the pharmaceutical action of the drug, reduces the toxicity in-vivo, overcomes the barriers, and delivers the drug at the targeted site is an exigent task [194]. Several methods have been developed in the last decade to enhance the target- specific delivery of therapeutic molecules. The use of viral vectors has been extensively employed in this approach but is limited because of their oncogenic effects and nonspecific immunological reactions [195, 196]. This article focuses on development of non-viral, ultrafine nanoparticles made of chitosan as a delivery system to pass through the BBB and deliver siRNA into neural cells for therapeutic purposes.

Chitosan and its derivatives have shown great potential in the areas of biotechnology, biomedicine, food ingredients, and cosmetics. Chitosan is a natural biocompatible polymer obtained from chitin by exhaustive deacetylation under high temperature and alkaline conditions. It has a unique chemical structure as a linear polyelectrolyte with a high charge density as well as reactive hydroxyl (OH) and amino groups (NH_2). This renders chitosan as an ideal delivery candidate for the delivery of oligonucleotides [197, 198]. Chitosan has been extensively studied because of its ideal properties including bioadhesiveness [199], biocompatibility [200], bioactivity, and biodegradability [201].

Furthermore, chitosan can be easily engineered to develop micro- and nanoparticles which can be subsequently targeted to the type of targeted tissue. At the same time the drug dose, stability, circulation time, and the in-vivo environment of the cell can be optimized. Because of its cationic charges, biocompatibility, and low toxicity [202], chitosan has been used as a vehicle system for genes, protein (including antibodies), and drugs [203–205]. The size, shape, and surface charge of chitosan- based micro- or nanoparticles are influenced by the DDA, molecular weight, and pH of the

chitosan solution [206–208]. The entrapment efficiency depends on the pKa, solubility of the molecule to be incorporated, the strength of electrostatic interactions, hydrogen bonds, and hydrophobic interactions between the molecule and chitosan [209]. Chitosan/DNA complexes especially from derivatized-chitosan have been reported to effectively transfect various cell types like THP-1 [210], HEK 293, CHO K1 [211], HeLa [212, 213], Caco-2, Cos-1 [204], HepG2 [214], and NIH 3T3 [78].

The mechanism of cellular uptake is facilitated by the presence of positively charged free amino groups ($-NH_2$) in chitosan, which become protonated on encountering an acidic pH in the endosome and form cationic amine groups ($-NH_3^+$), thereby leading to endosomal disruption [215, 216]. Various preparation techniques can be used to prepare chitosan nanocarriers by altering parameters such as concentration of the chitosan or the crosslinker, the molecular weight of chitosan ratio of drug:polymer, pH, and finally stabilizers or surfactants. All these factors collectively affect the structural and morphological properties of chitosan nanoparticles and the release rate of the loaded therapeutic molecule [217]. This article describes a method for the production of ultrafine nanoparticles and investigates the impact of various formulation and preparation parameters. The targeted delivery of siRNA using chitosan nanoparticles to the neural cells in vitro has been evaluated.

3.3. Materials and Methods

3.3.1 Materials

Low-molecular weight (LMW), medium-molecular weight (MMW), and high-molecular weight (HMW) chitosan were obtained from Wako (Richmond, VA, USA), each having a viscosity of 5–20 cP and degree of deacetylation of 80.0%. TPP and glacial acetic acid were obtained from Sigma (Oakville, ON, Canada). For dilution purposes ultrapure double-distilled water (ddH_2O) was used from laboratory - installed Barnstead Nanopure diamondTM water supply unit. siGLO (Green) transfection indicator (20 nm) was obtained from Dharmacon (Lafayette, IN, USA). Agarose (low gelling temperature) for gel electrophoresis was obtained from Sigma. Ethidium bromide (10 mg/mL) for band

visualization on electrophoretic gels was obtained from Sigma. Orange dye solution (6X) was obtained from Fermentas (Burlington, ON, Canada) and TrackIt 10-bp DNA ladder (0.5 μg/μL) was obtained from Invitrogen (Burlington, ON, Canada). Eagle's minimum essential medium (EMEM) was obtained from ATCC and supplemented with 10% fetal bovine serum (FBS).

3.3.2 Preparation of chitosan nanoparticles

Chitosan nanoparticles were prepared by an ionic gelation procedure as explained in previous studies [218]. Briefly, chitosan of different molecular weight were dissolved in 1% acetic acid solution to yield a concentration of 0.5 mg/mL at pH 5. TPP was dissolved in ddH_2O to obtain a concentration of 0.7 mg/mL and the pH was adjusted to 3 and 9. Nanoparticles were formed after addition of TPP (dropwise) to chitosan solution under constant magnetic stirring for an hour at room temperature. Different weight ratios of chitosan-TPP starting from 3:1 to 7:1 were used in a systemic study to yield the minimum possible size of nanoparticles (<100 nm).

3.3.3 Preparation of siGLO-entrapped chitosan nanoparticles

For siGLO to be entrapped into the chitosan nanoparticles, siGLO (266 μg/mL) was mixed with TPP, before adding it dropwise to the chitosan solution. The complete solution was kept under magnetic stirring for an hour at room temperature. The siGLO was mixed at varying weight ratios (50:1 to 250:1) with chitosan polymer to achieve maximum gene loading, forming nanoparticles. N:P ratio was calculated from weight ratios, using 325 Da for mass per phosphorous of siGLO and 168 for mass per charge of chitosan polymer.

3.3.4 Characterization of chitosan-TPP nanoparticles or chitosan-TPP/siGLO nanoparticles

Nanoparticles were characterized for mean particle diameter and size distribution using Brookhaven BI-90 Particle Nanosizer. Nanoparticle surface charge (zeta potential) was determined using Malvern Zeta sizer at 25°C.

3.3.5 Morphology

The nanoparticles were observed under high-resolution transmission electron microscope (TEM) (JEOL JEM 2000FX Electron Microscope). A drop of the sample containing the nanoparticles was placed on a carbon film-based copper mesh grid and allowed to air dry before observation.

3.3.6 siGLO-loading efficiency

The loading efficiency of siGLO to chitosan polymer was determined by gel electrophoresis with 48 μL of the sample on a 4% (w/v) agarose gel. Samples with chitosan- TPP:siGLO at a weight ratio of 50:1, 100:1, 150:1, 200:1, and 250:1, along with 1:6 dilution of the 6× orange dye was loaded onto the gel and was run for 4 hours at 55 V in Tris–borate EDTA (TBE) buffer (pH 8.3). The TBE buffer contained ethidium bromide at a concentration of 0.5 μg/mL, which is required for the visualization of RNA bands under UV transillumination at 365 nm.

3.3.7 Transfection efficiency

Transfection studies were performed on mouse neuroblastoma cells (Neuro2a). The cells after reaching a confluency of approximately 85% were sub-cultured and seeded in a 96-well plate at a density of 20,000 cells per well with 200 μL of complete growth media (antibiotics free EMEM with 10% serum). After 24 hours, transfection media containing 100 μL of serum-free medium along with 50 μL of sample was added onto the cells. The tested samples were; 50 μL of sample containing chitosan-TPP nanoparticles as positive control, free siGLO as negative control, and chitosan-TPP/siGLO nanoparticles at ascending weight ratios of 100:1, 150:1, 200:1, and 250:1 as treatment samples. The cells were then incubated at 37°C, 5% CO_2 for 4 h, after which the cells were observed under a fluorescence microscope (Nikon Eclipse TE2000-U) at a wavelength of 490 nm. siGLO is a transfection indicator gene, which fluoresces inside the cells and enable them to be visualized under fluorescent microscope. Quantitative measurement of transfection was done using a microtiter plate reader (Perkin Elmer® 1420 Multilabel Counter Victor 3TM V) at 490 nm.

3.4 Results and Discussion

3.4.1 Particle size and surface charge

Chitosan of different molecular weights LMW (10 K), MMW (100 K), and HMW (500 K) were crosslinked with TPP at varying pH conditions. While maintaining the same physiological conditions such as pH, temperature and concentration, the chitosan nanoparticles showed a continuous trend of increasing size as the molecular weight increased (**Figure 3.1**). In our attempts to reach the smallest possible particle size, different weight ratios of chitosan: TPP starting from 3:1 to 7:1 were tested. The smallest obtained particle size was approximately 76 ± 1 nm with LMW chitosan (solution pH value = 5) and TPP (solution pH value = 3) with a positive surface charge of 16.54 ± 1.64 mV at a weight ratio of 3:1 (as illustrated in **Figures 3.2 and 3.3**).

Indeed, TPP being an anionic reagent acts as a crosslinker and binds to the cationic chitosan because of electrostatic attraction [219]. While the concentration of chitosan increases progressively from 3:1 to 6:1, with TPP at a constant concentration, the positive zeta potential/surface charge on the nanoparticles increases (with an exception at 7:1, at which zeta potential drops down again to 14.97 ± 1.57 mV) as shown in **Figure 3.3**. Each particle sample was prepared in triplicates and assayed thrice on the Brookhaven BI-90 Particle Nano- sizer for particle sizing and Malvern Zeta sizer for zeta potential. The results obtained were highly redundant and reproducible. The distribution of nanoparticles is mainly expressed by the polydispersion index which shows the percentage variation in the particle size of a sample. The polydispersity obtained was less than 0.4 in each case (data not shown), which confirms the sample as highly monodispersed. The particle size and their surface charge have shown to be dependent on variable parameters like pH conditions and concentration. The particle size and surface charge were also affected by varying the molecular weight of chitosan and the different weight ratios of chitosan to TPP in the formulation [220].

3.4.2 Effect of pH on nanoparticle size

Results show that the chitosan solution at pH 5 yielded a smaller particle size, irrespective of the molecular weight of the chitosan. The LMW chitosan yielded the lowest particle size of 76 ± 1 nm. The effect of pH of the TPP solution on particle size was investigated. TPP at pH 3 and 9 was allowed to crosslink with chitosan solution at pH 5. Various molecular weights of chitosan (10, 100, and 500 kDa) were tested to determine the effect of pH change in TPP. Results (**Figure 3.4**) show that the chitosan nanoparticles formed at TPP at pH 3 were smaller in size compared to particles formed with TPP at pH 9. This may be because TPP at an acidic pH condition has a lower (negative) charge density, which becomes a limiting factor. It is known that TPP at acidic pH interacts with a lesser number of positively charged chitosan units [210]. This results in the formation of monodispersed nanoparticles of smaller size as a lesser number of chitosan units are involved in the formation of the nanoparticles. TPP at basic pH bears a more negative charge and is thus able to interact with higher number of counter charges available on chitosan, yielding larger particle size (**Figure 3.4**). pH of both TPP and chitosan was found to play a significant role in nanoparticle size.

3.4.3 Transmission electron microscopy study

Nanoparticles prepared using LMW chitosan were analyzed under TEM to study their morphological characteristics. Chitosan-TPP nanoparticles (without siGLO) were formed at chitosan solution pH 5 and TPP solution pH 3 and 9 at a weight ratio of 3:1. Chitosan-TPP nanoparticles (with entrapped siGLO) were formed at different weight ratios, ranging from 50:1 to 250:1 (w/w) (chitosan-TPP: siGLO). On observation of siGLO-free nanoparticles, it was found that nanoparticles were irregular in shape and smaller in size (ranging between 50 and 70 nm, at TPP pH 3) compared to nanoparticles formed with TPP solution at pH 9 (greater than 200 nm in size) as shown in **Figure 3.5b** and **c**. siGLO-loaded/entrapped nanoparticles consisting of varying weight ratios from 50:1 to 150:1 of chitosan-TPP:siGLO were approximately in the range of 100–170 nm in size (**Figure 3.5 d–f**). But at higher weight ratios of 200:1 and 250:1, the particles were monodispersed and effectively smaller (about 25 ± 5 and 50 ± 10 nm, respectively) as shown in **Figure 3.5g** and **h**. Interestingly, at these higher weight ratios, the smaller

particle size was accompanied by a better entrapment efficiency of siGLO (**Figure 3.6**), which is probably due to the stabilization of the surface charge on the nanoparticles. This may also facilitate the cellular uptake of the nanoparticles [205, 221]. Our results were in accordance with a recent study that showed that complete entrapment of siRNA depends on the molecular weight of chitosan and weight ratio of chitosan-TPP with siRNA [222].

At chitosan-TPP:siGLO weight ratio of 50:1 (N:P = 25), the nanoparticles appeared bigger and seemed to be aggregated. This could be because of the presence of free gene (siGLO) in the solution; being negatively charged it tends to attract the available positively charged chitosan units present in its vicinity. The unstable surface charge and the steric hindrance could lead to aggregation of nanoparticles. Our results are in accordance with reports in literature indicating that particle size decreases with decrease in molecular weight of chitosan but increases with increase in the concentration of the gene [197]. The TEM micrographs presented in **Figure 3.5** give an idea of the size and shape of the nanoparticles, attributes which play a major role in the transfection of nanoparticles across the cellular membrane. Our results show that the lowest particle size of approximately 20 nm showed maximum transfection efficiency, whereas, as the size of the particles increased, the transfection efficiency became low.

3.4.4 Gene-loading efficiency

We performed gel electrophoresis to evaluate the encapsulation of siGLO into the chitosan-TPP nanoparticles, prepared using LMW chitosan. In this agarose gel electrophoresis study, nanoparticles formed at different weight ratios were loaded into the 4% low gelling temperature agarose gel. 10-bp DNA ladder was used as a reference. The gel when observed under UV transilluminator, showed bands indicating the presence of an unbound siGLO in the suspension **(figure 3.6)**. As the concentration of chitosan in the chitosan-TPP:siGLO (w/w) complex increased from 100:1 to 250:1, there was a gradual decrease in the intensity of the bands. The change in the intensity of the bands was due to the increase in the weight ratio and consequently of the strong interaction of chitosan with the gene, siGLO. The strong interaction relates to the greater number of available positive charges on chitosan that interacts with negatively charged siGLO and TPP. This

study proves the complete complexation of siGLO into the nanoparticles at a weight ratio of 200:1 and 250:1. The amount of siGLO loaded at the weight ratio of 200:1 (N:P = 103) was 6 μg/mL of chitosan- TPP solution.

3.4.5 Gene delivery and transfection efficiency

Transfection was performed with different weight ratios of LMW chitosan-TPP:siGLO nanoparticles, on Neuro2a, mouse neuroblastoma cells. Transfection efficiency was analyzed by measuring the fluorescence intensity of the siGLO-loaded nanoparticles. siGLO is a transfection indicator, which is a fluorescent oligonucleotide that is localized into the nucleus of the mammalian cell (**Figure 3.7**). The transfected cells were observed using a fluorescein isothiocyanate filter. siGLO, chitosan solution, and regular cells without any treatment were used as controls. Maximum transfection efficiency was observed when chitosan-TPP:siGLO nanoparticles at a weight ratio of 200:1 were used (**Figures 3.7 and 3.8**). A negligible amount of transfection was obtained with only siGLO. This confirms the results in a recent study, which show that Chitosan-TPP nanoparticles, as a cationic polymer formulation are an effective delivery mechanism even in comparison to lipophilic formulations and that they facilitate the uptake of genes by cells [222]. Being cationic, chitosan complexes are readily taken up by cells via a mechanism of endocytosis [223]. In contrast, siGLO is negatively charged and is repelled by the negatively charged lipid-bilayer membrane of the cells. Fluorescence intensity, as an indication of the transfection efficiency, indicates the importance of particle size and surface charge on nanoparticle uptake [224, 225]. The particle formed with 200:1 (w/w) (N:P = 103) chitosan-TPP:siGLO exhibits maximum uptake by the cells (**Figures 3.7 c and 3.8**). The relation between weight ratios of chitosan-TPP:siGLO nanoparticles, particle size, and the transfection efficiency is more comprehensively expressed in **Table 3.1**. These results were in accordance with a previous study that showed LMW chitosan is an efficient nucleic acid-delivery system [216].

Like polyethyleneimine (PEI), chitosan is known to exhibit a proton sponge effect which is highly pH dependent [226]. At acidic pH, the chitosan attracts positively

charged H^+ ions and gets protonated. The protonated positively charged chitosan attracts negatively charged CI^- ions toward it. Therefore, an accumulation of H^+ and CI^- ions occurs within the cell's cytoplasm in the vicinity of the chitosan. This leads to an osmotic pressure difference between the exterior and the interior of the cell. Thus, the cell as well as the chitosan starts to absorb water and swell. This phenomenon is called "proton sponge effect". The swelling helps the chitosan to escape the endosomal cavity and reach the cytoplasm [227]. Moreover, it also helps entrapped genes to evade enzymatic attack by nucleases in endosomes, lysosomes, and follow the path toward nuclear import [225, 227, 228]. The transfection indicator siGLO used in our experiment was localized inside the nucleus, therefore, it is quite apparent that the chitosan-TPP nanoparticles were easily released from the endosomal compartment and that the gene was imported to the nucleus effectively. As explained in previous studies [206, 229], the pH of the medium and the molecular weight of the chitosan both play a key role in the transfection of nanoparticles. In a recent study, it was shown that the pH change of TPP from alkaline to acidic leads to controlled release of the oligonucleotides [230]. Also apart from being an efficient crosslinker TPP being negatively charged, enhances the release of the gene, as it competes for the available positively charged groups on chitosan inside the cell.

3.5 Conclusion

Chitosan-TPP nanoparticles are an efficient delivery system for oligonucleotides ranging from 18 to 21 bp (siRNAs) into neuronal cells. In our study we developed ultrafine, monodispersed, siRNA encapsulated chitosan- TPP nanoparticles of 20 nm size formed by ionic gelation. Furthermore, our LMW chitosan nanoparticles exhibited excellent transfection efficiency as an indication of biological activity in Neuro2a mouse neuroblastoma cells. The use of siGLO as a transfection agent is convenient and could prove to be superior to GFP and luciferase transfection agents. This chitosan nanoparticle delivery system needs to be further optimized using suitable surface coating molecules and ligands in order to represent a novel promising tool for gene delivery systems. Biocompatibility studies are needed to evaluate the suitability of these nanoparticles for in-vivo use.

3.6 Acknowledgements

We gratefully acknowledge the assistance received from the Canadian Institutes of Health Research (CIHR) and the Natural Sciences and Engineering Research Council of Canada (NSERC) to Dr. S. Prakash. The Centre of Biorecognition and Biosensors (CBB) for their support. We also acknowledge the support of the McGill Faculty of Medicine Internal Scholarship to M. Malhotra. A.K. acknowledges the Alexander Graham Bell Post Graduate Scholarship—Doctoral from NSERC. J.B. acknowledges a Doctoral Scholarship from CIHR. The authors acknowledge the technical support provided by Dr. Misara Hamoudeh. S.S. acknowledges the McGill Faculty of Medicine Internal Scholarship. We are grateful to Prof. Maryam Tabrizian for providing us with facilities (Malvern Particle Sizer and Brookhaven Zeta Potential) in her Laboratory at McGill University, Canada.

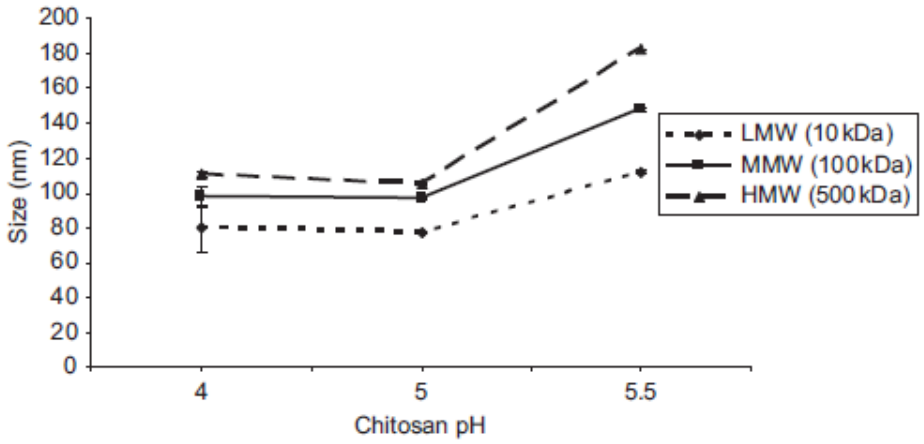

Figure 3.1: The influence of chitosan molecular weight on the nanoparticle size at three different pH values of chitosan solution. High molecular weight (HMW), medium-molecular weight (MMW), and low-molecular weight (LMW) chitosan.

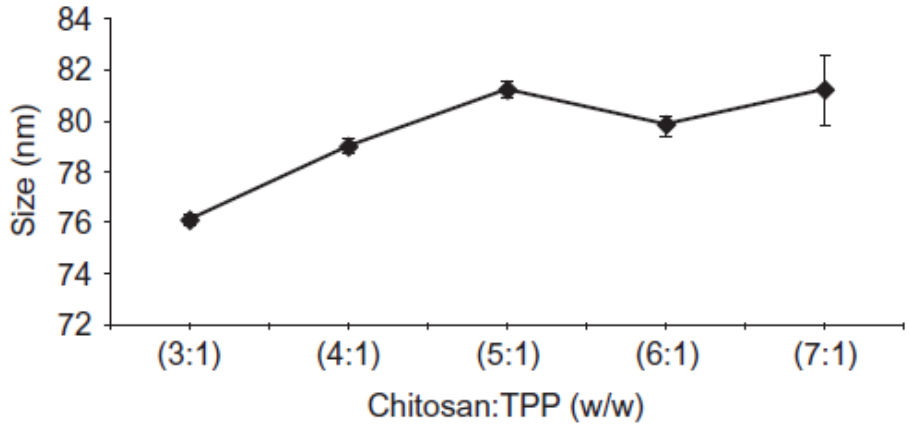

Figure 3.2: Effect of different weight ratios of low-molecular weight (LMW) chitosan (pH 5) crosslinked with TPP (pH 3) on nanoparticle size.

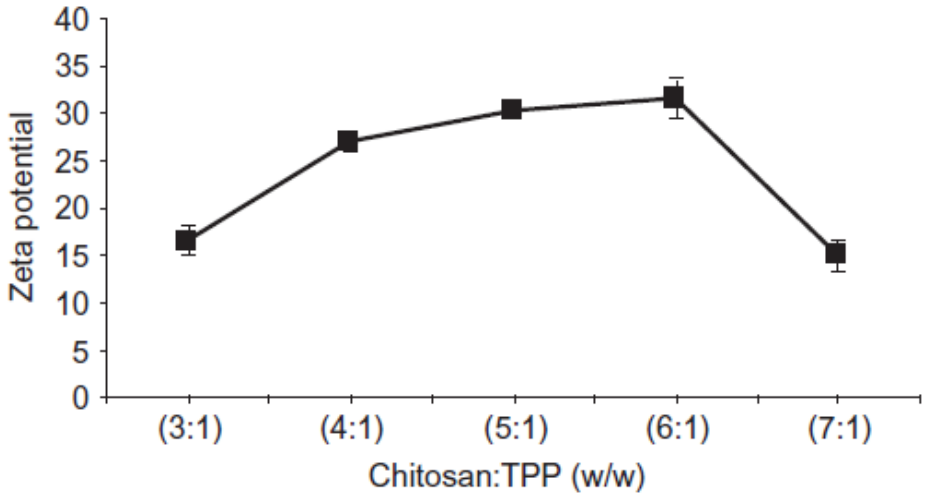

Figure 3.3: Effect of different weight ratio of low-molecular weight (LMW) chitosan (pH 5) crosslinked with TPP (pH 3) on zeta potential.

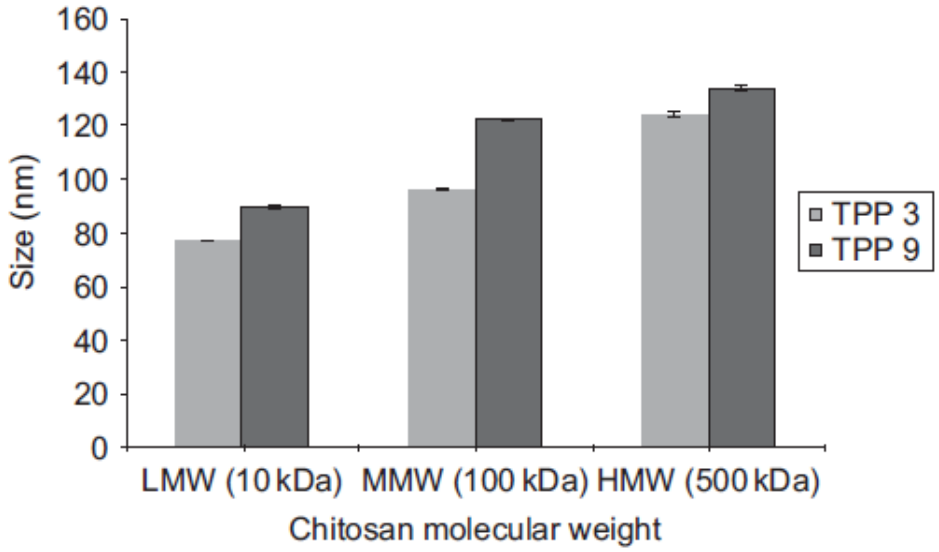

Figure 3.4: Effect of change of pH of TPP pH 3 and pH 9 on the formation of chitosan-TPP nanoparticles made from HMW, MMW, and LMW chitosan.

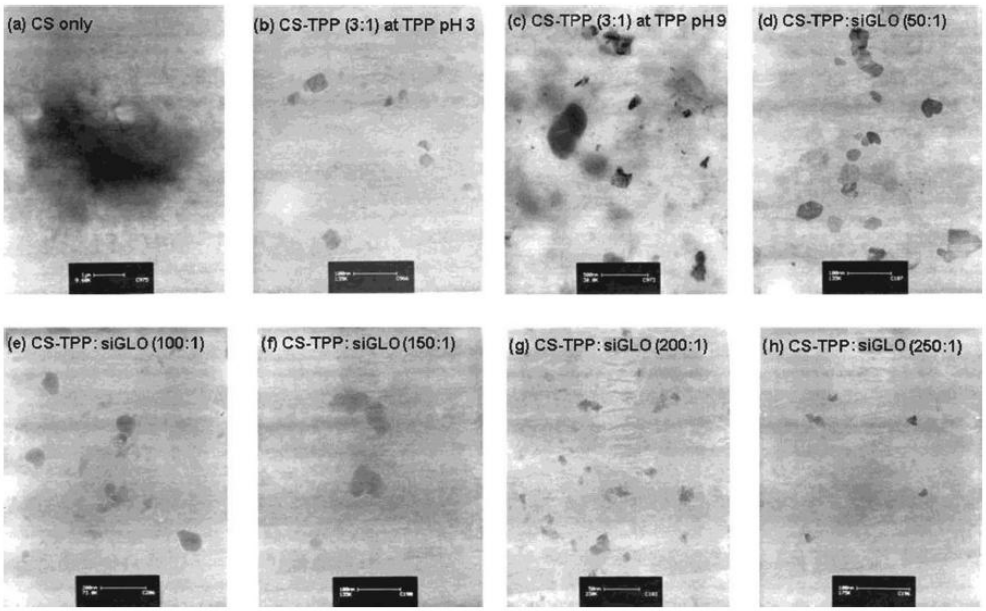

Figure 3.5: TEM micrographs of (a) chitosan polymer dissolved at pH 5, (b) Nanoparticles formed from complexation of chitosan and TPP with TPP at pH 3, (c) and TPP at pH 9, (d) siGLO-loaded chitosan-TPP nanoparticles with chitosan-TPP:gene weight ratio of 50:1, (e) 100:1, (f) 150:1, (g) 200:1, and (h) 250:1.

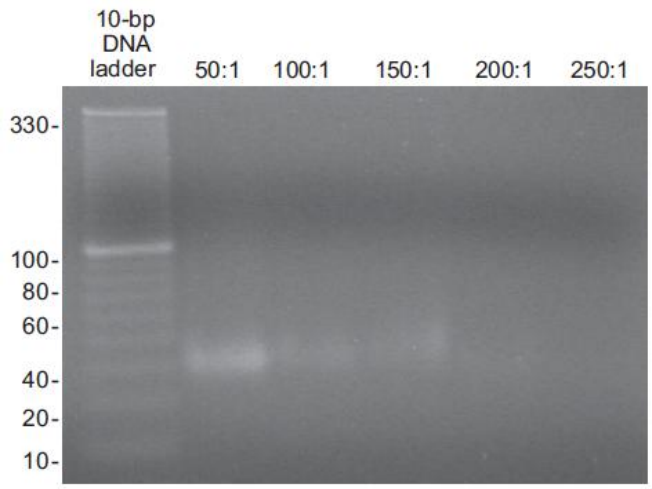

Figure 3.6: Agarose gel electrophoresis: Gel retardation assay of different weight ratios of chitosan-TPP with siGLO. Un-encapsulated siGLO in the suspension is observed in the 4% agarose gel. At 200:1 weight ratio of chitosan-TPP:siGLO, we achieved complete encapsulation of the gene, siGLO.

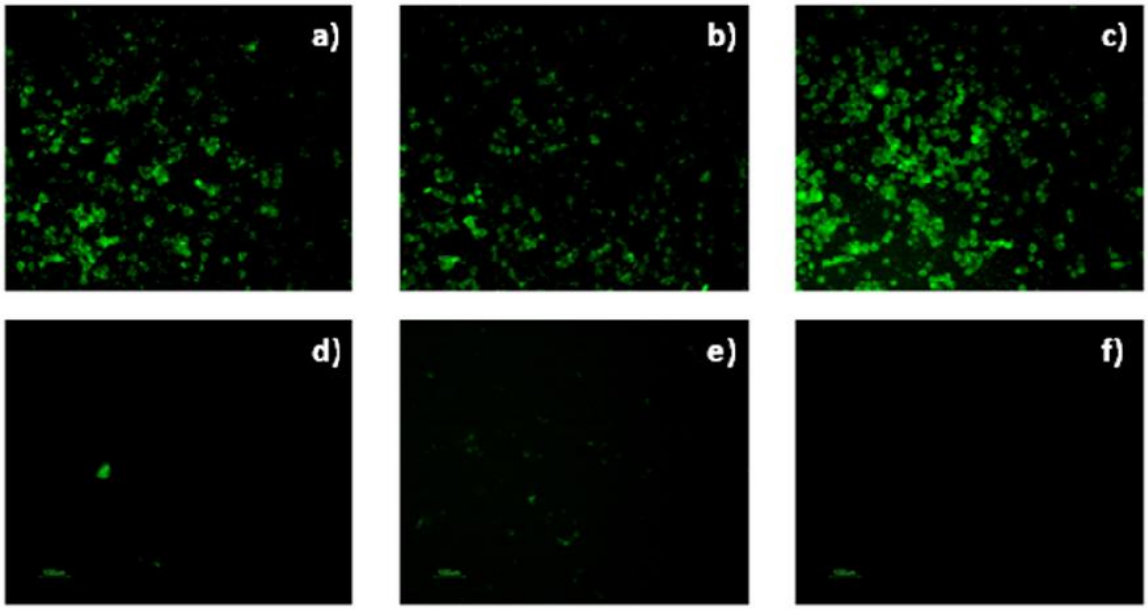

Figure 3.7: Evaluation of gene delivery and transfection efficiency: Neuro2a cells transfected with different weight ratios of chitosan-TPP:siGLO, (a) 100:1, (b) 150:1, (c) 200:1, (d) 250:1, (e) only siGLO, and (f) only cells (control).

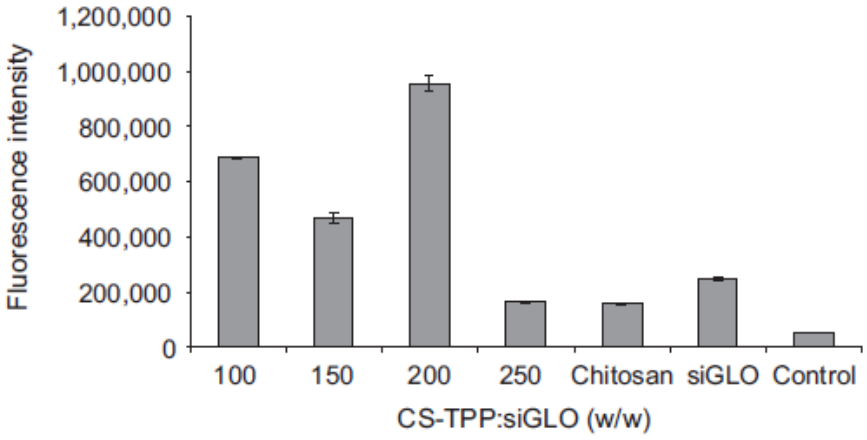

Figure 3.8: Transfection efficiency of siGLO-entrapped chitosan-TPP nanoparticles at different weight ratios starting from 100:1 to 250:1 (w/w) (chitosan-TPP:siGLO) in Neuro2a mouse neuroblastoma cells. For CS-TPP:siGLO weight ratio of 100:1, 150:1, 200:1, 250:1, the size of the nanoparticles were 110 ± 10, 150 ± 10, 25 ± 5, and 50 ± 10 nm, respectively. siGLO, chitosan, and regular cells were used as controls.

Table 3.1: The transfection efficiency of chitosan-TPP:siGLO nanoparticles in Neuro2a cells is represented. The lowest particle size obtained of ~20 nm at weight ratio 200:1 showed highest transfection efficiency; also, the siGLO was completely encapsulated at this ratio. It was observed that as the particle size increased the transfection efficiency decreased gradually with an exception at a weight ratio of 250:1. It is anticipated that at the ratio 250:1 (w/w), the siGLO amount as compared with the chitosan- TPP was too low to yield sufficient fluorescence. Weight ratios 100:1 and 150:1 lacked complete encapsulation of siGLO as shown in **figure 3.6** (gel electrophoresis data), and the particle size of more than 100 nm were anticipated to be the cause of low transfection efficiency in Neuro2a cells. The size of the nanoparticles was determined using TEM and the fluorescence intensity was measured using a microplate reader at 490 nm.

Sample	Chitosan-TPP: siGLO (w/w)	Particle size (nm)	Transfection efficiency (X: fluorescence intensity)
(a)	100:1	110 ± 10	XXX
(b)	150:1	150 ± 10	XX
(c)	200:1	25 ± 5	XXXX
(d)	250:1	50 ± 10	X

Original article 2

CHAPTER 4: A NOVEL METHOD FOR SYNTHESIZING PEGYLATED CHITOSAN NANOPARTICLES: STRATEGY, PREPARATION, AND IN VITRO ANALYSIS

Meenakshi Malhotra, Ciaran Lane, Catherine Tomaro-Duchesneau, Shyamali Saha and Satya Prakash*

Biomedical Technology and Cell Therapy Research Laboratory
Department of Biomedical Engineering, Artificial Cells and Organs Research Center
Faculty of Medicine, McGill University
3775 University Street, Montreal, Quebec, H3A2B4, Canada

*Corresponding author: Tel: 514-398-2736; Fax: 514-398-7461,
Email: satya.prakash@mcgill.ca

Preface: The nanoparticles as prepared in the previous chapter were tested for their transfection and cytotoxicity on Neuro2a cells. Though efficient transfection was achieved, however, the nanoparticles were cytotoxic. Towards this goal, this chapter demonstrates a novel synthesis scheme that was incorporated to reduce the toxicity of the nanoparticles. For which, the chitosan polymer was surface graft with a hydrophilic polymer, polyethylene glycol (PEG). The synthesized polymer was characterized by FTIR and nanoparticles were formed as previously described in chapter 3. The nanoparticles were tested for siRNA loading efficiency, transfection efficiency and cytotoxicity.

Article published in ***International Journal of Nanomedicine.*** **2011, 6: 485-494**
PMCID: PMC3088072

4.1 Abstract

Preparation of polyethylene glycol (PEG)-grafted chitosan is essential for improving the biocompatibility and water solubility of chitosan. Presently available methods for this have limitations. This article describes a new method for preparing PEGylated chitosan nanoparticles. For this chitosan was chemoselectively modified using a novel scheme at the C6 position of its repeating units by PEG. The amine groups at the C2 position of the chitosan were protected using phthalic anhydride. Sodium hydride was used to catalyze the etherification reaction between chlorinated chitosan and methyl-PEG, and PEG-grafted chitosan was successfully synthesized. Each step was characterized using ^{13}C nuclear magnetic resonance and Fourier transform infrared. After PEGylation the phthaloylated chitosan was successfully deprotected using hydrazine monohydrate. The synthetic scheme proposed demonstrates a new method for grafting PEG onto chitosan with a moderate degree of substitution. The potential of this polymer in nanoparticle preparation using an ionic gelation method and its gene delivery potentials were investigated by complexing a fluorescently labeled, scrambled siRNA. The result showed that suitable nanoparticles can be synthesized using this polymer and that they have capacity to carry genes and provide adequate transfection efficacy with no toxicity when tested on neuronal cells.

Key words: Nanoparticles, chitosan, polyethylene glycol, polymeric membrane, gene delivery

4.2 Introduction

Chitosan is a linear polymer composed of β-(1–4)-2-amino-2-deoxy-D-glucopyranose units. Being a polycationic, nontoxic, biodegradable, and biocompatible polymer, chitosan has attracted much attention and has wide applications in biotechnology, pharmaceutical, textile, food, cosmetics, and agricultural industries [6, 231]. Current research with chitosan focuses on its use as a novel drug, gene, peptide, and vaccine delivery vehicle, and scaffold for targeted delivery and tissue engineering applications [197, 232-234]. Chitosan has achieved much interest compared with chitin and cellulose due to the presence of primary amine groups present in its repeating units. The presence of primary amine groups makes chitosan an excellent cell transfectant. Like PEI, chitosan exhibits a "proton sponge" effect, which refers to the swelling behavior of the polymer on encountering an acidic pH inside the cell's endosome, making it an efficient carrier for therapeutic molecules [226-228]. A number of chitosan derivatives have been synthesized in the past with modification on the primary amine groups of the polymer [235, 236]. Chitosan is soluble only in acidic aqueous solutions due to the presence of amine groups that become protonated, and thus its poor solubility in other organic solvents has become a major drawback, limiting its effective utilization.

To facilitate the effective use of chitosan in gene delivery and other biomedical applications, it is necessary to make chitosan soluble either in water or organic solvents. Such attempts can be made by graft copolymerization of chitosan through chemical modifications with other polymers, such as PEG, of different molecular weights [237]. This allows chitosan to retain its inherent characteristics of, for example, molecular structure and length, and allows for a variety of chemical modifications or reactions on its side chain. However, chemical modification at amine groups leads to a change in the fundamental skeleton of chitosan, causing it to lose its original physiochemical and biochemical activities [237]. Recently, modifying hydroxyl groups of chitosan has gained much importance as it does not influence the characteristic structural and functional features of chitosan.

PEG is widely used as a graft-forming polymer. It is soluble in both water and organic solvents, has no toxicity, antigenicity, and immunogenicity, and is biodegradable and biocompatible [238]. PEGylation of chitosan through hydroxyl groups was first proposed by Gorochovceva and Makuska [239]. PEG has been used mainly as a graft polymer, where it is used as a crosslinker and forms interconnected channels to enable drug release [240, 241]. Various preparation techniques can be used to prepare chitosan nanocarriers by altering parameters such as concentration of the polymer or the crosslinker, the molecular weight of chitosan, the ratio of drug/gene:polymer, pH, and finally stabilizers or surfactants. All these factors collectively affect the structural and morphological properties of chitosan nanoparticles and the release rate of the loaded therapeutic molecule [217].

This study aims to achieve facile chemoselective conjugation of PEG at the hydroxyl group of chitosan, where the amine groups of chitosan were first protected using phthalic anhydride [242]. Nanoparticles were formed using an ionic gelation method. The concentration of the polymer versus crosslinker and the pH of the solution were adjusted with reference to our previously optimized study, as mentioned in chapter 3 [243]. The current study opens up the future application of forming PEG-grafted chitosan nanoparticles for efficient gene/drug delivery.

4.3 Materials and Methods

4.3.1 Materials

Low-molecular-weight chitosan was obtained from Wako (Richmond, VA, USA), having a viscosity of 5–20 cP and a degree of deacetylation of 80.0%. PEG monomethyl ether (MW 2000), phthalic anhydride, sodium hydride (NaH), pyridine, hydrazine monohydrate, TPP, glacial acetic acid, agarose (low gelling temperature), and ethidium bromide (10 mg/mL) of analytical grade were obtained from Sigma-Aldrich (Oakville, ON, Canada). Anhydrous tetrahydrofuran (THF), anhydrous N,N-dimethylformamide (DMF), sodium hydroxide (NaOH) and methanol were obtained from Thermo Fisher Scientific (Ottawa, ON, Canada). Thionyl chloride ($SOCl_2$) was obtained from VWR

(Mississauga, ON, Canada). For dilution purposes, ultra pure double distilled water (ddH_2O) was used from a laboratory-installed Barnstead Nanopure diamond™ water supply unit. siGLO (Green) transfection indicator (20 nmole) was obtained from Dharmacon (Lafayette, IN, USA). CellTiter 96® AQueous One Solution Reagent was purchased from Promega (Madison, WI, USA) to perform cell viability assay. TrackIt 10 bp DNA ladder (0.5 μg/μL) was obtained from Invitrogen (Burlington, ON, Canada). Neuro2a cell line and Eagle's minimum essential medium (EMEM) were obtained from Cedarlane (Burlington, ON, Canada) and supplemented with 10% fetal bovine serum (FBS) from Invitrogen (Burlington, ON, Canada).

4.3.2 Deacetylation of chitosan

Commercially available low-molecular-weight chitosan (5 g) was added to a 40% (w/v) aqueous NaOH solution. The mixture was stirred for 4 hours at 110°C under a nitrogen atmosphere. After 4 hours the mixture was vacuum filtered, pulverized, and was again treated with 40% (w/v) NaOH under similar conditions. The resultant product **(b) in Figure 4.1** was freeze-dried [244].

4.3.3 Phthaloylation of chitosan

Deacetylated chitosan (1.00 g) was added to a solution of phthalic anhydride (2.76 g) in 20 mL of DMF. The mixture was stirred for 8 hours at 120°C under a nitrogen atmosphere. The resultant product **(c) in Figure 4.1** was cooled to room temperature and precipitated in ice cold water. The precipitate was filtered, washed with methanol overnight, and vacuum dried [242, 245].

4.3.4 Synthesis of PEGylated chitosan (chitosan-O-PEG)

We employed a novel scheme to PEGylated chitosan chemoselectively. The scheme depicted in **Figure 4.1** utilizes the activation of PEG by NaH, used as a catalyst to conjugate PEG and chitosan. The synthesis was accomplished in 3 steps: 1) chlorination of chitosan, 2) activation of $OH\text{-}PEG\text{-}OCH_3$ (mPEG) with NaH, and 3) grafting activated mPEG onto chlorinated chitosan. To prepare chlorinated chitosan, $SOCl_2$ was added in 10-fold excess compared to phthaloylated chitosan (0.1 g) in 20 mL

of pyridine. The reaction was stirred at 80°C for 30 minutes under a nitrogen atmosphere. After 30 minutes, the reaction was cooled to room temperature, precipitated in ice cold water, filtered, and vacuum dried to yield chlorinated-phthaloyl chitosan, product **(d) in Figure 4.1**. PEG was activated by adding 4 g of OH-PEG-OCH_3 (mPEG) to a suspension of NaH (10 mg) in 50 mL of anhydrous THF. The reaction was stirred at 60°C for 2 hours under nitrogen atmosphere. After 2 hours, chlorinated-phthaloyl chitosan (60 mg) was added to the reaction mix and stirred for another 16 hours under similar conditions. After 16 hours the reaction was allowed to cool at room temperature and was precipitated in methanol, filtered, and vacuum dried to yield product **(e) in Figure 4.1**.

4.3.5 Deprotection of PEGylated-phthaloyl chitosan

PEGylated-phthaloyl chitosan (100 mg), hydrazine monohydrate (15 mL), and distilled water (30 mL) were mixed and heated at 100°C for 16 hours under constant magnetic stirring. Excess hydrazine monohydrate was removed by evaporating the mixture using a rotary evaporator until a viscous solution was left. The process was repeated 3 times by reconstituting the mix with distilled water each time and then rotary evaporating it until a solid residue was left. The final product was dried under vacuum to obtain the desired PEGylated chitosan.

4.3.6 Preparation of PEGylated chitosan nanoparticles

PEGylated chitosan nanoparticles were prepared by an ionic gelation procedure, as explained in previous studies [246]. After the deprotection of PEGylated-phthaloyl chitosan, the polymer was dissolved in 1% (v/v) acetic acid solution to yield a concentration of 0.5 mg/mL and the pH was adjusted to 5. TPP was dissolved in ddH_2O to obtain a concentration of 0.7 mg/mL and the pH was adjusted to 3 [243]. Nanoparticles were formed after the addition of TPP (drop-wise) to the chitosan solution under constant magnetic stirring for 1 hour at room temperature. The nanoparticles obtained were visualised under TEM, without any stain, for their morphology and size.

4.3.7. Gene loading efficiency by the gel retardation assay

The encapsulation/gene loading efficiency of PEGylated chitosan polymer was determined by complexing it with siGLO, a transfection indicator, to form nanoparticles following similar conditions as described in chapter 3 [243]. The free siGLO in PBS and siGLO complexed with nanoparticles were run in duplicates on a 4% w/v agarose gel electrophoresis for 4 hours at 55 V in Tris/Borate/EDTA (TBE) buffer (pH 8.3). The siGLO complexation with nanoparticles was performed at a ratio of 200:1 (polymer:gene) (w/w), with N:P of 103, as determined in our previous study [243]. The TBE Buffer used contained ethidium bromide at a concentration of 0.5 μg/mL, which is required for the visualization of the RNA bands under UV transilluminator at a wavelength of 365 nm using a ChemiDoc™ XRS System (Bio-Rad, Hercules, CA).

4.3.8 Transfection efficiency and cell viability assay

Mouse neuroblastoma cells (Neuro2a) were seeded in a 96-well plate at a density of 20,000 cells per well in complete growth media (antibiotics-free EMEM with 10% serum). The transfection study was performed after 24 hours of initial seeding. The different tested samples were: chitosan–TPP nanoparticles and free siGLO as controls, chitosan–TPP:siGLO nanoparticles, and PEGylated chitosan–TPP:siGLO nanoparticles (200:1 w/w), N:P = 103, as treatment samples. The cells were then incubated at 37°C, 5% CO_2 for 4 hours, after which the cells were observed under fluorescence microscope (Nikon Eclipse TE2000-U) at a wavelength of 490 nm. The same treatment and control samples were also used for a cytotoxicity assay. The cytotoxicity assay was performed after 4 hours using Cell-Titer 96® AQueous One Solution Reagent (MTS assay), as per manufacturer's protocol. After an additional incubation of 4 hours with the MTS assay the absorbance in each well was recorded at 490 nm using a microtiter plate reader (Perkin Elmer® 1420 Multilabel Counter Victor 3TM V). The cell study was performed in triplicate.

4.3.9 Statistical analysis

Values are expressed as means ± standard deviations (SD). The statistical significance was determined by using an independent t-test to compare the values of

chitosan-TPP nanoparticles with PEGylated chitosan–TPP nanoparticles (n = 3 for each group). P values of < 0.05 were considered significant. Statistical analysis was carried out using Minitab (Minitab, Version 14; Minitab Inc, State College, PA).

4.4 Results

4.4.1 Deacetylation of chitosan

The ^{13}C nuclear magnetic resonance (NMR) of deacetylated chitosan confirmed the absence of an acetyl peak (-CH_3) at 23.88 ppm and a carbonyl peak (−C=O) at 175.04 ppm present in the commercially available chitosan. NMR: (topological substructural molecular design (TOSS mode) of commercially available chitosan (**figure 4.2a**): δC 23.88 (CH_3), 59.01 (C-2), 61.76 (C-6), 75.64 (C-5, 3), 82.51 (C-4), 105.68 (C-1), 175.04 (C=O). ^{13}C CP/MAS NMR: (TOSS mode) of deacetylated chitosan (**figure 4.2b**): δC 60.76 (C-2, 6), 75.84 (C-4, 5, 3), 102.80 (C-1).

4.4.2 Phthaloylation of chitosan

The ^{13}C NMR in TOSS mode of phthaloylated chitosan confirmed the appearance of peaks Phth phenylene and Phth C=O at 134.42 ppm and 169.66 ppm, respectively (**figure 4.2c**), and the appearance of Phth C-1,2 and Phth C=O peaks at 131.63 ppm and 169.89 ppm, respectively, in TOSDL mode. ^{13}C CP/MAS NMR: (TOSS mode): δC 58.19 (C-2), 61.76 (C-6), 72.44 (C-3), 75.42 (C-5), 83.91 (C-4), 101.24 (C-1), 124.62, 131.70, 134.42 (Phth phenylene), and 169.66 (Phth C=O); (TOSDL mode): δC 131.63 (Phth C-1,2) and 169.89 (Phth C=O). FTIR of commercially available chitosan as shown in **Figure 4.3a**: ν_{max}/cm^{-1} 1630 (amide I), 1542 (amide II), and 1024 (pyranose). FTIR of phthaloylated chitosan as represented in **Figure 4.3b**: ν_{max}/cm^{-1} 3200–3400 (OH), 1774 (imide C=O), 1710 (imide C=O), 1150–1000 (pyranose), and 720 (arom).

4.4.3 Synthesis of PEGylated chitosan

The FTIR spectra presented in **Figure 2d** represent PEGylated chitosan with the characteristic peaks at ν_{max}/cm^{-1}: 2871 (C-H stretching), 1066 (C-O stretching), 1290, 1251, 950 and 837, confirming the PEG 2000 substitution when compared to **Figure 4.3c**

that represents the FTIR spectra of PEG only with the characteristic peaks at ν_{max}/cm^{-1}: 2878 (C-H stretching), 1100 (C-O stretching), 1466, and 1278.

4.4.4 Deprotection of PEGylated-phthaloyl chitosan

The FTIR spectra presented in **Figure 4.3e** represent deprotected PEGylated chitosan with the characteristic peaks at ν_{max}/cm^{-1}: 2878 (C-H stretching), 1066 (C-O stretching) belonging to PEG, the appearance of 1633 (amide I), 1582 (amide II), and 1024 (pyranose) belonging to chitosan, and the disappearance of 1774 (imide C=O), 1710 (imide C=O) belonging to the phthaloyl group, as shown in **Figure 4.3b.**

4.4.5 Preparation of PEGylated chitosan nanoparticles

Deprotected PEGylated chitosan polymer was crosslinked with TPP by the electrostatic interaction between the cationic charges of the primary amine groups on chitosan with the anionic charges of TPP. The crosslinking results in the formation of nanoparticles ranging from 100 to 150 nm in size as determined by transmission electron microscopy (TEM). **Figure 4.4a** represents the TEM image of the PEGylated chitosan polymer (magnification: 57000X). **Figure 4.4b** represents the chitosan–TPP nanoparticles (magnification: 22000X) and **Figure 4.4c** represents the PEGylated chitosan-TPP nanoparticle at magnification 57000X and **figure 4.4d** represents a much smaller PEGylated chitosan-TPP nanoparticle at a higher magnification; 135000X respectively. It was observed that PEGylation yielded a spherical shape to the nanoparticles. A distinct layer of PEG is observed around the nanoparticle in figure 4.4d.

4.4.6 Gene loading efficiency of PEGylated chitosan nanoparticles

In order to evaluate the complexation of siGLO with PEGylated chitosan-TPP nanoparticles, a gel retardation assay was performed, wherein a 10 bp DNA ladder was used as a reference, free siGLO at a concentration of 6 μg/mL of phosphate buffered saline (PBS) solution was used as the control and PEGylated chitosan–TPP nanoparticles complexing siGLO at a N:P ratio of 103, as determined in our previous study, was used as the treatment sample [243]. The gel, under a UV transilluminator, shows bands indicating the presence of unbound siGLO in the suspension, as shown in **Figure 4.5**, for

the control sample (i.e., free siGLO in PBS), whereas there is no band in a treatment sample, which confirms the complete complexation of the siGLO with PEGylated chitosan nanoparticles. The strong interaction pertains to the positive charges available on the chitosan chain after the deprotection procedure on the polymer allowing the interaction with the negatively charged siGLO and TPP.

4.4.7 Transfection efficiency and cell viability assay

The transfection efficiency was analyzed by measuring the fluorescence intensity of the siGLO-loaded nanoparticles. SiGLO is a transfection indicator, which is a fluorescent oligonucleotide that is localized in the nucleus of the mammalian cell (**Figure 4.6**). Free siGLO, chitosan–TPP nanoparticles, and cells without any treatment sample were used as negative controls. Efficient transfection efficiency was observed with both chitosan–TPP:siGLO and PEGylated chitosan–TPP:siGLO nanoparticles prepared at a weight ratio of 200:1 (**Figure 5**). The cell viability assay was performed on these cells after 4 hours, wherein it was observed that cells treated with PEGylated chitosan–TPP:siGLO nanoparticles showed significant increase in cell viability (≈70%) compared with the chitosan–TPP:siGLO nanoparticles (≈20%) (independent t-test, $p < 0.05$), as observed in **Figure 4.7**.

4.5 Discussion

The DA of chitin differentiates it from chitosan. The lower the DA of chitosan widens its application for chemical modifications with the amine groups, imparts greater solubility to the polymer, and enhances its biological properties. Unlike chitin, chitosan is soluble only in acidic aqueous solutions. The solubility of the polymer is an important parameter for having a homogeneous reaction mixture in order to obtain successful chemical modifications. The solubility of chitosan also depends on its molecular weight, its degree of neutralization of amine groups, the ionic strength of the solvent, and the distribution of N-acetyl glucosamine residues along the backbone of the chain [247]. In these experiments complete deacetylation of chitosan was achieved after treating it twice with a 40% (w/v) NaOH solution. Products **(a) and (b)** in **Figure 4.1** represent the

schematic of acetylated chitosan (commercially available) and deacetylated chitosan, respectively.

The complete deacetylation is required to achieve a chitosan with fully activated amine groups allowing for further chemical reactions but renders crystalline character to the polymer, making it insoluble in most organic solvents [245]. In order to solubilise chitosan in organic solvents and to avoid the interference of amine groups while performing chemical modifications on the backbone, the amine groups of chitosan were protected using phthalic anhydride [245]. Since it has been observed that phthaloylation of chitosan in 100% DMF yields partial O-phthaloylation along with N-phthaloylation, we attempted to use DMF/water (95:5 v/v) as a solvent [245]. However, it was observed that the product obtained did not solubilise homogeneously in most of the organic solvents, which in turn was a hindrance to perform further chemical reactions. Thus, in this chemical scheme we did not incorporate the use of DMF/water (95:5 v/v) as a solvent to synthesize phthaloylated chitosan.

^{13}C NMR data confirm the successful N-phthaloylation of the product. Product **(c) in Figure 4.1** shows the schematic representation of the N-phthaloyl chitosan. The total suppression of side bands (TOSS mode) exhibits peaks at 124.62 ppm, 131.70 ppm, 134.42 ppm corresponding to phenylene, and 169.66 ppm and carbonyl group of phthaloyl group and the TOSS – dipolar dephasing (TOSDL) mode confirms the absence of CH and CH_2 peaks due to their short relaxation time and presence of only 2 peaks 131.63 ppm and 169.89 ppm assigned to C 1, 2 and carbonyl of phthaloyl group, respectively. The FTIR data show distinct sharp peaks at 1774 cm^{-1} and 1702 cm^{-1} corresponding to imide of phthaloyl group (**Figure 4.2 b**). The phthaloyl chitosan prepared by this method becomes gel-like when precipitated in water, which supports the data shown by Kurita et al of formation of a uniform structure of phthaloylated chitosan [245].

The 2-N-phthaloylated chitosan formed was further reacted with thionyl chloride to obtain chlorinated chitosan as represented by product **(d) in Figure 4.1**. The FTIR data

in **Figure 4.3 b** show the disappearance of the OH peak in the range of 3200 cm^{-1} to 3400 cm^{-1} in chlorinated phthaloyl chitosan, confirming the replacement of hydroxyl groups with chlorine and the peaks pertaining to imide bond of phthaloyl group (1774 cm^{-1} and 1710 cm^{-1}) remain intact.

Simultaneously, mPEG (OH-PEG-OCH_3) was activated by NaH in THF to form PEG alkoxide (-O-PEG-OCH_3). To this intermediate, chlorinated phthaloyl chitosan was added to form PEG-grafted phthaloyl chitosan. The desired product was precipitated in methanol, with unreacted PEG being soluble in this solvent. This method is the most direct and the easiest way to obtain PEG-grafted chitosan and does not require any intensive purification procedures. Product **(e)** in **Figure 4.1** represents the schematic of PEGylated phthaloyl chitosan.

The deprotection of the chitosan was successfully achieved by treating the PEGylated phthaloyl chitosan, product **(e)** in **Figure 4.1**, with hydrazine monohydrate, which causes destabilization of the phthaloyl moiety by creating an excess alkaline condition of pH 12. Product **(f)** in **Figure 4.1** represents the final product achieved: PEG-grafted chitosan. The absence of peaks at 1774 cm^{-1} and 1710 cm^{-1} in product **(e)** confirms the complete dissociation of phthalimido group from chitosan and the appearance of peaks 1633 cm^{-1} (amide I) and 1582 cm^{-1} (amide II) corresponds to the presence of primary amine groups in chitosan. The peak at 2871 cm^{-1} refers to the presence of PEG in product **(e), Figure 4.1**. The data on ^1H NMR are not shown since it was observed that the multiple peaks of oxymethyl groups in PEG obtained at δ 3.3 to 3.7 cover over the signals of the pyranose ring of chitosan.

The reaction conditions used in the scheme for O-PEGylated chitosan are less intensive in terms of operation and purification. However, NaH, used as a catalyst, makes the reaction conditions alkaline which can potentially have a deleterious effect on the phthaloyl group of chitosan. But, a correct proportion of NaH, PEG, and chitosan can optimize the reaction conditions. In our study we used 2:4:1 molar ratio of NaH:PEG:chitosan. The studies conducted by Makuska's group used Ag_2O as a catalyst,

producing less alkalinity in the solution, suitable for the etherification reaction between chitosan and PEG. The reaction yielded a high degree of substitution of PEG on chitosan, but as stated by the researchers, the residual silver salts that remain in the reaction lead to degradation of chitosan polymer while undergoing deprotection with hydrazine [248]. Also, the overall yield of the PEGylated chitosan was less and involved 28 to 30 hours of reaction time. Even after implementing several cycles of purification on PEGylated chitosan intermediate, it could not completely remove the silver particles. Thus, the procedure involves intensive and multiple steps to obtain the desired product. The use of NaH as a catalyst is more promising than using Ag_2O as a catalyst. In our case, the degree of substitution of PEG on chitosan can be increased by using LMW PEG, but not, 1000 due to the high solubility of PEG in aqueous as well as organic solvents. We also tried PEGylating chitosan through a scheme followed by Jian and You-Lo, in which phthaloylated chitosan was first swelled in pyridine overnight [249]. Other researchers have used NaOH to swell chitosan prior to the reaction in order to achieve homogeneous conditions. NaOH can deprotect the phthaloyl group on chitosan, and therefore its use was avoided and using pyridine as a solvent was favored due to the solubility of phthaloylated chitosan in pyridine. We obtained similar results in terms of yield of PEGylated chitosan by following the protocol of Jian and You-Lo with the exception of the use of PEG acyl chloride followed by multiple steps that take more time (36–40 hours) in terms of reaction and purification at each step to obtain the final product. The total reaction time employed in this scheme, using NaH, was 18 to 20 hours.

The proposed scheme yielded a moderate (15%–50%) degree of substitution of PEG on chitosan, which was soluble in acetone, toluene, chloroform, DMF, and ethyl acetate at 50°C. Also, as reported earlier, O-PEGylated chitosans with free amino groups have a wider application in biotechnology and biomedical systems because of the unchanged poly (glucosamine) skeleton [238]. As PEG separates the chitosan backbone, thereby decreasing intermolecular hydrogen bonding and making it water soluble, it acts as an important intermediate to carry out further chemical modifications.

Chitosan nanoparticles were prepared by ionic gelation that involves a mixture of 2 aqueous phases, of which one is the polymer chitosan and the other is a polyanion TPP. The positively charged amino group of chitosan interacts with negatively charged TPP to form complex coacervates with a size of about 100 nm [250, 251]. The nanoparticles formed can have a significant application as a drug/gene carrier system for biomedical applications both in-vitro and in-vivo. In this study, we have complexed siGLO, a scrambled siRNA with a fluorescent tag with the nanoparticles prepared from the proposed formulation of PEGylated chitosan polymer. Complete complexation of the siGLO was achieved as confirmed by the gel retardation study. The optimal concentration of siGLO to be used for complexation was initially determined by our group and has been published previously as a characterization study [243]. The PEGylated chitosan polymer complexing siGLO was used as a nanocarrier to transfect a neuronal cell line in order to determine the transfection efficiency of the nanoparticle/carrier. It has been reported by many researchers that PEGylation reduces the transfection efficiency of the nanoparticles since PEG, being neutral in charge, does not efficiently interact with the negatively charged cell membrane. However, in this study, the facile chemoselective substitution of PEG on the C6 position was favored, especially so as not to affect the primary amine groups on chitosan that play a major role is gene complexation and cell transfection.

The transfection study, as shown in **Figure 4.6**, confirmed the efficient uptake of PEGylated chitosan nanoparticles (a) compared with chitosan nanoparticles alone (b). This proves that conjugating PEG on the C6 position of the chitosan polymer did not hinder the inherent character of the chitosan polymer to complex and to deliver the siGLO to neuronal cells. To further investigate the effect of nanoparticles on the cells, a cell viability assay was performed. This confirmed the stressed conditions of cells transfected with chitosan nanoparticles alone. The results indicated that although primary amine groups contribute significantly to transfection they may also disrupt the cellular integrity of the cell membrane due to an excessive positive charge on the nanoparticles. The presence of PEG on the nanoparticles makes them sterically stabilized and more hydrophilic. Also, as observed in **Figure 4.7**, the cytotoxicity was greater for the chitosan

nanoparticles complexing siGLO than the chitosan nanoparticles alone. This could be inferred from a reduction in size of the nanoparticles after complexing siGLO, which in turn allows more particle interaction with the cell membrane, thereby increasing the surface area. The optimization study based on the particle size and zeta potential of chitosan nanoparticles with and without siGLO has previously been published by our group [243].

4.6 Conclusion

We achieved successful grafting of PEG on chitosan polymer through a novel scheme of forming PEG alkoxide using NaH as a catalyst. The PEGylated chitosan polymer obtained was easily soluble in water and other organic solvents. The overall procedure is easier and requires less intensive reaction conditions and purification steps to obtain the desired product in a short period of time than the other methods used by other protocols reported in the literature. Also, the procedure does not impart any deleterious effect on the chitosan chain. The PEGylated chitosan nanoparticles successfully complexed siRNA and transfected into the neuronal cell line with minimal cytotoxicity effects. The proposed formulation could have a major implication for biomedical drug targeting strategies involving nanoparticle-mediated targeted delivery.

4.7 Acknowledgements

The authors would like to acknowledge the Canadian Institutes of Health Research (CIHR) grant (MOP-93641) to Dr S Prakash, the support of McGill Major Scholarship to M Malhotra, the support of Industrial Innovation Scholarship (IIS) BMP Innovation – NSERC, FQRNT scholarship and Micropharma Limited Scholarship to Catherine Tomaro- Duchesneau. We would like to acknowledge the support of the Centre of Biorecognition and Biosensors, the NMR Facility at Quebec/Eastern Canada High Field NMR Center, the Centre for self-assembled Chemical Structures (CSACS) and the facility of Electron Microscopy Research at McGill University. We would like to acknowledge the guidance of Dr Hani Al-Salami for statistical analysis.

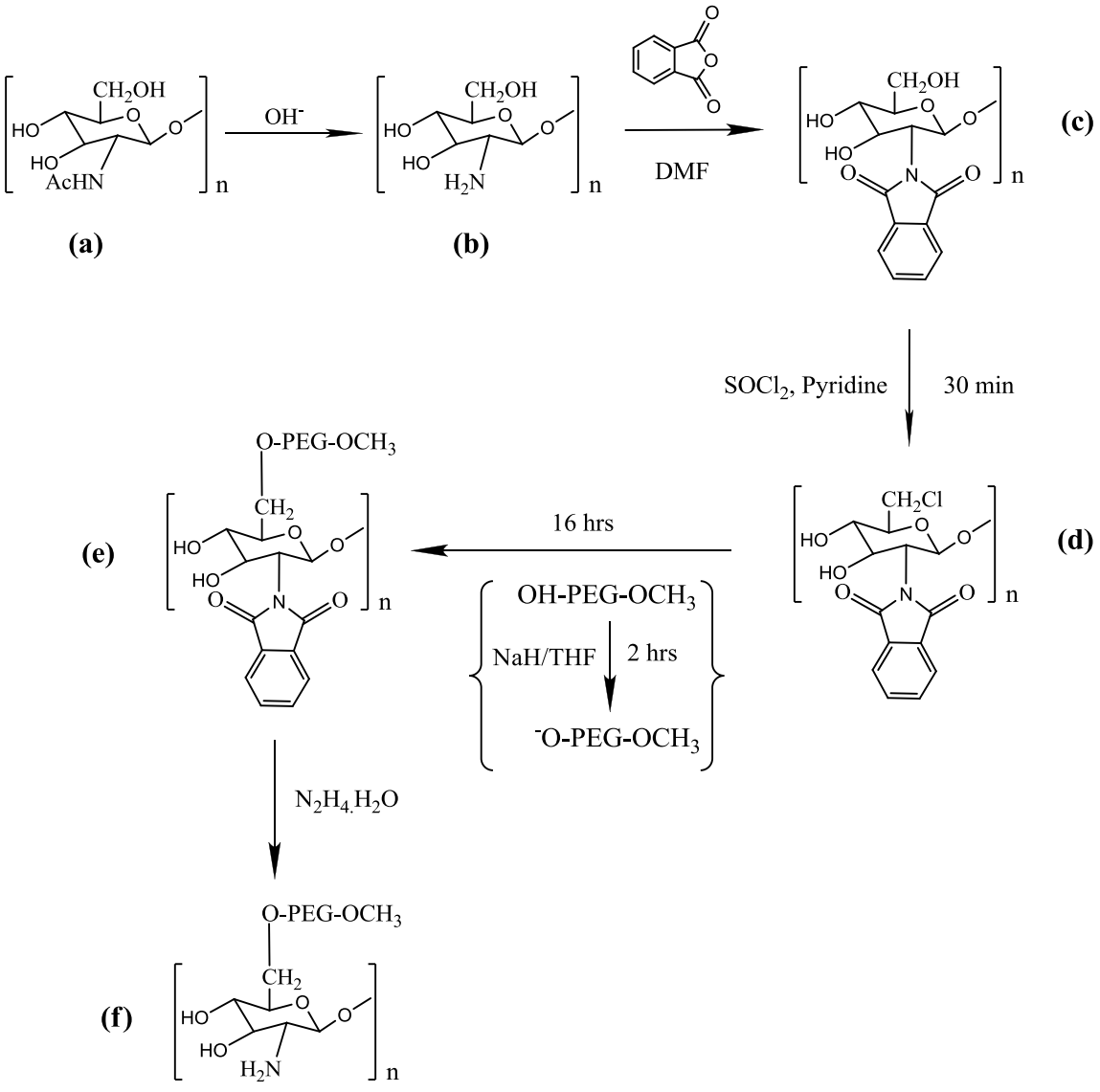

Figure 4.1: Schematic of O-PEGylated chitosan polymer preparation using NaH and THF: A) chitosan; B) deacetylated chitosan; C) phthaloyl chitosan; D) chlorinated phthaloyl chitosan intermediate; E) PEGylated phthaloyl chitosan; and F) PEGylated chitosan

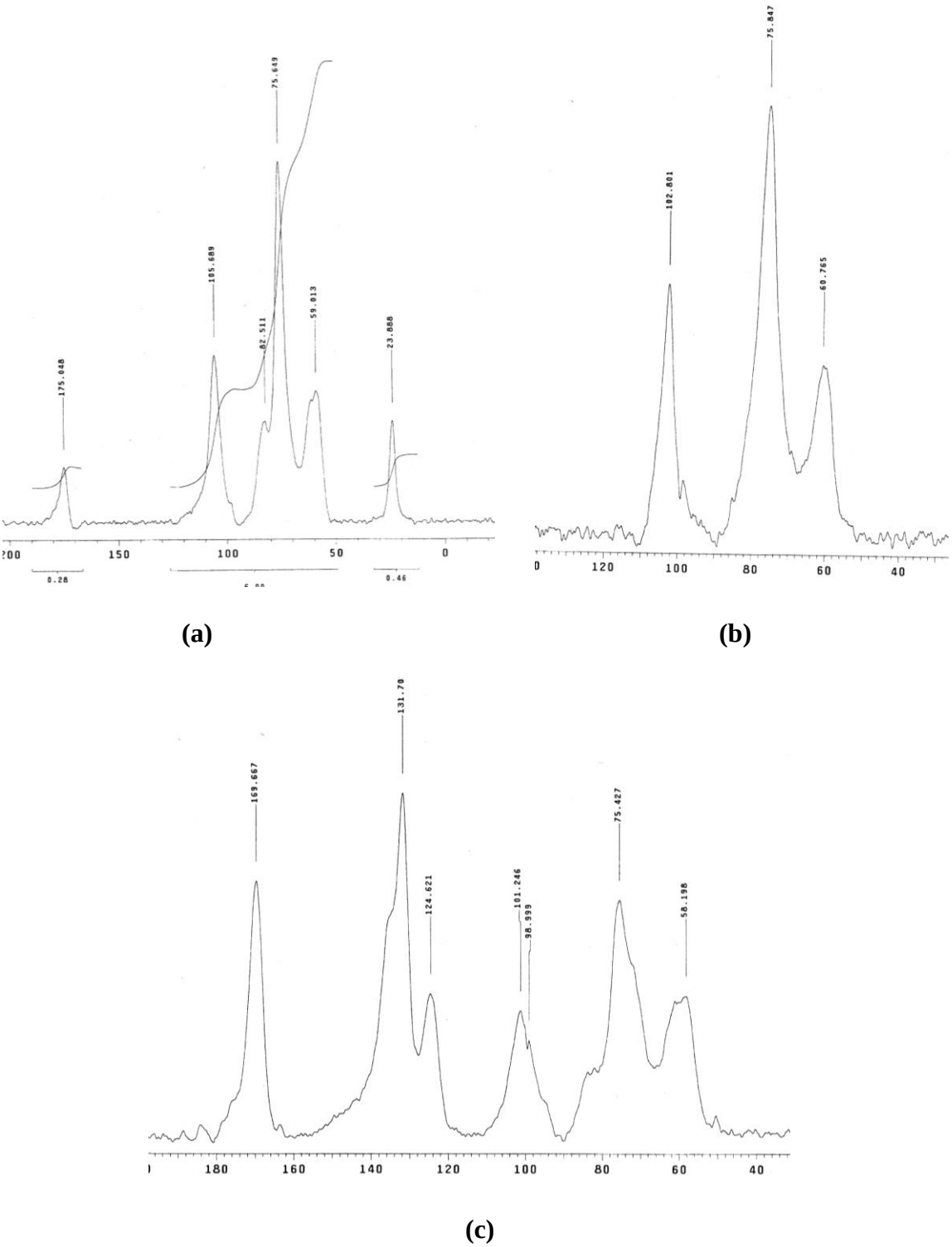

Figure 4.2: ^{13}C NMR of a) Commercially available chitosan, b) Deacetylated chitosan, c) Phthaloylated chitosan.

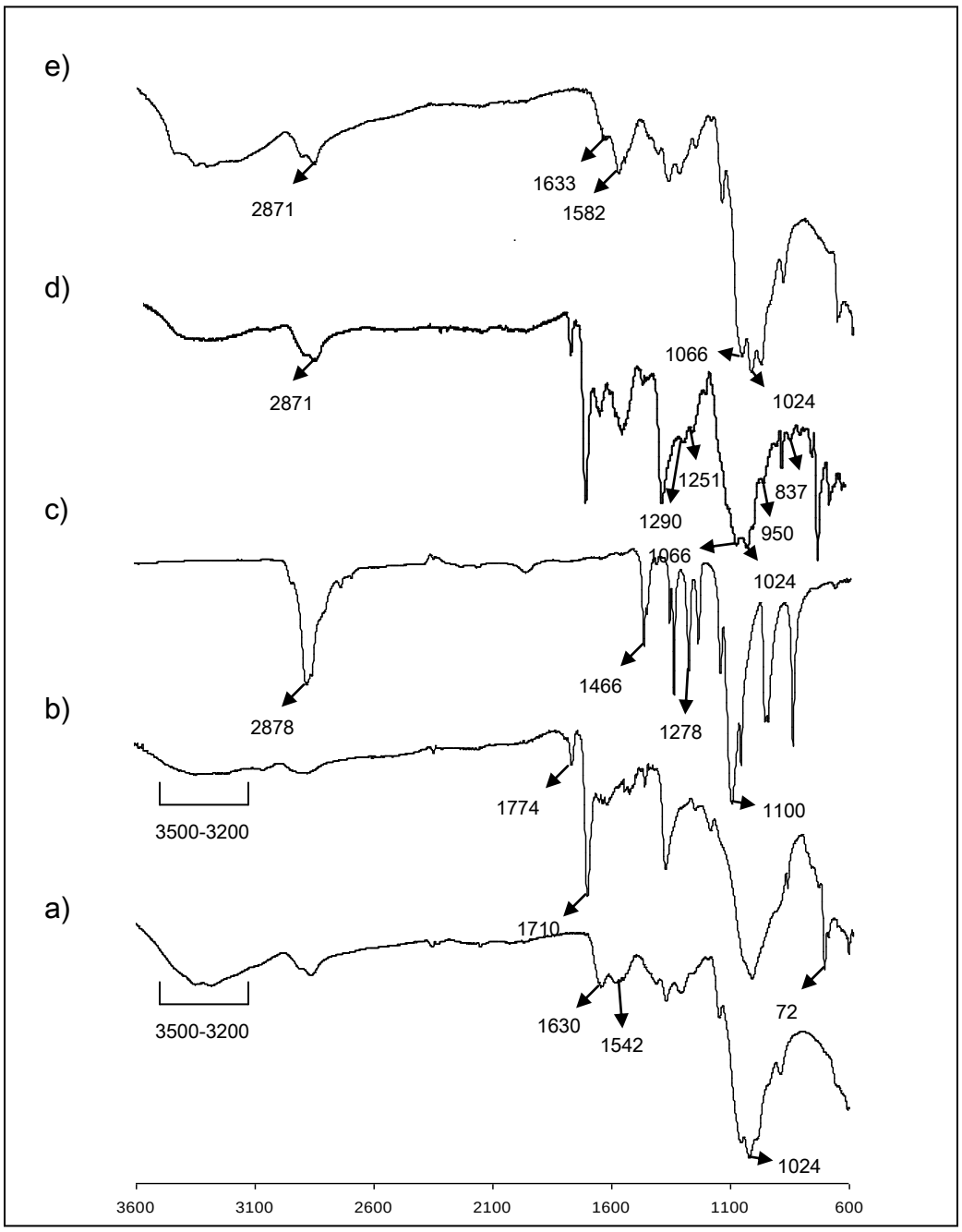

Figure 4.3: Fourier transform infrared spectra of the chitosan intermediates and O-PEGylated chitosan: A) deacetylated chitosan; B) phthaloylated chitosan: peaks at 1774 cm^{-1} and 1702 cm^{-1}. The OH groups of phthaloylated chitosan was chlorinated using thionyl chloride, represented by the reduction in peak: from 3500 to 3200 cm^{-1}; C) OH-PEG-OCH3, M.W. 5,000; D) 6-O-PEG-g-2-N-phthaloyl chitosan; E) PEG-grafted chitosan: disappearance of peaks 1774 cm^{-1} and 1702 cm^{-1}.

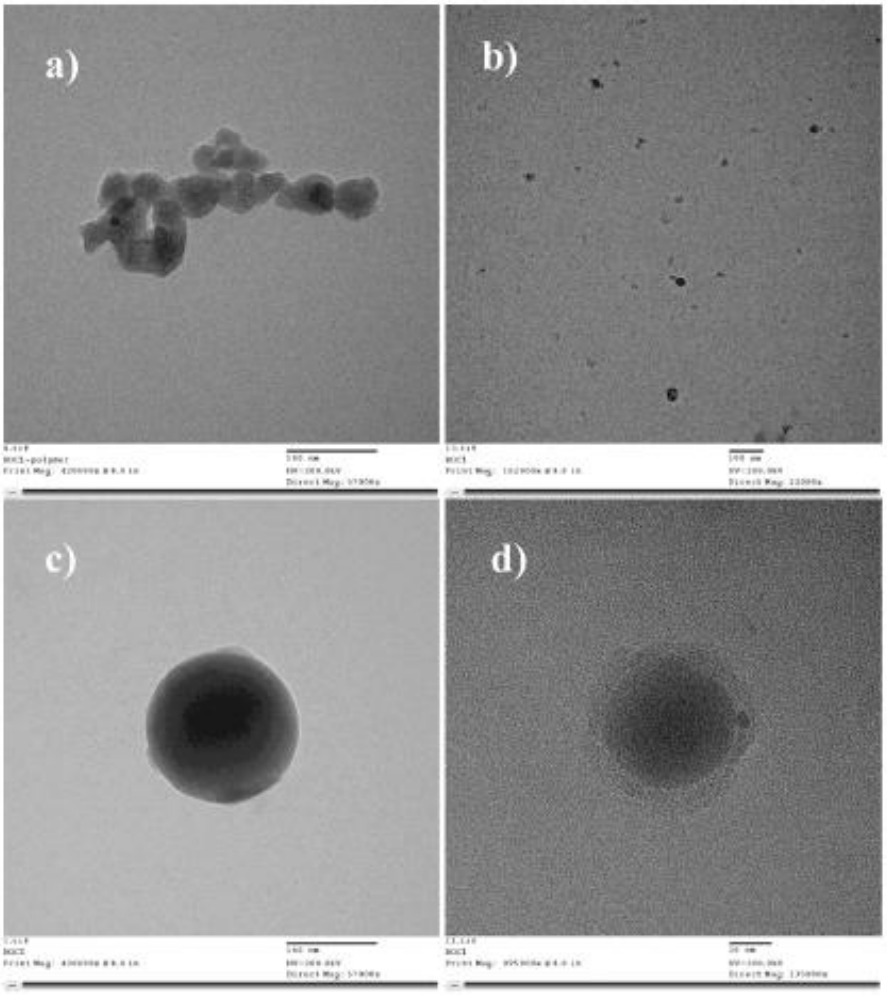

Figure 4.4: TEM images of a) PEGylated chitosan polymer (mag. 57,000×); b) chitosan–TPP nanoparticle (mag. 22,000×); c) PEGylated chitosan–TPP nanoparticle (mag. 57,000×) and d), PEGylated chitosan-TPP nanoparticle (mag. 135000×).

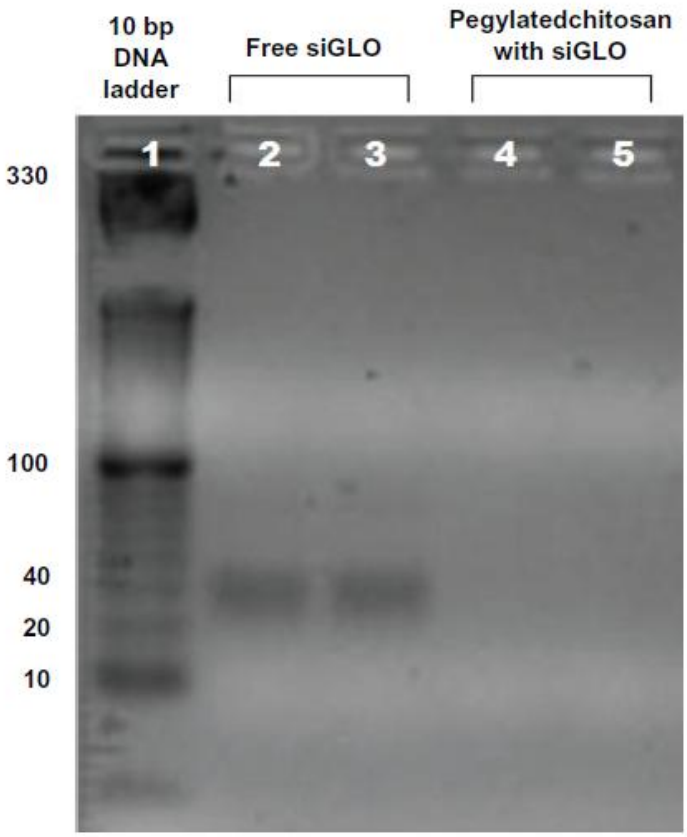

Figure 4.5: Gel retardation assay: lane 1) control 10 bp DNA ladder; lane 2 and 3 control siGLO, and lane 4 and 5 are PEGylated chitosan complexed siGLO at an N:P ratio of 103. In all groups the siGLO concentration was kept constant at 6 μg/mL. The disappearance of the band size at 40 bp in PEGylated chitosan complexed siGLO (lanes 4 and 5), compared to siGLO control (lanes 2 and 3), indicates the complete complexation of the siGLO.

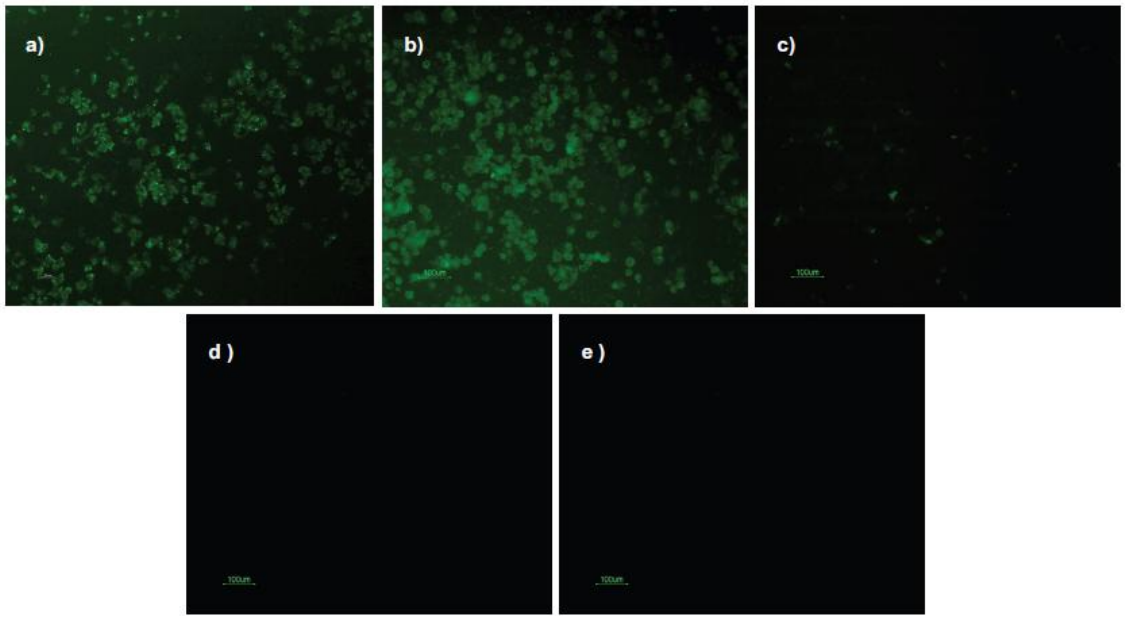

Figure 4.6: Transfection efficiency of nanoparticles on Neuro2a cells after 4 hours of incubation at 37°C and 5% CO2: a) PEGylated-chitosan-TPP:siGLO nanoparticles; b) chitosan-TPP:siGLO nanoparticles; c) siGLO only (negative control); d) chitosan-TPP nanoparticles (negative control); e) cells only (negative control).

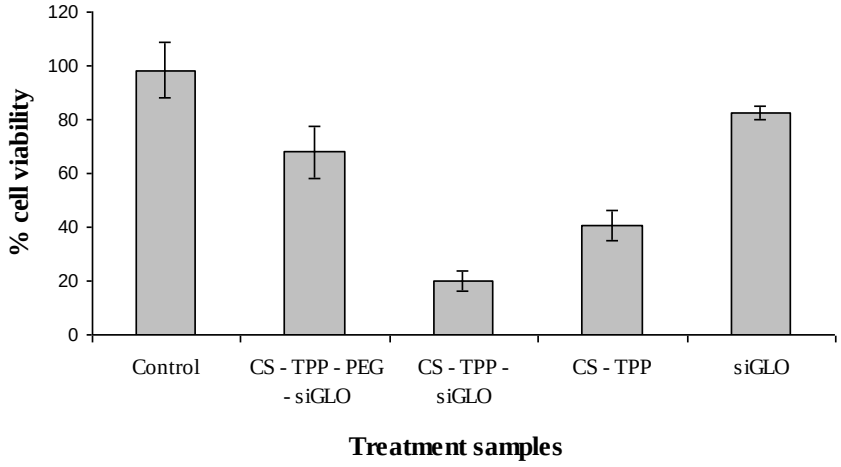

Figure 4.7: Designed CS-TPP-PEG-siGLO nanoparticle cytotoxicity was investigated using Neuro2a cells. For the experiment, various control nanoparticle formulations were used, the Neuro2a cells were exposed for 4 hours and cell viability was evaluated using spectrophotometer at 490 nm using standard MTS assays (n = 3).

Original article 3

CHAPTER 5: SYNTHESIS OF TAT PEPTIDE TAGGED PEGYLATED CHITOSAN NANOPARTICLES FOR SIRNA DELIVERY TARGETING NEURODEGENERATIVE DISEASES

Meenakshi Malhotra, Catherine Tomaro-Duchesneau and Satya Prakash*

Biomedical Technology and Cell Therapy Research Laboratory
Department of Biomedical Engineering, Artificial Cells and Organs Research Center
Faculty of Medicine, McGill University
3775 University Street, Montreal, Quebec, H3A2B4, Canada

*Corresponding author: Tel: 514-398-2736; Fax: 514-398-7461,
Email: satya.prakash@mcgill.ca

Preface: The PEGylated nanoparticles formed though were efficient for transfection and had reduced toxicity but were not suitable for specific targeting to be used in-vivo. Towards this goal, this chapter describes another novel synthesis scheme, wherein the chitosan polymer was surface grafted with PEG and was further tagged with a cell penetrating peptide, TAT, which was used as a model peptide, to form multifunctional nanoparticles. The synthesis was successfully performed and characterized by FTIR and NMR and nanoparticles were formed as described in chapter 3. These nanoparticles were then tested for transfection, cytotoxicity and their ability to deliver a functional siRNA in Neuro2a cells.

Article published in ***Biomaterials.*** **2013; 34,4:1270-1280**
http://dx.doi.org/10.1016/j.biomaterials.2012.10.013

5.1 Abstract

Delivery of therapeutic molecules to the brain for the treatment of Neurodegenerative diseases is a challenging task. This manuscript introduces a novel scheme of synthesizing peptide-tagged PEGylated chitosan polymer to develop nanoparticles for siRNA delivery for use in ND. Specifically, this manuscript proposes a facile chemoselective conjugation of monomethoxy PEG, at the C2 hydroxyl group of chitosan polymer, with conjugation of PEG to a cell-penetrating peptide, Trans-Activator of Transcription. The synthesized Chitosan-PEG-TAT polymer was used to form the nanoparticles of approximately 5 nm, complexing siRNA to be delivered in neuronal cells (Neuro 2a), with no/minimal toxicity. The various intermediates and the final product formed during the synthesis were characterized using ^{1}H Nuclear Magnetic Resonance and Fourier Transform Infrared Spectroscopy spectra. The morphological and size details of the nanoparticles were studied using Transmission Electron Microscopy. The nanoparticles were tested to deliver a functional siRNA against the Ataxin-1 gene in an in-vitro established model of a ND Spinocerebellar ataxia (SCA1) over-expressing ataxin protein. The results indicate successful suppression of the SCA1 protein following 48 hrs of transfection. Result of this study has potential in ND like SCA, Parkinson's, Alzheimer's and others.

Keywords: Chitosan, PEG, cell penetrating peptide, chemoselective conjugation, cationic polymer, TAT, siRNA, ataxia, nanoparticles, gene delivery

5.2 Introduction

Neurodegeneration is characterized by the progressive loss of structure and function of neurons. One among many neurodegenerative diseases is Spino Cerebellar Ataxia (SCA), characterized by loss of cells in the cerebellum and spinal cord affecting motor coordination, posture and balance. The international prevalence of SCA is estimated to be 0.3 to 2.0 per 100,000 [252]. SCA is caused by polyglutamine trinucleotide repeat expansion, CAG repeat and forms an abnormal/mutant protein when the CAG repeat unit is above the threshold level, i.e. approximately 35 repeat units [253]. The abnormal protein then accumulates in the Purkinje cells of the brain and also cytoplasm, dendrites and axonal processes [253]. A recent review by our group highlights the different subtypes of SCA and the current therapeutic methods and drugs used to alleviate the symptoms of this disease [253]. The reason for the absence of available medication could be attributed to the genetic problem associated with it. In the case of SCA, the cell production of poly glutamine cannot be halted as it would interfere with the function of the brain cells and, thus, would produce side effects which may in turn require further treatment. However, certain drugs like Deferipone and Idebenone [254] have reached phase II and III clinical trials, respectively, but are limited to Friedreich's ataxia (Autosomal Recessive Cerebellar Ataxia). Several other reports on the active and completed clinical trials of other related neurodegenerative diseases can also be found at clinicaltrials.gov.

RNA interference technology has been demonstrated as an effective therapeutic modality *in vivo* for the reduction of pathological molecules in neurons, for the treatment of SCA [255]. The other therapeutic targets that have been successfully inhibited with siRNA include ion channels [43], growth factors [256] growth factor receptors [257] and transcription factors [258]. The currently used drug/therapeutic delivery strategies such as implantation of catheters, intra-carotid infusions, surgeries and chemotherapies are invasive in nature and pose a greater risk of post-surgical complications like fluid retention in the ventricles etc, which lead to fatal side-effects. It has been estimated that up to 98% of the newly developed small molecules do not cross the blood-brain barrier [135]. Moreover, it is challenging to achieve sufficient distribution and diffusion of the

therapeutic drug within the brain. Although viral gene therapy vectors are the most efficient vectors available [255] concerns about their safety and immunogenicity [259] have triggered investigations of non-viral delivery systems. Thus, a need to develop an alternative non-invasive and targeted therapeutic delivery strategy exist which can cross/bypass the BBB.

The current research focuses on developing a scheme to synthesize non-viral, receptor-targeted nanoparticle formulation for the delivery of siRNA molecules capable of targeting neuronal cells. The scheme utilizes and preserves the unique characteristic of each component (Chitosan, PEG and a CPP). Chitosan is a polycationic polymer that has been regarded as a non-toxic [260], biodegradable [261] and biocompatible [262] polysaccharide. Due to the presence of primary amine groups, it is only soluble in dilute acids. The presence of free amine groups helps in complexing the negatively charged therapeutic molecules simply by ionic interactions. The free amine groups also help in cellular uptake of chitosan-derived nanoparticles, leading to a "proton sponge effect" in the endosomal compartment. The cationic biodegradable polymers are usually surface coated with hydrophilic polymers like PEG. PEG has been extensively used in biomedical and pharmaceutical applications because it is hydrophilic, non-toxic, non-antigenic and non-immunogenic [263]. PEG, helps eliminate phagocyte capture, providing better serum stability and extended blood circulation with low toxicity.

Many studies have conjugated PEG with amine groups of chitosan in view of improving its solubility in both aqueous as well as organic solvents [213, 264]. The most extensively used is α-Monomethoxy, ω-hydroxy PEG (MeO-PEG). The use of a monofunctional PEG is important to avoid crosslinking reactions between the two polymers [265]. Whereas, a bifunctional PEG serves as a linker for conjugating two different compounds, being neutral in charge, it reduces the steric-hindrance of the charged polymers and thus enables the efficient conjugation of two compounds linked on either side. However, PEG increases the blood clearance times of the nanoparticles but at the same time compromises its transfection efficiency, as PEG masks the overall charge on the surface of chitosan polymer. Therefore, a cationic CPP/CTP is required to interact

with the negatively charged cell surface proteoglycans [266]. The transfection efficiency of many other delivery vehicles apart from chitosan have been shown to improve with the incorporation of functional groups, such as targeting ligands or Nuclear localization signal (NLS) peptides [267].

This paper proposes a step-wise protocol for synthesizing peptide-tagged PEGylated chitosan, wherein PEG acts as a linker between chitosan and a CPP. We have employed the use of TAT oligopeptide, as a model CPP, covalently conjugated to the chitosan-PEG copolymer. The basic domain of TAT peptide (RKKRRQRRR) is comprised of arginine and lysine amino acid residues that can play an important role in the translocation across biological membrane due to its strong cell-adherence and is independent of receptors and temperature [268]. TAT has been shown to destabilize the lipid bilayer of the cell membrane through an energy independent pathway carrying hydrophilic or macromolecules as large as several hundred nanometers in size across the plasma membrane [269]. The current study shows the efficiency of TAT peptide tagged PEGylated chitosan nanoparticles formed after step-wise chemo-selective synthesis process, to deliver siRNA in neuronal cells and cause a therapeutic effect by suppressing the Ataxin 1 protein.

5.3 Materials and Methods

5.3.1 Materials

LMW chitosan was obtained from Wako (Richmond, VA, USA), having a viscosity of 5~20cP and degree of deacetylation of 80.0%. mPEG (M.W. 2,000), phthalic anhydride, pyridine, toluene, hydrazine monohydrate, succinic anhydride, ethanethiol, aluminum chloride, TPP and glacial acetic acid of analytical grade were obtained from Sigma (Oakville, ON, Canada). Anhydrous N,N-Dimethylformamide (DMF), 1-ethyl-3-[3-dimethylaminopropyl]carbodiimide hydrochloride (EDC), 4-(Dimethylamino) pyridine (DMAP), sodium hydroxide (NaOH), methanol, diethyl ether, chloroform and concentrated hydrochloric acid were obtained from Thermo Fisher Scientific (Ottawa, ON, Canada). Thionyl chloride ($SOCl_2$) was obtained from VWR (Mississauga, ON,

Canada). TAT peptide (NH_2-RKKRRQRRR) M.W. 1339.63 was synthesized by the Sheldon Biotechnology Centre, McGill University. Mouse Neuro2a cells and EMEM media were obtained from Cedarlane laboratories (Burlington, Ontario, Canada). 3-(4, 5-Dimethyl-2-thiazolyl)-2, 5-diphenyl-2H-tetrazolium bromide (MTS) cytotoxicity assay kit was obtained from Promega (Madison, WI, USA). Subcloning DH5-alpha competent cells and Lipofectamine 2000 were obtained from Invitrogen (Burlington, ON, Canada). pEGFP.ataxin1 (E3-82Q) plasmid is obtained from Dr. Zoghbi Huda from Baylor College of Medicine, Houston, TX, USA. Plasmid purification Maxi kit is from Qiagen (Mississauga, Ontario, Canada). Ataxin-1 siRNA (h), Ataxin-1(L-19) goat polyclonal antibody, Actin (I-19) goat polyclonal antibody and horse radish peroxide (HRP)-conjugated donkey anti-goat IgG antibody were procured from Santacruz Biotechnology (Santa Cruz, CA, USA). For dilution purposes ultra pure double distilled water (ddH_2O) was used from laboratory installed Barnstead Nanopure diamond™ water supply unit.

5.3.2 Synthesis of CSPH (phthaloyl chitosan)

Commercially available chitosan (CS) (1.00 g) was added to a solution of phthalic anhydride (PH) (2.76 g) in 20 ml of DMF. The mixture was stirred for 8 hrs at 110°C under nitrogen atmosphere. The resultant product **(c)** in **figure 5.1** was cooled to room temperature and precipitated in ice cold water [245]. The precipitate was filtered, washed with methanol overnight and vacuum dried.

5.3.3 Synthesis of mPEG-COCl

To 10 % solution of mPEG (M.W. 2000) in toluene, 4 molar excess of succinic anhydride dissolved in pyridine was added drop wise. The above reaction was set up under anhydrous conditions and refluxed for 6 hours. The product was precipitated with ether, filtered and again re-precipitated twice with chloroform and diethyl ether and finally vacuum dried. The final product obtained **(a)**, is shown in **figure 5.1**. To mPEG-COOH obtained, 2 fold molar excess of $SOCl_2$ was added under N_2 atmosphere. The reaction was refluxed to boil for 6 hours, followed by degassing to remove excess SO_2 and thionyl chloride. The product was marked as **(b)** in **figure 5.1**.

5.3.4 Synthesis of CSPH-O-mPEG (PEGylating phthaloyl chitosan)

Phthaloyl chitosan (CSPH) (300 mg), product **(c)**, was soaked in pyridine solution overnight and added to mPEG acylchloride (10 g), product **(b)**, in toluene. The reaction was stirred for 2 hours at room temperature and then refluxed to boil for 24 hrs [249]. The resultant product was allowed to cool to room temperature, precipitated in methanol and vacuum dried to yield product **(d)** in **figure 5.1**.

5.3.5 Synthesis of CSPH-PEG-TAT (Tagging TAT on PEGylated phthaloyl chitosan)

To conjugate TAT peptide onto PEGylated phthaloyl chitosan, the methoxy group of PEG was converted to hydroxyl group by following the procedure, as aforementioned [270]. In brief, equi-molar ratios of CS-mPEG and aluminum chloride were reacted together for 12 hrs at room temperature (RT) in 20 ml of ethanethiol. The reaction mix was diluted with water, acidified with 10% HCl, filtered and extracted thrice with dichloromethane to yield product **(e)** in **figure 5.1**. The hydroxyl groups were further converted to carboxyl groups by reacting it with 4 molar excess of succinic anhydride in toluene at 100°C for 12 hrs. The product obtained as **(f)** in **figure 5.1** was cooled to room temperature, precipitated with methanol, filtered and vacuum dried. The carboxylic groups of this product **(f)** i.e. CS-PEG-COOH (12 mM) was conjugated to the equi-molar ratio of TAT-NH_2 peptide (12 mM) in the presence of EDC (15.5 mM) and DMAP (1.2 mM) in 1 ml of DMF at RT for 24 hrs. This reaction mix was dialyzed against deionized water for 2 days, using a dialysis tube with a molecular weight cut-off of 3,500 Da. The resultant product **(g)** was obtained as shown in **figure 5.1**.

5.3.6 Synthesis of CS-PEG-TAT (deprotecting amine groups on chitosan)

As a last step of the synthesis, the amine groups of chitosan were deprotected using 4% (w/v) hydrazine monohydrate in DMF. The reaction was carried out at 100°C for 1 h under inert conditions. The mixture was allowed to cool to room temperature and was dialyzed against deionized water for 2 days, using a dialysis tube with molecular weight cut-off of 3,500 Da. Following dialysis, the sample was vacuum dried and marked as product **(h)** in **figure 5.1**.

5.3.7 Polymer characterization

The polymer CS-PEG-TAT was characterized and analyzed at every step of its derivation through FTIR (Perkin Elmer Spectrum BX), ^{13}C NMR (Varian 300 MHz broadband NMR) and ^{1}H NMR (Mercury 400 and 500 MHz NMR) and Transmission Electron Microscopy (Philips EM410 TEM).

5.3.8 Preparation of siRNA complexed CS-PEG-TAT nanoparticles

The obtained CS-PEG-TAT polymer was dissolved in ddH_2O at pH 5.0, and concentration of 0.5 mg/ml. To ensure maximum dissolution of the polymer, the solution was heated at 60°C and sonicated followed by stirring for 60 min. Before nanoparticle formation the polymer solution was filtered using 0.8 µm filter. The nanoparticles, complexing siRNA were prepared, as described in chapter 5 at an N:P ratio of 103. The nanoparticles obtained were viewed under TEM.

5.3.9 Plasmid Purification - ataxin -1 cDNA

The plasmid DNA containing ataxin -1 cDNA , purified and resuspended in Tris-EDTA buffered solution [pGFP-ataxin (Q82)] was a kind gift from Dr. Zoghbi Huda (Baylor college of medicine, Houston, TX, USA), and was used for the transformation experiment in DH5-alpha competent cells by means of chemical transformation also known as heat-shock transformation. The procedure for chemical transformation was followed according to the manufacturer's protocol (Invitrogen). The colony selective antibiotic for pGFP-ataxin was kanamycin (30 µg/mL). Stock cultures of transformed plasmid in DH5-alpha cells were made in sterilized 80% glycerol and were stored at -80°C. Plasmid purification was performed following the protocol of Qiagen's maxi kit. The purified plasmid obtained was quantified for its concentration and purity. The percentage purity of the plasmid was quantified using UV spectrophotometer. The ratio of Abs 260/280 obtained was 1.8 which signifies that the plasmid was purified and the concentration obtained was 266 µg/ml for pEGFP.ataxin1.

5.3.10 Cell study

Cell study with respect to transfection efficiency of the nanoparticles encapsulating siGLO red (Cy5-labelled transfection indicator) and cellular toxicity of nanoparticles using MTS assay was performed on mouse neuroblastoma cells (Neuro 2a).

5.3.10.1 Transfection efficiency of siRNA loaded nanoparticles on Neuro2a cells

The transfection studies were performed on mouse neuroblastoma cells (Neuro2a). The cells were allowed to reach 85% confluency sub-culture and seeding in a 96 well plate at a density of 20,000 cells per well. Twenty four hours before transfection, cell seeding was carried out with 200 µl of complete growth media (antibiotics-free EMEM with 10% serum) in each well. Following 24 hrs, the transfection media containing 100 µl of serum-free medium along with 50 µl of sample was added onto the cells. The different tested samples were: chitosan nanoparticles encapsulating siGLO-red and chitosan-PEG-TAT nanoparticles encapsulating siGLO-red The cells were then incubated at 37°C, 5% CO_2 for 4 hours, after which the cells were replaced with fresh complete media (with FBS). After 24 hrs, the cells were observed under a fluorescence microscope (Nikon Eclipse TE2000-U) at a wavelength of 660 nm. The property of siGLO-red as a transfection indicator gene, allows it to fluoresce inside the cell, enabling them to be viewed under a fluorescent microscope.

5.3.10.2 Cytotoxicity analysis

The cytotoxicity assay was performed on seeded cells following 4 hrs of transfection in 96 well plate. The transfection media was removed following 4 hrs and the cells were replenished with 100 µl of fresh serum-free media, to which 20 µl of MTS reagent was added and the cells were again incubated for another 4 hours at 37°C in 5% CO_2 incubator. The absorbance was measured using Varian multiplate reader set at 490 nm.

5.3.10.3 Over-expression of ataxic protein in Neuro2a cells and its suppression

Transfection studies were performed using a functional siRNA against the ataxin gene. 100,000 cells were seeded in a 12 well plate and were incubated for adherence for

24 hrs at 37°C, 5% CO_2. After 24 hrs, the cells were transfected with ataxin plasmid at a concentration of 250 ng/µl using lipofectamine. Optimal transfection efficiency with lipofectamine was determined experimentally. Following 6 hrs of transfection, the media was replaced with complete growth EMEM medium containing 10% FBS. Atxn-siRNA (Santacruz Biotechnology) was complexed with chitosan-PEG-TAT nanoparticles, as described in section 5.3.8. After 24 hrs, 40 µM per well of siRNA complexed with nanoparticles was used to transfect neuronal cells. Again, the transfection media was replaced with complete growth EMEM medium containing 10% FBS. Empty nanoparticles and nanoparticles containing scrambled siRNA were used as positive controls. The cells were harvested for ataxin protein estimation after 24 and 48 hrs.

5.3.11 Protein extraction and Western blot

Cultured cells were washed twice with cold PBS and lysed using 1% nonyl phenoxypolyethoxylethanol-40 (NP40) prepared in 50 mM Tris (pH 8.0), 150 mM NaCl, 5 mM EDTA lysis buffer; premixed with 2x sodium dodecyl sulfate (SDS) sample buffer (125 mM Tris· HCl, pH 6.8; 4% SDS; 20% glycerol; 100 mM Dithiotreitol (DTT), and 0.2% bromophenol blue) at 4°C on an orbital shaker. The cells were scrapped after 20 min (on ice). The extracted protein samples were heated at 70-100°C for 10 min, before loading on gels. The western blot was performed according to manufacturer's protocol (Invitrogen). Pre-cast Nupage Tris-Bis (4-10%) gels were used for running the protein samples. Magic mark 1Kb protein ladder was used as a standard. The gel was electrophoretically transferred to a nitrocellulose membrane using SemiDry blot apparatus (Invitrogen). The membrane was incubated for 1 hr in 5% non-fat powdered milk in 0.2% Tris buffered saline – tween (TBST). The membrane was then incubated overnight with goat ataxin-1 ImmunoglobulinG (IgG) polyclonal antibody (1:5,000 dilution; Santacruz Biotechnology). After three washes in TBST, the membrane was incubated with horseradish peroxidase (HRP)-conjugated donkey anti-goat IgG antibody (1:2,000 dilution; Santacruz Biotechnology). The membranes were then washed three times in TBST followed by detection of signal with a chemiluminescence detection kit (Roche). To control the protein loading, the membrane was stripped at 60°C using

stripping solution (10 mM β-mercaptoethanol, 2% SDS, and 62.5 mM Tris·HCl, pH 6.8) before reprobing with antibody to α-Actin (1:10,000; Santa Cruz Biotechnology).

5.3.12 Statistical analysis

Values are expressed as means ± Standard Deviation. Statistical analysis was carried out using SPSS Version 17.0 (Statistical Product and Service Solutions, IBM Corporation, New York, NY, USA). Statistical comparisons were carried out by using Tukey's post-hoc analysis. Statistical significance was set at $p < 0.05$ and *p*-values less than 0.01 were considered highly significant.

5.4 Results

5.4.1 Synthesis of CSPH (phthaloyl chitosan)

The commercially available chitosan polymer with DA of 80% was first protected with phthalic anhydride in order to protect the amine groups. This is the key step in carrying forward any further chemical reactions with chitosan, as chitosan being soluble only in acidic conditions becomes soluble in most organic solvents such as dimethylsulfoxide (DMSO), DMF, THF, Pyridine etc. following protection with phthalic anhydride. ^{13}C NMR data confirms successful N-phthaloylation of the product. Product **(c)** in **figure 5.1** shows the schematic representation of the N-phthaloyl chitosan. The Total Suppression of Side bands (TOSS) mode exhibit peaks at 124.62 ppm, 131.70 ppm, 134.42 ppm corresponding to phenylene, and 169.66 ppm and carbonyl group of phthaloyl group and the TOSS and dipolar dephasing (TOSDL) mode confirms the absence of CH and CH_2 peaks due to their short relaxation time and presence of only two peaks 131.63 ppm and 169.89 ppm assigned to C 1, 2 and carbonyl of phthaloyl group respectively. The infrared (IR) data shows distinct sharp peaks at 1774 cm^{-1} and 1702 cm^{-1} corresponding to the imide of phthaloyl group in **figure 5.2**. The phthaloyl chitosan prepared by this method becomes gel-like when precipitated in water, which supports the data shown by Kurita, of formation of a uniform structure of phthaloylated chitosan [245].

^{13}C CP/MAS NMR: (TOSS mode): δC 58.19 (C-2), 61.76 (C-6), 72.44 (C-3), 75.42 (C-5), 83.91 (C-4), 101.24 (C-1), 124.62, 131.70, 134.42 (Phth phenylene), and 169.66 (Phth C=O); (TOSDL mode): δC 131.63 (Phth C-1,2) and 169.89 (Phth C=O).

FTIR: ν_{max}/cm^{-1} 3200-3400 (OH), 1774, 1710 (carbonyl anhydride), 1150-1000 (pyranose), and 720 (arom).

5.4.2 Synthesis of mPEG-COCl

The monomethoxy PEG (OH-PEG-OCH_3) (M.W. 2,000) was converted to carboxyl ate-terminated PEG (COOH-PEG-OCH_3) by reacting monomethoxy PEG with four molar excess of succinic anhydride. **Figure 5.3** represents the IR spectra that shows the presence of carboxylic peak at 1732 cm^{-1}, confirming the presence of (-C=O) carbonyl groups on PEG. This product was further reacted with thionyl chloride to form PEG acyl chloride (COCl-PEG-OCH_3) (product **b** in **figure 5.1**) as an active intermediate of PEG to be further conjugated to hydroxyls of 2-*N*-phthaloyl chitosan (Product **c** in **figure 5.1**).

FTIR: ν_{max}/cm^{-1} 1732 (C=O), 2878 (C-H stretching), 1100 (C-O stretching).

5.4.3 Synthesis of CSPH-O-mPEG (PEGylating phthaloyl chitosan)

The FTIR spectra in figure 4 shows PEG grafted phthaloylated chitosan with characteristic peaks at 2921 cm^{-1} (C-H stretching), 1066 cm^{-1} (C-O stretching), 1491, 1451 and 1254 belong to PEG. Also the reduction in hydroxyl peaks of chitosan at 3500 cm^{-1}, indicates the grafting of PEG onto chitosan forming 2-N-phthaloyl chitosan-O-MPEG, product **(d)** in **figure 5.1**.

FTIR: ν_{max}/cm^{-1} 2873 (C-H stretching), 1068 (C-O stretching) of PEG, 1774, 1710 (carbonyl anhydride) and 720 (arom) of phthalimido group on chitosan.

5.4.4 Synthesis of CSPH-PEG-TAT (Tagging TAT on PEGylated phthaloyl chitosan)

To attach a ligand or a cell penetrating peptide, NH_2-TAT on PEG, demethylation was performed on 2-*N*-phthaloyl chitosan-*O*-MPEG to obtain 2-*N*-phthaloyl chitosan-*O*-PEG, product **(e)** as shown in **figure 5.1**. This was performed by following steps as

mentioned previously by Lin et al. [270]. This step was performed in order to obtain a reactive form of PEG that facilitates the further conjugation of compounds. The product **(e)** was further reacted with four molar excess of succinic anhydride under similar conditions as before. The formation of the carboxyl group at the other end of the PEG conjugated to phthaloyl chitosan enables the attachment of amine terminated TAT peptide to yield product **(f)** as show in **figure 5.1**. The IR spectra in figure 4 shows the appearance of a new peak at 1636 cm^{-1} that shows the presence of amide bonds and confirms the conjugation of TAT peptide onto the polymer forming 2-*N*-phthaloyl chitosan-*O*-PEG-*CONH*-TAT, product **(g)** in **figure 5.1**.

FTIR: ν_{max}/cm^{-1} 2919 (C-H stretching), 1067 (C-O stretching) of PEG, 1774, 1710 (carbonyl anhydride) and 720 (arom) of phthalimido group on chitosan, 1659 (amides) in TAT peptide.

5.4.5 Synthesis of CS-PEG-TAT (deprotecting amine groups on chitosan)

The final step following TAT tagging was the deprotection of the amine groups from chitosan. This was successfully achieved by treating the 2-*N*-phthaloyl chitosan-*O*-PEG-*CONH*-TAT with 4% hydrazine monohydrate solution in DMF. Hydrazine monohydrate being basic in nature causes the destabilization of the phthaloyl moiety by creating an excess alkaline condition of pH > 12. The resultant product **(h)** as represented in **figure 5.1** was obtained. The removal of the phthaloyl group from the polymer was confirmed by FTIR, where the absence of peaks at 1774 cm^{-1} and 1710 cm^{-1} confirmed the complete dissociation of the phthalimido group from chitosan. It was observed that the reaction conditions followed in the scheme had no deleterious effects on any of the previous bonds formed. The peak representing the presence of amides due to TAT peptide shifts from 1659 cm^{-1} to 1644 cm^{-1} and the peak at 1582 cm^{-1} (amide II) belongs to the chitosan. The peaks at 2918 cm^{-1} and 1061 cm^{-1} refer to the presence of (CH_2) groups and (C-O stretch) of PEG respectively as observed in **figure 5.4.** The final product was dialyzed for 2 days against deionized water in order to get rid of any impurity or byproduct left from the reaction.

FTIR: ν_{max}/cm^{-1} 2918 (C-H stretching), 1061 (C-O stretching) of PEG, 1644 amides of TAT peptide, and 1543 (amides) in chitosan.

5.4.6 Polymer characterization by ^{1}H NMR

Figure 5.5 represents the ^{1}H NMR spectra of 2-*N*-phthlaoyl chitosan **(figure 5.5a)**, 2-*N*-phthlaoyl chitosan-*O*-mPEG **(figure 5.5b)**, 2-*N*-phthaloyl chitosan-*O*-PEG-*CONH*-TAT **(figure 5.5c)** and chitosan-*O*-PEG-*CONH*-TAT **(figure 5.5d)**. The chemical shift at δ 7.78 belongs to the aromatic protons of the phthaloyl moiety, which is present in the spectra of 2-*N*-Phthaloyl chitosan-*O*-mPEG, 2-*N*-phthaloyl chitosan-*O*-PEG-*CONH*-TAT but disappeared in chitosan-*O*-PEG-*CONH*-TAT spectrum. The multiple peaks of oxymethyl groups in PEG at δ 3.3 to 3.7 cover the signals of the pyranose ring of chitosan in all three spectras. The weak and broad peak at δ 4.3 - 4.5 were from the protons of –NH-CH(CH_2)-CO- in the TAT peptide, as observed in the spectrum of 2-*N*-phthaloyl chitosan-*O*-PEG-*CONH*-TAT. The peak at δ 2.7-2.8 is from the protons of –CH_2-NH-NH-NH_2 in arginine and the weak and multiple peaks at δ 1.3-1.7 are from the –CH_2-CH_2-CH_2-NH-NH-NH_2 in arginine as observed in spectra 2-*N*-phthaloyl chitosan-*O*-PEG-*CONH*-TAT and chitosan-*O*-PEG-*CONH*-TAT . The multiple peaks at δ 7.0-8.0 belong to the amines in the TAT peptide sequence (**figure 5.5e**).

5.4.7 Preparation of siRNA complexed CS-PEG-TAT nanoparticles

Figure 5.6 represents TEM images of the polymer chitosan-O-PEG-CONH-peptide dissolved in dilute acetic acid at pH 6 and a concentration of 0.5 mg/ml, sonicated for 10 min before being observed under the TEM. **Figure 5.6a** shows nanoparticles formed with the modified Chitosan-PEG-peptide polymer, without siRNA, using TPP as a crosslinker. The nanoparticles range in the size of 50-100 nm. **Figure 5.6(b)** and **5.6(c)** represent nanoparticles formed with unmodified chitosan complexing siRNA and Chitosan-PEG-peptide polymer complexing siRNA respectively. On encapsulating siRNA, the nanoparticles obtained from chitosan-PEG-peptide polymer were smaller than 5 nm and appeared more spherical and monodispersed, as compared to the particles obtained by unmodified chitosan polymer, which were 20-50 nm and non-spherical.

5.4.8 Cell study

Figure 5.7b and **5.7d** represent 100% transfection efficiency, achieved with both unmodified chitosan nanoparticles and chitosan-PEG-TAT nanoparticles encapsulating siGLO-red. The nanoparticle treatment was replaced by fresh media after 4 hrs and the fluorescence at a wavelength of 660 nm was observed after 24 hours. The cells' morphology as observed under bright field revealed that the cells treated with unmodified chitosan nanoparticles (**figure 5.7a**) were stressed as compared to the cells treated with nanoparticles formed from chitosan-PEG-TAT polymer (**figure 5.7c**). The quantitative and comparative analysis of the cellular toxicity of the two nanoparticle formulations were also tested using the MTS assay, which proved that unmodified chitosan nanoparticles were highly toxic on cells as compared to modified chitosan-PEG-TAT nanoparticles ($p = 0.00004$) (**figure 5.8**). The modified chitosan-PEG-TAT nanoparticles did not induce any significant toxicity when compared to the untreated cells ($p = 0.507$).

5.4.9 Protein extraction and Western blot

Neuro2a cells, over-expressing Ataxin 1 protein, in-vitro were established prior to the treatment with nanoparticles. Suppression of ataxin protein by Atxn-siRNA delivered through chitosan-PEG-TAT nanoparticles is depicted in **figure 5.9**. The nanoparticle treatment was replaced after 4 hrs with complete fresh media and the cells were harvested after 24 and 48 hrs for protein quantification. Sample A was treated with nanoparticles without siRNA, Sample B had nanoparticles with Atx-siRNA and sample C had nanoparticles with scrambled siRNA, siGLO. The silencing was observed after 48 hours in sample B. A non-specific effect in downregulation of target with no or scrambled siRNA sample is also seen. This confirmed our hypothesis that nanoparticles prepared using the proposed synthetic scheme successfully and efficiently transfected functional siRNA causing suppression of ataxin protein in neuronal cells in-vitro.

5.5 Discussion

The BBB is characterized by tight junctions between cerebral endothelial cells that guard the selective diffusion of blood borne compounds from entering the brain [271]. However, small lipophilic molecules such as glucose, amino acids and gases

diffuse freely across the plasma membrane either via carrier-mediated or receptor-mediated mechanisms [272]. Thus, importing drugs or therapeutic molecules across the BBB is a major challenge for the treatment of neurodegenerative diseases. Most of the non-viral nanoparticles widely being accepted as an alternative approach to gene delivery are developed from polyethyleneimine (PEI) [54], chitosan [211], cyclodextrin polycations [57], poly- L Lysine [273] and polyamidoamines [274] to deliver siRNA for on-target gene silencing. The characteristic features encompassing the non-viral nanoparticles for an effective gene delivery system are: 1) the polymeric material should be inert and have low integration with the physiological system, 2) it should handle more payload, 3) can be modified with appropriate ligands for specific cell targeting, 4) be administrated repeatedly without fretting about delivery induced toxicity or immunogenicity, 5) should ideally be ≤100 nm in size with a positive surface charge, 6) should be able to overcome anatomical, biophysical and physiological barriers, 7) should be able to safe-guard the payload against degradative enzymes before reaching the targeted site and 8) be able to be administered non-invasively. As per these key features of non-viral nanoparticles, having a small size range is one of the key factors to cross the BBB. Lipid nanoparticles have been used for drug delivery, targeting the brain [275]; however, such formulations lack active targeting to the tissue of interest. Partridge has explained the use of monoclonal antibody as a targeting moiety on a non-viral liposome nanoparticle targeting the brain [276]. Various other BBB targeting antibodies have been detailed by Shusta et al. [277]. However, the high molecular weight of antibodies makes the overall size of the nanoparticles big, which acts as a hindrance to achieve optimal bio-distribution at the targeted site. In view of size, specific peptides, which have much smaller molecular weight as compared to antibodies have also been utilized as targeting ligands for brain delivery [278].

Chitosan is a cationic polymer, whose use has been widely explored in biomedical fields for its biological activities and neuroprotective properties, such as suppression of beta amyloid formation, acetyl cholinesterase inhibitory activity, anti-neuroinflammatory and anti-apoptotic activities [279]. A recent study demonstrates the use and characterization of chitosan nanoparticles loaded with dopamine for future application

towards PD [280]. Another study demonstrated the use of chitosan nanoparticles for targeted peptide delivery, such as caspase inhibitor Z-DEVD-FMK or a fibroblast growth factor to the brain [281]. In this study we used chitosan as a parent polymer to develop nanoparticles, surface grafted with PEG and a cell penetrating peptide, TAT. Chitosan derives its cationic property from the amine groups present at the C2 position of its pyranose ring. These amine groups are responsible for its solubility only in mild acidic conditions. Though, solubility of chitosan is a major challenge faced when utilizing it for biological applications, it can be controlled by specifically modifying/protecting the primary amine groups thereby making it soluble in solvents like DMSO, DMF, Pyridine, THF etc. [282]. In our study, we protected the amine groups of chitosan by using phthalic anhydride. This property enables it to take part in further chemical reactions. Most of the chitosan derivatives are derived from the chemical modification of NH_2 groups [236]. However, in this study, to form a nanoparticle formulation complexing siRNA, we have employed the use of monomethoxy PEG, a hydrophilic polymer, which was conjugated to the C6 hydroxyl groups of chitosan polymer. This protocol was adapted from Jian Du, et al. [249] with a modification of using phthaloyl chitosan. In their procedure they achieved N-substitution as well as O-substitution of chitosan with PEG as their objective did not require protecting primary amines of chitosan, whereas we attempted to obtain chemoselective O-substitution of PEG onto the chitosan [263]. This chemo-selective conjugation helps preserve the inherent nature of the cationic polymer by protecting its amine groups with phthalic anhydride [283]. In our previous study, we developed PEGylated chitosan nanoparticles via chemoselective O-substitution of PEG onto chitosan using sodium hydride (NaH) as a catalyst [283]. However, the current method does not incorporate the use of NaH in the synthesis because the current method yields a higher rate of PEGylated chitosan polymer than the previous method. The conjugation of a hydrophilic polymer (PEG) helps reduce the steric hindrance and cyto-toxicity of formed nanoparticles and also acts as a linker to further conjugate a CPP, (TAT), which was incorporated to enhance the cellular uptake profile of nanoparticles.

The polymer characterization in terms of pH, concentration and siRNA loading etc. was previously reported by us for preparing chitosan nanoparticles [243] and

therefore we used same optimized conditions for unmodified and modified chitosan-PEG-TAT nanoparticles. The TEM image in **figure 5.6** represent the nanoparticles developed before and after complexing siRNA with TAT tagged chitosan-PEG-TAT, **figure 5.6a** and **5.6c** respectively. The reduction in size from 100 to approximately 5 nm after complexing siRNA is because of the negatively charged siRNA, which forms tight complexes with cationic polymer via electrostatic interactions. Also during the polymer synthesis, the use of hydrazine monohydrate involved in the last step of the synthesis to deprotect the chitosan amine groups, is thought to break the backbone of chitosan chain, yielding smaller chain lengths, allowing us to achieve a smaller particle size. **Figure 5.6b** represents nanoparticles formed with unmodified chitosan complexing siRNA. The particles obtained were in the range of 50-80 nm in size, were polydispersed and non-spherical in shape. The spherical shape of the nanoparticles in **figure 5.6a** and **5.6c** is attributed to the PEG in the formulation, which is hydrophilic in nature.

As observed in **figure 5.7**, the modified chitosan-PEG-TAT nanoparticles were as efficient in delivering siGLO (scrambled siRNA) to neuronal cells (Neuro2a) (**figure 5.7d**) as the unmodified chitosan nanoparticles (**figure 5.7b**). However, the morphology of the cells in bright-field for modified chitosan-PEG-TAT nanoparticles looked much healthier than unmodified chitosan nanoparticles. This effect was further evaluated with MTS, a cytotoxicity assay in **figure 5.8**, which clearly indicates that the modified chitosan-PEG and chitosan-PEG-TAT nanoparticles were significantly less toxic to the cells than the unmodified chitosan nanoparticles. The use of chitosan polymer, TPP and siGLO alone were used as controls to indicate that the major toxic effect in the unmodified chitosan nanoparticles came from chitosan polymer alone, which is again attributed to free amine groups on chitosan. Though, it is known that chitosan is a non-toxic polymer however excess of positive charge on its surface can break the integrity of the cell membrane, causing cell death. Thus, we attempted to modify chitosan's surface before forming nanoparticles in order to reduce the toxic effects, without compromising its transfection efficiency. Lastly, to determine whether these modified chitosan-PEG-TAT nanoparticles can deliver a functional siRNA, we attempted to prove that in an established in-vitro model of SCA1, wherein the neuronal cells were transfected with

ataxin 1 plasmid using lipofectamine to overexpress ataxin 1 protein. After 24 hrs of expression the cells were transfected with ataxin 1 siRNA delivered through modified chitosan-PEG-TAT nanoparticles. The results indicate ataxin1 protein suppression after 48 hrs, as analyzed by western blot. Thus, this study confirms that we successfully achieved 100% transfection of siRNA in neuronal cells with minimal toxicity, with ability to silence a diseased gene causing a therapeutic effect.

5.6 Conclusion

The article details a scheme for tagging TAT peptide onto the PEGylated chitosan polymer and the formation of nanoparticles capable of delivering siRNA to neuronal cells. The chitosan polymer formulations were characterized using FTIR and NMR at each step of synthesis. The morphological studies were performed using TEM, which revealed nanoparticles as small as 5 nm in size. The chitosan-PEG-TAT nanoparticles were shown to deliver siRNA to neuronal cells with minimal toxicity. They also had an important therapeutic effect in an in-vitro model of SCA. Thus, these nanoparticles hold great promise for biomedical engineering applications, specifically for the delivery of therapeutic molecules targeting neurodegenerative diseases. However, it may be noted that the synthesis and development of these nanoparticles is not limited to one application but represents a platform technology in which the nanoparticles can be custom-made to target any disease application by simply replacing the targeting moiety on the surface of the nanoparticles and the therapeutic payload.

5.7 Acknowledgements

We gratefully acknowledge the assistance Natural Sciences and Engineering Research Council of Canada (NSERC) to Dr. S. Prakash, the support of FRSQ doctoral scholarship to M. Malhotra and an NSERC Alexander Graham Bell Graduate doctoral scholarship to C. Tomaro-Duchesneau. We also acknowledge the support of colleagues Rishi Sharma and Anjali Sharma Department of Chemistry, Otto Maas chemistry Building, McGill University and Ambika Srinivasan, Montreal Neurological Institute, McGill University for their expert opinion to M. Malhotra. We would also like to thank Dr. Zoghbi Huda (Baylor College of medicine, Houston, TX, USA) for providing [pGFP-

ataxin (Q82)] was a kind gift, Dr. Jing Hu for synthesizing peptide sequences at Sheldon Biotechnology, McGill University. Dr. Tara Sprules, NMR Facility Manager of Quebec/Eastern Canada NMR Centre for processing our NMR samples, Mr. Petr Fiurasek, Centre for self-assembled Chemical Structures (CSACS) for the FTIR facility, Mr. Xu Dong Liu for processing TEM images at (FEMR) Facility of Electron Microscopy Research at McGill University.

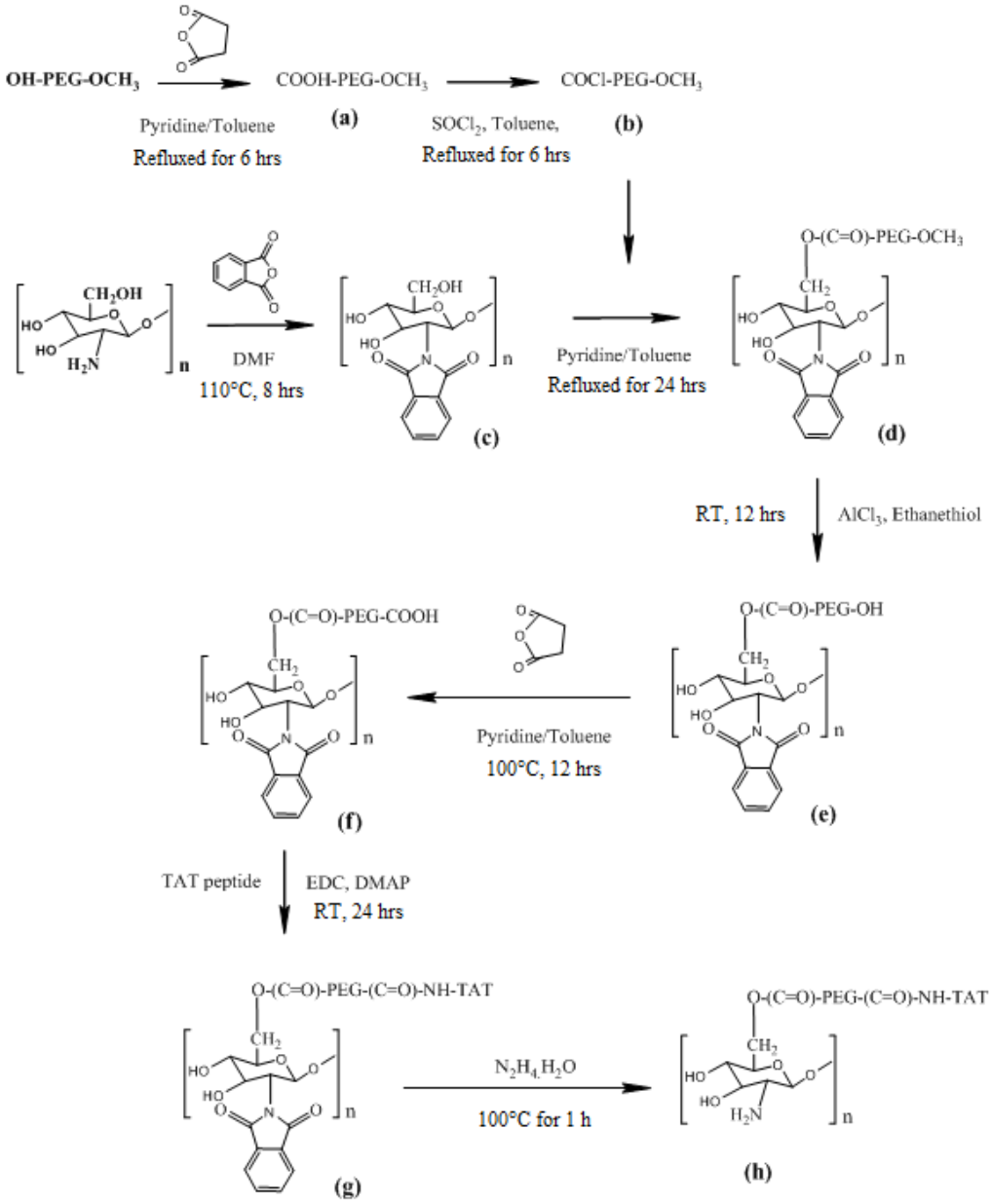

Figure 5.1: Chemoselective synthesis of chitosan polymer: Schematic representing the synthesis route of peptide tagged PEGylated chitosan polymer for the development of receptor-targeted nanoparticles.

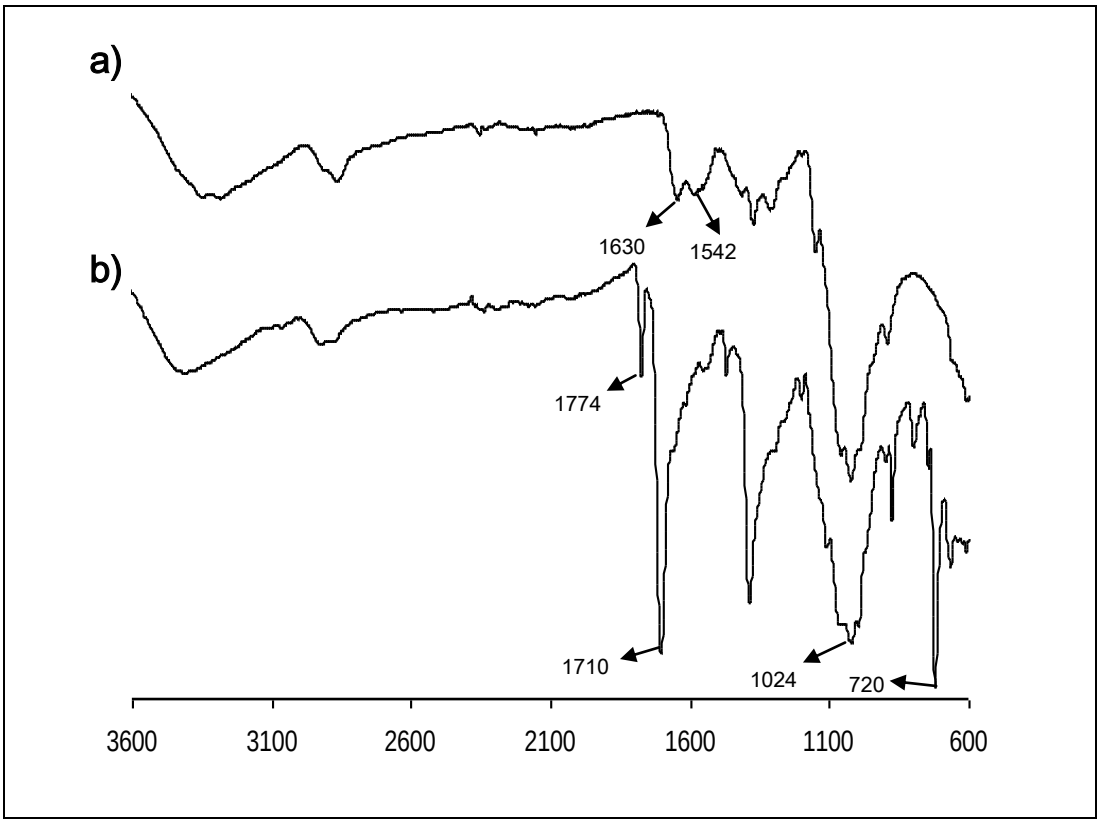

Figure 5.2: Polymer characterization using FTIR: (a) commercially available chitosan (CS) and (b) 2-N-phthaloylated chitosan: νmax/cm-1 3200-3400 (OH), 1774, 1710 (carbonyl anhydride), 1150-1000 (pyranose), and 720 (arom). The appearance of peak 1774 and 1710 in (b) indicate the presence of phthaloyl group on chitosan.

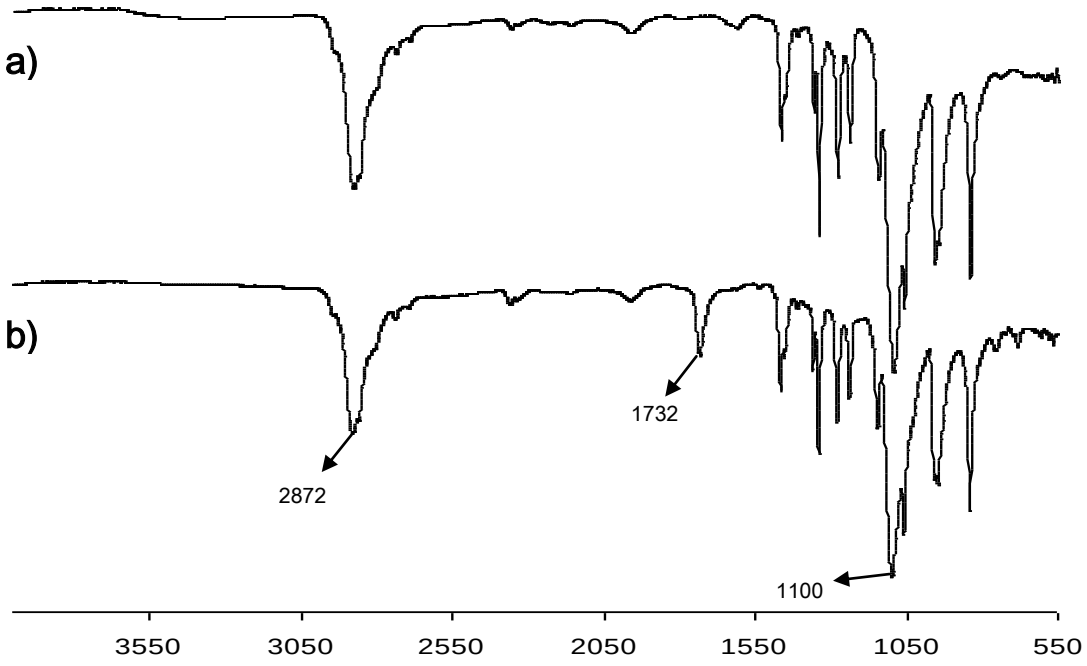

Figure 5.3: Polymer characterization using FTIR: (a) Polyethylene glycol monomethyl ether (mPEG-OH) and (b) Carboxylated mPEG (mPEG-COOH): ν_{max}/cm^{-1} 1732 (C=O), 2878 (C-H stretching), 1100 (C-O stretching). The appearance of peak 1732 in (b), indicate the successful modification of hydroxyl group to carboxyl group on PEG.

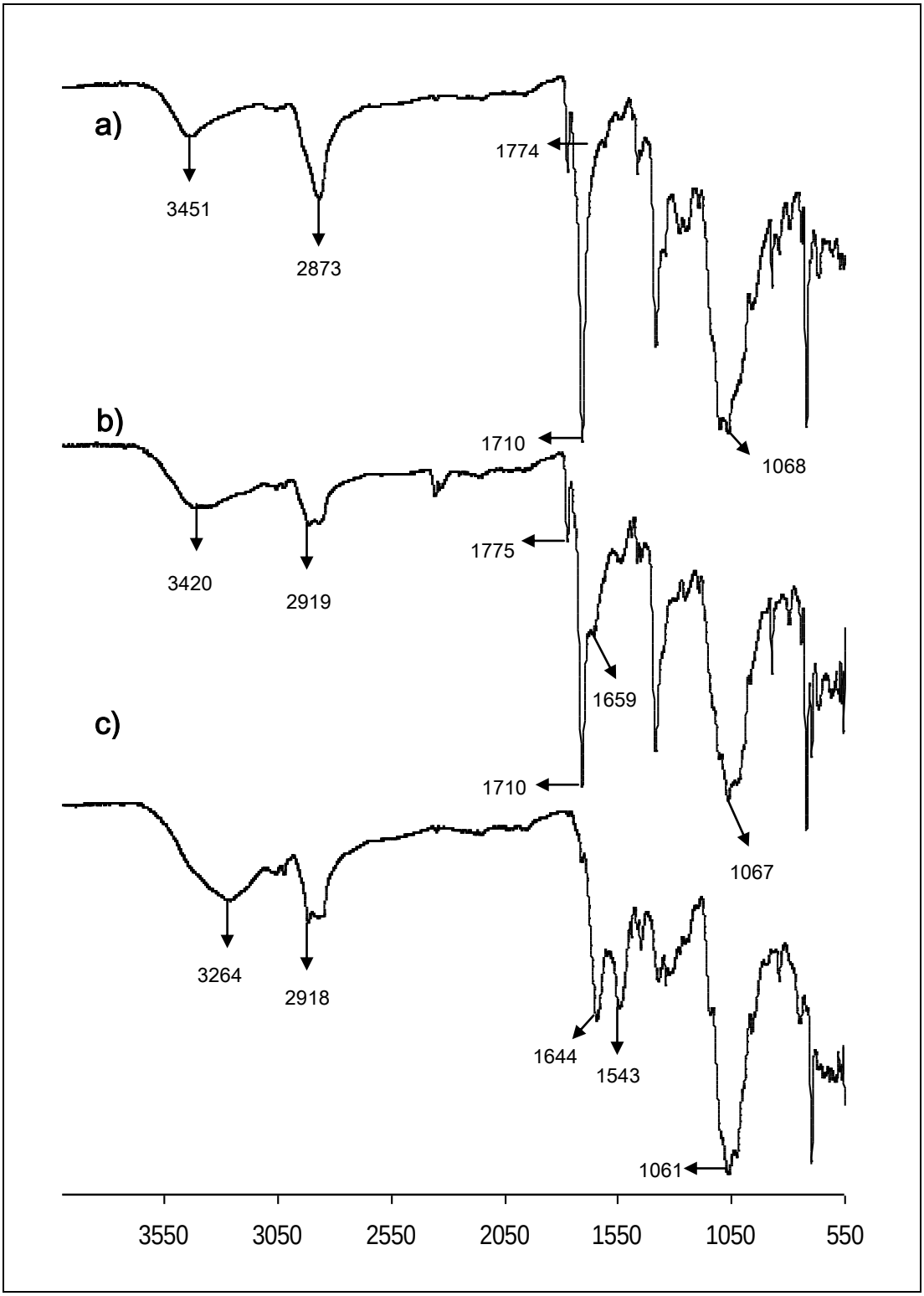
a)
3451
2873
1774
1710
1068
b)
3420
2919
1775
1659
1067
c)
3264
2918
1644
1543
1061
3550
3050
2550
2050
1550
1050
550

Figure 5.4: Polymer characterization using FTIR: (a) 2-N-phthaloyl chitosan-O-PEG: ν_{max}/cm^{-1} 2873 (C-H stretching), 1068 (C-O stretching) of PEG, 1774, 1710 (carbonyl anhydride) and 720 (arom) of phthalimido group on chitosan. (b) TAT tagged PEGylated phthaloyl chitosan (2-*N*-phthaloyl chitosan-*O*-PEG-*CONH*-TAT): ν_{max}/cm^{-1} 2919 (C-H stretching), 1067 (C-O stretching) of PEG, 1774, 1710 (carbonyl anhydride) and 720 (arom) of phthalimido group on chitosan, 1659 (amides) in TAT peptide. (c) Deprotected TAT tagged PEGylated chitosan (chitosan-*O*-PEG-*CONH*-TAT): ν_{max}/cm^{-1} 2918 (C-H stretching), 1061 (C-O stretching) of PEG, 1644 amides of TAT peptide, and 1543 (amides) in chitosan. The presence of peak 1659 in (b) in comparison to (a), indicate the conjugation of TAT peptide onto the polymer, as this peak shows the presence of amides that belong to TAT peptide. The absence of peak 1775 and 1740 in (c), as compared to (a and b) indicate the complete removal of phthaloyl (protecting) group from the polymer and the emergence of peak 1644 and 1543 belong to the peaks of TAT and chitosan respectively.

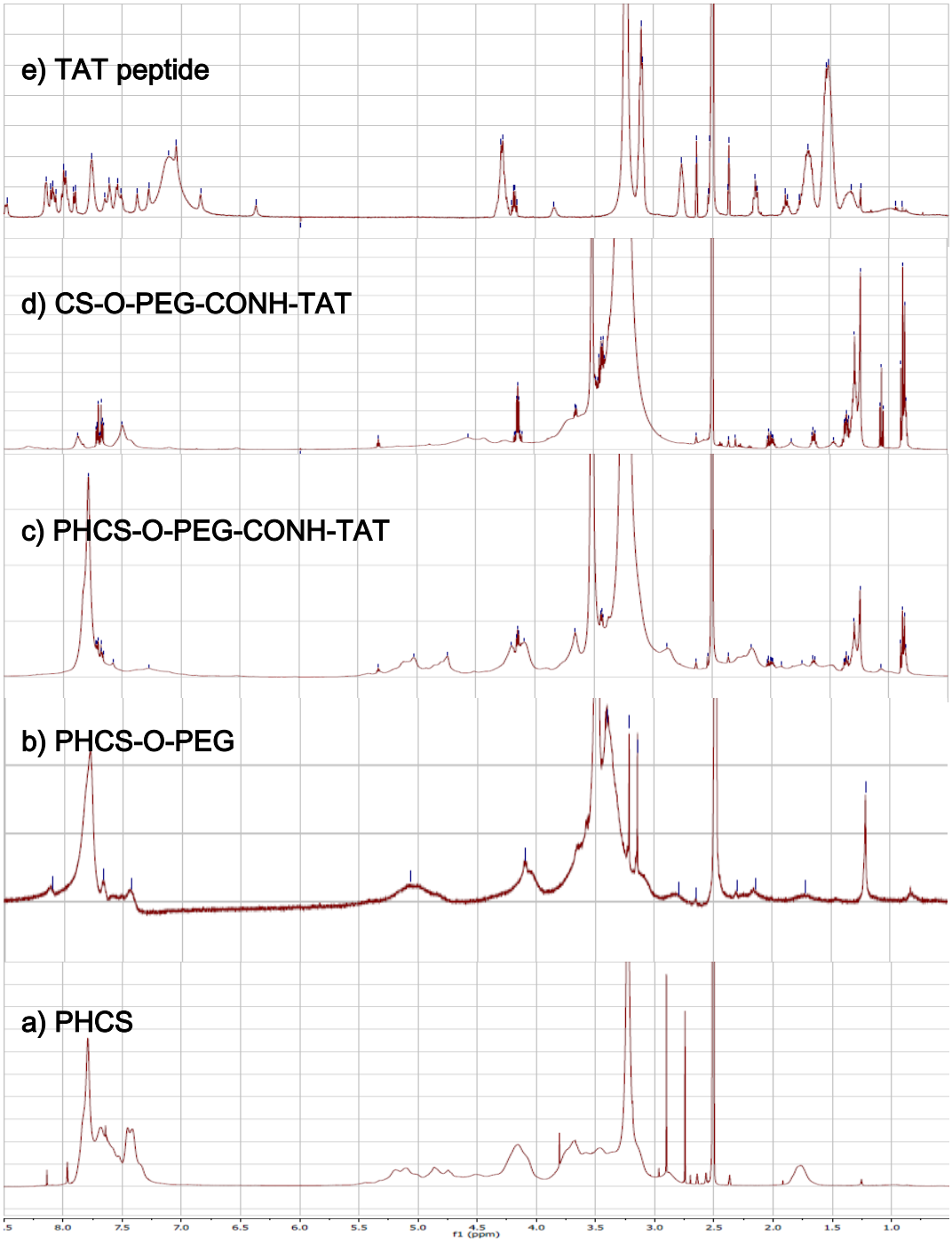
e) TAT peptide
d) CS-O-PEG-CONH-TAT
c) PHCS-O-PEG-CONH-TAT
b) PHCS-O-PEG
a) PHCS
8.0
7.5
7.0
6.5
6.0
5.5
5.0
4.5
f1 (ppm)
4.0
3.5
3.0
2.5
2.0
1.5
1.0

Figure 5.5: Polymer characterization using ^{1}H NMR: (a) phthaloylated chitosan (PHCS), (b) PEGylated phthaloyl chitosan (PHCS-*O*-PEG), (c) TAT tagged PEGylated phthaloyl chitosan (PHCS-*O*-PEG-*CONH*-TAT), (d) Deprotected TAT tagged PEGylated chitosan (CS-*O*-PEG-*CONH*-TAT), (e) TAT peptide. The chemical shift at δ 7.78 belongs to the aromatic protons of the phthaloyl moiety, which is present in the spectra (a), (b) and (c) but disappeared after deprotection in as observed in spectra (d). The multiple peaks of oxymethyl groups in PEG at δ 3.3 to 3.7 cover the signals of the pyranose ring of chitosan in the spectras of (b), (c) and (d). The weak and broad peak at δ 4.3 - 4.5 were from the protons of –NH-CH(CH_2)-CO- in the TAT peptide (e), whose presence is also observed in spectra (d) . The peak at δ 2.7-2.8 is from the protons of –CH_2-NH-NH-NH_2 in arginine and the weak and multiple peaks at δ 1.3-1.7 are from the –CH_2-CH_2-CH_2-NH-NH-NH_2 in arginine are observed in spectra (c) and (d), which confirms the presence of TAT, when compared to spectra (e). The multiple peaks at δ 7.0-8.0 belong to the amines in the TAT peptide sequence (e) and the similar peaks are observed in the final derivatized polymer (d).

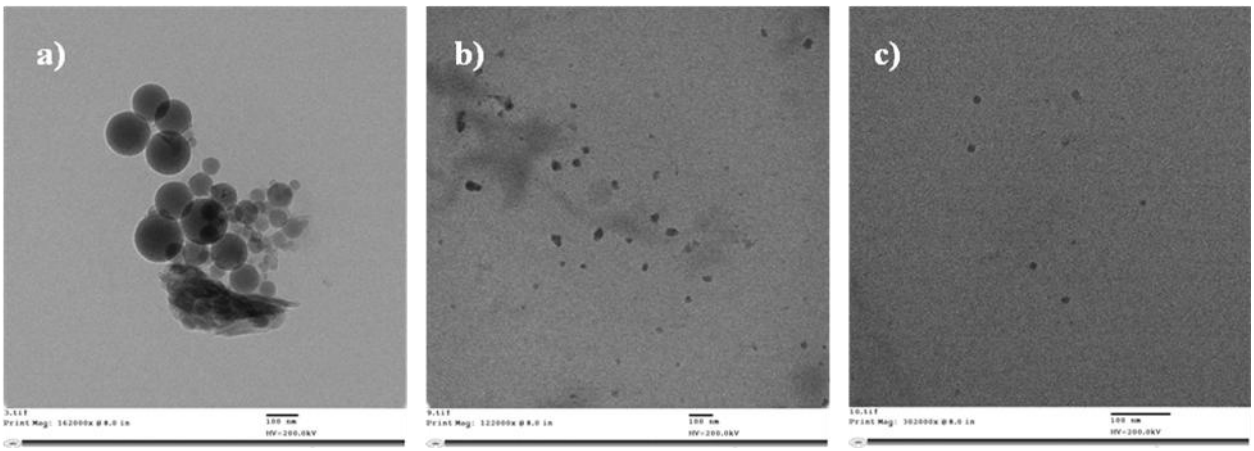

Figure 5.6: Nanoparticle characterization using TEM: (a) Empty TAT tagged PEGylated chitosan nanoparticles; magnification: 162,000X (b) Unmodified chitosan-siRNA nanoparticles; magnification: 122,000X; (c) Chitosan-PEG-TAT-siRNA nanoparticles; magnification: 302000 X.

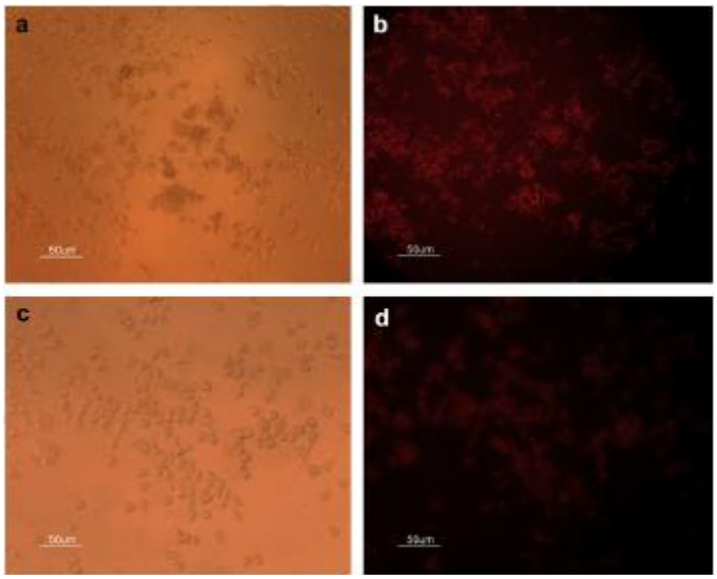

Figure 5.7: Cell transfection study on Mouse neuroblastoma cells (Neuro2a) transfected with nanoparticles formulation carrying non-targeting Cy-5 labeled scrambled siRNA: (a, b) Cells transfected with unmodified chitosan nanoparticles; (c, d) Cell transfection with modified chitosan-PEG-TAT nanoparticles. It is observed that modified chitosan nanoparticles (d) were equally efficient in transfecting siGLO as unmodified chitosan nanoparticles (b). When compared to the bright field images of the cells, it is clear that the modified nanoparticles (c) pose less cytotoxicity as compared to the unmodified ones (a).

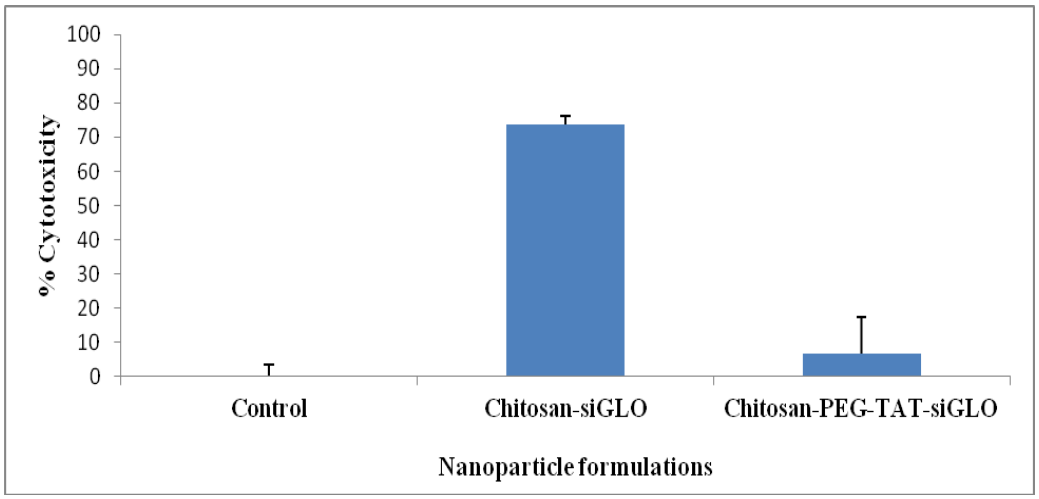

Figure 5.8: Cytotoxicity study on mouse neuroblastoma cells (Neuro2a) with various treatments using MTS assay: Unmodified chitosan nanoparticles were highly toxic on cells as compared to modified chitosan-PEG-TAT nanoparticles (p = 0.00004). The modified chitosan-PEG-TAT nanoparticles did not induce any significant toxicity when compared to the untreated cells (p = 0.507). Data is presented as mean ± standard deviation, n = 3.

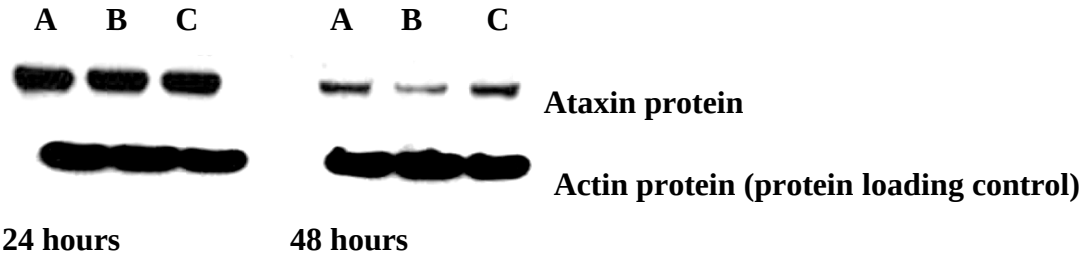

Figure 5.9: Western blot analysis of ataxin protein performed after 24 and 48 hours: Sample A and C are positive controls with nanoparticles containing no siRNA and scrambled siRNA (siGLO) respectively. Sample B contains nanoparticles with Atxn-siRNA. Silencing is observed after 48 hrs in sample B. Actin is used as a protein loading control.

Original article 4

CHAPTER 6: siRNA DELIVERY BY NOVEL TAT/MGF TAGGED PEGYLATED CHITOSAN NANOPARTICLES TARGETING ALZHEIMER'S DISEASE

Meenakshi Malhotra, Catherine Tomaro-Duchesneau, Shyamali Saha and Satya Prakash*

Biomedical Technology and Cell Therapy Research Laboratory
Department of Biomedical Engineering, Artificial Cells and Organs Research Center
Faculty of Medicine, McGill University
3775 University Street, Montreal, Quebec, H3A2B4, Canada

*Corresponding author: Tel: 514-398-2736; Fax: 514-398-7461,
Email: satya.prakash@mcgill.ca

Preface: As surface functionalized, peptide tagged PEGylated chitosan nanoparticles were prepared in the previous chapter. The similar synthesis scheme was utilized to form nanoparticles tagged with a cell penetrating peptide, TAT and a cell targeting peptide, MGF. The nanoparticles were prepared to deliver siRNA to the brain, when administered intranasally. The purpose of the study was to enable the therapeutic delivery non-invasively with high efficiency. Towards this goal, this chapter demonstrates a pilot study, wherein the siRNA delivery, to the brain, through the nanoparticles was investigated in an experimental animal model C57BL/6J. The analysis was performed based on safety, biodistribution and toxicity of the nanoparticles in the organ tissues. This study was further extended to an animal model of Alzheimer's disease as most of the nanoparticles were observed to target the cerebral cortex of the brain, which is the most affected area of degeneration in Alzheimer's disease. This extended study illustrates delivery of a functional siRNA targeting Presenilin 1 (PSN1) gene by nanoparticles, via intranasal route to an animal model of Alzheimer's disease.

Article submitted to Journal of Drug Delivery

6.1 Abstract

Neurodegeneration is characterized by progressive loss of structure and function of neurons. Several therapeutic methods and drugs are available to alleviate the symptoms of these diseases. However, a need for a suitable therapeutic method that can halt the progression of the disease is yet to be found. The currently used delivery strategies such as implantation of catheters, intra-carotid infusions, surgeries and chemotherapies are invasive in nature and pose a greater risk of post-surgical complications like fluid retention in the ventricles etc, which can have fatal side-effects. Thus, a need to develop an alternative non-invasive and targeted therapeutic delivery strategy exist which can cross/bypass the blood-brain barrier. The proposed research utilizes a peptide tagged PEGylated chitosan nanoparticle formulation for siRNA delivery, administered intranasally and investigates its preclinical efficacy and safety in experimental animals. Preliminary result indicates that this novel formulation has potential to deliver siRNA, targeting cerebral cortex and cerebellum. The study also indicates successful delivery of siRNA against presinilin1 gene, which causes approximately 20% gene reduction at the targeted site. This study shows the potential of peptide tagged PEGylated chitosan nanoparticles to be delivered intranasally and target brain tissue for the treatment of neurodegenerative diseases, such as Alzheimer's disease.

Keywords: Alzheimer's disease, PSN1, siRNA, gene silencing, nanoparticles, MGF, TAT

6.2 Introduction

NDDs are characterized by progressive, age-related loss of specific subsets of neural cells, which lead to diverse clinical phenotypes depending on the underlying anatomical involvement [284]. The etiology of NDDs is most often multifactorial, likely a result of gene–environmental interaction [285], which may lead to diseases like PD, AD, HD, ALS and SCA. These diseases tend to progress slowly over the time and generally target older population. Alzheimer's is the most common form of dementia, which is incurable and degenerative. It is characterized by the presence of misfolded protein in the form of senile plaques and neurofibrillary tangles in the brain [155]. It is predicted to affect 1 in 85 people globally by 2050 [156]. The mean life expectancy of an individual is drastically reduced to 7 years after the onset of the disease. Currently, there is no cure available that can halt the progression of the disease. However, therapies and drugs are available in the markets that merely mitigate the symptoms of the disease.

The underlying pathological mechanism of AD is still unknown but the accumulation of amyloid-beta peptides is thought to be the central triggering event of the disease, which is believed to disrupt the cell's calcium ion homeostatis, leading to apoptosis [158]. The amyloid plaques in Alzheimer's disease are composed of dense, insoluble deposits of amyloid-beta peptide in and around the neuron. These peptides are the fragment of a larger transmembrane protein called amyloid precursor protein (APP) [159-161]. APP is essential for neurons growth survival and post injury repair [162, 163]. The formation of amyloid-beta peptides is initiated by a sequential cleavage of APP by an enzyme, protease beta-secretase, also known as BACE1 (beta site APP cleaving enzyme) and then by a gamma–secretase, an aspartyl protease complex, which generates toxic C-terminal fragments inside the cell and releases a fragment called amyloid-beta peptide extra cellularly [159, 164].

The identification of the biological and pathological abnormalities triggered the studies on recognizing the genes responsible for causing inherited forms of AD [158]. On such form is autosomal dominant familial AD, which is caused due to the mutations in the APP and components of gamma-secretase (Presenilins 1 and 2) [165-167] that lead to

increased production of amyloid-beta 2 protein, the main component of senile plaques [168, 169]. Several transgenic animal models have been developed based on various genetic mutations to understand the etiology and possible pathological mechanism of the disease and to investigate various therapeutic options [170, 171].

Advancement in RNAi therapy has facilitated the understanding of pathobiological mechanisms of the disease with most of the researches focusing on phenotype rescue due to dominantly acting mutant genes and loss-of function analysis [172, 173]. Based on the etiology of the AD, the key targets for RNAi therapy are assumed to be APP, BACE [174] and gamma-secretase [175, 176] and tau, which can eliminate the production of toxic C-terminal fragments and amyloid-beta peptides. siRNAs has been delivered to the central nervous system both naked or with the help of some transfection reagents in-vivo, targeting different molecular targets in different parts of the nervous system, showing effective gene silencing.

Direct doses of siRNAs administered intrathecally or intracerebro-ventricularly [1] pose a widespread inhibition of molecular targets that are broadly expressed in different parts of the brain but may also lead to off-targeting. A significant limitation is the inability of the therapeutic molecules to cross the BBB and other physiological barriers. Though, various siRNA delivery strategies have been explored, but they have not proved to be as effective and have created concerns with safety issues, thus a polymeric approach of delivering siRNA molecules, which is target specific, multifunctional, biodegradable and biocompatible is more appealing. We have developed a self-assembled, functionalized receptor targeting nanoparticles from chitosan that are biodegradable and biocompatible in nature, as represented in **figure 6.1.** The nanoparticles prepared were used to perform target specific delivery of siRNA, when delivered intranasally to the cerebral cortex of the brain.

The animal study in this chapter is divided in two sections. The first section **(A)** was a preliminary study performed to analyse the nanoparticles ability to intranasally deliver the siRNA, in-vivo in four weeks old C57BL/6J male mice. The objective of the

study was to optimize the dose, duration, biodistribution, toxicity and target specificity of the nanoparticles. The second section **(B)** was an extension of the preliminary study, in which the optimized dose of the nanoparticle formulation complexing siRNA was administered intranasally to an animal model of AD (Tg(APPSwFlLon,PSEN1*M146L*L286V)6799Vas). These transgenic mice overexpresses both mutant human APP(695) [Swedish (K670N, M671L), Florida (I716V), and London (V717I)] Familial Alzheimer's Disease (FAD) mutations and human PSN1 harboring two FAD mutations, M146L and L286V. This transgenic mice model was chosen as it over expresses amyloid-beta 42 protein in cerebral cortex and hippocampus, resulting in amyloid plaque pathology as early as 2 months of age [286]. The objective of this study was to determine the ability of nanoparticles to deliver a functional siRNA against PSN1 gene and to cause a gene silencing.

6.3. Materials and Methods

6.3.1 Materials

Materials used to synthesize peptide-tagged PEGylated chitosan polymer were as described in chapter 5. Other materials used were; TAT peptide (NH_2-RKKRRQRRR) M.W. 1339.63 and MGF peptide (YQPPSTNKNTKSQRRKGSTFEEHK- NH_2) M.W. 2848.14, were synthesized by Sheldon Biotech, McGill University. Biotin-tagged scrambled siRNA, siGENOME Non-Targeting siRNA #2: D-001210-02, was procured from Dharmacon Inc. (Lafayette, CO, USA). siRNA targeting PSN1 (Accession #: NM_000021.3) targeting sequence: 5' AAG GUC CAC UUC GUA UGC UGG was synthesized from Dharmacon (Lafayette, CO, USA).

6.3.2 Preparation of siRNA-nanoparticle formulation

The nanoparticles were prepared from a synthesized peptide-tagged PEGylated chitosan polymer, as described in chapter 5. The peptides used in this study were MGF and TAT. The nanoparticles were synthesized as described previously in chapter 3 and 5 [243, 287]. In brief, the nanoparticles were prepared using an aqueous solution of derivatized polymer CS-PEG-TAT/MGF at 0.5 mg/ml, pH 6.0, complexing siRNA at an

N:P ratio of 103. TPP at 0.7 mg/ml, pH 3.0 was used as a crosslinker to form nanoparticles. Biotin-tagged scrambled siRNA, siGENOME Non-Targeting siRNA #2: D-001210-02 and PSN1 siRNA against the target mRNA gene 5' AAG GUC CAC UUC GUA UGC UGG were procured from Dharmacon Inc. (Lafayette, CO, USA).

6.3.3 Animals

For the preliminary study, four-week old C57BL/6J male mice, weighing 10-15 g were purchased and for the Alzheimer's study, four weeks old, heterozygous female, transgenic mice model Tg(APPSwFlLon,PSEN1*M146L*L286V)6799Vas, weighing 10-15 g were purchased from MMRC facility in Jackson Laboratory (Bar Harbor, ME, USA). The animals were housed in an environment with controlled temperature (22°C), humidity, and a 12 h light/dark cycle at McGill's animal care facility. The animal experiment was conducted as per the protocol approved by the animal care committee at McGill University (Montreal, QC, Canada). Standard mouse chow and water were supplied ad libitum. Animals were acclimatized for a week before the experiment.

6.3.3.1 Animal experimental study

For the preliminary study, the animals were randomized into 4 groups to receive non-targeting (NT) biotin-siRNA complexed with CS-PEG-TAT/MGF nanoparticles (n = 2). One animal in each group received PBS, as untreated control. CS-PEG-TAT/MGF nanoparticle formulations complexing NT biotin-siRNA was concentrated to 4 different doses: (a) 0.25 (b) 0.5 (c) 1 and (d) 2 mg/kg siRNA using Amicon Ultra-15 centrifugal filters (MW cut-off 3000 Daltons, Millipore). The animals were anesthetized with 75-100 µl cocktail comprising ketamine (100 mg/kg), xylazine (10 mg/kg) and acepromazine (3 mg/kg) via intraperitoneal administration. A total of 30 µl of the nanoparticle formulation was administered intranasally once (5 µl/drop) over 15-20 minutes. The experimental end-points were 4, 16, 24 and 48 h.

For the Alzheimer's study, the animals were divided in 2 groups (n=4). The first group received nanoparticles with siRNA against PSN1 gene and the second group received PBS, as untreated control. The treatment began at 6 weeks of animal age. The

siRNA dose administered through nanoparticles was 0.5 mg/kg of animal weight as optimized in the preliminary study. Due to daily administration of dose, the animals were preferred to be anesthetized with isoflurane, gas anesthesia, as approved by the animal use protocol of McGill University. The treatment doses were given daily, intranasally, for a total of 3 weeks. All the animals were sacrificed at the end of 4 weeks. Brain and blood were harvested for mRNA and serum safety marker analysis, respectively.

6.3.4 Histology: Preliminary study

Histology sections were prepared from preliminary study, wherein the animals were anesthetized using the aforementioned cocktail and perfusion fixed with 4% paraformaldehyde (PFA) (Sigma Aldrich, Canada), at each end point. Brain, lungs, heart, stomach, kidney and liver were harvested and kept at 4°C in 4% PFA for 48 hrs. The tissues were trimmed to 3 mm thick sections and stored in 70% ethanol in histology cassettes. The tissues were paraffin-embedded and processed into 4 μm thick section on slides (The Rosalind and Morris Goodman Cancer Research Centre, McGill University). The tissue slides were stained with Vectastain elite ABC kit (Vector laboratories; Burlingame, CA, USA) as per the manufacturer's protocol and Diaminobenzidine (DAB) was used as a substrate to assess the presence of biotin tag present on siRNA (brown staining). Hematoxylin was used as a counterstain and slides were mounted with permount (Vector laboratories; Burlingame, CA, USA) and observed by compound microscopy (Leica DM500; ON, Canada) at 400X.

6.3.5 Toxicity analysis: Preliminary study

Analysis of apoptotic cells was performed using Terminal deoxynucleotidyl transferase-mediated dUTP nick-end labeling (TUNEL) staining (Promega, Madison, Wisc., USA) as per the manufacturer's protocol after blocking biotin-siRNA. The tissue sections in paraffin block were dewaxed in xylene and rehydrated in decreasing concentrations of ethanol and washed with PBS. The tissue sections were then incubated with Streptavidin-HRP reagent (Roche Diagnostics) for 10 min, washed in PBS. Then the sections were incubated with 3% H_2O_2 for another 10 min and washed in PBS. The rest of the TUNEL assay was performed as per the manufacturer's instructions. The tissue

sections were counterstained with hematoxylin, washed in distilled water, dehydrated and mounted with permount (Vector laboratories; Burlingame, CA, USA) and observed by compound microscopy at 400X.

6.3.6 Percentage PSN1 mRNA knockdown by siRNA delivered through novel nanoparticles: Alzheimer's study

To validate the knockdown of endogenous PSN1 expression in the Alzheimer's study, a quantitative real time polymerase chain reaction (PCR) was performed on the brain tissues excised from both treatment and control groups (n=4) after 3 weeks. The total RNA was extracted using RN*easy*® Lipid tissue mini kit from Qiagen and the total RNA was quantified using Nanodrop 2000 spectrophotometer. The reverse transcription on total RNA was performed to obtain complementary DNA (cDNA) using a QuantiTect Reverse Transcription kit from Qiagen. A quantitative real time PCR was performed using MBI Evolution Evagreen Master Mix following the manufacturer's protocol (MBI, Montreal, Canada) on ECO RT PCR machine from Illumina. The relative expression levels of the targeted gene were compared with the housekeeping gene glyceraldehyde 3-phosphate dehydrogenase (GAPDH). The primer sequences used were as follows: PSN1: F 5'-CCGAAATCACAGCCAAGA-3'; R: 5'-CATTCACAGAAGATACCAAGAC-3'. GAPDH, F: 5'-TAAAGGGCATCCTGGGCTACACT-3'; R: 5'-TTACTCCTTGGAGGCCATGTAGG-3'. The PCR was run for 40 cycles with a 95°C denaturing step (15 s), a 56°C annealing step (1 min), and a 72°C extension step (15 s), plus final incubation at 72°C for 10 min.

6.3.7 Systemic safety and toxicity of novel siRNA-nanoparticle formulation: Alzheimer's study

Serum was collected via cardiac puncture from the animals in Alzheimer's study using a sterile 23G/25mm needle. Approximately 400 µl of blood was collected in the Microtainer® serum separator tubes (Becton Dickinson, NJ, USA). The blood was allowed to clot at room temperature for 30 minutes and subsequently placed on ice until centrifugation. Serum was separated by low-speed centrifugation at 3600 rpm for 8 min at 4°C. The separated serum was frozen at -80°C until analysis. Serum was used to test for C-reactive protein (CRP) and liver function tests, alkaline phosphatase (ALP), alanine

aminotransferase (ALT) and aspartate transaminase (AST). Urea, creatinine (CRE) and uric acid (UA) were also tested for renal functionality in the animals using a conventional enzymatic method on Hitachi 911 automated clinical chemistry auto-analyzer (Roche Diagnostics, USA).

6.3.8 Statistical analysis

Experimental results are expressed as means ± standard error of the mean (SEM). Statistical analysis was carried out using SPSS Version 17.0 (Statistical Product and Service Solutions, IBM Corporation, New York, NY, USA). Statistical comparisons were carried out using Tukey's post-hoc analysis and Levene's T test, assuming equal variances. Statistical significance was set at $p < 0.05$ and p-values less than 0.01 were considered highly significant.

6.4 Results

6.4.1 Dose optimization of siRNA/nanoparticle formulation to target brain tissue in-vivo: preliminary study

The optimal dose to be delivered to the four-week old C57BL/6J male mice was determined by administering the animals (divided in 5 groups (n=2) with different doses of NT-biotin-tagged siRNA, (A) 0.25 mg/kg; (B) 0.5 mg/kg; (C) 1 mg/kg; (D) 2 mg/kg and (E) 0.85% (w/v) NaCl. **Figure 6.2a** represents histopathological sections of the cerebral cortex and cerebellum from animals receiving different concentrations of nanoparticle-NT siRNA formulations. The animals were sacrificed after 4 h. The dark brown stained neuronal cells obtained with 0.5 mg/kg of NT biotin-siRNA complexed nanoparticles, ensured the delivery of siRNA in the neuronal cells of cerebral cortex ($p < 0.01$) and in the Purkinje cells of cerebellum ($p < 0.01$) as compared to the untreated control. Other animals that received 0.25 mg/kg of NT biotin-siRNA showed faint staining in the neuronal cells of cerebral cortex ($p = 0.006$) whereas, animals that received 1 and 2 mg/kg of NT biotin-siRNA dose, did not show any staining in the tissue. **Figure 6.2b** represents the quantitative analysis of the tissues using ImageJ, which confirmed the above observation.

The histopathological sections of the cerebral cortex and cerebellum at 0.5 mg/kg (determined as the optimal dose) at A) 4, B) 16, C) 24 and D) 48 h, as represented in **figure 6.2c** shows significant dark brown staining in the neuronal cells of both cerebral cortex and cerebellum ($p < 0.01$) at 4 hrs. The staining was observed only until 16 h in the cerebral cortex ($p < 0.01$) and faded thereof, with no staining observed at 24 and 48 h. The result was quantified using Image J as represented in **Figure 6.2d.** This study revealed that the delivery of NT biotin-siRNA by the peptide tagged PEGylated chitosan nanoparticles was achieved within 4 hrs of intranasal administration and was cleared after 16 h of administration.

6.4.2 Biodistribution of siRNA/nanoparticle formulation in-vivo: preliminary study

The biodistribution study was performed with animals receiving biotin-siRNA/nanoparticle dose at (A) 0.25 mg/kg; (B) 0.5 mg/kg; (C) 1 mg/kg; (D) 2 mg/kg and (E) 0.85% (w/v) NaCl. **Figure 6.3a** represents histopathological sections of tissues from different organs receiving 0.5 mg/kg of biotin-siRNA/nanoparticle dose (left column) compared to untreated control (right column), sacrificed after 4 hrs of dose administration. The staining in the brain tissue was highly significant with 0.5 mg/kg NT biotin siRNA/nanoparticle dose in both cerebral cortex and cerebellum ($p < 0.01$) and also with 0.25 mg/kg but only in the cerebral cortex ($p = 0.006$), as represented in **figure 6.3b**. The expression of siRNA/nanoparticle dose at 0.5 mg/kg was also observed to target heart sarcomeres ($p < 0.01$), with a significant expression as compared to other dose concentrations; 0.25 mg/kg ($p = 0.403$), 1 mg/kg ($p = 0.562$), 2 mg/kg ($p = 0.999$) **(figure 6.3b)**. Renal cells in the medulla region of the kidney and hepatic cells showed brown-colored staining in the cells, with 0.5 mg/kg of siRNA/nanoparticle formulation ($p < 0.01$) as compared to the untreated control **(figure 6.3b)**. The glandular cells of the stomach and alveoli in lungs showed no significant difference as compared with the untreated control. Among all the concentrations of different treatment doses tested, the highest expression of siRNA delivery was observed with 0.5 mg/kg of NT-biotin siRNA/nanoparticle formulation in the cerebral cortex and cerebellum ($p < 0.01$), when compared with expression in other organs, except the heart.

6.4.3 Toxicity of siRNA/nanoparticle formulation in-vivo: preliminary study

Toxicity analysis was performed on the animals that received 0.5 mg/kg of the nanoparticles containing NT biotin-siRNA dose, euthanized after 4 h, as represented in **figure 6.4**. The tissue sections of various organs, such as brain, heart, lungs, kidney and liver were stained with TUNEL assay. The assay helps locate DNA damage in the cells resulting from apoptotic signaling cascades. The TUNEL assay was first modified to block the siRNA biotin tag to avoid any false positive results. Our results indicate that the NT biotin-siRNA/nanoparticle formulation had no toxicity/apoptotic effect, as no brown staining was detected in any of the tissues from different organs.

6.4.4 Percentage PSN1 mRNA knockdown by siRNA delivered through novel nanoparticles: Alzheimer's study

The second part of the study was to evaluate the ability of the nanoparticles to deliver a functional siRNA in an animal model of AD. For this, the treatment group of the animals (n=4) were intranasally administered with 0.5 mg/kg of PSN1-siRNA, complexed with nanoparticles and the control group (n=4) received 0.85% (w/v) NaCl**.** The brain tissues were harvested after the end of 3 weeks and were processed and quantified for QPCR analysis to determine the percentage PSN1 gene knockdown. The relative expression of PSN1 was quantified with reference to the GAPDH expression in the tissues. The results, as represented in **figure 6.5** indicate a 21.34% reduction in PSN1 gene expression with nanoparticles carrying siRNA against PSN1 gene ($p = 0.162$), when compared with the untreated control.

6.4.5 Systemic safety and toxicity of novel siRNA-nanoparticle formulation: Alzheimer's study

Safety markers were analyzed from the serum collected from the animals that received 0.5 mg/kg of PSN1-siRNA, complexed with peptide tagged PEGylated chitosan nanoparticles. The liver function and toxicity tests were performed using alkaline phosphatase (ALP) and aspartate aminotransferase/alkaline aminotransferase (AST/ALT) respectively. The results as indicated in **figure 6.6** for ALP though show a significant difference between the treatment and control group ($p = 0.036$) but had values that fall in

the normal range of 44 to 147 IU/L. For AST/ALT, the results indicate no significant difference between the treatment and the control group (p = 0.379). Another test performed was CRP, which is an indicative of systemic inflammation the results showed no significant difference between the treatment and the control (p = 0.472). Urea, CRE and UA tests were performed indicating the renal function in animals. The results indicate no significant difference in urea (p = 0.535) and UA (p = 0.737) levels, however the creatinine was found to be elevated in the treatment group as compared to the control (p = 0.025), but the values in both the groups were all found to be in the normal range i.e. 38.13 to 91.5 µmol/L.

6.5 Discussion

Self-assembled, functionalized peptide tagged PEGylated chitosan nanoparticles that are biodegradable and biocompatible in nature and capable of specific siRNA delivery were prepared, as mentioned in chapter 5 [287]. The nanoparticles were developed using a novel synthetic scheme, comprising a parent polymer, chitosan, and a hydrophilic polymer, PEG, a CPP (TAT) and a CTP (MGF) (**figure 6.1**). As per the nanoparticle formulation of CS-PEG-TAT/MGF, chitosan is a mucoadhesive agent, that helps reduce clearance rate from nasal cavity [288]. The intranasal delivery is achieved by the absorption of the formulation across the nasal epithelia tissue, following the olfactory/trigeminal neural pathways [289]. PEG was utilized in the synthesis as a linker between chitosan and peptide, and was also used to avoid nanoparticle aggregation. PEG is hydrophilic, non-toxic and non-immunogenic [290]. The incorporation of TAT peptide provided a moiety for cell penetration [1] and MGF peptide was used as a neuronal targeting peptide [291].

This modified polymer was used to form nanoparticles complexing siRNA following a previously established protocol, as described in chapter 3 [243]. The current study investigates the potential of these nanoparticles to deliver siRNA to the brain (cerebral cortex and cerebellum) via intranasal route of administration, in-vivo. The preliminary proof-of-concept study was performed in four-week old C57BL/6J male mice. Wherein, the animals were divided in 5 groups (n=2) receiving different doses of

NT biotin-siRNA, (A) 0.25 mg/kg; (B) 0.5 mg/kg; (C) 1 mg/kg; (D) 2 mg/kg and (E) 0.85% (w/v) NaCl. The animals were sacrificed at 4, 16, 24 and 48 hrs. The analysis was performed to determine the optimal dose, specific site delivery of siRNA through nanoparticles and the extent of biodistribution and its related toxicity in the associated tissues.

The encouraging results obtained in the preliminary study (**figure 6.2 – 6.4**), indicate an optimal siRNA dose of 0.5 mg/kg was delivered in the neuronal cells of cerebral cortex and the Purkinje cells of cerebellum, when administered intranasally. The expression was quantified by analysing the intensity of the brown colored stain, as an indicator of siRNA delivery. The intensity was quantified by calculating the mean percentage area of the dark brown stained cells using image J software. The absence of stained cells at higher concentration, i.e. 1 and 2 mg/kg of siRNA was due to the clumping and aggregation. The aggregation caused due to precipitation of nanoparticles at higher concentration resulted in increased particle size thereby, preventing neuron penetration. The study also determined the pharmacokinetics of the siRNA/nanoparticle formulation and observed that the highest expression was observed at 4 h time point and was sustained until 16 h in the cerebral cortex. No staining was observed in any tissue sections at the 24 and 48 h time points. This reveals that the siRNA delivered and the nanoparticles were degraded/cleared from the system after 16 h of dose administration.

The current study also evaluated the site-specific delivery of the nanoparticles to the brain tissue by performing biodistribution analysis. As observed in **figure 6.3a** the neurons in the cerebral cortex especially, the anterior olfactory bulb, hippocampus, thalamus and hypothalamus and the Purkinje cells of the cerebellum were intensely stained brown in color. However, a fair amount of staining was also observed in the heart tissue. The staining in the heart tissue is attributed to the small size of the nanoparticles of 5 nm (as optimized in chapter 5) that excavates into the systemic route and gets accumulated in other organs. The staining could also be attributed to the use of targeting peptide, MGF, which has also shown to have affinity towards heart sarcomeres [292]. However, to confirm this statement, further studies would be required to test the

biodistribution of siRNA delivered through chitosan-PEG without a targeting moiety, delivered the similar way. The nanoparticles were also observed to be accumulated in the kidney and liver, which is again attributed to the small size (5-10 nm) of the nanoparticles that leaked into the systemic route and were captured by the reticuloendothelial system and underwent hepatic filtration [84]. A slight peripheral staining in the lungs and stomach was also observed.

The toxicity analysis performed on the tissues of animals that received 0.5 mg/kg of siRNA dose in peptide tagged PEGylated chitosan nanoparticles showed no apparent toxicity at the tissue level. These results led to the investigation of using these nanoparticles to deliver a functional siRNA against Presenilin 1 gene in an animal model of AD. For this study, the animals were divided in 2 groups (n=4), with one group receiving the optimal dose of 0.5 mg/kg siRNA, complexed with nanoparticles, as determined in the preliminary study and the other 0.85% (w/v) NaCl. The results show 21.34% of PSN1 gene knockdown in the treatment group as compared to the untreated control. No systemic toxicity was observed as indicated in data obtained from serum safety analysis.

The 21.34% of gene silencing observed in the animal model of AD, though not significant, but does show a promise of using these nanoparticles to deliver siRNA and cause gene silencing of the diseased gene. A limitation that was encountered from carrying the study from proof-of-concept to therapeutic level was the mode of dose administration. The success of siRNA delivery as achieved in the preliminary study, with highest siRNA expression within 4 hours of administration was dependent on the effect of anesthesia provided to the animals. The cocktail of anesthesia administered intra-peritoneally to the animals in our preliminary study was just once after which the animals were sacrificed at the desired time points. This cocktail anesthesia causes muscle relaxation in the animals with revival within 20-30 minutes, which lets the animals to take the treatment intranasally without any movements and complications. However, in the case of proving the therapeutic potential of nanoparticle-siRNA formulation, the dose had to be administered daily for a fixed period of time, for which, the animals could not

be sedated using a cocktail, as the higher dose of anesthesia can itself cause toxicity to the animals. Thus, the animals were mildly sedated using isoflurane, a general gas anesthesia, with which the animals revive back within a few seconds. Other studies have also shown that this method may lead to slipping of the dose through animal throat or sniffing-off, which may cause loss of therapeutic efficacy at the targeted site [293, 294].

Moreover, dose in the form of nasal drops administered to animals, which are strongly sedated with cocktail anesthesia, is much easier, wherein, the animals can be laid on a "head back" position for at least 10-15 minutes, without any movement complications and the drops can be alternately administered to each nostril. This technique becomes a challenge when the animals are not strongly sedated. A study by Harris et al. showed that the use of nasal spray is far more effective than the use of nasal drops [295]. Moreover, it is essential to split the medication in fine droplets in order to increase the efficiency of dose uptake across the olfactory epithelium. A total volume of dose split in half and administered twice daily, improves efficiency. These were the limitations faced, where the use of nasal spray and frequent dosing could not be incorporated in the study. Thus, a formulation of an enhanced strategy would have to be taken into consideration with different ways of non-invasive dose-administration techniques, in order to achieve efficient therapeutic efficacy. However, keeping the limitations aside the trend with approximate 20% reduction in the gene expression is definitely encouraging. This study is an example to show the potential of delivering a functional siRNA by the developed nanoparticles targeting neurodegenerative diseases but is not limited to the AD.

6.6 Conclusion

In recent years there have been important advances in the field of nanotechnology, specifically with regards to the delivery of drugs and therapeutics. The research presented in this article demonstrates the use of a novel surface functionalized, peptide tagged PEGylated chitosan nanoparticles capable of delivering siRNA to the cerebral cortex and cerebellum by bypassing the BBB. The study shows a potential to cause knockdown of the diseased gene in an animal model of AD. Furthermore, the

biodistribution and toxicity characterization demonstrated, no visible toxic effects linked to delivery of the nanoparticle formulation at cellular and systemic levels. Hence, the developed siRNA/nanoparticle formulation shows great promise for use as a therapeutic modality in the treatment and prevention of NDDs.

6.7 Acknowledgements

We gratefully acknowledge the assistance Canadian Institute of Health Research (CIHR) to Dr. S. Prakash and the support of McGill Major Scholarship to M. Malhotra. We would also like to thank Dr. Jing Hu for synthesizing peptide sequences at Sheldon Biotechnology, McGill University. Dr. Tara Sprules, NMR Facility Manager of Quebec/Eastern Canada NMR Centre for processing our NMR samples, Mr. Petr Fiurasek, Centre for self-assembled Chemical Structures (CSACS) for the FTIR facility, Mr. Xu Dong Liu for processing TEM images at (FEMR) Facility of Electron Microscopy Research at McGill University, Mrs. Anna Jimenez for help with animal study, Dr. Marilene Paquet for her expert advice and analytical help on histology slides and the histology facility at Goodman Cancer Research Centre at McGill University for preparation and processing of histology slides.

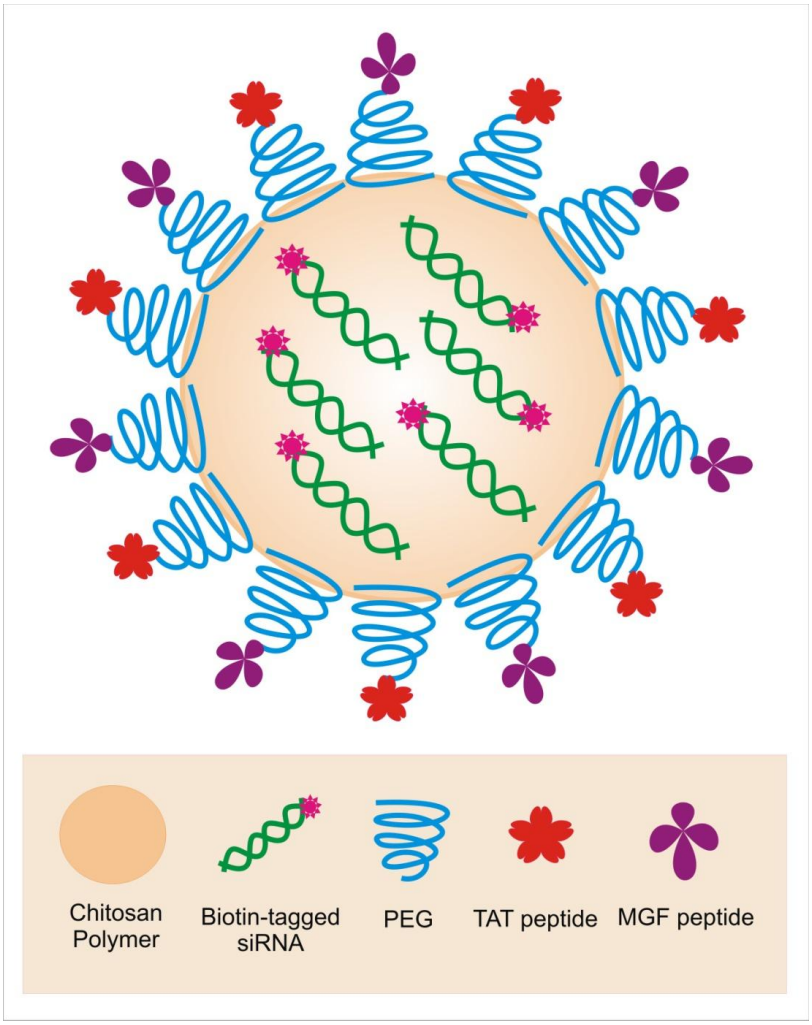

Figure 6.1: The multifunctional siRNA/nanoparticle formulation, comprising a core formed by chitosan polymer, tagged with PEG, cell penetrating (TAT) and cell targeting peptide (MGF) on its surface. The formulation complexes biotin- tagged siRNA for intranasal delivery to the brain.

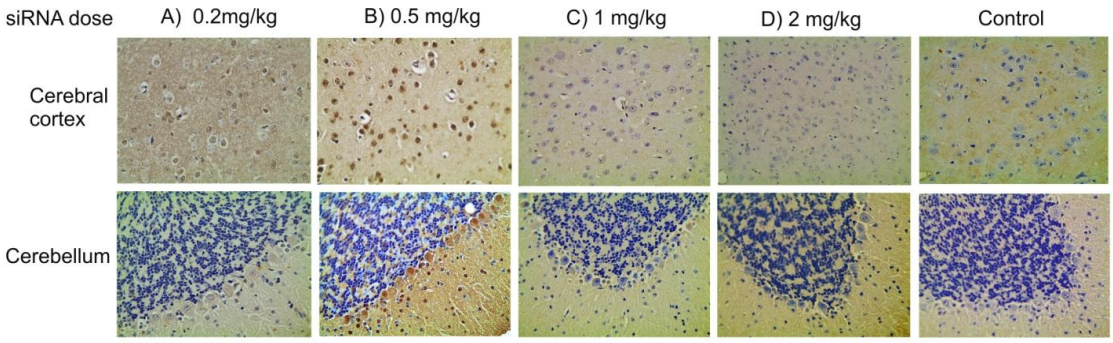
siRNA dose
A) 0.2mg/kg
B) 0.5 mg/kg
C) 1 mg/kg
D) 2 mg/kg
Control
Cerebral cortex
Cerebellum

(A)

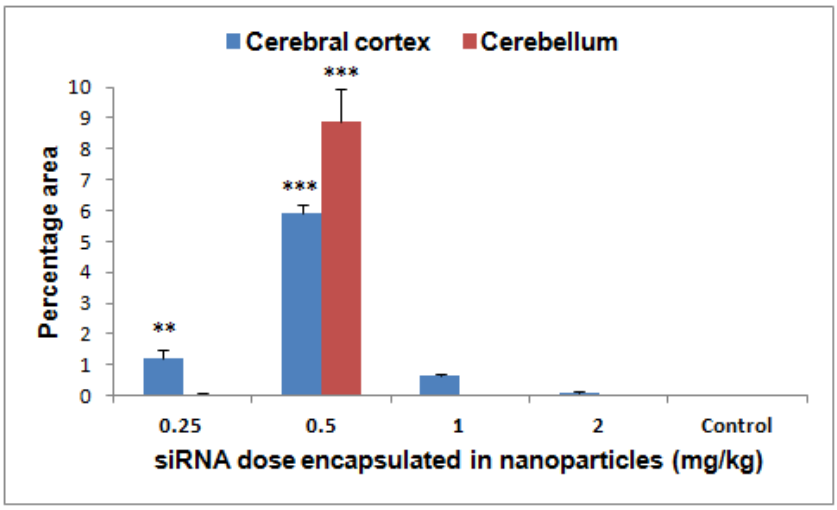
Cerebral cortex
Cerebellum
Percentage area
10
9
8
7
6
5
4
3
2
1
0
**
***
***
0.25
0.5
1
2
Control
siRNA dose encapsulated in nanoparticles (mg/kg)

(B)

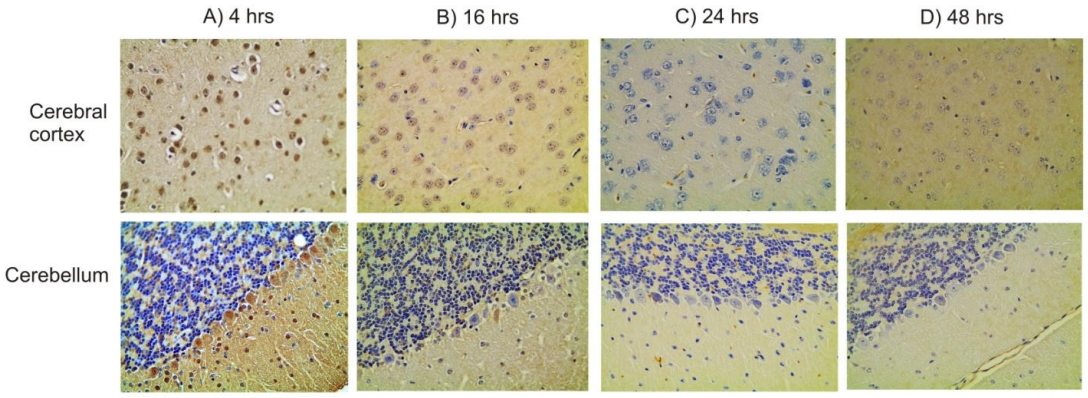
A) 4 hrs
B) 16 hrs
C) 24 hrs
D) 48 hrs
Cerebral cortex
Cerebellum

(C)

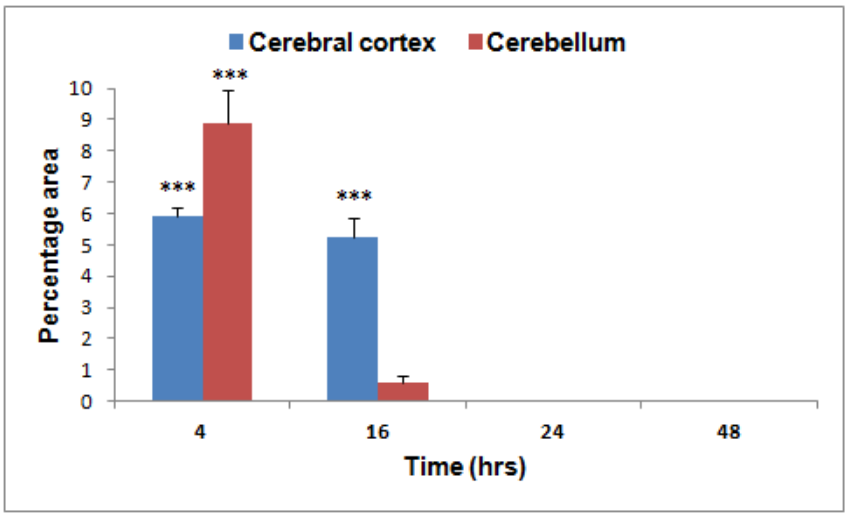

(D)

Figure 6.2(a): Histopathological images of brain tissue (cerebral cortex and cerebellum) 4 hrs after receiving the nanoparticle formulation carrying doses of biotin-siRNA: A) 0.25 mg/kg, B) 0.5 mg/kg, C) 1 mg/kg, D) 2 mg/kg and E) Control. **(b)** Quantitative analysis of the stained area in tissues using Image J. This study proved that the novel nanoparticle formulation successfully delivered the biotin-siRNA with high efficiency and selective targeting. The optimal dose of siRNA delivered via nanoparticles was determined to be 0.5 mg/kg. **(c)** Histopathological images of the cerebral cortex and cerebellum with nanoparticles carrying 0.5 mg/kg of biotin-siRNA at different time points, A) 4hrs, B) 16 hrs, C) 24 hrs and D) 48 hrs. **(d)** Quantitative analysis of the stained area in tissues using Image J. This study confirmed successful delivery of biotin-siRNA to the brain within 4 hrs of intranasal administration, with its clearance after 16 h. The graph shows a representative result of the average of two random sections (n=2) measured per animal tissue. mean±s.d. ***P <0.01 was considered highly significant based on Tukey's post-hoc analysis, when compared with other groups.

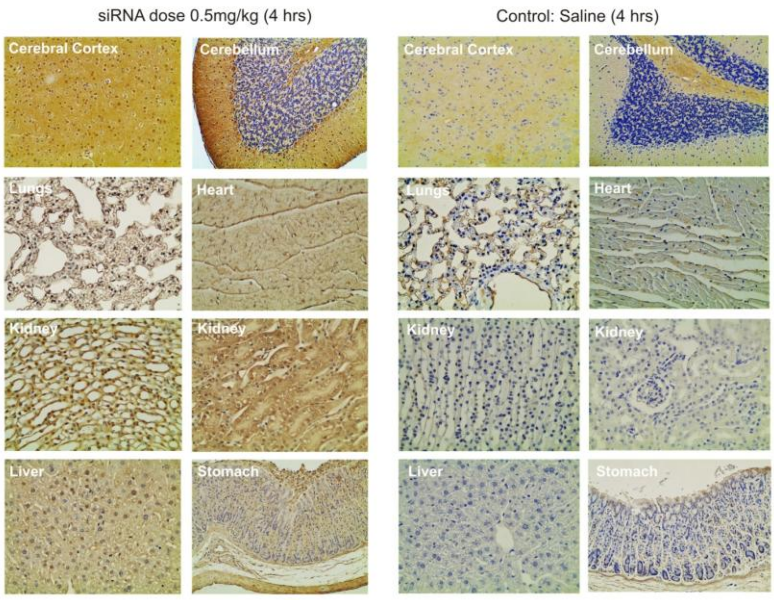

(A)

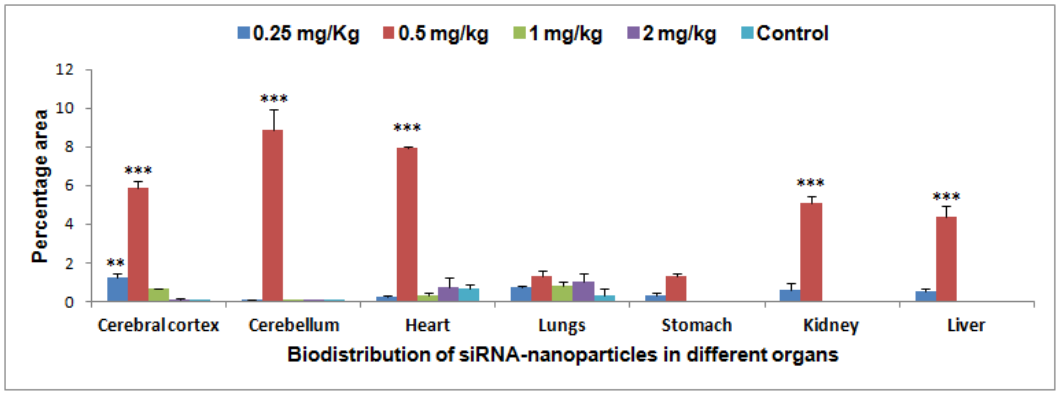

(B)

Figure 6.3(a): Histopathological images of organ tissues collected 4 h following administration of the novel nanoparticle formulation containing biotin-siRNA dose at 0.5 mg/kg in animals, indicating biodistribution. The study confirmed maximum delivery of biotin-siRNA in the brain (cerebral cortex and cerebellum), with a lesser extent in the heart, kidney, liver lungs and stomach. The results of nanoparticle-based siRNA delivery on the left were compared to the untreated control animals on the right. **(b):** Quantitative analysis using Image J of the stained area in tissues from animals receiving NT-biotin siRNA dose, complexed in nanoparticles at; 0.25 mg/kg, 0.5 mg/kg, 1mg/kg and 2 mg/kg, comapred with the untreated control receiving 0.85% w/v NaCl. The graph shows a representative result of the average of two random sections (n=2) measured per animal

tissue mean±s.d. ***P <0.01 was considered highly significant based on Tukey's post-hoc analysis, when compared with other groups

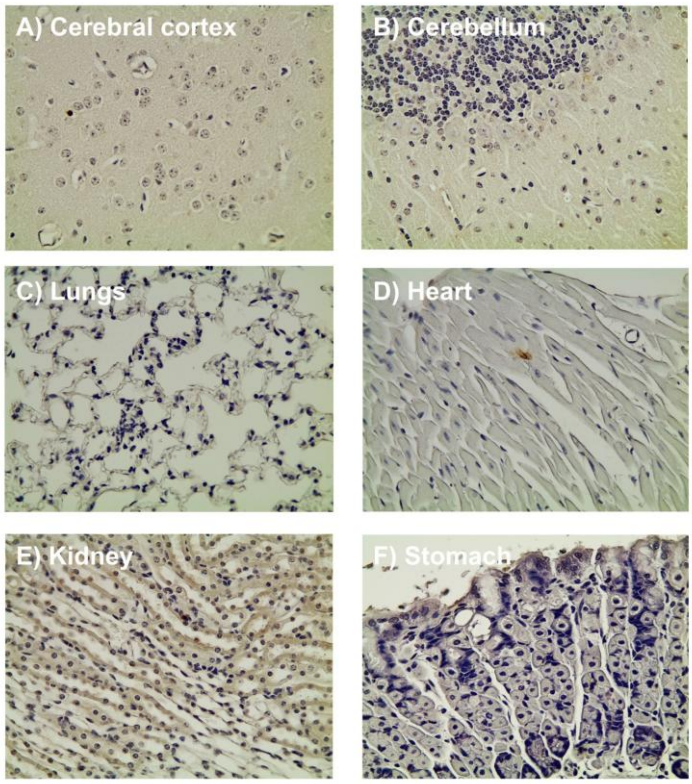

Figure 6.4: Histopathological images of various organ tissues collected 4 h following intranasal administration of multifunctional siRNA/nanoparticle formulation containing biotin-siRNA at a dose of 0.5 mg/kg. The tissues were stained with TUNEL – cell apoptosis assay. As indicated in the images, no apparent cell toxicity/apoptosis was observed in these tissues. This study confirms that the novel peptide-tagged nanoparticles were safe and did not cause any toxic effects.

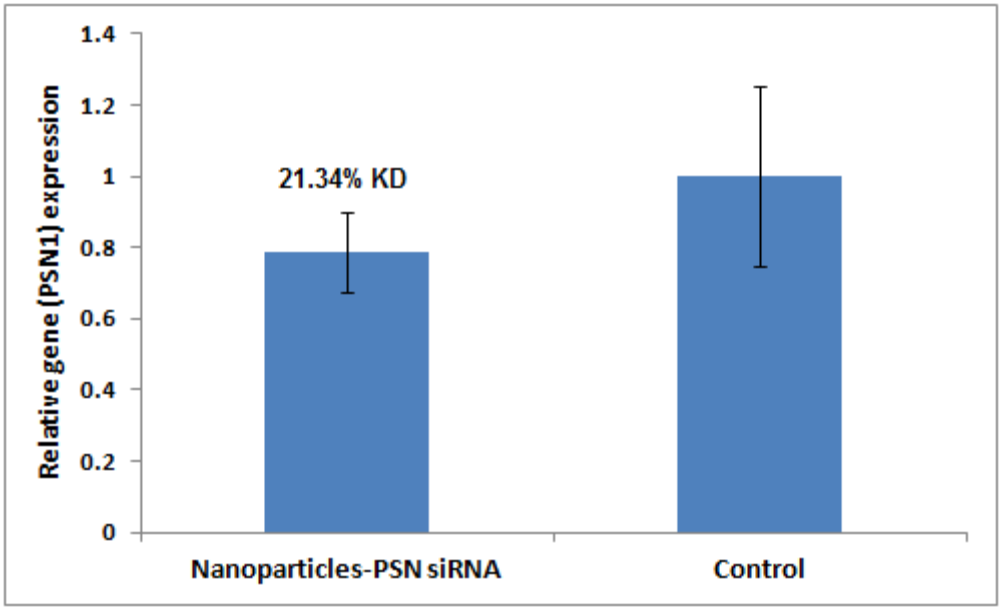

Figure 6.5: Relative PSN1 gene expression: Results are shown as relative expression (in function of GADPH) of PSN1 for animals treated with the nanoparticles bearing a PSN1 siRNA (left column) and for control (untreated) animals (right column). The results indicate a 21.34% KD (knockdown) in PSN1 gene expression with nanoparticles carrying siRNA against PSN1 gene, when compared with untreated control. The graph shows a representative result (average of n = 4 ± S.E.), with no statistical significance according to student t-test.

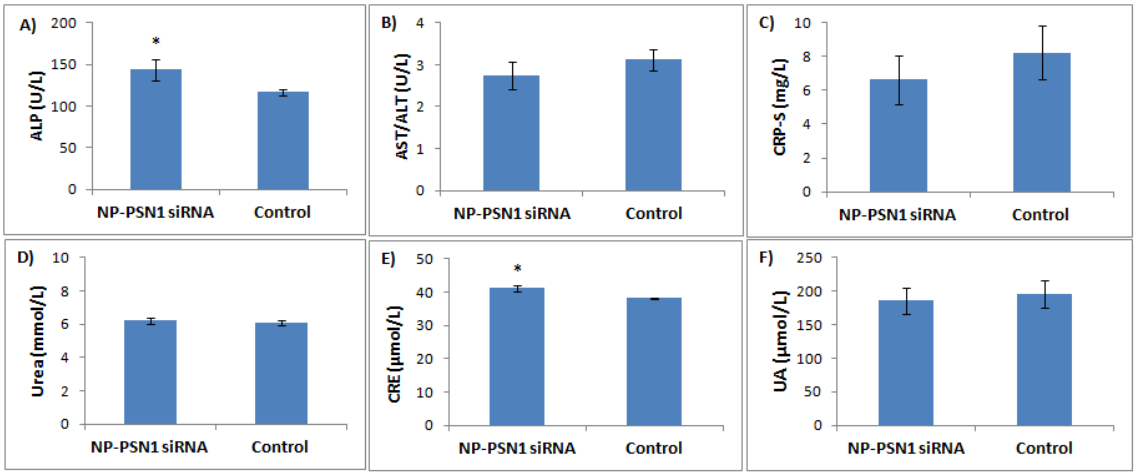

Figure 6.6: Serum analysis performed as a safety test for comparing the (A) ALP, (B) AST/ALT levels as liver function test, (C) CRP as an inflammatory test, (D) Urea; (E) CRE and (F) UA as kidney function tests. The graph shows a representative result (average of n = 4 ± S.E.). *P <0.05 was considered significant based on student t-test.

Original article 5

CHAPTER 7: NOVEL CP-15 TAGGED PEGYLATED CHITOSAN NANOPARTICLE FORMULATION FOR siRNA DELIVERY, SYSTEMICALLY, IN A MOUSE XENOGRAFT MODEL OF COLORECTAL CANCER

Meenakshi Malhotra, Catherine Tomaro-Duchesneau, Shyamali Saha and Satya Prakash*

Biomedical Technology and Cell Therapy Research Laboratory
Department of Biomedical Engineering, Artificial Cells and Organs Research Center
Faculty of Medicine, McGill University
3775 University Street, Montreal, Quebec, H3A2B4, Canada

*Corresponding author: Tel: 514-398-2736; Fax: 514-398-7461,
Email: satya.prakash@mcgill.ca

Preface: This study was performed to explore the multifunctionality of the nanoparticles prepared through a synthetic scheme, as described in chapter 5. The synthetic scheme developed enables to tag any peptide on the nanoparticles, which is specific to target a particular cell surface receptor. Towards this goal, we utilized CP15 peptide on PEGylated chitosan nanoparticles to target colorectal cancer tissue in-vivo. The siRNA used in this study was targeted against a pro-oncogene polo-like kinase 1 (PLK1), which is highly expressed in most of the tumor tissue types. The study analyzed the relative gene expression (mRNA) and protein suppression by the siRNA delivered by nanoparticles in comparison to other treatment groups and the control group. The biodistribution, tumor accumulation, serum safety analysis was also performed.

Article to be submitted

7.1 Abstract

Novel polymeric nanoparticles were developed to specifically target tumor tissue when administered systemically. The polymeric nanoparticles were developed using a novel synthetic scheme following a series of chemical reactions, which involved grafting of chitosan polymer with PEG and conjugating it further with a CTP (CP15). The synthesized polymer was used to form nanoparticles complexing siRNA at an N:P ratio of 129.2. The CP-15 tagged PEGylated chitosan nanoparticles were optimized and characterized to achieve a nanoparticle size of 80-120 nm with 100% siRNA loading efficiency. These multifunctional nanoparticles were tested for their optimal dosage, efficient delivery, cytotoxicity and bio-distribution in a mouse xenograft model of colorectal cancer. In-vivo results indicate efficient delivery of siRNA (0.5 mg/kg) by the CP-15 tagged PEGylated chitosan nanoparticles with approximately 50% gene silencing when administered intra-peritoneally in the mouse xenograft model of colorectal cancer. Gene silencing was obtained with no detectable toxicity. These results indicate a potential of using multifunctional nanoparticles for systemic delivery of siRNA at the targeted tumor site.

Key words: Chitosan, PEG, peptide, CP-15, nanoparticle, colon cancer, siRNA, gene silencing

7.2 Introduction

Cancer is characterized by the uncontrolled growth of a group of cells that infest adjacent tissues and often metastasize to other organs via the lymphatic or circulatory system. It is primarily caused by environmental factors (90-95%), but also by genetic factors (5-10%) [296]. Typically the alteration in cell growth promoting oncogenes and cell division inhibiting tumor suppressive genes lead to the formation of cancer cells [297]. Depending on the stage of the cancer, the treatment options available include surgical removal, chemotherapy with anticancer drugs, such as 5-Fluorouracil, oxaliplatin and Leucovorin [185], radiation therapy, immunotherapy [298] and hormone therapy with drugs like cetuximab and panitumumab [299]. However, it has been shown that cancers with genetic origin are not benefitted with these chemotherapies [299]. Moreover, the toxicity and side-effects have severely limited the safety and effectiveness of these methods.

One of the target proteins in cancer therapy is serine/threonine-protein kinase (PLK1), a key regulator of mitosis in mammalian cells. PLK1 is a proto-oncogene over-expressed in a variety of human cancers [300, 301]. It is directly associated with p53, a tumor suppressor protein and on interaction with p53, it inhibits the latter's transactivation and pro-apoptotic activity [302], leading to uncontrolled cell proliferation. Recently, the inhibition of PLK1 with antibodies, antisense oligonucleotides (ASO's), small interfering RNA (siRNA) or dominant negative mutants that suppress tumor growth by causing increased apoptosis have gained much interest as therapeutic options to treat cancer [303-308]. Although antineoplastic drugs have shown great success as a treatment for cancer therapy, many carcinomas are resistant to these agents and thus, chemotherapy with these agents has become a major restriction at an advanced cancer stage [309, 310]. Current clinical trial with PLK1 inhibitors are being conducted by Tekmira pharmaceuticals (TKM03081), wherein the formulation comprises of a stable nucleic acid lipid particle containing siRNA against PLK1 targeted towards late stage solid tumors [www.clinicaltrials.gov]. Thus, siRNAs targeted against proliferation-associated signal transduction pathways, which can halt the tumor progression in animal models is emerging as an appealing approach.

The delivery of siRNAs in-vivo has been challenging for anti-tumor therapy due to their instability in physiological conditions, improper cellular distribution, low bioactivity, high dosage requirement, and the necessity for continuous long-term infusions [49]. Various commercially available delivery/transfection reagents can provide better siRNA delivery in substantially lower doses than siRNA delivered alone, but these have concerns of target specificity, cytotoxicity, immunological responses, stable systemic delivery and off-target effects of these reagents. Moreover, the efficacy of most of these commercially available transfection reagents is limited to in-vitro use. For in-vivo applications, delivery via a systemic route targets multiple sites, which may not be an ideal deal for many biomedical applications [30-33]. Thus, the development of a delivery vehicle that can overcome these issues and identify cell-specific receptors, expressed as tumor biomarkers, with an ability to distinguish between cancer and normal cells will be an effective approach to overcome the limitations of currently used therapeutics. Most of the nanoparticles that are widely being accepted as an alternative approach to gene delivery are developed from cyclodextrin polycations, poly-l-lysine (PLL), polyamidoamines, chitosan, quantum dots and liposomes to deliver siRNA for on-target gene silencing [36, 311, 312].

The current study proposes a peptide tagged PEGylated chitosan nanoparticle for in-vivo siRNA delivery. The target specificity of the nanoparticles is attributed to a peptide that guides the nanoparticle system carrying siRNA to specific tissues, when administered via a systemic route. In this study, we have used peptide CP15 on the nanoparticles, which was identified by the generation of phage displayed libraries [313]. This method for identifying specific binding ligands has found wide application in isolating peptides that have high binding affinity for cancer cells [313]. The advantage of using peptide-based tumor targeting is their rapid clearance from the blood because of their small size and lack of immunogenicity. CP15 peptide has shown to be the most effective peptide targeting colon tumor cells, while not recognizing normal human intestinal epithelial cells [314]. The nanoparticle formulation developed in this study was used to selectively target the tumor tissue, expressing affinity towards CP15 peptide, in a mouse xenograft model of colon cancer developed from SW480 epithelial colon cancer

cells. This current study illustrates an example and potential use for the siRNA/nanoparticle formulation in cancer therapy.

7.3 Materials and methods

7.3.1. Materials

Materials used to synthesize modified chitosan polymer are as described in Chapter 5, with an exception of using Chitosan at a molecular weight of 50 KDa – 190 KDa, with viscosity 20-300cP and degree of deacetylation of 75-85%, obtained from Sigma (Oakville, ON, Canada). Other materials used include: CP15 (VHLGYAT- NH_2) M.W. 758.3, were synthesized by Sheldon Biotech, McGill University. Scrambled siRNA tagged with biotin, and PLK1 siRNA (h) with sequence; PLK1 (sense strand) - 5' AGAmUCACCCmUCCUmUAAAmUAUU 3' and PLK1 (antisense strand) - 5' UAUUUAAmGGAGGGUGAmUCUUU 3' from Dharmacon (Lafayette, CO, USA), where "m" represents 2'Omethylated nucleotide. Primary antibodies; PLK1 (F-8) mouse monoclonal antibody, β-Actin (C-4) mouse monoclonal antibody, probed with secondary antibodies; (HRP)-conjugated goat antimouse antibody. All the antibodies were procured from Santacruz Biotechnology (Santa Cruz, CA, USA).

7.3.2. Synthesis of peptide (CP-15) tagged PEGylated chitosan polymer

The polymer CS-PEG-CP15 was synthesized as described in chapter 5. The modified polymer was characterized and analyzed using 1H (Mercury 400 and 500 MHz NMR) and Transmission Electron Microscopy (Philips EM410 TEM).

7.3.3. Preparation of novel polymeric nanoparticles from CP-15 tagged PEGylated chitosan polymer

The nanoparticles were prepared from the chemically modified polymer (CS-PEG-CP-15). The nanoparticles complexing siRNA were developed at varying N:P ratios as described in chapter 3 [243]. The characterization of nanoparticles size and dispersivity was analyzed by TEM and the siRNA loading efficiency was determined by gel retardation assay.

7.3.4. Animal study and in-vivo tumor induction

Six week old Balb/c nude mice, weighing 15-20 g were purchased from Charles River Laboratories (Wilmington, MA, USA) and housed in an environment with controlled temperature (22°C), humidity, and a 12 h light/dark cycle at McGill's Animal care facility. The animal experiment was conducted as per the protocol approved by the Animal care committee at McGill University (Montreal, QC, Canada). Standard mouse chow pellets and water were supplied ad libitum. Animals were acclimatized for a week before the start of the experiment. For tumor induction, animals were subcutaneously injected with 100 µl of SW480 colon cancer cells (2×10^6) mixed with an equal volume of matrigel (BD). The treatment began after the tumor reached a volume of 100 mm^3. The tumor size was measured using a digital caliper and was calculated by the formula: volume = $(\text{width})^2 \times \text{length}/2$. The animals were randomized into 4 treatment groups (n=6) to receive treatment formulations: 1) CS-PEG-CP15 with PLK1 siRNA; 2) CS-PEG-CP15 with NT siRNA, 3) PLK1 siRNA alone and 4) Untreated control. In each treatment group the animals received a total siRNA dose of 0.5 mg/kg animal mass, as optimized in chapter 6. 100 µl of treatment formulations were administered every alternate day via intra-peritoneal injections for a period of 2 weeks.

7.3.5. Tumor accumulation and biodistribution study to identify siRNA delivery via nanoparticles in different tissues

Accumulation of nanoparticles at the tumor site and biodistribution in other organs of the animal was performed separately on one animal (n=1) receiving different kind of formulations as a) CS-PEG-CP15 with NT biotin-siRNA, b) Chitosan with NT biotin-siRNA, c) NT biotin-siRNA and d) Untreated control. The animals were sacrificed after 4 h of intraperitoneal treatment administration. Histopathological analysis was performed on tumor, lungs, heart, kidney, spleen and liver. In brief, the tissues were harvested and kept at 4°C in 10% phosphate buffered formalin for 48 hours. The tissues were then trimmed to 3 mm thick sections and stored at 70% ethanol in histology cassettes. The tissues were paraffin embedded and processed into 4 µm thick section on slides at the histology core facility (The Rosalind and Morris Goodman Cancer Research Centre, McGill University). The tissue section on slides were stained with Vectastain

elite ABC kit (Vector laboratories; Burlingame, CA, USA) as per the manufacturer's protocol and Diaminobenzidine (DAB) was used as a substrate to assess the presence of biotin, used as a tag on siRNA for histology identification purposes. Haematoxylin was used as a counterstain and slides were mounted with permount (Vector laboratories; Burlingame, CA, USA) and observed under compound microscope (Leica DM500; Ontario, Canada) at 400X.

7.3.6. RNA extraction and QPCR analysis to determine percentage of PLK1 gene knockdown

To further validate the knockdown effects of the endogenous PLK1 expression after nanoparticle-based PLK1-siRNA delivery in animals (n=6) from each group, a quantitative real time PCR was performed, as described in chapter 6. The relative expression levels of PLK1 gene were normalized with the housekeeping gene GAPDH. The primer sequences used were as follows: PLK1, 5'-GGCAACCTTTTCCTGAATGA-3'and 5'-AATGGACCACACATCCACCT-3'; GAPDH, 5'-TAAAGGGCATCCTGGGCTACACT-3' and 5'-TTACTCCTTGGAGGCCATGTAGG-3'. The PCR was run for 30 to 40 cycles with a 95°C denaturing step (5 s), a 60°C annealing step (15 s), and a 72°C extension step (15 s), plus final incubation at 72°C for 10 min.

7.3.7 Protein extraction and western blot analysis to determine PLK1 protein suppression

After 2 weeks of treatment, the animals (n=6) from each group were sacrificed and the tumor tissues were harvested and preserved in "All protect tissue reagent" from Qiagen (Toronto, ON, Canada). The tissue samples were homogenized using a PowerGen Model 125 Homogenizer from Fisher Scientific (Ottawa, Ontario, Canada) at 26,300 rpm in 2 mL of ice cold RIPA buffer (20 mM Tris pH 8, 150 mM NaCl, 5 mM EDTA, 1% Nonidet P-40, 0.1 % SDS, 10.0% Glycerol, 10 mM $Na_2HPO_4.7H_20$, 1% Sodium deoxycholate) containing phenylmethylsulfonyl fluoride (PMSF) and protease inhibitor cocktail from Roche Diagnostics (Laval, QC, Canada). The crude extract was incubated on ice for 30 minutes and centrifuged at 10,000 xg for 10 minutes at 4°C to remove tissue debris. The supernatant was collected and the protein concentration was determined using

Pierce® Bicinchoninic acid (BCA) Protein assay kit from Thermo Scientific (Rockford, IL, USA). Briefly, aliquots containing 100 µg of protein were heated at 70°C for 15 minutes with Nupage LDS sample buffer supplemented with 100 mM DTT. The proteins were fractionated on precast NuPAGE® 4-12% Bis Tris Gel from Invitrogen (Ontario, Canada) at 200 V for 35 minutes in MES SDS running buffer. Magic mark 1Kb protein ladder was used as a standard. The gel was electrophoretically transferred to a 0.45 µm pore size Novex® nitrocellulose membrane using Nupage transfer buffer on a Novex® SemiDry blotter (Invitrogen, ON, Canada). After transfer, the nitrocellulose membrane was incubated for 1 hr in 5% non-fat powdered milk in 1X Tris buffered saline (TBS) buffer supplemented with 0.2% Tween 20. The membrane was then incubated overnight at 4°C with mouse PLK (F-8) monoclonal antibody (1:100 dilution). The next day, the membrane was washed thrice with TBST for 15 minutes each, and then incubated with (HRP)-conjugated goat antimouse IgG secondary antibody (1:2,000 dilution). The membrane was again washed thrice with TBST followed by the detection of the signal with chemiluminescent agents (ECL, Amersham) from GE healthcare. The bound antibody was visualized using autoluminography. To control the protein loading, the membrane was reprobed with primary mouse monoclonal β-Actin (C-4) antibody (1:1000) with an overnight incubation at 4°C, followed by three washes in TBST and detection with HRP-conjugated goat anti-mouse IgG secondary antibody (1:2,000) and development with chemiluminescent agents, as described earlier.

7.3.8. Serum collection and analysis

Serum was collected and analysed as described in chapter 6. Serum analysis was performed to test for CRP and liver function tests; ALT and AST, using a conventional enzymatic method on Hitachi 911 automated clinical chemistry auto-analyzer (Roche Diagnostics, USA).

7.3.9. Statistical analysis

Experimental results are expressed as scattered dot plots with median. Statistical analysis was carried out using SPSS Version 17.0 (Statistical Product and Service Solutions, IBM Corporation, New York, NY, USA). Statistical comparisons were carried

out using Tukey's post-hoc analysis. Statistical significance was set at $p < 0.05$ and p-values less than 0.01 were considered highly significant.

7.4 Results

7.4.1 Synthesis of CP-15 tagged PEGylated chitosan polymer and preparation of nanoparticles

The peptide tagged PEGylated chitosan polymer was synthesized following a series of chemical reactions as described in chapter 5 [287]. Each intermediate step and the final product of the synthesis were characterized for the functional group modification and substitution by FTIR and ^{1}H NMR as described in chapter 5. **Figure 7.1** illustrates, NMR spectra of the final product obtained (CS-PEG-CP15) after the synthesis. The multiple peaks of oxymethyl groups in PEG at δ 3.3 to 3.7 cover over the signals of pyranose ring of chitosan in the spectra. The weak and broad peak at δ 4.3 - 4.5 are from the protons of –NH-CH(CH_2)-CO- in CP-15 peptide. The multiple peaks at δ 6.0-9.0 belong to the CP-15 peptide sequence.

7.4.2 Characterization of nanoparticles

Nanoparticles were prepared following an ionic gelation scheme, as described in chapter 3, wherein the cationic polymer complexes the anionic molecule due to electrostatic interaction. **Figure 7.2** represents a gel retardation assay, which was performed to determine the N:P ratio to achieve complete complexation of siRNA. Results indicate that at N:P ratio of 129.2, siRNA was completely complexed with the CP15 tagged PEGylated chitosan polymer to form nanoparticles. **Figure 7.3** represent nanoparticles as observed under TEM. The nanoparticles obtained were polydispersed and ranged from 100-120 nm in size.

7.4.3 Evaluation of siRNA/nanoparticle formulation to systemically deliver siRNA at the targeted tumor site

The nanoparticles developed from CP15 tagged PEGylated chitosan polymer were evaluated for their ability to deliver siRNA at the targeted tumor site through

systemic route, in comparison to unmodified chitosan nanoparticles, siRNA delivered alone and untreated control. For this experiment, the treatment formulations were separately prepared with 1) chemically modified polymer, CS-PEG-CP15, and 2) Chitosan polymer alone complexing NT biotin-siRNA at 0.5 mg/kg, as optimized and presented in our previous study, mentioned in chapter 6. NT biotin siRNA was also administered as a control. The animals were sacrificed after 4 h of dose administration. As represented in **figure 7.4(i),** the histopathological images from a mouse xenograft model of SW480 colon cancer. The dark brown stained tumor cells represent the presence of NT biotin-siRNA at the tumor site. The intensity of siRNA expression was found to be approximately equal for both CP-15 tagged PEGylated chitosan/siRNA nanoparticle formulation (p = 0.00043) and b) unmodified chitosan/siRNA nanoparticle formulation (p = 0.0011). The expression of NT biotin-siRNA, delivered alone was comparatively less and was not found to be significant, when compared to the untreated control (p = 0.062) **Figure 7.4(ii)** represents the mean of percentage area analysed for intensity (n=3) using Image J software. **Figure 7.5A** represents the biodistribution analysis of the above mentioned 3 treatments in heart, lungs, kidney, liver and spleen, as compared to the untreated control. The results indicate significant biodistribution of unmodified chitosan nanoparticles in all the organs ($p < 0.05$), whereas with CP-15 tagged PEGylated chitosan nanoparticles, the biodistribution was only found to be significant in heart (p = 0.001) and lungs (p = 0.017). The expression was followed by siRNA delivered alone with its significant expression in heart (p = 0.009) and lungs (p = 0.043) **Figure 7.5B** indicates the mean percentage area analysed for intensity (n=2) using Image J software.

7.4.4 Analysis of Percentage PLK1 gene knockdown

The PLK 1 gene knockdown was evaluated by extracting total RNA form the tumor tissues, then reverse transcribing it to form a cDNA and running a Real time PCR on cDNA using primers specific for PLK 1 gene. The percentage gene knockdown of PLK1 gene by siRNA delivered through CP-15 tagged PEGylated chitosan nanoparticles was evaluated by comparing the treatment group with other controls; mock transfections (CS-PEG-CP15 with NT siRNA), PLK1 siRNA alone and untreated control. As represented in **figure 7.6**, the treatment group showed a 50% PLK1 gene knockdown (p = 0.031) when

compared with the untreated control (n=6). No significant difference was observed between the groups of mock transfections and untreated control.

7.4.5 Analysis of PLK1 protein suppression

To evaluate and compare the amount of protein expression in various treatment groups, the total protein was extracted from the tumor tissue, quantified using BCA assay and 100 µg of total protein was loaded onto NuPAGE® 4-12% Bis Tris gels for western blot analysis. The gel was electrophoretically transferred to a nitrocellulose membrane and probed with appropriate antibodies. The protein bands developed using autoluminiscence were quantified using an Image J software and plotted with animal numbers, n=6 in each group. The relative protein expression as observed in **figure 7.7** shows that the animals receiving CS-PEG-CP15/siRNA(PLK1) nanoparticle formulation showed significantly lower expression of PLK1 (p = 0.038), when compared to the untreated control. However, no difference was observed among the mock transfection groups i.e. nanoparticles with NT siRNA and PLK siRNA alone when compared with the control untreated group.

7.4.6 Serum analysis for safety and toxicity study

200 µl of blood was collected in microtainer serum separating tubes just before the experimental end point, from jugular vein of all the animals in each group. The experimental end-point was at 2 weeks after the commencement of the treatment formulation. The serum was analyzed for safety tests especially for CRP and liver function tests ALT/AST as represented in **figure 7.8A and 7.8B**, respectively. No significant difference was observed among any treatment groups when compared to the untreated control (n=5) for both CRP and ALT/AST. Thus, with this study we can conclude that the synthesized CP15-tagged PEGylated chitosan nanoparticle formulation did not cause any systemic toxicity to the animals.

7.5 Discussion

The benefit of nano-delivery vehicles to facilitate the delivery and targeting of therapeutic molecules is becoming of great interest, wherein the targeted delivery

approach can increase the bioavailability of the drug at the tumor site. In addition, it encases the therapeutic minimizing its toxic exposure to the surrounding tissue and also providing it with stability by protecting from degrading enzymes. The hyper-proliferative environment of the tumor demands additional energy from its surroundings resulting in the generation of an acidic environment [84]. The disorganized and leaky endothelial junctions can facilitate the uptake of nanovectors via passive targeting by a phenomenon called EPR effect. However, active targeting can also take place by using ligands showing specific affinity towards a particular cell [313].

In this study we utilized a CP15 peptide on the surface of PEGylated chitosan nanoparticles, which have shown to have affinity towards SW480 colon cancer cells [314]. The nanoparticles were prepared from a series of polymeric chemical reactions, characterized and tested for their ability to deliver siRNA in-vitro, as presented in chapter 5 [287]. Moreover, the nanoparticles developed from the modified synthetic scheme were observed to have minimal/no toxic effect as compared to unmodified chitosan nanoparticles. In this study, these nanoparticles were used to complex siRNA against PLK1 gene, which is a known proto-oncogene. The nanoparticles developed at an N:P ratio of 129.5 had size in the range of 100-120 nm. The size of the nanoparticle depends on the molecular weight of the parent (chitosan) polymer, which was 50-190KDa. This size range was essential, when administering a formulation systemically as it has been described earlier that a size < 100 nm leads to glomerular filtration and the size above >200 nm leads to opsonisation of nanoparticles by reticuloendothelial system [84, 116].

The nanoparticles prepared with CS-PEG-CP15 polymer, complexing siRNA showed equivalent degree of accumulation as the unmodified chitosan nanoparticles at the tumor site. The delivery in the tumor was determined by the dark brown stained cells in the tissue, as represented in **figure 7.4(i)** and the intensity of the staining was evaluated by using Image J software, **figure 7.4(ii)**. Though both modified and unmodified chitosan nanoparticles were observed to efficiently accumulate in the tumor tissue, however the biodistribution study as presented in **figure 7.5 (A, B)** showed that the modified chitosan nanoparticles accumulated more at the tumor site than other organs, when compared to

unmodified chitosan nanoparticles. It is noted that the effect of specific tumor delivery may not necessarily be targeting alone but also due to the EPR effect which enhances the accumulation of nanoparticles at the tumor site due to leaky vasculature system [116]. However, the presence of targeting moieties on nanoparticles restricts them from being taken up by other tissues [117]. High degree of siRNA expression was observed for both modified and unmodified chitosan nanoparticles in heart and lungs after 4 h of intraperitoneal dose administration. A significantly lesser expression was observed in kidneys and liver with the modified chitosan nanoparticles, when compared with the unmodified chitosan nanoparticles ($p < 0.046$). This effect is seen due to the incorporation of PEG in the modified chitosan nanoparticles, which caters to the increased stability and circulation of the nanoparticles in the blood, without being degraded or filtered by kidneys [82, 315]. It is noted that the expression of NT biotin-siRNA delivered alone was not significantly observed in most of the tissues, as it is known that an siRNA delivered without a carrier is rapidly cleared from the system, within 15 min of administration [316].

The efficacy study was performed with 6 animals in each group receiving different treatment formulations for 2 weeks. For this study, the unmodified chitosan with PLK1 siRNA was not used as we have previously reported about its toxicity in in-vitro studies, mentioned in chapter 5 [287]. Thus, this study was aimed to see the anticancer effect due to the therapeutic (siRNA) targeted against the PLK gene delivered by the nanoparticles but not by the nanoparticles itself. The RTPCR study performed on the harvested tumor tissues reveal approximately 50 % gene silencing (p=0.031) with PLK1 siRNA delivered by CP-15 tagged PEGylated chitosan nanoparticles as compared to the untreated control. The animals receiving CS-PEG-CP15 nanoparticles with NT siRNA had no effect on the PLK1 gene expression as compared to the untreated control. That shows that the derivatized polymer, had no toxic effect of its own and the PLK1-siRNA was solely responsible for silencing of the gene. The similar results were obtained in protein analysis, where the treatment group with PLK 1-siRNA delivered by CS-PEG-CP15 nanoparticles show significant suppression of PLK1 protein (p=0.038) as compared to the untreated control. The serum safety markers analysed for liver function tests and

inflammation showed no significant difference among different treatments, which concludes that the treatment formulation had no apparent systemic toxicity.

7.6 Conclusion

The current study projects the potential of synthesized peptide-tagged PEGylated chitosan nanoparticle formulation to be used in-vivo in a mouse xenograft model of colorectal cancer. These nanoparticles prepared from a chemically modified polymer have the ability to be modified by incorporation of a specific peptide which shows affinity towards a particular cell line. The nanoparticles delivered the siRNA at the targeted site and caused 50% reduction in the expression of PLK1, at mRNA level. These nanoparticles did not induce any immunological reactions and liver toxicity as determined by the serum analysis. This study shows a potential of using nanoparticles mediated gene delivery that can be achieved via non-invasive strategy. This study can further be improved by prolonging the treatment duration and increasing animal number per group to see a therapeutic effect on the animal's tumor tissue. Our future studies will also include the extra controls in the experiment, such as other commercially available drug/gene delivery devices/ transfection reagents, non targeted nanoparticles to more conclusively comment on the targeting ability of the developed nanoparticles.

7.7 Acknowledgements

We gratefully acknowledge the assistance Canadian Institute of Health Research (CIHR) to Dr. S. Prakash and the support of McGill Major Scholarship to M. Malhotra. We would also like to thank Dr. Jing Hu for synthesizing peptide sequences at Sheldon Biotechnology, McGill University. Dr. Tara Sprules, NMR Facility Manager of Quebec/Eastern Canada NMR Centre for processing our NMR samples, Mr. Petr Fiurasek, Centre for self-assembled Chemical Structures (CSACS) for the FTIR facility, Mr. Xu Dong Liu for processing TEM images at (FEMR) Facility of Electron Microscopy Research at McGill University, Mrs. Anna Jimenez for help with animal study, Dr. Marilene Paquet for her expert advice and analytical help on histology slides and the histology facility at Goodman Cancer Research Centre at McGill University for preparation and processing of histology slides.

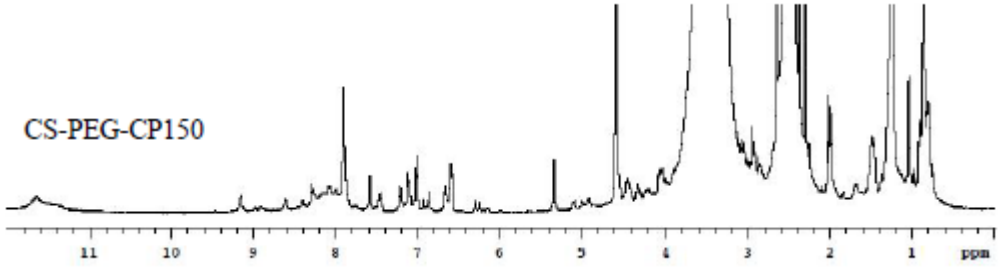

Figure 7.1: ^{1}H NMR spectra of (A) Chitosan-PEG-CP15 (CS-O-PEG-CONH-CP15). The multiple peaks of oxymethyl groups in PEG at δ 3.3 to 3.7 cover over the signals of pyranose ring of chitosan. The multiple peaks at δ 6.0-9.0 belong to the peptide CP15 sequence respectively.

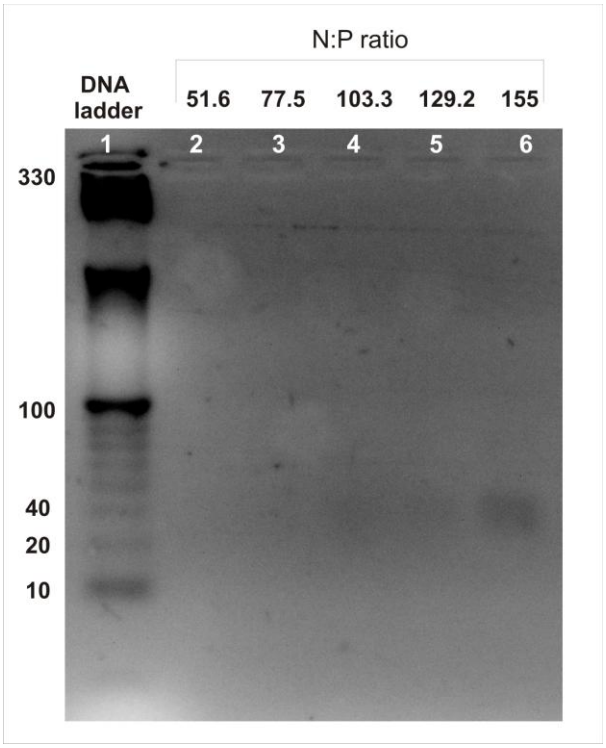

Figure 7.2: Gel retardation assay was performed to evaluate the maximum gene (siRNA) loading efficiency of nanoparticles for application in cancer therapy. Lane 1 represents a 10bp DNA ladder used as a reference. Lane 2, 3, 4, 5 and 6 represent various N:P ratios tested to achieve maximum siRNA loading into nanoparticles. The N:P ratio of 129.2 showed optimal siRNA loading with 8μg/ml of siRNA loaded in 0.5mg/ml of CS-PEG-CP15 polymer solution.

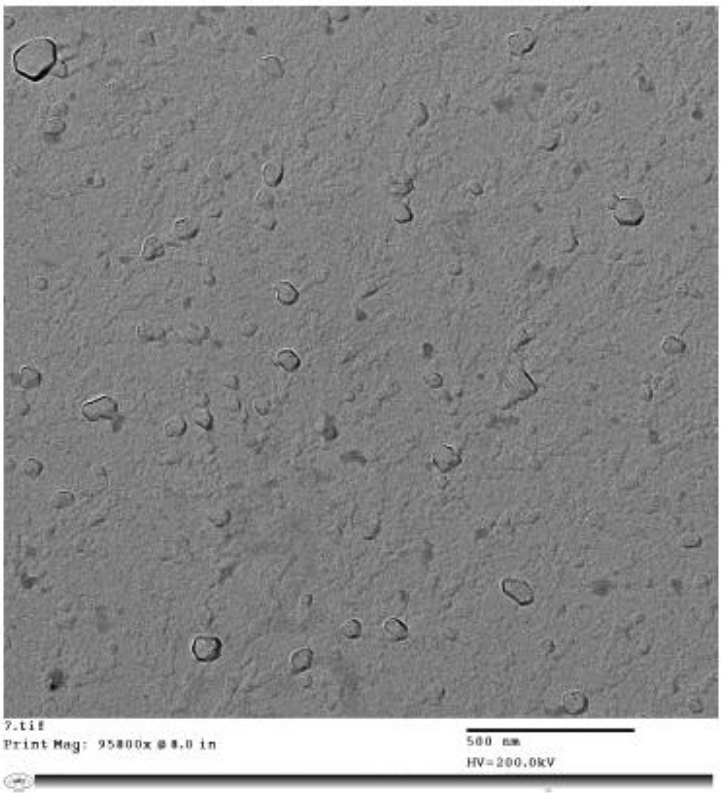

Figure 7.3: TEM image of CS-PEG-CP15/siRNA nanoparticles complexing siRNA at an N:P ratio of 129.2. Magnification at 95800X. The average size of the nanoparticles ranged from 100 to 120 nm.

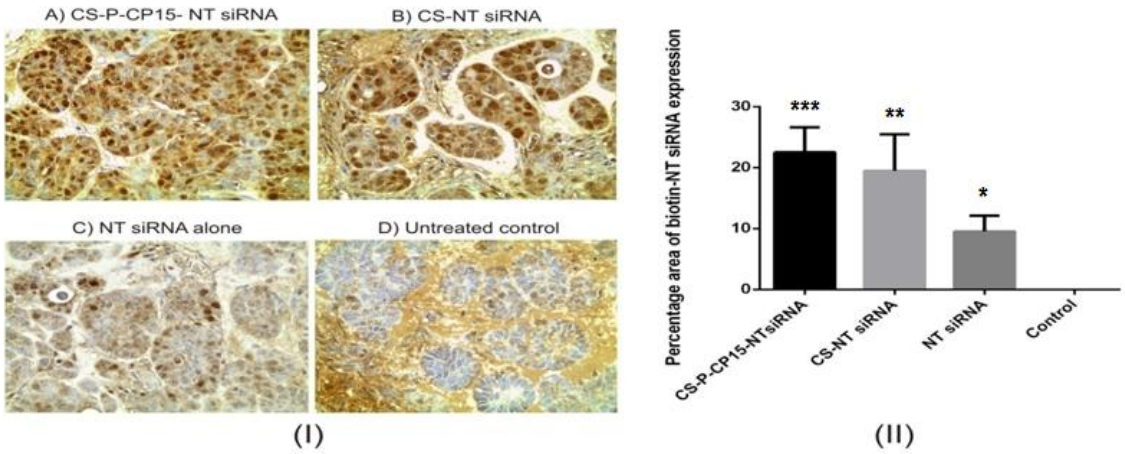

Figure 7.4(I): Histopathological images of SW480 colon cancer tissue stained dark brown in color, indicating the presence of scrambled biotinylated siRNA (0.5 mg/kg) in the tumor tissue after intraperitoneal administration of the treatment nanoparticle formulation. Animals were sacrificed after 4 hrs. (A) Chitosan-PEG-CP15, (B) Unmodified chitosan nanoparticles (C) Non-targeting biotin siRNA alone (D) Control: Untreated. **(II)** Image analysis of the mean percent area stained in the tumor tissues. The graph shows a representative result of the average of three random sections (n=3) measured per animal tissue, mean ± s.d. * $P < 0.05$, ** $P < 0.01$.

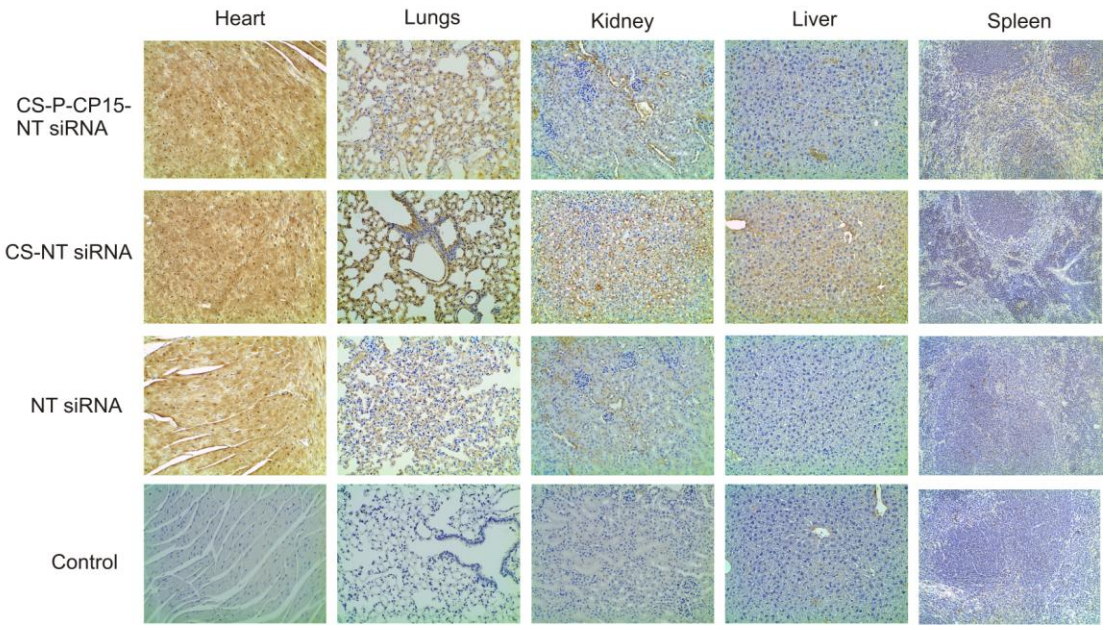

(A)

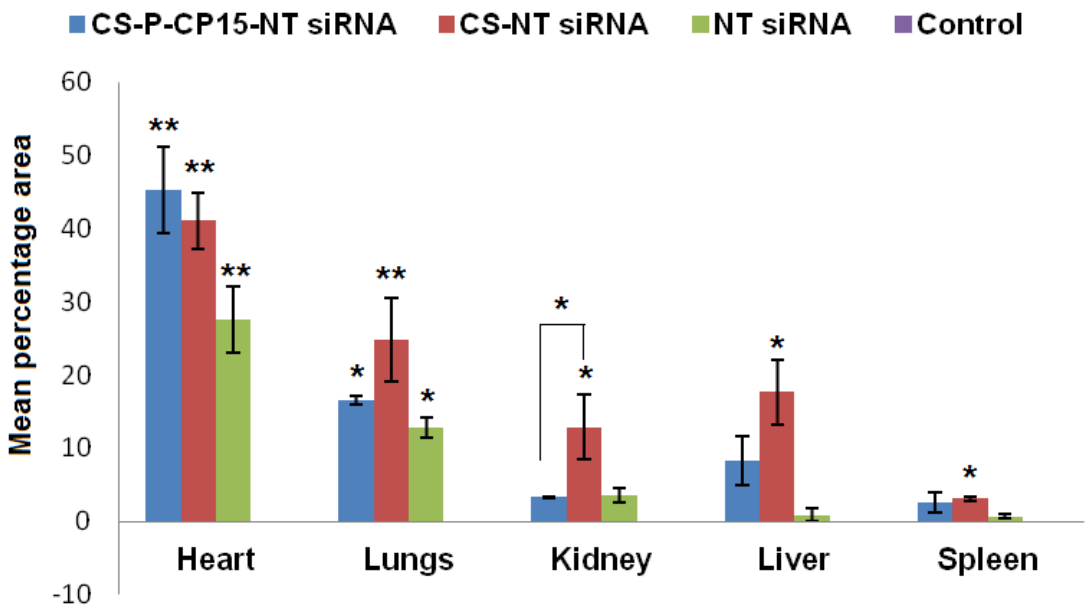

(B)

Figure 7.5A: Analysis of biodistribution of novel receptor-targeted nanoparticles in various tissues after 4 hours when administered intraperitoneally. Histopathological images of heart, lungs, kidney, liver and spleen obtained from a mouse xenograft model of colon cancer. The represented dark brown staining in the tissues emphasizes the presence of scrambled biotinylated siRNA (0.5 mg/kg) with different treatment

formulations: Chitosan-PEG-CP15, Unmodified chitosan nanoparticles, non-targeting biotin-siRNA alone and control as untreated. **(B)** Image analysis of the mean percent area stained in the tumor tissues. The graph shows a representative result of the average of two random sections measured per animal tissue, mean±s.d. *P<0.05, **P <0.01.

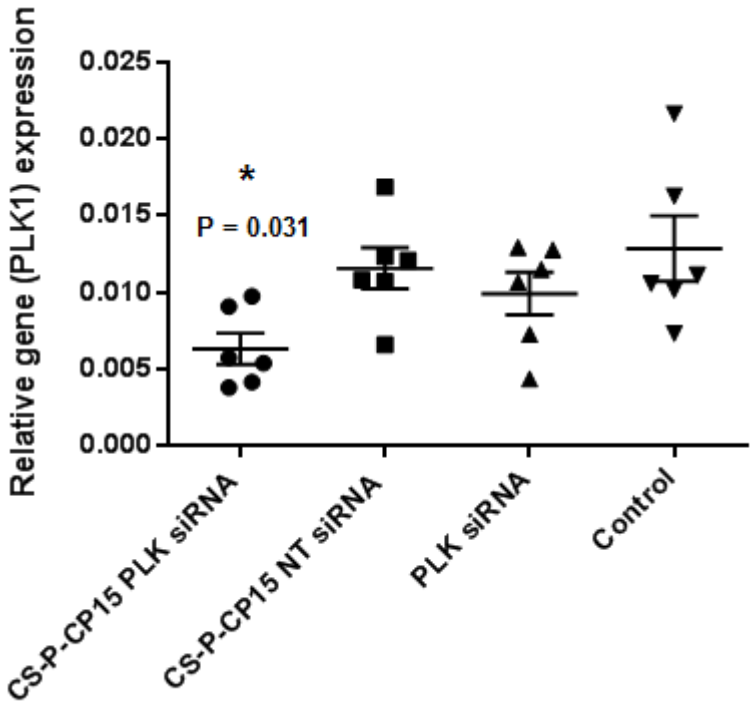

Figure 7.6: Quantitative Real Time PCR analysis from RNA extracted from tumor tissues of colon cancer. The PLK1 gene expression was compared among different groups after normalizing the GAPDH levels among all the animals The graph represents relative gene expression of PLK1 gene in tumor tissue after intra-peritoneal administration of various treatment formulations; A) CS-PEG-CP15 with siRNA against PLK1 gene, B) CS-PEG-CP15 with non-targeting biotin-siRNA, C) PLK1 siRNA alone and D) Untreated control: Saline. A 50% reduction in PLK1 gene expression was observed with treatment formulation (B) as compared with untreated control. The graph shows a scatter dot plot with n = 6 and mean±SE, *P<0.05.

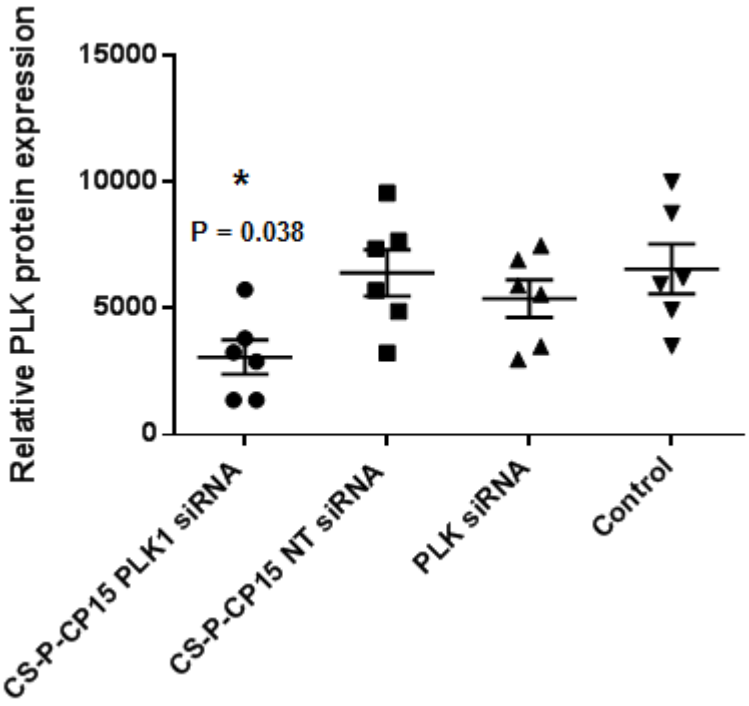

Figure 7.7: Western blot analysis from 100 μg of total protein extracted from tumor tissues of colon cancer. The PLK1 protein expression was compared among different groups after normalizing the β-actin levels among all the animals. The graph represents relative protein expression of PLK1 gene in tumor tissue after intra-peritoneal administration of various treatment formulations; A) CS-PEG-CP15 with siRNA against PLK1 gene, B) CS-PEG-CP15 with non-targeting biotin-siRNA, C) PLK1 siRNA alone and D) Untreated control: Saline. Reduction in PLK1 protein expression was observed with treatment formulation (A) as compared with untreated and mock transfection controls. The graph shows a scatter dot plot with n = 6 and mean±SE, *P<0.05.

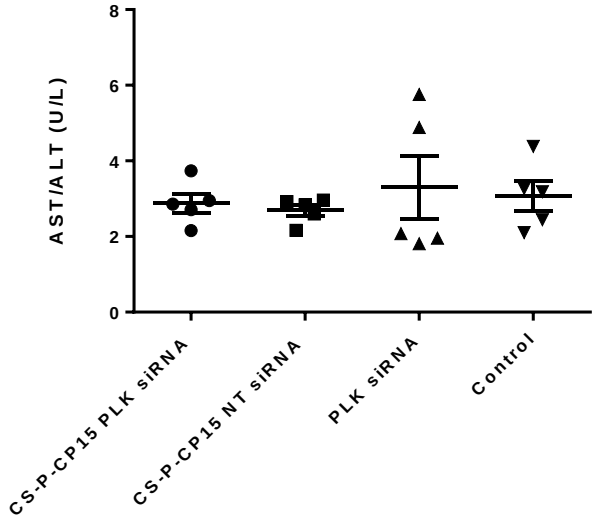

(A)

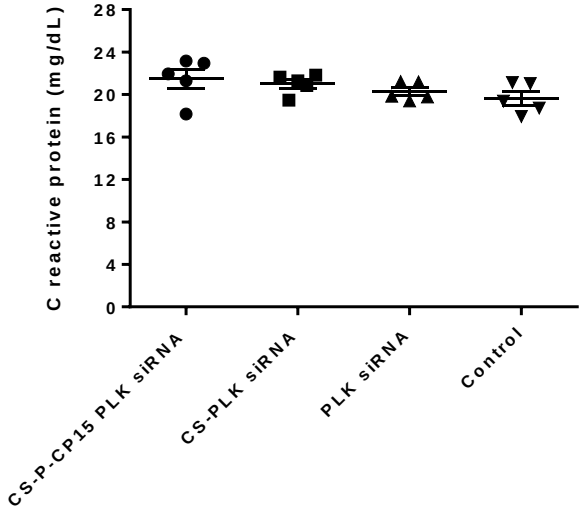

(B)

Figure 7.8: Serum analysis was performed as a safety test for comparing the (A) CRP and (B) ALT, AST levels among different treatment groups. The results indicate no significant difference between the treatment group (CS-PEG-CP15 containing siRNA against PLK1 gene with mock transfections and untreated controls. This concludes that the treatment formulation had no deleterious effect in terms of toxicity and immunological reactions on the animals. The graph shows a scatter dot plot with n = 5 and mean±SE.

CHAPTER 8: GENERAL DISCUSSION

The thesis in its first chapter gives a general introduction on nanomedicine and focuses on the components that are used to make an efficient multifunctional nanoparticle formulation for delivery of therapeutics across the biological barriers. This introduction forms the core of the thesis, introducing the main features of the components and their advantages. The thesis also outlines the rationale behind the research and the main objectives of the study.

The second chapter of the thesis summarises the recent advancements on nanoparticles based siRNA delivery strategies targeting neurodegenerative diseases and cancer. It describes the current limitations and challenges faced with various therapeutic modalities to deliver drugs/gene across the physiological and anatomical barriers of the body, highlighting the invasive procedures performed and their drawbacks. The review also focuses and on RNAi technology, as a new class of therapeutic drugs and the design and delivery aspects employed with RNAi research. The review further focuses on the current research in nanoparticles-based targeted delivery approaches. It further discusses the limitations of nanoparticles with respect to toxicity, efficiency, stability and off-target effects. The review comprehensively talks about the methods to improvise the target specificity of nanoparticles using cell specific ligands/peptides, their advantages and their specific pathway of being taken-up by the cell membrane. The overall story sums up with examples from in-vitro and in-vivo studies performed with various synthetic nanoparticles developed utilizing cell specific ligands and their promise to be used as a drug/gene delivery device.

The third chapter summarises the characterization and optimization performed with siRNA complexed chitosan nanoparticles, in view to achieve smallest particle size, with efficient gene loading and transfection capability. To achieve this objective, the commercially available chitosan of various molecular weights (high, medium and low) were tested to form nanoparticles on interacting with sodium tripolyphosphate (TPP), which was used as a crosslinker. The nanoparticles were prepared at various pH

conditions of both chitosan and TPP. The smallest particle size was achieved with low molecular weight chitosan at a Chitosan to TPP ratio of 3:1 (w/w) and at pH 5 for chitosan and at pH 3 for TPP. This data was supported with particle size, zeta potential and TEM analysis. The particles achieved after siRNA complexation were of approximately 20 nm in size. Complete gene (siRNA) loading efficiency was achieved at chitosan to siRNA ratio of 200:1 (w/w), i.e. N:P ratio of 103. This data was supported by gel retardation assay. The transfection efficiency of these nanoparticles was performed on mouse neuroblastoma cells. This study was regarded as the preliminary study in order to optimize the conditions for forming smallest particle size that can be proposed for delivering therapeutics across the biological barriers in-vivo. However toxicity of the nanoparticles developed, was one of the concerns in this study.

The fourth chapter comprises of a novel synthetic scheme that was employed to achieve chemoselective conjugation of PEG on C6 hydroxyl group of chitosan. The motive behind this study was to protect amine groups of chitosan using phthalic anhydride, which play a key role for chitosan to act as an efficient transfecting agent. Moreover, phthaloyl moiety on chitosan enables its character to be soluble in various solvents and be able to take part in further chemical reactions. Also, it is known that high density of amine groups can disrupt the cell surface integrity, thus causing toxicity. Therefore, incorporation of PEG was preferred to alleviate the cytotoxicity of nanoparticles. In brief, this chapter illustrates the utilization of sodium hydride (NaH) as a catalyst to facilitate the reaction between monomethoxy PEG and phthaloyl chitosan. This study is the first to report the use of NaH for a reaction between PEG and chitosan. This chapter compared and discussed the advantage of this scheme with other methods known in the literature to form PEG grafted chitosan polymer, with a focus on purification methods, reactions conditions and final yield of the product. The chapter also focused on the ability of the PEG grafted chitosan polymer to form nanoparticles and deliver siRNA into neuronal cells, in-vitro. The characterization of the polymer performed through FTIR reported successful grafting of PEG on chitosan. The nanoparticle size and morphology was characterized by TEM analysis, which yielded, nanoparticles of the range 50-100 nm. The siRNA loading efficiency was supported by

gel retardation assay and transfection and cytotoxicity was determined via spectrometric analysis.

The fifth chapter introduces another novel scheme of synthesizing TAT peptide tagged PEGylated chitosan polymer. This study was performed to address the question of target specificity and enhanced transfection ability of the nanoparticles when delivered via systemic route, in-vivo. This chapter described the synthesis, characterization and in-vitro study of the nanoparticle formulation. The derivatized product was synthesized by functionalizing the hydroxyl groups of chitosan. Before which, the amine groups on the chitosan were protected using phthalic anhydride, as described in chapter 4. This step was performed to make chitosan organosoluble, which leads to a homogeneous solution of the polymer for further chemical reactions. The protected chitosan polymer was PEGylated followed by a chemoselective conjugation of a cationic, CPP (TAT). The final product was obtained by deprotecting the amine groups on chitosan polymer. Here, PEG acts as a linker to conjugate two compounds on its either side. The various intermediates and the final product formed during the synthesis were characterized using ^{1}H NMR and FTIR spectra, which showed successful grafting of the conjugants. The morphological details of the final polymer were studied using TEM. The implication of the proposed synthetic scheme was utilized to form nanoparticles and deliver small interfering RNA's as a model therapeutic molecule, in an in-vitro model of mouse neuroblastoma cells over-expressing ataxin protein. The siRNA delivered through these nanoparticles exhibited efficient suppression of the diseased protein as determined by western blot analysis.

The sixth chapter of this thesis explores the ability of the novel peptide-tagged PEGylated chitosan nanoparticles to deliver siRNA bypassing the BBB, when administered intranasally. For this study, the nanoparticles were tagged with an MGF and TAT peptide. The MGF peptide has shown to have an affinity towards neuronal tissue. Thus, MGF was considered as a targeting peptide on the nanoparticles in this study. The TAT peptide was used as a cell penetrating peptide to enhance the transfection ability of the nanoparticles. The study aimed to achieve two objectives: The first objective was to determine preclinical efficacy, optimal dose, duration, dose frequency, toxicity and

biodistribution of the nanoparticles to deliver siRNA targeting brain. Preliminary result from this study indicated that this novel formulation has potential to deliver siRNA, via intranasal route of administration, bypassing the BBB and targeting a specific region of the brain. The second objective is an extension of the preliminary study which aimed to evaluate and determine percentage gene knockdown by siRNA delivered through these novel nanoparticles in an animal model of AD. This study showed that these nanoparticles can safely deliver the functional siRNA at the targeted site (cerebral cortex) and cause silencing of PSN1 gene, chosen as a model for therapeutic study. However, the gene knockdown study did not turn to be significant, but nevertheless its shows a trend and a potential towards the therapeutic efficacy. This study shows the promise of using nanoparticles mediated siRNA delivery, administered intranasally, for use NDDs, such as AD.

The seventh chapter describes another application with peptide-tagged PEGylated chitosan nanoparticles to be used in-vivo in a mouse xenograft model of colorectal cancer. This study was performed with an objective to evaluate the target specificity and serum stability of the nanoparticles to protect siRNA before reaching the targeted tumor tissue, when administered systemically. The advantage of the proposed nanoparticle formulation is that it can be tailor-made by incorporating a specific peptide or a cell targeting ligand/moiety that has an affinity towards the targeted cell type. In this study a CTP (CP-15) was utilized, which has shown to have affinity towards the SW480 colon cancer cells. The nanoparticles prepared showed efficient siRNA complexation, at an N:P ratio of 129.2. The nanoparticles safe guarded the siRNA when administered systemically and specifically released it at the tumor site. This was confirmed by data that showed 50% reduction in the expression of PLK1 oncogene, as determined by quantitative PCR analysis. These nanoparticles did not induce any immunological reactions and liver toxicity as determined by the serum analysis. This study showed that the siRNA delivered through peptide-tagged PEGylated chitosan nanoparticles can cause efficient gene silencing, following non-invasive delivery approach.

Though nanotechnology shows an extensive potential in the coming future, there are few concerns associated with its use. The primary concern is their toxicity. This would require an exhaustive study on the nanoparticle's interaction with the physiochemical and physiological processes in the system. The biodistribution of nanoparticles have to be extensively studied to avoid its uptake by unintended molecules such as MPS, consisting of monocytes and macrophages. However, the mask of PEG on nanoparticles has helped in excavating the opsonisation. Another concern of nanoparticles is that they are active and have a large surface area capable of interacting with unintended sites if not tagged properly with targeting molecules. Several strategies have been proposed in literature to efficiently tag the nanoparticles with ligands that specifically identify the surface signatures at the targeted site. Another important study would be to investigate how these nanoparticles are metabolically processed or excreted from the system, without causing any toxic effects. Though, biodegradable polymers are being used for this approach but its application in in-vivo use is most crucial. Thus, care has to be taken to implement this technology in a way as to avoid environmental, socio-economic and toxic side-effects.

The efficacy of nanomedicine needs to be analyzed on the basis of pharmacogenetics due to known population variability in drug sensitivity. There is a possibility of "varying" specific and non-specific interactions due to nanoparticle contact based on cell and tissue type. Currently, there are no established methodologies or model system(s) to study such intricacies to rule out the possibility of any hazardous effects of nanoparticles delivered in-vivo. It is not the high surface area of small nanoparticles, that make them toxic but its accumulation in certain un-intended organs. In this scenario, vital questions need to be addressed further: how do these nanomaterials interact with other types of drugs, foods and secondary metabolites of a tissue/organ, will there be any induction or interference mediated by these nanomaterials, and do they influence macromolecular interactions happening in a cell in response to different signals? An emphasis on non-specific adsorption, organ distribution, metabolism, residence time, degradation, clearance and bioaccumulation of nanomaterials remains to be addressed. Moreover, the pharmacokinetic behavior, the production reproducibility of nanoparticle

formulations and their size distribution need to be validated both in-vitro and in-vivo before their use is implemented.

A multi dimensional investigation is needed to rule out all of the possible short-term and long-term toxicological effects. Efforts to ensure the safety of nanomaterials require manufacturers to fully assess how the "nanosizing" of drugs affects dissolution rate, solubility and therapeutic action. Safety has to be given higher priority for the in-vivo use of nanoparticles, particularly those in the size of 50 nm, which can enter cells via adsorptive endocytosis. Validated assays are mandatory for detecting and quantifying nanoparticles in tissues and medical products. Additional standard test methods may be needed to ensure the appropriate formulation of nanoparticles for drugs and biologics. However, a major challenge is to find a reliable and affordable method of connecting the steering (delivery) system to the payload (drug). Having described nanoparticles should be efficiently used and functionalized based on the desired applications.

The characteristics, both physical and biochemical, of each delivery system should be considered in the design and drug functionalization processes. Furthermore, current preclinical studies focus on a number of different animal models, including tumor-induced and genetically encoded cancers. This makes it difficult to compare and contrast the efficiency of each delivery system and drug combination. In addition, the route of administration, the targeted site, the stage of the cancer and the physiological stability of the formulation are all aspects that need to be addressed to conclude on the efficacy of any developed therapeutic. For this analysis, established clinical trial methods would need to be employed. There are still several questions that remain unanswered concerning the fate of these nanomaterials in-vivo and their long term effects on gene expression, interaction/interference with the normal physiology, dose effect and drug–drug interactions. These properties have to be validated in addition to the conventional methods of ADMETox. The answers may start coming from the clinical research and trials in cancer and neurodegenerative and infectious diseases, provided that the drug manufacturers can resolve technical challenges, unwanted cellular/immunological reactions, in-vivo stability and limitations in delivery.

Industrial scale-up of nanotechnologies is required for future clinical studies. Efficient studies, using preclinical and clinical studies, must continue to ensure efficiency and safety of any developed formulation. One also must consider that drug delivery systems are inherently limited by the payload they deliver. Anti-cancer drug research must progress to allow any delivery system formulation, to be effective in the future.

CHAPTER 9: CLAIMED ORIGINAL CONTRIBUTIONS TO KNOWLEDGE AND CONCLUSIONS

9.1 Claimed original contributions to knowledge

In this thesis, we have shown that peptide-tagged PEGylated chitosan nanoparticles can be successfully used to deliver siRNA, noninvasively to target neurodegenerative diseases and cancer.

The following novel research findings have been demonstrated:

1. Chitosan nanoparticles were developed with size in the range of 20 nm and N:P ratio of 103. These nanoparticles showed efficient delivery of siRNA in neuronal cells, in-vitro.

2. A novel synthetic scheme was developed to surface-graft PEG on chitosan polymer using sodium hydride as a catalyst. The nanoparticles developed, complexing siRNA, showed efficient siRNA delivery, with no/minimal cytotoxicity in neuronal cells, in-vitro.

3. Another novel synthetic scheme was developed to form multifunctional nanoparticles. The synthesis scheme utilized PEG grafting on chitosan polymer followed by attachment of a CPP/CTP ligand for active targeting.

4. The modified chitosan polymer (peptide tagged PEGylated chitosan) developed was observed to complex siRNA and parameters like gene loading efficiency, size, surface charge were optimized. The nanoparticles obtained were of 5-10 nm in size.

5. The multifunctional nanoparticles developed using the novel synthetic scheme, showed ability to be custom made in terms of size and attachment of a targeting moiety with respect to the application in use. In this study we used MGF peptide,

that is known to have affinity towards neuronal cells and CP-15 peptide that is known to have affinity towards colorectal cancer cells.

6. The multifunctional nanoparticles developed, presented enhanced transfection ability with minimal/no toxicity in in-vitro model of neuronal cells, as compared to the unmodified nanoparticles.

7. The multifunctional nanoparticles developed have shown to successfully bypass the BBB to deliver siRNA intranasally to the cerebral cortex and cerebellum. The optimal dose of siRNA delivered was 0.5 mg/kg of animal weight, with no toxicity at the tissue level.

8. The multifunctional nanoparticles developed showed a potential to deliver a functional siRNA to cause approximately 20% reduction in the relative gene expression (Presenilin 1) of the diseased gene in an animal model of AD. However, it was not a significant result.

9. The multifunctional nanoparticles showed ability to be tailor-made in terms of size (100-120 nm), complexing siRNA at an N:P ratio of 129.2 for cancer study.

10. The nanoparticles systemically delivered siRNA to an animal model of colorectal cancer and showed a significant 50% reduction in the relative gene expression (PLK1) in the tumor tissues.

11. The biodistribution study in the cancer model, showed multifunctional nanoparticles were accumulated more at the targeted site as compared to other organs.

12. The in-vivo toxicity in the AD and cancer study has indicated that the multifunctional nanoparticles show no apparent tissue or systemic toxicity in the animals.

13. The proposed synthesis scheme of the multifunctional nanoparticle developed is highly reproducible and can be easily scaled up for in-vivo applications.

14. The proposed nanoparticle formulation has a potential be used as a therapeutic intervention, delivering drugs, vaccines, peptides, proteins, genes etc for a specific application.

15. The nanoparticle formulation has the ability to be custom-made in terms of size, surface charge and attaching a targeting moiety as per the specific cell/tissue to be targeted.

16. The multifunctional nanoparticle developed can address an urgent need to deliver the therapeutics across the blood-brain-barrier and other physiological barriers, without interfering with the membrane's integrity and be used for clinical applications.

9.2 Conclusions

Nanomedicine holds a promise to bring about the next therapeutic intervention in the health science. With its versatile applications in drug delivery, diagnosis and regenerative medicine, it has the potential to bridge the gap between early stage diagnoses to the treatment of diseases. In future, it can provide a window for "personalised medicine", which will specifically cater to the need of an individual, by providing improved therapeutic efficiency with reduced side-effects. RNAi technology can fight the diseases that have genetic origin. However, owing to the transient nature of siRNA's, shRNAs, a combination of a delivery vehicle that is biocompatible, biodegradable and poses efficient targeting and delivery abilities, appears as an appealing approach for RNAi. Moreover, nanoparticles based delivery vehicles have an advantage to be surface functionalised, to be accumulated at a targeted site, with increased stability and blood circulation. Also, the ability to be functionalised gives a creative opportunity to address the unseen challenges that may appear or be discovered in future. It is important to establish a delivery vehicle

that if needed be equipped with various moieties, this will aid in responding to evolutionary changes such as multidrug resistance with certain cancer types.

In this research thesis, we have developed a novel multifunctional nanoparticle device, that can efficiently complex siRNA and deliver it non-invasively. This siRNA/nanoparticle formulation showed successful delivery in two in-vivo models namely, Alzheimer's disease and a xenograft model of a colorectal cancer, respectively.

In this thesis the suitability of the siRNA/nanoparticle formulation in terms of size, gene loading efficiency, delivery and toxicity was tested in both in-vitro and in-vivo. The application of siRNA/nanoparticle formulation tested in animal models show better improved bioavailability of the therapeutic at the targeted site, with better circulation and reduced accumulation in other organs. The formulation developed shows an ability to be targeted towards a specific cell type or tissue based on the affinity of the attached ligand on the nanoparticle's surface towards a cell surface receptor. The advantage of free amines on the surface of chitosan polymer helps complex siRNA, via ionic interaction and moreover helps release the siRNA in the cell's cytoplasm due to "proton sponge effect". These characteristics truly enhance the quality of this formulation in comparison to other delivery formulations that exist in literature. Moreover the formulation has the ability to be tailor-made in terms of functionality, targeting ligands, payload and size as per the delivery application in use. Thus, this work demonstrates the effectiveness of using our developed siRNA/nanoparticle formulation as a therapeutic modality to aid the process of therapeutic delivery in the animal models of neurodegenerative diseases and cancer model but is not limited to it.

This thesis presents the potential of multifunctional siRNA/nanoparticle formulation to be delivered non-invasively in the animal models of NDDs and cancer. However, further study would be required to clarify and improve the nanoparticle's efficacy.

The preparation of the synthesized polymer, though is highly reproducible, but has number of steps to follow. The use of chemical, ethanethiol to remove the methyl group on PEG for its further conjugation should thought to be replaced, due to the stinky character of the chemical. This step was the major hindrance while performing the experiments in the lab and if possible a better and enhanced method can be utilized that uses odorless chemicals.

The nanoparticle prepared from the synthesized polymer should be tested for their shelf-life stability to be considered for effective clinical practice. Studies of lyophilization and stability of the therapeutic after lyophilization over a period of time should be performed and tested both in-vitro and in-vivo.

A well suitable method for delivering the siRNA/nanoparticle formulation for intranasal delivery has to be formulated. Methods have to be developed to be able to deliver the formulation at a required dose, without compromising the efficacy, either as sniffing lyophilized powder, intranasal spray or drops. Else a study on a bigger animal model should be considered for proper intranasal, dose administration.

An elaborative study in a cancer model with more animal numbers and controls should be performed to gain a deeper insight on the targeting of the proposed siRNA/nanoparticle formulation. Such as chitosan-PEG nanoparticle would serve as a better control with chitosan-PEG-peptide nanoparticle. As the presence of PEG helps improve steric stability of the nanoparticle providing better circulation however the

effectiveness of targeting can only be proved best with comparing these two formulations. This control is necessary and should be considered for future work.

The multifunctional nanoparticles developed should also be explored in the area of delivering drugs etc. The nanoparticles developed in the proposed scheme were prepared keeping in mind its wide application and use in future, wherein not only extra targeting moieties but also various other kind of payloads can also be delivered by utilizing the available functional groups on the polymer. This can also be performed by incorporating combinatorial approaches i.e. delivering genes and drugs together in one formulation.

Currently there are no clinical trials with siRNA nanoparticle formulation for NDDs, especially addressing the non-invasive delivery approach. Thus, there is an urgent need to address this situation by providing a successful therapeutic intervention. Our developed siRNA/nanoparticle formulation shows a potential to not only bring about new studies being conducted at clinical trials but also revive back the clinical trials existed with therapeutics that failed to prove their efficacy or cross the BBB.

Thus, it brings about a joint effort where the goodness of each molecule can be explored to fasten the process of drug development and its efficient delivery.

1. Malhotra M and Prakash S. Targeted Drug Delivery Across Blood-Brain-Barrier Using Cell Penetrating Peptides Tagged Nanoparticles. Current Nanoscience. 2011;7:81-93
2. Neurodegenerative disease: a major market in the making. http://pharmalicensing.com/public/articles/view/1134396614_439d84c67e5bf/neurodegenerative-disease-a-major-market-in-the-making
3. World Health Organization, Cancer, Fact Sheet #297, 2009.
4. Malhotra M, Nambiar S, Swamy VR and Prakash S. Small interfering ribonucleic acid design strategies for effective targeting and gene silencing. Expert Opin. Drug Discov. 2011;6:269-289
5. Mourya VK and Inamdar NN. Chitosan-modifications and applications: Opportunities galore. Reactive & Functional Polymers. 2008;68:1013–1051
6. Kumar MNVR. A review of chitin and chitosan applications. Reactive & Functional Polymers. 2000;46:1–27
7. Napoli C, Lemieux C, Jorgensen R. Introduction of a chimeric chalcone synthase gene into petunia results in reversible cosuppression of homologous genes in trans. Plant Cell. 1990;2:279-89
8. Fire A, Xu S, Montgomery MK, et al. Potent and specific genetic interference by double-stranded RNA in Caenorhabditis elegans. Nature. 1998;391:806-11
9. Elbashir SM, Harborth J, Lendeckel W, et al. Duplexes of 21-nucleotide RNAs mediate RNA interference in mammalian cell culture. Nature. 2001;411:494-8
10. Yang WQ and Zhang Y. RNAi-mediated gene silencing in cancer therapy. Expert Opin. Biol. Ther. 2012;12:1495-1504
11. Sharp PA. RNA interference-2001. Genes Dev. 2001;15:485-90
12. Hutvagner G, Zamore PD. RNAi: nature abhors a double-strand. Curr Opin Genet Dev 2002;12:225-32
13. Jackson AL, Bartz SR, Schelter J, et al. Expression profiling reveals off-target gene regulation by RNAi. Nat Biotechnol. 2003;21:635-7.
14. Persengiev SP, Zhu X, Green MR. Nonspecific, concentration-dependent stimulation and repression of mammalian gene expression by small interfering RNAs (siRNAs). RNA. 2004;10:12-18
15. Birmingham A, Anderson EM, Reynolds A, et al. 3’ UTR seed matches, but not overall identity, are associated with RNAi off-targets. Nat Methods. 2006;3:199-204
16. Anderson EM, Birmingham A, Baskerville S, et al. Experimental validation of the importance of seed complement frequency to siRNA specificity. RNA. 2008;4:853-61

17. Stein P, Zeng F, Pan H, et al. Absence of non-specific effects of RNA interference triggered by long double-stranded RNA in mouse oocytes. Dev Biol. 2005;286:464-71
18. Cullen BR. Enhancing and confirming the specificity of RNAi experiments. Nat Methods. 2006;3:677-81
19. Hornung V, Guenthner-Biller M, Bourquin C, et al. Sequence-specific potent induction of IFN-alpha by short interfering RNA in plasmacytoid dendritic cells through TLR7. Nat Med. 2005;11:263-70
20. Judge AD, Sood V, Shaw JR, et al. Sequence-dependent stimulation of the mammalian innate immune response by synthetic siRNA. Nat Biotechnol. 2005;23:457-62
21. Poeck H, Besch R, Maihoefer C, et al. 5'-Triphosphate-siRNA: turning gene silencing and Rig-I activation against melanoma. Nat Med. 2008;14:1256-63
22. Behlke MA. Chemical modification of siRNAs for in vivo use. Oligonucleotides. 2008;18:305-19
23. Eberle F, Giessler K, Deck C, et al. Modifications in small interfering RNA that separate immunostimulation from RNA interference. J Immunol. 2008;180:3229-37
24. Gantier MP, Tong S, Behlke MA, et al. Rational design of immunostimulatory siRNAs. Mol Ther. 2010;18:785-95
25. Jackson AL, Linsley PS. Recognizing and avoiding siRNA off-target effects for target identification and therapeutic application. Nat Rev Drug Discov. 2010;9:57-67
26. Mazarakis ND, Azzouz M, Rohll JB. Rabies virus glycoprotein pseudotyping of lentiviral vectors enables retrograde axonal transport and access to the nervous system after peripheral delivery. Hum Mol Genet. 2001;10:2109–21
27. Rao DD, Vorhies JS, Senzer N, Nemunaitis J. siRNA vs. shRNA: similarities and differences. Adv Drug Deliv Rev. 2009:61(9):746-59.
28. Davis ME, Pun SH, Bellocq NC, Reineke TM, Popielarski SR, Mishra S, Heidel JD. Self-assembling nucleic acid delivery vehicles via linear, water-soluble, cyclodextrin-containing polymers. Curr. Med. Chem. 2004;11:179–197.
29. Lu PY, Xie F, Woodle MC. In vivo application of RNA interference: from functional genomics to therapeutics. Adv Genet. 2005;54:117-42
30. Mirus - The transfection experts. 2011.
31. Polyplus - The delivery experts. 2011.
32. Turbofect invivo transfection reagent - Fermentas. 2011.
33. Sigma Aldrich. N-TER™ Nanoparticle siRNA Transfection System. 2011.
34. Morar AS, Schrimsher JL, Mark D. Pegylation of proteins a structural approach. Biopharm Int. 2006;19:34-49

35. Schiffelers RM, Mixsonb AJ, Ansari AM, et al. Transporting silence: design of carriers for siRNA to angiogenic endothelium. J Control Release. 2005;109:5-14
36. McNeil SE. Nanotechnology for the biologist. J Leukoc Biol. 2005;78:585-94
37. Reich SJ, Fosnot J, Kuroki A, et al. Small interfering RNA (siRNA) targeting VEGF effectively inhibits ocular neovascularization in a mouse model. Mol Vision. 2003;9:210-16
38. Tolentino MJ, Brucker AJ, Fosnot J, et al. Intravitreal injection of vascular endothelial growth factor small interfering RNA inhibits growth and leakage in a nonhuman primate, laser-induced model of choroidal neovascularization. Retina. 2004;24:132-8
39. Shen J, Samul R, Silva RL, et al. Suppression of ocular neovascularization with siRNA targeting VEGF receptor 1.Gene Ther. 2006;13:225-34
40. Bitko V, Musiyenko A, Shulyayeva O, et al. Inhibition of respiratory viruses by nasally administered siRNA. Nat Med. 2005;11:50-5
41. Li BJ, Tang Q, Cheng D, et al. Using siRNA in prophylactic and therapeutic regimens against SARS coronavirus in Rhesus macaque. Nat Med. 2005;11:944-51
42. Thakker DR, Natt F, Husken D, et al. Neurochemical and behavioral consequences of widespread gene knockdown in the adult mouse brain by using nonviral RNA interference. Proc Natl Acad Sci USA. 2004;101:17270-5
43. Dorn G, Patel S, Wotherspoon G, et al. SiRNA relieves chronic neuropathic pain. Nucleic Acids Res. 2004;32:e49
44. Tan PH, Yang LC, Shih HC, Lan KC Cheng JT. Gene knockdown with intrathecal siRNA of NMDA receptor NR2B subunit reduces formalin-induced nociception in the rat. Gene Ther. 2005;12:59–66
45. Luo MC, Zhang DQ, Ma SW, et al. An efficient intrathecal delivery of small interfering RNA to the spinal cord and peripheral neurons. Mol Pain. 2005;1:29
46. Oh YK, Park TG. siRNA delivery systems for cancer treatment. Adv Drug Deliv Rev. 2009;61:850-62
47. Whitehead KA, Langer R, Anderson DG. Knocking down barriers: advances in siRNA delivery. Nat Rev Drug Discov. 2009;8:129-38
48. de Fougerolles A, Vornlocher HP, Maraganore J, et al. Interfering with disease: a progress report on siRNA-based therapeutics. Nat Rev Drug Discov. 2007;6:443-53
49. Chen SH, Zhaori G. Potential clinical applications of siRNA technique: benefits and limitations. Eur J Clin Invest 2011;41:221-32
50. Dubin, CH. Special delivery: pharmaceutical companies aim to target their drugs with nano precision. Mech. Eng. Nanotechnol. 2004;126:10-12.
51. Dass CR, Su T. Particle-mediated intravascular delivery of oligonucleotides to tumors, associated biology and lessons from genotherapy. Drug Deliv. 2001;8:191-213

52. Kumar MNVR. Nano and Microparticles as controlled drug Delivery Devices. J. Pharm. Pharmaceut. Sci. 2000;3:234-258
53. LaVan DA, McGuire T, Langer R. Small-scale systems for in vivo drug delivery. Nat. Biotechnol. 2003;21:1184-1191
54. Schiffelers RM, Ansari A, Xu J. Cancer siRNA therapy by tumor selective delivery with ligand-targeted sterically stabilized nanoparticle. Nucleic Acids Res. 2004;32:e149
55. Hu-Lieskovan S, Heidel JD, Bartlett DW, et al. Sequence-specific knockdown of EWS-FLI1 by targeted, nonviral delivery of small interfering RNA inhibits tumor growth in a murine model of metastatic Ewing's sarcoma. Cancer Res. 2005;65:8984-92
56. Heidel JD, Yu Z, Liu JYC, et al. Administration in non-human primates of escalating intravenous doses of targeted nanoparticles containing ribonucleotide reductase subunit M2 siRNA. Proc Natl Acad Sci USA. 2007;104:5715-21
57. Bartlett DW, Davis ME. Impact of tumor-specific targeting and dosing schedule on tumor growth inhibition after intravenous administration of siRNA containing nanoparticles. Biotechnol Bioeng. 2008;99:975-85
58. Santhakumaran LM, Thomas T, Thomas TJ. Enhanced cellular uptake of a triplex-forming oligonucleotide by nanoparticle formation in the presence of polypropylenimine dendrimers. Nucleic Acids Res. 2004;32:2102-12
59. Hollins AJ, Benboubetra M, Omidi Y, et al. Evaluation of generation 2 and 3 poly propylenimine) dendrimers for the potential cellular delivery of antisense oligonucleotides targeting the epidermal growth factor receptor. Pharm Res. 2004;21:458-66
60. Ulrich KE, Cannizzaro SM, Langer RS, Shakeshelf KM. Polymeric systems for controlled drug release. Chem. Rev. 1999;99:3181-3198
61. Singh R, James W, Lillard J. Nanoparticle-based targeted drug delivery. Exp. Mol. Pathol. 2009;86:215-223
62. Torchilin VP. Recent advances with liposomes as pharmaceutical carriers. Nat Rev Drug Discov. 2005;4:145-60
63. MacLachlan I. In: Crooke ST, editor, Antisense drug technology: principles, strategies and applications. 2nd edition. Chapter 9. CRC, Boca Raton; 2007. p. 237-70
64. Felgner PL, Gadek TR, Holm M, et al. Lipofection: a highly efficient, lipid-mediated DNA-transfection procedure. Proc Natl Acad Sci USA. 1987;84:7413-17
65. Malone RW, Felgner PL, Verma IM. Cationic liposome-mediated RNA transfection. Proc Natl Acad Sci USA. 1989;86:6077-81
66. Zimmermann TS, Lee ACH, Akinc A, et al. RNAi-mediated gene silencing in non-human primates. Nature. 2006;441:111-14

67. Geisbert TW, Hensley LE, Kagan E, et al. Postexposure protection of guinea pigs against a lethal ebola virus challenge is conferred by RNA interference. J Infect Dis. 2006;193:1650-7
68. Panyam J, Labhasetwar V. Biodegradable nanoparticles for drug and gene delivery to cells and tissue. Adv. Drug Deliv. Rev. 2003;55:329-347
69. Panyam J, Dali MM, Sahoo SK, Ma W, Chakravarthi SS, Amidon GL. Polymer degradation and in vitro release of a model protein from poly(d,l-lactide-co-glycolide) nano- and microparticles. J. Control. Release. 2003;92:173-187
70. Nugent J, Wan Po, AL, Scott EM. Design and delivery of nonparenteral vaccines. J. Clin. Pharm. Ther. 1998;23:257-285
71. Katare YK, Panda AK, Lalwani K, Haque IU, Ali MM. Potentiation of immune response from polymer-entrapped antigen: toward development of single dose tetanus toxoid vaccine. Drug Deliv. 2003;10:231-238
72. Lee KE, Kim BK, Yuk SH. Biodegradable polymeric nanospheres formed by temperature-induced phase transition in a mixture of poly(lactideco-glycolide) and poly(ethylene oxide)-poly(propylene oxide)-poly(ethylene oxide) triblock copolymer. Biomacromolecules, 2002;3:1115-1119
73. Brannon-Peppas L, Blanchette JO. Nanoparticle and targeted systems for cancer therapy. Adv. Drug Deliv. Rev. 2004;56:1649-1659
74. Rosiak JM, Janik I, Kadlubowski S, Kozicki M, Kujawa P, Stasica P. Nano-, micro- and macroscopic hydrogels synthesized by radiation technique. Nucl. Instrum. Methods Phys. Res. B, 2003;208:325-330
75. Ggiannavola C, Bucolo C, Maltese A, Paolino D, Vandelli MA, Puglisi G. Influence of preparation conditions on acyclovirloaded poly-d,llactic acid nanospheres and effect of PEG coating on ocular drug bioavailability. Pharm. Res. 2003;20:584-590
76. Kompella UB, Bandi N, Ayalasomayajula SP. Subconjunctival nanoand microparticles sustain retinal delivery of budesonide, a corticosteroid capable of inhibiting VEGF expression. Invest. Ophthalmol. Visual Sci. 2003;44:1192-1201
77. Sanchez A, Tobio M, Gonzalez L, Fabra A, Alonso MJ. Biodegradable micro- and nanoparticles as long-term delivery vehicles for interferon alpha. Eur. J. Pharm. Sci. 2003;18:221-229
78. Howard KA, Rahbek UL, Liu X, et al. RNA interference in vitro and in vivo using a novel chitosan/siRNA nanoparticle system. Mol Ther. 2006;14:476-84
79. Pille JY, Li H, Blot E. Intravenous delivery of anti-RhoA small interfering RNA loaded in nanoparticles of chitosan in mice: safety and efficacy in xenografted aggressive breast cancer. Hum Gene Ther. 2006;17:1019-26
80. Ochiya T, Takahama Y, Nagahara S, et al. New delivery system for plasmid DNA in vivo using atelocollagen as a carrier material: the Minipellet. Nat Med. 1999;5:707-10

81. Takeshita F, Minakuchi Y, Nagahara S, et al. Efficient delivery of small interfering RNA to bone-metastatic tumors by using atelocollagen in vivo. Proc Natl Acad Sci USA. 2005;102:12177-82
82. Sanvicens N and Marco MP. Multifunctional nanoparticles – properties and prospects for their use in human medicine. Trends in Biotechnology. 2008;26:425-433
83. Malam Y, Loizidou M, Seifalian AM. Liposomes and nanoparticles: nanosized vehicles for drug delivery in cancer. Trends Pharmacol. Sci. 2009;30:592–599
84. Prakash S, Malhotra M, Shao W, Tomaro-Duchesneau C, Abbasi S. Polymeric nanohybrids and functionalized carbon nanotubes as drug delivery carriers for cancer therapy. Advanced Drug Delivery Reviews. 2012;63:1340-1351
85. Yang J. et al. Multifunctional magneto-polymeric nanohybrids for targeted detection and synergistic therapeutic effects on breast cancer. Angew. Chem. Int. Ed. Engl. 2007;46:8836–8839
86. Farokhzad OC. et al. Targeted nanoparticle-aptamer bioconjugates for cancer chemotherapy in vivo. Proc. Natl. Acad. Sci. U. S. A. 2006;103:6315–6320
87. Tosi G et al. Targeting the central nervous system: in vivo experiments with peptide-derivatized nanoparticles loaded with Loperamide and Rhodamine-123. J. Control. Release. 2007;122:1–9
88. Vail DM et al. Pegylated liposomal doxorubicin: proof of principle using preclinical animal models and pharmacokinetic studies. Semin. Oncol. 2004;31:16–35
89. Wagner V et al. The emerging nanomedicine landscape. Nat.Biotechnol. 2006;24:1211–1217
90. Zhang Y et al. Organ-specific gene expression in the rhesus monkey eye following intravenous non-viral gene transfer. Mol. Vis. 2003;9:465–472
91. Carmeliet P, Jain RK, Angiogenesis in cancer and other diseases, Nature. 2000;407:249–257
92. Pelicano H, Martin DS, Xu RH, Huang P. Glycolysis inhibition for anticancer treatment, Oncogene. 2006;25:4633–4646
93. Jain RK. Delivery of molecular medicine to solid tumors: lessons from in vivo imaging of gene expression and function, J. Control. Release. 2001;74:7–25
94. Maeda H. SMANCS and polymer-conjugated macromolecular drugs: advantages in cancer chemotherapy, Adv. Drug Deliv. Rev. 2001;46:169–185
95. Maeda H, Matsumura Y. Tumoritropic and lymphotropic principles of macromolecular drugs, Crit. Rev. Ther. Drug Carrier Syst. 1989;6:193–210
96. Matsumura Y, Maeda H. A new concept for macromolecular therapeutics in cancer chemotherapy: mechanism of tumoritropic accumulation of proteins and the anti-tumor agent smancs. Cancer Res. 1986;46:6387–6392

97. Hume DA. The mononuclear phagocyte system. Curr. Opin. Immunol. 2006;18:49–53
98. Peracchia MT, Vauthier C, Desmaele D, et al. Pegylated nanoparticles from a novel methoxypolyethylene glycol cyanoacrylate-hexadecyl cyanoacrylate amphiphilic copolymer. Pharm. Res. 1998;15:550–56
99. Casettari L, Vllasaliu D, Castagnino E, Stolnik S, Howdle S, Illum L. PEGylated chitosan derivatives: Synthesis, characterizations and pharmaceutical applications. Progress in Polymer Science. 2012;37:659– 685
100. Brenner BM, Hostetter TH, Humes HD. Glomerular permselectivity: barrier function based on discrimination of molecular size and charge, Am. J. Physiol. 1978;234:F455–F460
101. Maack T, Johnson V, Kau ST, Figueiredo J, Sigulem D. Renal filtration, transport, and metabolism of low-molecular-weight proteins: a review, Kidney Int. 1979;16:251–270
102. Mihara K, Hojo T, Fujikawa M, Takakura Y, Sezaki H, Hashida M. Disposition characteristics of protein drugs in the perfused rat kidney, Pharm. Res. 1993;10:823–827
103. Mihara K, Mori M, Hojo T, Takakura Y, Sezaki H, Hashida M. Disposition characteristics of model macromolecules in the perfused rat kidney, Biol. Pharm. Bull. 1993;16:158–162
104. Perrault SD, Walkey C, Jennings T, et al. Mediating tumor targeting efficiency of nanoparticles through design. Nano Lett. 2009;9:1909–15
105. Dreher MR, Liu W, Michelich CR, Dewhirst MW, Yuan F, Chilkoti A. Tumor vascular permeability, accumulation, and penetration of macromolecular drug carriers. J Natl Cancer Inst. 2006;98:335–44
106. Fujita T, Nishikawa M, Tamaki C, Takakura Y, Hashida M, Sezaki H. Targeted delivery of human recombinant superoxide dismutase by chemical modification with mono and polysaccharide derivatives, J. Pharmacol. Exp. Ther. 1992;263:971–978
107. Mahato RI, Kawabata K, Takakura Y, Hashida M. In vivo disposition characteristics of plasmid DNA complexed with cationic liposomes. J. Drug Target. 1995;3:149–157
108. Ma SF, Nishikawa M, Katsumi H, Yamashita F, Hashida M. Cationic charge dependent hepatic delivery of amidated serum albumin, J. Control Release. 2005;102:583–594
109. Kim SH, Jeong JH, Chun KW, Park TG. Target-specific cellular uptake of PLGA nanoparticles coated with poly(Llysine)-poly(ethylene glycol)-folate conjugate. Langmuir. 2005;21:8852–7

110. Dhar S, Gu FX, Langer R, Farokhzad OC, Lippard SJ. Targeted delivery of cisplatin to prostate cancer cells by aptamer functionalized Pt(IV) prodrug-PLGA-PEG nanoparticles. Proc Natl Acad Sci USA. 2008;105:17356–61
111. Juliano RL, Alam R, Dixit V, Kang HM. Cell-targeting and cell penetrating peptides for delivery of therapeutics and imaging agents. Wiley Interdiscip Rev Nanomed Nanobiotechnol. 2009;1:324–35
112. Mamot C, Drummond DC,Noble CO,Kallab V, Guo Z,Hong K, et al. Epidermal growth factor receptor-targeted immunoliposomes significantly enhance the efficacy of multiple anticancer drugs in vivo. Cancer Res. 2005;65:11631–8.
113. Brooks H, Lebleu B and Vives E. Tat peptide-mediated cellular delivery: back to basics, Adv Drug Deliv Rev. 2005;57:559-577
114. Kirpotin DB, Drummond DC, Shao Y, Shalaby MR, Hong K, Nielsen UB, et al. Antibody targeting of long-circulating lipidic nanoparticles does not increase tumor localization but does increase internalization in animal models. Cancer Res. 2006;66:6732–40
115. Gabizon A, Horowitz AT, Goren D, Tzemach D, Shmeeda H, Zalipsky S. In vivo fate of folate-targeted polyethylene-glycol liposomes in tumor-bearing mice. Clin Cancer Res. 2003;9:6551–9
116. Schmidt MM, Wittrup KD. A modeling analysis of the effects of molecular size and binding affinity on tumor targeting. Mol Cancer Ther. 2009;8:2861–71
117. Choi CH, Alabi CA, Webster P, Davis ME. Mechanism of active targeting in solid tumors with transferrin-containing gold nanoparticles. Proc Natl Acad Sci USA. 2010;107:1235–40
118. Vives E, Richard JP, Rispal C and Lebleu B. TAT Peptide Internalization: Seeking the Mechanism of Entry, Curr Protein Pept Sci. 2003;4:125-132
119. Nakase I, Tadokoro A, Kawabata N, Takeuchi T, Katoh H, Hiramoto K, Negishi M, Nomizu M, Sugiura Y and Futaki S. Interaction of arginine-rich peptides with membrane-associated proteoglycans is crucial for induction of actin organization and macropinocytosis, Biochemistry. 2007;46:492-501
120. Muratovska A, Eccles MR. Conjugate for efficient delivery of short interferin RNA (siRNA) into mammalian cells. FEBS Lett. 2004;558:63-8
121. Simeoni F, Morris MC, Heitz F, et al. Insight into the mechanism of the peptide-based gene delivery system MPG: implications for delivery of siRNA into mammalian cells. Nucleic Acids Res. 2003;31:2717-24
122. Kim WJ, Christensen LV, Jo S, et al. Cholesteryl oligoarginine delivering vascular endothelial growth factor siRNA effectively inhibits tumor growth in colon adenocarcinoma. Mol Ther. 2006;14:343-50
123. Fittipaldi A, Ferrari A, Zoppe M, Arcangeli C, Pellegrini V, Beltram F and Giacca M. Cell membrane lipid rafts mediate caveolar endocytosis of HIV-1 tat fusion proteins. J Biol Chem. 2003;278:34141-9

124. Kaplan IM, Wadia JS and Dowdy SF. Cationic TAT peptide transduction domain enters cells by macropinocytosis. J Control Release. 2005;102:247-253
125. Nakase I, Niwa M, Takeuchi T, Sonomura K, Kawabata N, Koike Y, Takehashi M, Tanaka S, Ueda K, Simpson JC, Jones AT, Sugiura Y and Futaki S. Cellular uptake of arginine-rich peptides: roles for macropinocytosis and actin rearrangement, Mol Ther. 2004;10:1011-1022
126. Richard JP, Melikov K, Brooks H, Prevot P, Lebleu B and Chernomordik LV. Cellular uptake of unconjugated TAT peptide involves clathrin-dependent endocytosis and heparan sulfate receptors, J Biol Chem. 2005;280:15300-6
127. Vandenbroucke RE, Smedt SC, Demeester J and Sanders NN. Cellular entry pathway and gene transfer capacity of TAT-modified lipoplexes. Biochim Biophys Acta. 2007;1768:571-579
128. Fischer R, Kohler K, Fotin-Mleczek M and Brock R. A Stepwise Dissection of the Intracellular Fate of Cationic Cell-penetrating Peptides. J Biol Chem. 2004;279:12625-12635
129. Duchardt F, Fotin-Mleczek M, Schwarz H, Fischer R and Brock R. A comprehensive model for the cellular uptake of cationic cell-penetrating peptides, Traffic. 2007;8:848-866
130. Josephson, L.; Tung C.H.; Moore, A.; Weissleder, R. High-efficiency intracellular magnetic labeling with novel superparamagnetic-Tat peptide conjugates. Bioconjug. Chem., 1999, 10, 186-191.
131. Santra, S.; Yang, H.; Dutta, D.; Stanley, J.T.; Holloway, P.H.; Tan, W.; Moudgil, B.M.; Mericle, R.A. TAT conjugated, FITC doped silica nanoparticles for bioimaging applications. Chem. Commun. (Camb), 2004, 24, 2810-2811.
132. Pasqualini R, Koivunen E and Ruoslahti E. Alpha v integrins as receptors for tumor targeting by circulating ligands. Nat Biotechnol. 1997;15:542-546
133. Scott JK and Smith GP. Searching for peptide ligands with an epitope library, Science. 1990;249:386-390
134. Ballabh P, Braun A, Nedergaard M. The blood-brain barrier: an overview: structure, regulation, and clinical implications. Neurobiol. Dis. 2004;16:1-13
135. Pardridge WM. Blood-brain barrier drug targeting: the future of brain drug development. Mol. Interv. 2003;3:90-105
136. Pardridge WM. Drug and gene targeting to the brain with molecular trojan horses. Nat. Rev. Drug Discov. 2002;1:131-139
137. Yaksh TL, Provencher JC, Rathbun ML, Myers RR, Powell H, Richter P, Kohn FR. Safety assessment of encapsulated morphine delivered epidurally in a sustained-release multivesicular liposome preparation in dogs. Drug Deliv. 2000;7:7-36
138. Misra A, Ganesh S, Shrenik P. Drug delivery to the central nervous system: a review. J. Pharm. Pharmaceut. Sci. 2003;6:252-273

139. Bodor N, Buchwald P. Recent advances in the brain targeting of neiropharmaceuticals by chemical delivery systems. Adv. Drug. Deliv. Rev. 1999; 36:229-254
140. Rockwell S. Use of hypoxia directed drugs in the therapy of solid tumors. Semin. Oncol. 1992;19:29-40
141. Risau W. Molecular biology of blood-brain barrier ontogenesis and function. Acta. Neurochir. 1994;60:109-112
142. Fung LK, Ewend MG, Sills A, Sipos EP, Thompson R, Watts M, Colvin OM, Brem H, Saltzman WM. Pharmacokinetics of interstitial delivery of carmustine, 4-hydroperoxycyclophosphamide, and paclitaxel from a biodegradable polymer implant in the monkey brain. Cancer Res. 1998;58:672-684
143. Bobo RH, Laske DW, Akbasak A, Morrison PF, Dedrick RL. Oldfield, E.H. Convection-enhanced delivery of macromolecules in the brain. Proc. Natl. Acad. Sci. USA. 1994;91: 2076-2082
144. Carter, B.S.; Zervas, N.T.; Chiocca, E.A. Neurogenetic surgery: current limitations and the promise of gene- and virus-based therapies. Clin. Neurosurg.,1999, 45, 226-246.
145. Shapiro, W.; Shapiro, J.; Walker, R.; Central nervous system. In: Abeloff, M.; Armitage, J.; Lichter, A.N.J. Eds, Clinical oncology. New York, Churchill Livingstone, 2000, 1103-1193.
146. Markowitz, D.C.; Fernstorm, J.D. Diet and uptake of Aldomet by the brain: competition with natural large neutral amino acids. Science, 1977, 197, 1014-1015.
147. Taylor, E.M. The impact of efflux transporters in the brain on the development of drugs for CNS disorders. Clin. Pharmacokinet., 2002, 14, 81-92.
148. VanBree, J.B.M.M.; Audus, K.L.; Borchardt, R.T. Carrier mediated transport of baclofen across monolayers of bovine brain endothelial cells in primary culture. Pharm. Res., 1988, 5, 369-371.
149. Nutt, J.G.; Woodward, W.R.; Hammerstad, J.P.; Carter, M.N.; Anderson, J.L. The "on-off" mechanism in Parkinson's disease. Relation to levodopa absorption and transport. N. Engl. J. Med., 1984, 310, 483-488.
150. Pratt, O.E. In: Physiology and Pharmacology of the blood-brain barrier. Bradbury, M.W.B., Ed.; Springer-Verlag: Berlin, 1992, 205-220.
151. Thorne, R.G.; Frey, W.H. Delivery of neurotropic factor to the central nervous system: pharmacokinetic consideration. Clin. Pharmacokinet., 2001, 40, 907-946.
152. Born, J.; Lange, T.; Kern, W. Sniffing neuropeptides: a transnasal approach to the human brain. Nat. Neurosci., 2002, 5, 514-516.
153. Illum, L. Nasal drug delivery: new development strategies. Drug Discov. Today, 2002, 7, 1184-1189.
154. Thorne, R.G.; Emory, C.R.; Ala, T.A.; Fery, W.H. Quantitative analysis of the olfactory pathway for drug delivery to the brain. Brain Res., 1995, 692, 278-282.

155. Tiraboschi P, Hansen LA, Thal LJ, Corey-Bloom J: The importance of neuritic plaques and tangles to the development and evolution of AD. Neurology. 2004;62:1984-1989
156. Brookmeyer R, Johnson E, Ziegler-Graham K, Arrighi HM: Forecasting the global burden of Alzheimer's disease. Alzheimers Dement. 2007;3:186-91
157. Neurodegenerative Disease Market to 2017 - Patent Expiries of High Selling Drugs Such as Aricept, Namenda, Avonex, Rebif and Copaxone will Restrain Growth. GBI research. Oct 15, 2011. http://www.marketresearch.com/GBI-Research-v3759/Neurodegenerative-Disease-Patent-Expiries-High-6623005/
158. Bertram L, Tanzi RE. Thirty years of Alzheimer's disease genetics: the implications of systematic meta-analyses. Nat Rev Neurosci. 2008;9:768-778
159. Yankner BA, Duffy LK, Kirschner DA. Neurotrophic and neurotoxic effects of amyloid beta protein: reversal by tachykinin neuropeptides. Science. 1990;250:279-282
160. Hashimoto M, Rockenstein E, Crews L, Masliah E. Role of protein aggregation in mitochondrial dysfunction and neurodegeneration in Alzheimer's and Parkinson's diseases. NeuroMolecular Medicine. 2003;4:21-35
161. Priller C, Bauer T, Mitteregger G, Krebs B, Kretzschmar HA, Herms J. Synapse Formation and Function Is Modulated by the Amyloid Precursor Protein. The Journal of Neuroscience. 2006;26:7212-7221
162. Turner PR, O'Connor K, Tate WP, Abraham WC. Roles of amyloid precursor protein and its fragments in regulating neural activity, plasticity and memory. Progress in Neurobiology. 2003;70:1-32
163. Lefort R. Investigating the Role of the Amyloid Precursor Protein in the Pathogenesis of Alzheimer's Disease. 2011. 201 pages
164. Selkoe DJ. Deciphering the genesis and fate of amyloid beta protein yields novel therapies for Alzheimer disease. J Clin Invest. 2002;110:1375-1381
165. Williamson J, Goldman J, Marder KS. Genetic Aspects of Alzheimer Disease. The Neurologist. 2009;15
166. Ertekin-Taner,N: Genetics of Alzheimer's Disease: A Centennial Review. Neurologic Clinics. 2007;25:611-667
167. Waring,SC, Rosenberg,RN: Genome-Wide Association Studies in Alzheimer Disease. Arch Neurol. 2008;65:329-334
168. Tomlin S. Microtechnology: Laying it on thick. Nature 1999;399:23
169. Gotz J, Ittner LM. Animal models of Alzheimer's disease and frontotemporal dementia. Nat Rev Neurosci. 2008;9:532-544
170. Gotz J, Streffer JR, David D, Schild A, Hoerndli F, Pennanen L, Kurosinski P, Chen F. Transgenic animal models of Alzheimer's disease and related disorders: histopathology, behavior and therapy. Mol Psychiatry. 2004;9:664-683

171. Janus C, Westaway D. Transgenic mouse models of Alzheimer's disease. Physiology & Behavior. 2001;73:873-886
172. Azorsa D, Robeson R, Frost D, Hoovet B, Brautigam G, Dickey C, Beaudry C, Basu G, Holz D, Hernandez J, Bisanz K, Gwinn L, Grover A, Rogers J, Reiman E, Hutton M, Stephan D, Mousses S, Dunckley T. High-content siRNA screening of the kinome identifies kinases involved in Alzheimer's disease-related tau hyperphosphorylation. BMC Genomics 2010;11:25
173. Marine S, Stec EM, Chase P, Hoffman I, Szymanski S, Simon A, Shi XP, Bartz S, Bagchi S, Minch E, Majercak J, Koblan K, Hazuda D, Shearman M, Gates A, Xu M, Rosahl T, Beher D, Ray WJ, Stone, Espeseth A, Ferrer M, Strulovici B. Activity profile-based siRNA screen to explore the functional genomics of Alzheimer's disease. BioTechniques. 2007;43:Sxxii-Sxxvii
174. Kao SC, Krichevsky AM, Kosik KS, Tsai LH. BACE1 Suppression by RNA Interference in Primary Cortical Neurons. Journal of Biological Chemistry. 2004;279:1942-1949
175. Xie Z, Romano DM, Kovacs DM, Tanzi RE. Effects of RNA interference-mediated silencing of gamma-secretase complex components on cell sensitivity to caspase-3 activation. Journal of Biological Chemistry. 2004;279:34130-34137
176. He G, Luo W, Li P, Remmers C, Netzer WJ, Hendrick J, Bettayeb K, Flajolet M, Gorelick F, Wennogle LP, Greengard P. Gamma-secretase activating protein is a therapeutic target for Alzheimer/'s disease. Nature. 2010;467:95-98
177. Luo J, Solimini NL, Elledge SJ, Principles of cancer therapy: oncogene and non oncogene addiction. Cell. 2009;136:823–837
178. Hanahan D, Weinberg RA, The hallmarks of cancer, Cell. 2000;100:57–70
179. Reticker-Flynn NE, Malta DFB, Winslow MM, Lamar JM, Xu MJ, Underhill GH, Hynes RO, Jacks TE and Bhatia SN. A combinatorial extracellular matrix platform identifies cell-extracellular matrix interactions that correlate with metastasis. Nature Communications 3, Article number: 1122
180. Anand P, Kunnumakkara AB, Sundaram C, Harikumar KB, Tharakan ST, Lai OS, Sung B, Aggarwal BB. Cancer is a preventable disease that requires major lifestyle changes. Pharm Res. 2008; 25:2097-116
181. Harris AL. Hochhauser D. Mechanisms of multidrug resistance in cancer treatment. Acta Oncol. 1992;31:205–213
182. Aggarwal S. Targeted cancer therapies. Nat. Rev. Drug Discov. 2010;9:427–428
183. Shih HA, Loeffler JS, Tarbell NJ. Late Effects of CNS Radiation Therapy. 2009;150:23–41
184. Helleday T, Petermann E, Lundin C, Hodgson B, Sharma RA. DNA repair pathways as targets for cancer therapy. Nat. Rev. Cancer. 2008;8:193–204
185. Sargent D, Sobrero A, Grothey A, O'Connell MJ, Buyse M, Andre T, Zheng Y, Green E, Labianca R, O'Callaghan C, Seitz JF, Francini G, Haller D, Yothers G,

Goldberg R, de Gramont A. Evidence for Cure by Adjuvant Therapy in Colon Cancer: Observations Based on Individual Patient Data From 20,898 Patients on 18 Randomized Trials. Journal of Clinical Oncology. 2009;27:872-877

186. Tsuruo T, Naito M, Tomida A, Fujita N, Mashima T, Sakamoto H, Haga N. Molecular targeting therapy of cancer: drug resistance, apoptosis and survival signal. Cancer Sci. 2005;94:15–21
187. Jabr-Milane LS, Vlerken LE, Yadav S, Amiji MM. Multi-functional nanocarriers to overcome tumor drug resistance. Cancer Treat. Rev. 2008;34:592–602
188. Cappell MS. The pathophysiology, clinical presentation, and diagnosis of colon cancer and adenomatous polyps. Med Clin N Am 89 (2005) 1–42.
189. Conlin A, Smith G, Carey FA, Wolf CR, Steele RJC. The prognostic significance of K-ras, p53, and APC mutations in colorectal carcinoma. Gut 2005;54:1283–1286
190. Eckerdt F, Yuan,J, Strebhardt,K: Polo-like kinases and oncogenesis. Oncogene. 2005; 24:267-276
191. Takai N, Hamanaka,R, Yoshimatsu,J, Miyakawa,I: Polo-like kinases (Plks) and cancer. Oncogene. 2005;24:287-291
192. Ando K, Ozaki T, Yamamoto H, Furuya K, Hosoda M, Hayashi S, Fukuzawa M, Nakagawara A. Polo-like Kinase 1 (Plk1) Inhibits p53 Function by Physical Interaction and Phosphorylation. Journal of Biological Chemistry. 2004;279:25549-25561
193. Sanovich E, Bartus RT, Friden PM, et al. (1995). Pathway across blood-brain barrier opened by the bradykinin agonist, RMP-7. Brain Res, 705.
194. Molas M, Gomez-Valadés AG, Vidal-Alabró A, Miquel-Turu M, Bermudez J, Bartrons R, et al. Receptor mediated gene transfer vectors: Progress towards genetic pharmaceuticals. Curr Gene Ther. 2003;3:468–85
195. Peden CS, Burger C, Muzyczka N, Mandel RJ. Circulating anti wild type adeno associated virus type 2 (AAV2 antibodies inhibit recombinant AAV2 (rAAV2)-mediated, but not rAAV5 mediated, gene transfer in the brain. J Virol. 2004;78:6344–59
196. Lu PY, Xie F, Woodle MC. In vivo application of RNA interference: From functional genomics to therapeutics. Adv Genet. 2005;54:117–42
197. Liu WG, Yao K. Chitosan and its derivatives: A promising non-viral vector for gene transfection. J Controll Release. 2002; 83:1–11
198. Borchard G. Chitosans for gene delivery. Adv Drug Deliv Rev. 2001;52:145–50
199. Dodane V, Vilivalum VD. Pharmaceutical applications of chitosan. Pharm Sci Technol Today. 1998;1:246–53
200. Tomihata K, Ikada Y. In vitro and in vivo degradation of films of chitin and its deacetylation derivatives. Biomaterials. 1997;18:567–75

201. Onishi H, Machida Y. Biodegradation and distribution of water-soluble chitosan in mice. Biomaterials. 1999;20:175–82.
202. Rao SB, Sharma CP. Use of chitosan as a biomaterial: Studies on its safety and hemostatic potential. J Biomed Mater Res. 1997;34:21–8
203. Mao H-Q, Roy K, Walsch SM, et al. DNA-chitosan nanospheres for gene delivery. Proc Int Symp Control Rel Bioact Mater. 1996;23:401–2
204. Roy K, Mao H-Q, Leong KW. DNA-chitosan nanospheres: Transfection efficiency and cellular uptake. Proc Int Symp Control Rel Bioact Mater. 1997;24:673–4
205. Lee KY, Kwon IC, Kim YH, Jo WH, Jeong, SY. Preparation of chitosan self-aggregates as a gene delivery system. J Controll Release. 1998;51:213–20
206. Kiang T, Wen J, Lim HW, Leong KW. The effect of the degree of chitosan deacetylation on the efficiency of gene transfection. Biomaterials. 2004;25;5293–301
207. Sato T, Ishii T, Okahata Y. In vitro gene delivery mediated by chitosan. Effect of pH, serum, and molecular mass of chitosan on the transfection efficiency. Biomaterials. 2001;22:2075–80
208. Huang M, Fong CW, Khor E, Lim LY. Transfection efficiency of chitosan vectors: Effect of polymer molecular weight and degree of deacetylation. J Control Release. 2005;106: 391–406
209. Xu S, Dong M, Liu X, Howard KA, Kjems J, Besenbacher F. Direct force measurements between siRNA and chitosan molecules using force spectroscopy. Biophys J. 2007;93: 952–9
210. Chellat F, Grandjean-laquerriere A, Naour R, Fernandes J, Yahia L, Guenounou M, et al. Metalloproteinase and cytokine production by THP-1 macrophages following exposure to chitosan-DNA nanoparticles. Biomaterials. 2005;26:961–70
211. Katas H, Alpar HO. Development and characterization of chitosan nanoparticles for siRNA delivery. J Control Release. 2006;115:216–25
212. Murata J, Ohya Y, Ouchi T. Possibility of application of quaternary chitosan having pendant galactose residues as gene delivery tool. Carbohydrate polymers. 1996;29:69–74
213. Erbacher P, Zhou S, Bettinger T, Steffan AM, Remy JS. Chitosan based vector/DNA complexes for gene delivery: Biophysical characteristics and transfection ability. Pharm Res. 1998;15:1332–9
214. Lee MK, Chun SK, Choi WJ, Kim JK, Choi SH, Kim A, et al. The use of chitosan as a condensing agent to enhance emulsion mediated gene transfer. Biomaterials. 2005;26: 2147–56
215. Illum L, Farraj NF, Davis SS. Chitosan as a novel nasal delivery system for peptide drugs. Pharm Res. 1994;11:1186–9

216. Verhoef JC, Junginger HE, Thanou M. Chitosan and its derivatives as intestinal absorption enhancers. Adv Drug Deliver Rev. 2001;50:S91–S101
217. Liu X, Howard KA, Dong M, Anderson MO, Rahbek UL, Johnsen MG, et al. The influence of polymeric properties on chitosan/siRNA nanoparticle formulation and gene silencing. Biomaterials. 2007;28:1280–8
218. Calvo P, Remunan-lopez C, Vila-Jato JL, Alonso MJ. Novel hydrophilic chitosan-polyethylene oxide nanoparticles as protein carriers. J Appl Polym Sci. 1997;63:125–32
219. Shu XZ, Zhu KJ. A novel approach to prepare tripolyphosphate/ chitosan complex beads for controlled drug delivery. Int J Pharm. 2000;201:51–8
220. Rojanarata T, Opanasopit P, Techaarpornkul S, Ngawhirunpat T, Ruktanonchai U. Chitosan-Thiamine pyrophosphate as a novel carrier for siRNA delivery. Pharm Res. 2008;25:2807-14
221. MacLaughlin FC, Mumper RJ, Wang J, Tagliaferri JM, Gill I, Hinchcliffe M, et al. Chitosan and depolymerised chitosan oligomers as condensing carriers for in vivo plasmid delivery. J Control Release, 1998;56:259–72
222. Andersen MO, Howard KA, Paludan SR, Besenbacher F, Kjems J. Delivery of siRNA from lyophilized polymeric surfaces. Biomaterials. 2007;29:506–12
223. Liu WG, Zhang X, Sun SJ, Sun GJ, Yao KD, Liang DC, et al. N-alkylated chitosan as a potential nonviral vector for gene delivery. Bioconjug Chem. 2003;14:782–9
224. Wolfert MA, Seymour LW. Characterization of vectors for gene therapy formed by self-assembly of DNA with synthetic block copolymers. Human Gene Ther. 1996;3:269–73
225. Mao H-Q, Roy K, Troung-Le VL, Janes KA, Lin KY, Wang Y, August JT, Leong KW. Chitosan-DNA nanoparticles as gene carriers: Synthesis, characterization and transfection efficiency. J Control Release. 2001;70:399–421
226. Boussif O, Lezoualch F, Zanta MA, Mergny MD, Scherman D, Demeneix B, et al. A versatile vector for gene and oligonucleotide transfer into cells in culture and in vivo: Polyethylenimine. Proc Natl Acad Sci USA. 1995;92:7297–301
227. Cho YW, Kim JD, Park K. Polycation gene delivery system: Escape from endosomes to cytosol. J Pharm Pharmacol. 2003;55:721–34
228. Ishii T, Okahata Y, Sato T. Mechanism of cell transfection with plasmid/chitosan compleses. Biochim Biophys Acta. 2001;1514:51–64
229. Fang N, Chan V, Mao H-Q, Leong KW. Interactions of phopholipid bilayer with Chitosan: effect of molecular weight and pH. Biomacromolecules. 2001;2:1161–8
230. Dung TH, Lee S-R, Han S-D, Kim SJ, Ju YM, Kim MS, et al. Chitosan-TPP nanoparticle as a release system of antisense oligonucleotide in the oral environment. J Nanosci Nanotechnol. 2007;7:3695–9

231. Li Q, Dunn ET, Grandmasion EW, Goosen MFA. Applications and properties of chitosan. In: Goosen MFA, editor. Applications of Chitin and Chitosan. Lancaster: Technomic Publishing Company, Inc.; 1992: 3–29
232. Bernkop-Schnurch A. Chitosan and its derivatives: potential excipients for peroral peptide delivery systems. Int J Pharm. 2000;194:1–13
233. Illum L, Jabbal-Gill I, Hinchcliffe M, Fisher AN, Davis SS. Chitosan as a novel nasal delivery system for vaccines. Adv Drug Del Rev. 2001;51:81–96
234. Sundararajan VM, Howard WTM. Porous chitosan scaffolds for tissue engineering. Biomaterials. 1999;20:1133–1142
235. Skryabin KG, Vikhoreva GA, Varlamov VP. Chitin and chitosan. Production properties and usage. Moscow: Nauka; 2002 [in Russian]
236. Ravi-Kumar MNV, Muzzarelli RAA, Muzzarelli C, Sashiwa H, Domb AJ. Chitosan chemistry and pharmaceutical perspectives. Chem Rev. 2004;104:6017–6084
237. Sugimoto M, Morimoto M, Sashiwa H, Saimoto H, Shigemasa Y. Chitin and chitosan derivatives. Carbohydr Polym. 1998;36:49–59
238. Harris JM, Zalipsky S. Poly (ethylene glycol) Chemistry: and Biological Applications. Washington, DC: American Chemical Society: 1997;489
239. Gorochovceva N, Makuska R. Synthesis and study of water-soluble chitosan-O-poly (ethylene glycol) graft copolymers. European Polymer Journal. 2004;40:685–691
240. Lin WJ, Lee HG. Design of a microporous controlled delivery system for theophylline tablets. J Control Release. 2003;89:179–187
241. Lin WJ, Lee HG, Wang DM. The influence of plasticizers on the release of theophylline from microporous-controlled tablets. J Control Release. 2004;99:415–421
242. Nishimura S, Kohgo O, Kuzuhara H, Kurita K. Chemospecific manipulations of a rigid polysaccharide: syntheses of novel chitosan derivatives with excellent solubility in common organic solvents by regioselective chemical modifications. Macromolecules. 1991;24: 4745–4748
243. Malhotra M, Kulamarva A, Sebak S, Paul A, Bhathena J, et al. Ultrafine chitosan nanoparticles as an efficient nucleic acid delivery system targeting neuronal cells. Drug Dev Ind Pharm. 2009;35: 719–726
244. Torii Y, Ikeda H, Shimojoh M, Kurita K. Chemoselective protection of chitosan by dichlorophthaloylation: preparation of a key intermediate for chemical modifications. Polym Bull. 2009;62:749–759
245. Kurita K, Ikeda H, Yoshida Y, Shimojoh M, Harata M. Chemoselective protection of amino groups of chitosan by controlled phthaloylation: Facile preparation of a precursor useful for chemical modifications. Biomacromolecules. 2002;3:1–4

246. Calvo P, Remunan-lopez C, Vila-Jato JL, Alonso MJ. Novel hydrophilic chitosan-polyethylene oxide nanoparticles as protein carriers. J Appl Polym Sci. 2007;63:125–132
247. Kasaai MR. Various methods for determination of the degree of N-acetylation of chitin and chitosan: a review. J Agric Food Chem. 2009;57:1667–1676
248. Makuska R, Gorochvceva N. Regioselective grafting of poly(ethylene glycol) onto chitosan through C-6 position of glucosamine units. Carbohydr Polym. 2006;64:319–327
249. Jian Du, You-Lo H. PEGylation of chitosan for improved solubility and fiber formation via electrospinning. Cellulose. 2007;14:543–552
250. Janes KA, Fresneau MP, Marazuela A, Fabra A, Alonso MJ. Polysaccharide colloidal particles as delivery systems for macromolecules. J Control Release. 2001;73:255–267
251. Pan Y, Li Y, Zhao H, Zheng J, Xu H, et al. Bioadhesive polysaccharide in protein delivery system: chitosan nanoparticles improve the intestinal absorption of insulin in vivo. Int J Pharm. 2002;249:139–147
252. Bettencourt C, Lima M. Machado-joseph disease: from first descriptions to new perspectives. Orphanet J Rare Dis. 2011;6:35
253. Prakash S, Malhotra M. Recent advancements in targeted delivery of therapeutic molecules in neurodegenerative disease—spinocerebellar ataxia—opportunities and challenges. Drug Target Insights. 2008;3:99–117
254. Di Prospero NA, Baker A, Jeffries N, Fischbeck KH. Neurological effects of high-dose idebenone in patients with friedreich's ataxia: a randomized, placebo-controlled trial. Lancet Neurol. 2007;6:878–86
255. Xia H, Mao Q, Eliason SL, Harper SQ, Martins IH, Orr HT, et al. RNAi suppresses polyglutamine-induced neurodegeneration in a model of spinocerebellar ataxia. Nat Med. 2004;10:816-820
256. Takei Y, Kadomatsu K, Yuzawa Y, Matsuo S and Muramatsu T. A small interfering RNA targeting vascular endothelial growth factor as cancer therapeutics. Cancer Res. 2004;64:3365-3370
257. Zhang Y, Zhang YF, Bryant J, Charles A, Boado RJ, Pardridge WM. Intravenous RNA interference gene therapy targeting the human epidermal growth factor receptor prolongs survival in intracranial brain cancer. Clin Cancer Res. 2004;10:3667–3677
258. Bhoumik A, Jones N, Ronai Z. Transcriptional switch by activating transcription factor 2-derived peptide sensitizes melanoma cells to apoptosis and inhibits their tumorigenicity. PNAS 2004;101:4222–4227
259. Lu PY, Xie F, Woodle MC. In vivo application of RNA interference: from functional genomics to therapeutics. Adv Genet. 2005;54:117-142

260. Arai K, Kineemaki T, Fujita T. Toxicity of chitosan. Bull Tokai Reg Fish Res Lab. 1968;56:89-94
261. Yamamoto H, Amaike M. Biodegradation of cross-linked chitosan gels by microorganisms. Macromolecules. 1997;30:3936-3937
262. Risbud MV, Bhonde RR. Polyacrylamide-chitosan hydrogels: in vitro biocompatibility and sustained antibiotic release studies. Drug Deliv. 2000;7:69–75
263. P.K. et al. Safety of poly(ethylene glycol) and poly(ethylene glycol) derivatives. In Harris, J.M., and Zalipsky, S. (eds), Polyethylene Glycol Chemistry and Biological Applications, American Chemical Society, Washington DC,1997. p. 45
264. Ouchi T, Nishizawa H, Ohya Y. Aggregation phenomenon of peg-grafted chitosan in aqueous solution, Polymer. 1998;39:5171–5175
265. Lebouc F, Dez I, Desbrieres J, Picton L, Madec PJ. Different ways for grafting ester derivatives of poly(ethylene glycol) onto chitosan : related characteristics and potential properties. Polymer. 2005;46:639-651
266. Kircheis R, Kichler A, Wallner G, Kursa M, Ogris M, Felzmann T et al. Coupling of cell-binding ligands to polyethyleneimine for targeted gene delivery. Gen Ther. 1997;4:409-418
267. Moore NM, Sheppard CL, Sakiyama-Elbert SE. Characterization of a multifunctional peg-based gene delivery system containing nuclear localization signals and endosomal escape peptides. Acta Biomater. 2009;5:854-864
268. Torchilin VP, Rammohan R, Weissig V, Lev chenko TS. TAT peptide on the surface of liposomes affords their efficient intracellular delivery even at low temperature and in the presence of metabolic inhibitors. Proc Natl Acad Sci USA. 2001;98:8786-8791
269. Tseng YL, Liu JJ, Hong RL. Translocation of liposomes into cancer cells by cell-penetrating peptides penetratin and TAT: a kinetic and efficacy study. Mol pharmacol. 2002;62:864-872
270. Lin WJ, Chen MH, Synthesis of multifunctional chitosan with galactose as a targeting ligand for glycoprotein receptor. Carbohydr polym. 2007;67:474-480
271. Rubin LL, Staddon JM. The cell biology of the blood-brain barrier. Annu Rev Neurosci 1999;22:11-28
272. Pardridge WM. In: Peptide drug Delivery to the Brain, Raven Press: New York, 1991. p. 1-357.
273. Inoue Y, Kurihara R, Tsuchida A, Hasegawa M, Nagashima T, Mori T, et al. Efficient delivery of siRNA using dendritic poly(l-lysine) for loss-of-function analysis. J Control Release. 2008;126:59-66
274. Patil ML, Zhang M, Betigeri S, Taratula O, He H, Minko T. Surface-modified and internally cationic polyamidoamine dendrimers for efficient siRNA delivery. Bioconjug Chem. 2008;19:1396-1403

275. Wissing SA, Kayser O, Müller RH. Solid lipid nanoparticles for parenteral drug delivery. Adv Drug Deliv Rev. 2004;56:1257-1272
276. Xia CF, Zhang Y, Zhang Y, Boado RJ, Pardridge WM. Intravenous siRNA of brain cancer with receptor targeting and avidin–biotin technology. Pharm Res. 2007;24:2309–2316
277. Jones AR, Shusta EV. Antibodies and the blood-brain barrier. In therapeutic monoclonal antibodies: from bench to clinic. John Wiley & Sons, Inc. 483-502
278. Sharma V, Piwnica-Worms D. Blood-brain barrier permeation peptides. US Patent No. US7,803,351 B2, 2010
279. Pangestuti R, Kim SK. Neuroprotective properties of chitosan and its derivatives. Mar Drugs. 2010;8:2117-2128
280. Giglio E, Trapani A, Cafagna D, Sabbatini L, Cometa S. Dopamine-loaded chitosan nanoparticles: formulation and analytical characterization. Anal Bioanal Chem. 2011; 400:1997-2002
281. Caban S, Capan, Y, Couvreur P and Dalkara T. Preparation and characterization of biocompatible chitosan nanoparticles for targeted brain delivery of peptides. Methods Mol Biol. 2012;846:321-322
282. Yoksan R, Matsusaki M, Akashi M Chirachanchai S. Controlled hydrophobic/ hydrophilic chitosan: colloidal phenomena and nanosphere formation. Colloid Polym Sci. 2004;282:337-342
283. Malhotra M, Lane C, Tomaro-Duchesneau C, Saha S and Prakash S, A novel method for synthesizing pegylated chitosan nanoparticles: strategy, preparation and in-vitro analysis. Int J Nanomedicine. 2011;6:485-494
284. Gonzalez-Alegre P: Therapeutic RNA interference for neurodegenerative diseases: From promise to progress. Pharmacology & Therapeutics 2007;114:34-55
285. Brown RC, Lockwood AH, Sonawane BR: Neurodegenerative Diseases: An Overview of Environmental Risk Factors. Environ Health Perspect. 2005;1131250-1256
286. Oakley H, Cole SL, Logan S, Maus E, Shao P, Craft J, Guillozet-Bongaarts A, Ohno M, Disterhoft J, et al. Intraneuronal Amyloid Aggregates, Neurodegeneration, and Neuron Loss in Transgenic Mice with Five Familial Alzheimer's Disease Mutations: Potential Factors in Amyloid Plaque Formation. The Journal of Neuroscience. 2006;26:10129-10140.
287. Malhotra, M., Tomaro-Duchesneau, C., & Prakash, S. Synthesis of TAT peptide tagged PEGylated chitosan nanoparticles for siRNA delivery targeting neurodegenerative diseases. Biomaterials. 2013;34:1270-1280
288. Vila A, Sanchez A, Janes K, Behrens I, Kissel T, Jato JLV and Alonso MJ. Low molecular weight chitosan nanoparticles as new carriers for nasal vaccine delivery

in mice. European Journal of pharmaceutics and biopharmaceutics. 2004;57:123-131

289. Zhang YJ, Ma CH, Lu WL, Zhang X, Wang XL, Sun JN, Zhang Q. Permeation-enhancing effects of chitosan formulations on recombinant hirudin-2 by nasal delivery in vitro and in vivo. Acta Pharmacol Sin. 2005;26:1402-8
290. Inada Y, Furukawa M, Sasaki H, Kodera Y, Hiroto M, Nishimura H and Matsushima A. Biomedical and biotechnological applications of PEG- and PM-modified proteins. Trends Biotechnol 1995;13:86-91
291. Matheny, R. W., Nindl, B. C., Adamo, M. L. Minireview: mechano growth factor: a putative product of IGF-1gene expression involved in tissue repair and regeneration. Endocrinology. 2010;151:865-875
292. Carpenter V, Matthews J, Devlin G, Stuartb S, Jensen J, Conaglen J, Jeanplong F, Goldspink P, Yang SY, Goldspink G, Basss J, McMahon C. Mechano growth factor reduces loss of cardiac function in acute myocardial infarction. Heart, lung and circulation. 2008;17:33-39
293. Merkus P, et al. Influence of anatomy and head position on intranasal drug deposition. Eur Arch Otorhinolaryngol, 2006;263:827-32.
294. Merkus, P. et al. The 'best method' of topical nasal drug delivery: comparison of seven techniques. Rhinology. 2006;44:102-7.
295. Harris AS, Nilson IM, Wagner Z-G, Alkner U. Intranasal administration of peptides: Nasal deposition, biological response, and absorption of desmopressin. J Pharm Sci. 1986;75:1085-1088
296. Anand P, Kunnumakara A, Sundaram C, Harikumar K, Tharakan S, Lai O, Sung B, Aggarwal B. Cancer is a Preventable Disease that Requires Major Lifestyle Changes. Pharmaceutical Research. 2008;25:2097-2116
297. Knudson AG. Two genetic hits (more or less) to cancer. Nat Rev Cancer. 2001;1:157- 162

298. Mosolits S, Nilsson B, Mellstedt H. Towards therapeutic vaccines for colorectal carcinoma: a review of clinical trials. Expert Rev Vaccines. 2005;4:329-350
299. Wang G, Kelley RK, GAPPNet. KRAS mutational analysis for colorectal cancer Application: Pharmacogenomic. PLoS Curr. 2010;2:RRN1175
300. Eckerdt F, Yuan,J, Strebhardt,K: Polo-like kinases and oncogenesis. Oncogene. 2005; 24:267-276
301. Takai N, Hamanaka,R, Yoshimatsu,J, Miyakawa,I: Polo-like kinases (Plks) and cancer. Oncogene. 2005;24:287-291
302. Ando K, Ozaki T, Yamamoto H, Furuya K, Hosoda M, Hayashi S, Fukuzawa M, Nakagawara A. Polo-like Kinase 1 (Plk1) Inhibits p53 Function by Physical Interaction and Phosphorylation. Journal of Biological Chemistry. 2004;279:25549-25561

303. Spañnkuch-Schmitt B, Bereiter-Hahn J, Kaufmann M, Strebhardt K. Effect of RNA Silencing of Polo-Like Kinase-1 (PLK1) on Apoptosis and Spindle Formation in Human Cancer Cells. Journal of the National Cancer Institute. 2002;94:1863-1877
304. Liu X, Erikson RL. Polo-like kinase (Plk)1 depletion induces apoptosis in cancer cells. Proceedings of the National Academy of Sciences. 2003;100:5789-5794
305. Liu X, Lei M, Erikson RL. Normal Cells, but Not Cancer Cells, Survive Severe Plk1 Depletion. Mol Cell Biol. 2006;26:2093-2108
306. Guan R, Tapang P, Leverson JD, Albert D, Giranda VL, Luo Y. Small Interfering RNAi-mediated polo-like kinase depletion preferentially reduces the survival of p53-defective, oncogenic transformed cells and inhibits tumor growth in animals. Cancer Research 2005;65:2698-2704
307. Lane HA, Nigg EA. Antibody microinjection reveals an essential role for human polo-like kinase 1 (Plk1) in the functional maturation of mitotic centrosomes. The Journal of Cell Biology. 1996;135:1701-1713
308. Cogswell JP, Brown CE, Bisi JE, Neill SD. Dominant-Negative Polo-like Kinase 1 Induces Mitotic Catastrophe Independent of cdc25C Function. Cell Growth Differ. 2000; 11:615-623
309. Nahta R, Esteva FJ. Herceptin: mechanisms of action and resistance. Cancer Letters. 2006;232:123-138
310. Valabrega G, Montemurro F, Aglietta M. Trastuzumab: mechanism of action, resistance and future perspectives in HER2-overexpressing breast cancer. Annals of Oncology. 2007; 18:977-984
311. Aigner A. Delivery systems for the direct application of siRNAs to induce RNA Interference (RNAi) in vivo. Journal of Biomedicine and Biotechnology. 2006;1-15
312. Yang X, Dou S, Wang Y, Long H, Xiong M, Mao C, Yao Y, and Wang J.Single-Step Assembly of Cationic LipidPolymer Hybrid Nanoparticles for Systemic Delivery of siRNA. ACS nano. 2012;6:4955–4965
313. Baea YH, Park P. Targeted drug delivery to tumors: Myths, reality and possibility. J Control Release. 2011;153:198–205
314. Zhang Y, Chen J, Zhang Y, Hu Z, Hu D, Pan Y, Ou S, Liu G, Yin X, Zhao J, Ren L, Wang J. Panning and identification of a colon tumor binding peptide from a phage display peptide library. Journal of Biomolecular Screening. 20
315. Wang AZ, Langer R, Farokhzad OC. Nanoparticle Delivery of Cancer Drugs. Annual Review of Medicine: Nanoparticle chemotherapeutics. 2012;63: 186-198
316. Tech note: In vivo RNAi: Biodistribution, delivery, and applications. Thermoscientificbio

Original research articles included in the thesis:

1. **Malhotra M**, Kulamarva A, Sebak S, Paul A, Bhathena J, Mirzaei M and Prakash S (2009). Ultra-small nanoparticles of low molecular weight Chitosan as an efficient delivery system targeting neuronal cells. Drug Development and Industrial Pharmacy. Vol. 35, 6:719-726.
2. **Malhotra M**, Lane C, Tomaro-Duchesneau C, Saha and Prakash S (2011). A novel scheme for synthesis of PEG-grafted-chitosan polymer for preparation of nanoparticles and other applications. International Journal of Nanomedicine. Vol. 2011, 6: 485-494.
3. **Malhotra M**, Tomaro-Duchesneau C and Prakash S (2013). Synthesis of TAT peptide tagged PEGylated chitosan nanoparticles for siRNA delivery targeting neurodegenerative diseases. Biomaterials Vol. 34, 1270-1280.
4. **Malhotra M**, Tomaro-Duchesneau C, Saha S and Prakash S. siRNA delivery by novel TAT/MGF tagged PEGylated chitosan nanoparticles targeting Alzheimer's disease. (Submitted to Journal of Drug Delivery)
5. **Malhotra M**, Tomaro-Duchesneau C, Saha S and Prakash S. Novel CP-15 tagged PEGylated chitosan nanoparticle formulation for siRNA delivery, systemically, in a mouse xenograft model of colorectal cancer. (To be submitted)

Original research articles not included in the thesis (published/accepted/submitted):

6. **Malhotra M**, Nambiar S, Swamy VR and Prakash S (2011). Small interfering ribonucleic acid design strategies for effective targeting and gene silencing. Expert Opinion on Drug Discovery. Vol. 6, 3: 269-289.
7. **Malhotra M** and Prakash S (2011). Targeted Drug Delivery Across Blood-Brain-Barrier Using Cell Penetrating Peptides Tagged Nanoparticles. Current Nanosciences. Vol. 7, 1: 81-93.
8. **Malhotra M**, Tomaro-Duchesneau C, Saha S, Kahouli I and Prakash S. Development and characterization of novel chitosan-PEG-TAT nanoparticles for intracellular delivery of siRNA. Biomacromolecules. Submission ID: bm-2012-01522s.

9. Bhathena J, Martoni C, Kulamarva A, Tomaro-Duchesneau C, **Malhotra M**, Paul A, Prakash S. Oral probiotic microcapsule formulation ameliorates non-alcoholic fatty liver disease in Bio F1B Golden Syrian hamsters. PLOS one. (Submitted)
10. Prakash S, Tomaro-Duchesneau C, Saha S, Rodes L, Kahouli I, **Malhotra M**. Probiotics for the prevention and treatment of allergies, with an emphasis on mode of delivery and mechanism of action. Current Pharmaceutical Design. (Submitted)
11. Prakash S and **Malhotra M** (2008). Recent advancements in targeted delivery of therapeutic molecules in neurodegenerative disease - spinocerebellar ataxia - opportunities and challenges. Drug Target Insights. Vol. 3, 99-117.
12. Marinescu D, Tomaro-Duchesneau C, **Malhotra M**, Kahouli I, Jones M. L, Rodes L, Prakash S. Effect of orally administered APA microencapsulated BSH-active Lactobacillus reuteri NCIMB 30242 on markers of obesity: an in-vivo analysis. Journal of Medical Microbiology. (Accepted) Submission ID: JMM/2012/048298
13. Tomaro-Duchesneau C, Saha S, **Malhotra M**, Kahouli I and Prakash S. Microencapsulation for the therapeutic delivery of drugs, live mammalian and bacterial cells and other biopharmaceutics: current status and future directions. Journal of Pharmaceutics (In press) Submission ID: 103527.
14. Saha S, Tomaro-Duchesneau C, **Malhotra M**, Tabrizian M and Prakash S. Suppression of Streptococcus mutans and Candida albicans by probiotics: an in vitro study. Dentistry. Vol. 2, 6:1-8.
15. Sinno H, **Malhotra M**, Lutfy J, Jardin BA, Winocour S, Brimo F, Beckman L, Watters K, Philips A, Williams B and Prakash S (2012). The effects of topical collagen treatment on wound strength and scar cosmesis in rats. The Canadian Journal of Plastic Surgery. Vol. 20, 3:181-185.
16. Sinno H, **Malhotra M**, Lutfy J, Jardin BA, Winocour S, Brimo F, Beckman L, Watters K, Philips A, Williams B and Prakash S (2012). Accelerated Wound Healing with Topical Application of Complement C5. Plastic and Reconstructive Surgery journal. Vol. 130, 3:523-529.
17. Salehi P, Makhoul G, Roy R, **Malhotra M**, Mood ZA and Daniel SJ (2012) Curcumin loaded NIPAAM/VP/PEG-A nanoparticles: Physicochemical and chemopreventive properties. Journal of Biomaterials Science: Polymer Edition: 1-15.

18. Bhathena J*, Tomaro-Duchesneau C*, Martoni C, **Malhotra M**, Kulamarva A, Urbanska AM, Paul A and Prakash S (2012). Effects of orally administered microencapsulated FA-producing L. fermentum on markers of metabolic syndrome: an in vivo analysis. Journal of Diabetes and Metabolism. [* denotes equal contribution]. S2-009.
19. Tomaro-Duchesneau C, Saha S, **Malhotra M**, Coussa-Charley M, Jones M, Labbé A, Prakash S (2012) Probiotic ferulic acid esterase active Lactobacillus fermentum NCIMB 5221 cells APA microcapsules for oral delivery: preparation and in-vitro characterization. Pharmaceuticals. Vol. 5, 2: 236-248.
20. Tomaro-Duchesneau C, Saha S, **Malhotra M**, Coussa-Charley M, Al-Salami H, Mitchell L. Jones, Alain Labbé and Satya Prakash (2012). Lactobacillus fermentum NCIMB 5221 has a greater ferulic acid production compared to other ferulic acid esterase producing Lactobacilli. International Journal of Probiotics and Prebiotics. Vol. 7, 1:23-32.
21. Coussa R, Shah S, Jain P, Martoni C, Bhathena J, **Malhotra M** and Prakash S (2012). Microencapsulated Saccharomyces cerevisiae column bioreactor for potential use in renal failure uremia. Artifical cells, Blood Substitutes and Biotechnology, An International Journal. Vol. 2012, 40: 103-112.
22. Prakash S, **Malhotra M**, Shao W, Tomaro-Duchesneau C and Abassi S (2011). Polymeric nanohybrids as drug delivery carriers for cancer therapy. Advanced Drug Delivery Reviews. Vol. 63, 14-15: 1340-1351.
23. Sinno H, **Malhotra M**, Lutfy J, Jardin B, Winocour S, Brimo F, Beckman L, Watters K, Philips A, Williams B and Prakash S. (2011) Topical Application of Complement C3 in Collagen Formulation Increases Early Wound Healing. Journal of dermatological treatment. doi:10.3109/09546634.2011.631977.
24. Bhathena J, Kulamarva A, Martoni C, Urbanska AM, **Malhotra M**, Paul A and Prakash S (2011). Diet induced metabolic hamster model of non-alcoholic fatty liver disease. Diabetes, Metabolic Syndrome and Obesity: Targets and Therapy. Vol. 2011, 4: 195-203.
25. Sebak S, Mirzaei M, **Malhotra M**, Kulamarva A and Prakash S (2010). Human serum albumin nanoparticles as an efficient noscapine drug delivery system for

potential use in breast cancer: preparation and in-vitro analysis. International Journal of Nanomedicine. Vol. 2010, 5: 525-532.

26. Paul A, Jardin BA, Kulamarva A*, **Malhotra M***, Elias CB and Prakash S (2010) Recombinant Baculovirus as a highly potent vector for gene therapy of human colorectal carcinoma: Molecular cloning, expression, and in vitro characterization. Molecular Biotechnology [* denotes equal contribution]. Vol. 45, 2: 129-39.
27. Bhathena J, Martoni C, Kulamarva A, Urbanska AM, **Malhotra M**, and Prakash S (2009). Orally delivered microencapsulated live probiotic formulation lowers serum lipids in hypercholesterolemic hamsters. Journal of Medicinal Food. Vol. 12, 2:310-9.
28. Kulamarva A, Bhathena J, **Malhotra M**, Sebak S, Ajayan P and Prakash S (2008). In-vitro cytotoxicity of functionalized single walled carbon nanotubes for targeted gene delivery applications. Nanotoxicology. Vol. 2, 4:184-188.

Book chapter

29. Prakash S, **Malhotra M**, Swamy VR (2010) Non-viral siRNA delivery and gene silencing for neurodegenerative diseases; RNA interference from laboratory to clinical application. Methods in Molecular Biology Vol. 623, 211-229.

Provisional Patent

30. Prakash S and **Malhotra M.** Non-viral nanaoparticle based delivery system U.S. Provisional Patent. US 61/660,139 (June 15, 2012) / US 61/497,088 (June 15, 2011).

Other refereed contributions (abstracts/posters/presentations):

1. **Malhotra M** and Prakash S. Smart nanoparticles for siRNA delivery targeting neurodegenerative diseases. Neurodegeneration: Causes and Therapeutics. A joint workshop by McGill University and UNICAMP. Nov 22-23, 2012. Campinas, Sao Paulo, Brazil. ***Oral presentation***
2. **Malhotra M** and Prakash S. Non-viral nanoparticle based delivery system. Techconnect World- summit and innovation showcase 2012. June 18-21, 2012. Santa Clara, California, USA. ***Intellectual Property Oral Presentation***.

3. **Malhotra M**, Tomaro-Duchesneau C, Saha S and Prakash S. Novel nanoparticles for targeted delivery of siRNA in CNS diseases. Techconnect World- summit and innovation showcase 2012. June 18-21, 2012. Santa Clara, California, USA. ***Oral Presentation***
4. Tomaro-Duchesneau C, Saha S, Jones ML, Labbé A, **Malhotra M**, Kahouli I, Rodes L and Prakash S. APA microcapsules for the delivery of Lactobacillus fermentum NCIMB 5221: an in-vitro study. *Canadian Society for Pharmaceutical Sciences–Modern Therapeutics 2012: Advances in Physiology, Pharmacology and Pharmaceutical Sciences,* Toronto, ON, Canada. June 12-15 2012. ***Poster***
5. Tomaro-Duchesneau C, Saha S, Jones ML, Labbé A, **Malhotra M**, Kahouli I and Prakash S. Lactobacillus fermentum NCIMB 5221 ferulic acid production for human health. "Reflections" The 9th Annual NHP Conference and Tradeshow. May 22-25, 2012. Kelowna, BC, Canada. ***Abstract***
6. Saha S, Tomaro-Duchesneau C, **Malhotra M**, Kahouli I, Tabrizian M and Prakash S. Probiotics for the prevention and treatment of dental caries and oral candidiasis. Exploring Human Host-Microbiome Interactions in Health and Disease, Cambridge, UK May 8-10, 2012. ***Abstract***
7. Saha S, Tomaro-Duchesneau C, **Malhotra M**, Kahouli I, Tabrizian M and Prakash S. Potential role of probiotics for the inhibition of S. mutans and C. albicans. "Reflections"9th Annual NHP Conference and Tradeshow, Kelowna, BC, Canada. May 22-25, 2012. ***Abstract***
8. Saha S, Tomaro-Duchesneau C, **Malhotra M**, Kahouli I, Tabrizian M and Prakash S. Probiotics: bio-therapeutics for the prevention and treatment of oral diseases such as dental caries and oral candidiasis. CSPS–Modern Therapeutics 2012: Advances in Physiology, Pharmacology and Pharmaceutical Sciences, Toronto, Ontario, Canada. June 12-15 2012. ***Poster***
9. Saha S, Tomaro-Duchesneau C, **Malhotra M**, Kahouli I, Tabrizian M, Prakash S. Probiotic Replacement Therapy for the Prevention and Treatment of Dental Caries and Oral Candidiasis - McGill University ,Faculty of Dentistry – 7th Annual Research Day, Montreal, QC. March 29th, 2011. ***Poster***

10. Saha S, Tomaro-Duchesneau C, **Malhotra M**, Al-Salami H, Kahouli I, Tabrizian M and Prakash S. Development of an oral ecosystem model to study the oral microflora. McGill Bioengineering Symposium 2011. September 15, 2011. Montreal, Quebec. ***Poster***
11. **Malhotra M**, Tomaro-Duchesneau C, Saha S and Prakash S. Ligand-guided polymeric nanoparticles mediating site-specific delivery of siRNA - a promising approach to target neurodegenerative diseases. BioEngineering Symposium 2011. September 15, 2011. Montreal, QC, Canada. ***Abstract***
12. Chemali R, **Malhotra M**, Tomaro-Duchesneau C, Saha S, Kahouli I, Jackson C, Al-Salami H and Prakash S. Surface functionalized single walled carbon nanotubes for tumor specific targeting: characterization and in vitro studies. Canadian Society for Pharmaceutical Sciences – 2011 Annual Symposium (Multidisciplinary Approaches to Modern Therapeutics: Joining Forces for a Healthier Tomorrow). May 24 – 27, 2011. Montreal, QC, Canada. ***Abstract***
13. Tomaro-Duchesneau C, Saha S, **Malhotra M**, Al-Salami H, Kahouli I and Prakash S. Artificial cell APA microcapsules for the delivery of a Lactobacillus fermentum based therapeutic. Canadian Society for Pharmaceutical Sciences – 2011 Annual Symposium (Multidisciplinary Approaches to Modern Therapeutics: Joining Forces for a Healthier Tomorrow). May 24 – 27, 2011. Montreal, QC, Canada. ***Poster***
14. Kahouli I, Tomaro-Duchesneau C, **Malhotra M**, Al-Salami H, Saha S and Prakash S. Effect of Lactobacillus acidophilus supernatant on colon cancer cell proliferation and polyamine synthesis. Canadian Society for Pharmaceutical Sciences – 2011 Annual Symposium (Multidisciplinary Approaches to Modern Therapeutics: Joining Forces for a Healthier Tomorrow). May 24 – 27, 2011 Montreal, QC, Canada. ***Poster***
15. Saha S, Tomaro-Duchesneau C, **Malhotra M**, Al-Salami H, Kahouli I and Prakash S. Development of an in vitro oral ecosystem model to investigate probiotics as a therapeutic for maintaining oral health. Canadian Society for Pharmaceutical Sciences – 2011 Annual Symposium (Multidisciplinary Approaches to Modern Therapeutics: Joining Forces for a Healthier Tomorrow). May 24 – 27, 2011. Montreal, QC, Canada. ***Poster***

16. Tomaro-Duchesneau C, Saha S, **Malhotra M**, Al-Salami H, Coussa-Charley M and Prakash S. Selection and characterization of FAE active probiotic bacteria for the development of therapeutics. International Scientific Conference on Probiotics and Prebiotics – IPC 2011. June 14th-16th 2011. Kosice, Slovakia. ***Abstract***
17. Saha S, Tomaro-Duchesneau C, **Malhotra M**, Tabrizian M and Prakash S. Role of probiotics in dental caries causing organism Streptococcus mutans and other bacterial systems: In vitro analysis. 6th McGill Dentistry Research Day. Feb 21st 2011. Montreal, QC, Canada. ***Oral Presentation***
18. **Malhotra M**, Tomaro-Duchesneau C, Saha S, Chemali R and Prakash S. Nanocarriers for siRNA brain delivery to silence neurodegenerative diseases in pets and humans. 38th Annual Meeting and Exposition of the Controlled Release Society – Delivering Bioactives 2011. July 30 - August 3, 2011. National Harbor, Maryland, U.S.A - ***Abstract***
19. **Malhotra M** and Prakash S. Surface functionalized chitosan nanoparticles for gene delivery. Particles 2010. May 22-25, 2010. Lake Buena Vista, Florida, USA. ***Poster***
20. **Malhotra M**, Paul A and Prakash S. Peptide tagged, non-toxic chitosan nanoparticles for enhanced siRNA delivery. RNAi and miRNA world congress. May 5-7, 2010. Boston, MA, USA. ***Abstract***
21. Sinno H, Lutfy J, Jardin B, Brimo, F, **Malhotra M**, Beckman L, Winocour S, Williams B, Prakash S. Topical Complement C3 in Collagen Formulation Accelerates Wound Healing. 89th annual meeting for the American Association of Plastic Surgeons (oral presentation) Plastic & Reconstructive Surgery Journal Monday, March 22, 2010. Abstract No. 1, Page 113 *Best Prize for* ***Poster presentation*** *(2nd Place).*
22. Sinno H, Lutfy J, Jardin B, Brimo, F, **Malhotra M**, Beckman L, Winocour S, Williams B, Prakash S. Early Increased Wound Healing Strength with Topical Complement C3. 63rd annual meeting for the Canadian Society of Plastic Surgeons Canadian Journal of Plastic Surgery. 2009 Vol 17 (2) pg 50 Abstract No.42. ***Oral Presentation***

23. **Malhotra M**, Paul A, Kulamarva A and Prakash S. Nanonoparticles mediated delivery of siRNA in neuronal cells, RNAi Congress 2009. May14-15, 2009. Boston, MA, USA. ***Poster***
24. Sinno H, Lutfy J, Jardin B, Brimo F, **Malhotra M**, Beckman L, Winocour S, Williams B. and Prakash S. Complement C3 increases wound healing in rats. Association for Specialists in Plastic and Aesthetic Surgery of Quebec –ASCPEQ. March 2009. Quebec, Canada. Abstract No. 23, pg 27. ***Poster***
25. Paul A, Kulamarva A, **Malhotra M**, Elhayek E and Prakash S. Rapid Expression of Transporter Gene in Mammalian Cells using Recombinant Viruses: Focus on Cancer Gene Therapy, 12th Canadian Society for Pharmaceutical Sciences (CSPS) Annual Symposium, June 3-6, 2009, Toronto, Canada. ***Abstract***
26. Paul A, **Malhotra M**, Jardin B.A, Elias C.B and Prakash S. Baculovirus mediated gene delivery for rapid expression of transporter gene in mouse neuroblastoma cells: In vitro analysis. Dendritic Cells Conference 2009, Banff. ***Abstract***
27. Paul A, Kulamarva A, **Malhotra M** and Prakash S. Viral Gene Therapy for Expression of Transporter Gene in Pancreatic Tumor Cells: A Novel Approach. Nanotech, Cleantech, TechConnect Conference & Expo 2009, May3-7, 2009 Houston, Texas, U.S.A. ***Abstract***
28. Kulamarva A, Bhathena J, Paul A, **Malhotra M** and Prakash S. Microcapsule carbon nanotube devices for targeted delivery. Nanotoday 2009, August 2-5 2009, Singapore. ***Abstract***
29. Kulamarva A, **Malhotra M**, Paul A and Prakash S. Polymeric membrane carbon nanotube devices for targeted drug delivery. NSTI Nanotechnology Conference and Trade Show, May 3-7 2009, Houston, Texas, U.S.A. ***Abstract***
30. **Malhotra M**, Kulamarva A, Paul A and Prakash S. Surface functionalized chitosan nanoparticles for targeted gene delivery in-vitro. Nanotoday 2009, August 2-5 2009, Singapore. ***Abstract***
31. **Malhotra M**, Paul A, Kulamarva A and Prakash S. Improved tranfection of chitosan nanoparticles, surface coated with cell penetrating peptides. 6th Interdisciplinary Graduate Student Research Symposim (IGSRS), March 26-27 2009, McGill University, Montreal, Canada. ***Poster***

32. **Malhotra M**, Kulamarva A, Paul A and Prakash S. Characterizing PEGylated chitosan nanoparticles in terms of size and zeta potential for gene delivery applications. NSTI Nanotech 2009, May 3-7 2009, Houston, TX. ***Abstract***
33. **Malhotra M**, Kulamarva A, Paul A and Prakash S. Surface functionalized chitosan nanoparticles for gene delivery. 32nd Canadian Medical and Biological Engineering Conference CMBEC32, May 20-22, 2009. Calgary, Alberta. ***Abstract***
34. Kulamarva A, Bhathena J, **Malhotra M**, Paul A and Prakash S. Targeted carbon nanotube delivery for biomedical applications: preparation and in-vitro analysis. Nanomaterials Conference 2008, December 7- 10, 2008. Playa del Carmen, Mexico. ***Abstract***
35. Kulamarva A, Bhathena J, Paul A, Sinno H, **Malhotra M** and Prakash S. Polymeric membrane microcapsule carbon nanotube devices for targeted delivery. Nanobiophysics, Nanochemistry, Nanomedicine & Nanotoxicology Conference 2009, January 21 – 25, 2009. Antigua and Barbuda. ***Poster***
36. **Malhotra M**, Nambiar S and Swamy V.R. Analyzing molecular interaction at nanoscale through confocal live cell imaging. – 77th Society of Biological Chemists (SBC India), December 18-20, 2008. Chennai, India. ***Oral Presentation***
37. Paul A, Hamoudeh M, **Malhotra M**, Elias C.B, Prakash S. Viral vector based gene therapy for angiogenesis of damaged cardiac tissues: A novel approach. Canadian Cardiovascular Congress, October 25-29, 2008. Toronto, Canada. ***Abstract***
38. **Malhotra M**, Kulamarva A, Sebak S, Bhathena J, Prakash S. Cationic chitosans as efficient non-viral nano-carriers for gene delivery. 31st Canadian Medical and Biological Engineering Conference (CMBEC31), June 11-13, 2008. Montreal, QC, Canada. ***Poster***
39. **Malhotra M**, Kulamarva A, Sebak S, Bhathena J, Prakash S. In vitro transfection efficiency of chitosan nanoparticles for gene delivery. NSTI Nanotech 2008, June1-5, 2008. Boston Masachussets, U.S.A. ***Poster***
40. Kulamarva A, **Malhotra M**, Bhathena J, Sebak S and Prakash S. In-vitro evaluation of carbon nanotube mediated gene delivery for colon cancer. NSTI Nanotech 2008, June 1-5, 2008. Boston, Massachusetts, U.S.A. ***Abstract***

41. **Malhotra M**, Kulamarva A, Paul A, Hamoudeh M, Sebak S, Bhathena J, Prakash S. Non-Viral Nanonoparticles for Targeted Delivery of siRNA- A Promising Approach for the Treatment of Neurodegenerative Diseases. RNAi Congress, April 30 – May 2, 2008. Boston MA, U.S.A. ***Poster***
42. Bhathena J, Martoni C, Kulamarva A, Urbanska A, **Malhotra M**, Prakash S. In-vitro analysis of microencapsulated bacterial cells for augmentation of ferulic acid in the gastrointestinal tract. Ferulate 08 - An International Conference on Hydroxycinnamates and Related Plant Phenolics, August 25-27, 2008, Minneapolis/St. Paul, U.S.A. ***Poster***
43. Kulamarva A, Bhathena J, **Malhotra M**, Sebak S and Prakash S. In-vitro cytotoxicity of carbon nanotubes for targeted delivery applications. 11th Canadian Society for Pharmaceutical Sciences (CSPS) Annual Meeting. May 22-25, 2008, Banff, Alberta, Canada. ***Best Poster Award***
44. Kulamarva A, Bhathena J, **Malhotra M**, Sebak S, Ajayan P and Prakash S. In-vitro cytotoxicity of functionalized single walled carbon nanotubes for targeted gene delivery applications. International Conference on Nanomaterial Toxicology, February 2008. Lucknow, India. – ***Oral Presentation***
45. **Malhotra M**, Kulamarva A, Sebak S, Bhathena J, Prakash S. Characterization of low molecular weight chitosan nanoparticles as a delivery carrier for therapeutic molecules. 8th Annual McGill Biomedical Graduate Conference, February 26, 2008, McGill University, Montreal, Canada. ***Poster***
46. Sebak S, Mirzaei M, **Malhotra M**, Kulamrava A and Prakash S. Human Serum Albumin Nano devices as efficient drug delivery systems. 8th Annual McGill Biomedical Graduate Conference, February 26, 2008. McGill University, Montreal Canada. ***Poster***
47. **Malhotra M**, Kulamarva A, Sebak S, Bhathena J, Mirzaei M, Prakash S. Nanoparticles for targeted delivery of therapeutic molecules for use in neurodegenerative diseases. International Conference of Neurons and Brain Disease, August 29-31,2007 University of Toronto, Canada. ***Abstract***
48. **Malhotra M**, Sebak S, Mirzaei M, Kulamarva A, Bhathena J, Prakash S. Optimizing the design principles of cationic chitosan nanoparticles as an efficient gene delivery

system. 2nd Annual Conference of the CSLSR, July 13-14, 2007 at McGill Unversity, Montreal, QC, Canada. ***Poster***

49. Safaa S, Mirzaei M, **Malhotra M**, Kulamarva A, Prakash S. Preparation and characterization of Human Serum Albumin for Drug Delivery Applications. 2nd Annual Conference of the CSLSR, July 13-14, 2007 at McGill Unversity, Montreal, QC, Canada. ***Poster***